

## **INFORMATION TO USERS**

This manuscript has been reproduced from the microfilm master. UMI films the text directly from the original or copy submitted. Thus, some thesis and dissertation copies are in typewriter face, while others may be from any type of computer printer.

**The quality of this reproduction is dependent upon the quality of the copy submitted.** Broken or indistinct print, colored or poor quality illustrations and photographs, print bleedthrough, substandard margins, and improper alignment can adversely affect reproduction.

In the unlikely event that the author did not send UMI a complete manuscript and there are missing pages, these will be noted. Also, if unauthorized copyright material had to be removed, a note will indicate the deletion.

Oversize materials (e.g., maps, drawings, charts) are reproduced by sectioning the original, beginning at the upper left-hand corner and continuing from left to right in equal sections with small overlaps.

Photographs included in the original manuscript have been reproduced xerographically in this copy. Higher quality 6" x 9" black and white photographic prints are available for any photographs or illustrations appearing in this copy for an additional charge. Contact UMI directly to order.

ProQuest Information and Learning  
300 North Zeeb Road, Ann Arbor, MI 48106-1346 USA  
800-521-0600

**UMI<sup>®</sup>**



## **NOTE TO USERS**

**Page(s) not included in the original manuscript and are unavailable from the author or university. The manuscript was microfilmed as received.**

**35, 189**

**This reproduction is the best copy available.**

**UMI**



**University of Alberta**

**Characterization of Bacterial and Mammalian Recombinant Nucleoside Transport Proteins**

= 3

**By**

**Mark F. Vickers**



**A thesis submitted to the Faculty of Graduate Studies and Research in partial fulfillment of the requirements for a degree of Doctor of Philosophy**

**Department of Biochemistry**

**Edmonton, Alberta**

**Fall, 2000**

~



**National Library  
of Canada**

**Acquisitions and  
Bibliographic Services**

**395 Wellington Street  
Ottawa ON K1A 0N4  
Canada**

**Bibliothèque nationale  
du Canada**

**Acquisitions et  
services bibliographiques**

**395, rue Wellington  
Ottawa ON K1A 0N4  
Canada**

*Your file Votre référence*

*Our file Notre référence*

**The author has granted a non-exclusive licence allowing the National Library of Canada to reproduce, loan, distribute or sell copies of this thesis in microform, paper or electronic formats.**

**The author retains ownership of the copyright in this thesis. Neither the thesis nor substantial extracts from it may be printed or otherwise reproduced without the author's permission.**

**L'auteur a accordé une licence non exclusive permettant à la Bibliothèque nationale du Canada de reproduire, prêter, distribuer ou vendre des copies de cette thèse sous la forme de microfiche/film, de reproduction sur papier ou sur format électronique.**

**L'auteur conserve la propriété du droit d'auteur qui protège cette thèse. Ni la thèse ni des extraits substantiels de celle-ci ne doivent être imprimés ou autrement reproduits sans son autorisation.**

**0-612-59688-5**

**Canada**

**University of Alberta  
Library Release Form**

**Name of Author:** Mark F. Vickers  
**Title of thesis:** Characterization of Bacterial and Mammalian  
Recombinant Nucleoside Transport Proteins  
**Degree:** Doctor of Philosophy  
**Year This Degree Granted:** 2000

Permission is hereby granted to the University of Alberta Library to reproduce single copies of this thesis, and to lend or sell copies for private, scholarly or scientific research purposes only.

The author reserves all other publication and other rights in association with the copyright in the thesis, and except as hereinbefore or otherwise reproduced in any material from whatever without the author's prior written permission.



**Mark F. Vickers**

**45 Dunfield Ave. # 608**

**Toronto Ontario**

**Canada**

**M4S 2H4**

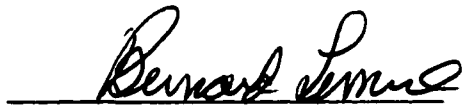
*August 21 2000*

University of Alberta  
Faculty of Graduate Studies and Research

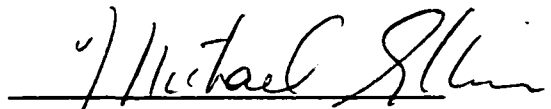
The undersigned certify that they have read, and recommended to the Faculty of Graduate Studies and Research for acceptance, a thesis entitled "Characterization of Bacterial, Yeast and Mammalian Recombinant Nucleoside Transport Proteins" submitted by Mark F. Vickers in partial fulfillment of the requirements for the degree of Doctor of Philosophy.



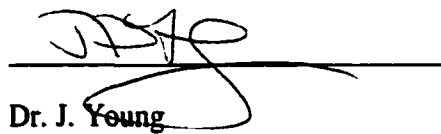
Dr. C. E. Cass (supervisor)



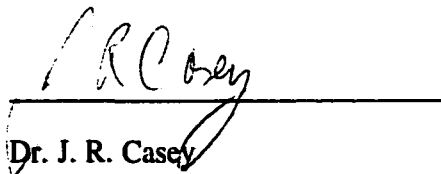
Dr. B. Lemire



Dr. M. Ellison



Dr. J. Young



Dr. J. R. Casey



Dr. R. Reithmeier (external examiner)

August 10 2000



## ABSTRACT

Nucleoside transporter proteins have been divided into two structurally distinct families: (i) the equilibrative nucleoside transporters (ENTs) that mediate the passage of substrate down a concentration gradient, and (ii) the concentrative nucleoside transporters (CNTs) that mediate the passage of substrate against a concentration gradient in a sodium-dependent fashion. The isolation of cDNAs encoding proteins with known nucleoside transport activity and the identification of cDNAs encoding proteins with sequence similarity to known nucleoside transporters has stimulated the development of model expression systems to examine recombinant nucleoside transporter proteins. Described here is the identification and characterization of two endogenous nucleoside transport proteins from *Saccharomyces cerevisiae* and the subsequent use of this organism as an expression system to functionally characterize three prokaryotic and four mammalian recombinant nucleoside transporter proteins.

It was demonstrated that *S. cerevisiae* possess two, structurally distinct, nucleoside transporter proteins: FUI1, a uridine-specific transporter protein of the "uracil/allantoin" family of transporters which functions at the yeast cell surface, and FUN26, a broadly specific, transporter protein of the ENT family, which apparently functions in intracellular membranes.

Procedures were then developed to functionally express cDNAs encoding members of the CNT family in *S. cerevisiae*. The pyrimidine nucleoside specific transporters from rat (rCNT1), human (hCNT1) and *Escherichia coli* (NUPC) were functionally produced and shown to retain their pyrimidine nucleoside specific substrate specificity. Open reading frames from *Haemophilus influenzae* (HI0519) and *Helicobacter pylori* (HP1180) that are predicted to encode proteins that are members of the CNT family were shown by phenotypic complementation in yeast to have thymidine transport activity.

Yeast expression studies were also undertaken with the human nitrobenzylmercaptapurine ribonucleoside (NBMPR)-sensitive ENT protein, hENT1.

Recombinant hENT1 was functionally produced in *S. cerevisiae* and methods were developed to measure the interaction of NBMPR with recombinant hENT1. NBMPR bound to hENT1 with high-affinity ( $K_d$  1.2 nM) and a mutant version of hENT1 that lacked the capacity for N-linked glycosylation bound with reduced affinity ( $K_d$  10.5 nM).

The human NBMPR-insensitive ENT protein, hENT2, was also functionally produced in *S. cerevisiae*. hENT2-mediated transport of uridine was inhibited by several purine and pyrimidine nucleosides as well as by the nucleobases hypoxanthine and thymine. Additionally, scanning N-linked glycosylation mutagenesis established that the loop region between predicted transmembrane spanning domains 1 and 2 is extracellular and the loop region between predicted transmembrane spanning domains 6 and 7 is intracellular.

## Acknowledgements

The work presented here would not have been possible without the support of many people. I am very grateful to Carol Cass for the opportunity to pursue a wide range of projects during the course of my studies. Past and present members of Carol's lab and our collaborators labs have my gratitude and thanks for their intellectual and technical assistance, colleagues and cohorts one and all. From the lab of Carol Cass: C. Boumah, M. Cabrita, P. Carpenter, I. Coe, X. Fang, K. Graham, D. Hogue, L. Jennings, K. King, T. Lang, J. Leithoff, R. Mani, J. Marjan, S. Modi, D. Mowles, K. Panayides, P. Panayides, M. Selner, F. Visser, K. Wong, L. Zombar. From the lab of John Mackey: C. Lee, C. Santos. From the lab of Jim Young: E. Chomey, S. Loewen, A. Ng, M. Ritzel, M. Sundaram, S. Yao. I also thank members of the Molecular Biology of Membranes Research Group and the Membrane Transport Research Group for helpful suggestions as well as the coffee and donuts. My final thanks go to Jen and Kitty without whose support...

## TABLE OF CONTENTS

<b>I.</b>	<b>Introduction</b>	<b>1</b>
<b>I.</b>	<b>Nucleoside transport proteins</b>	<b>2</b>
<b>I.A.</b>	<b>General introduction</b>	<b>2</b>
<b>I.B.</b>	<b>Mammalian concentrative nucleoside transporters</b>	<b>5</b>
<b>I.B.i</b>	<b>Pyrimidine nucleoside selective CNTs</b>	<b>5</b>
<b>I.B.i.a</b>	<b>rCNT1</b>	<b>5</b>
<b>I.B.i.b</b>	<b>hCNT1</b>	<b>6</b>
<b>I.B.i.c</b>	<b>pkCNT1</b>	<b>6</b>
<b>I.B.ii</b>	<b>Purine nucleoside selective CNTs</b>	<b>7</b>
<b>I.B.ii.a</b>	<b>rCNT2</b>	<b>7</b>
<b>I.B.ii.b</b>	<b>hCNT2</b>	<b>7</b>
<b>I.B.ii.c</b>	<b>mCNT2</b>	<b>8</b>
<b>I.B.iii.</b>	<b>Functional domains of the mammalian CNT proteins</b>	<b>8</b>
<b>I.B.iii.a</b>	<b>Amino acids involved in substrate recognition in the CNTs</b>	<b>9</b>
<b>I.C</b>	<b>Mammalian equilibrative nucleoside transporters</b>	<b>10</b>
<b>I.C.i.</b>	<b>NBMPR-sensitive equilibrative nucleoside transporters</b>	<b>10</b>
<b>I.C.i.a</b>	<b>hENT1</b>	<b>10</b>
<b>I.C.i.b</b>	<b>rENT1</b>	<b>11</b>
<b>I.C.ii.</b>	<b>NBMPR-insensitive equilibrative nucleoside transporters</b>	<b>12</b>
<b>I.C.ii.a</b>	<b>hENT2</b>	<b>12</b>
<b>I.C.ii.b</b>	<b>rENT2</b>	<b>12</b>
<b>I.C.iii</b>	<b>Functional domains of the mammalian ENT proteins</b>	<b>13</b>
<b>I.C.iii.a</b>	<b>Region of hENT1 responsible for conferring dipyrindamole sensitivity</b>	<b>13</b>
<b>I.D</b>	<b>“Orphan” nucleoside transport processes</b>	<b>14</b>
<b>I.E</b>	<b>Nucleoside transporters of parasitic protozoans</b>	<b>15</b>
<b>I.E.i</b>	<b>LdNT1 and LdNT2</b>	<b>15</b>
<b>I.E.i.a</b>	<b>LdNT1</b>	<b>15</b>
<b>I.E.i.b</b>	<b>LdNT2</b>	<b>16</b>
<b>I.E.ii</b>	<b>TbAT1 and TbNT2</b>	<b>16</b>
<b>I.E.ii.a</b>	<b>TbAT1</b>	<b>16</b>
<b>I.E.ii.b</b>	<b>TbNT2</b>	<b>17</b>
<b>I.E.iv</b>	<b>PfNT1 and PfENT1</b>	<b>18</b>
<b>I.F.</b>	<b>Nucleoside transporters of yeast</b>	<b>19</b>
<b>I.F.i</b>	<b><i>Candida albicans</i></b>	<b>19</b>
<b>I.E.ii</b>	<b><i>Saccharomyces cerevisiae</i></b>	<b>20</b>
<b>I.G</b>	<b>Nucleobase transport processes of <i>S. cerevisiae</i>.</b>	<b>21</b>
<b>I.H</b>	<b>Nucleoside transport processes of <i>S. cerevisiae</i>.</b>	<b>22</b>
<b>I.I</b>	<b>Bacterial nucleoside transporters</b>	<b>23</b>
<b>I.I.i</b>	<b>NUPC and NUPG</b>	<b>23</b>
<b>I.J</b>	<b>Expression systems for analysis of recombinant nucleoside transporters</b>	<b>24</b>
<b>I.J.i</b>	<b>Oocytes of <i>X. laevis</i></b>	<b>24</b>
<b>I.J.ii</b>	<b>Cultured mammalian cells</b>	<b>25</b>
<b>I.J.iii</b>	<b><i>S. cerevisiae</i></b>	<b>25</b>
<b>I.K</b>	<b>Objectives of the study</b>	<b>27</b>

<b>II.</b>	<b>Materials and methods</b>	<b>49</b>
II.A.i	Yeast Strains, media and plasmids	50
II.A.ii	Plasmid construction in Chapter III	50
II.A.iii	Plasmid construction in Chapter IV	51
II.A.iv	Plasmid construction in Chapter V	53
II.A.v	Plasmid construction in Chapter VI	53
II.B.	Phenotypic complementation assay	54
II.C.	Cell culture	55
II.D.	RNA isolation and Northern analysis	56
II.E.	Preparation of yeast membranes	56
II.F.	Preparation of CHO membranes	57
II.G.	Protein determination	57
II.G.i.	Modified Lowry assay	57
II.G.ii	Bradford assay	58
II.H.	Peptide-N-Glycosidase F treatment of proteins from membranes of transfected CHO cells	58
II.I.	Electrophoresis and immunoblotting	59
II.J.	Nucleoside uptake	59
II.J.i.	<i>S. cerevisiae</i>	59
II.J.ii.	HeLa cells	60
II.J.iii.	<i>X. laevis</i> oocytes	61
II.K.	[ <sup>3</sup> H]NBMPR binding	62
II.L.	Kinetics of dissociation and association of [ <sup>3</sup> H]NBMPR	63
II.M.	Reconstitution of hENT1 and hENT2-mediated thymidine transport into proteoliposomes	63
II.N	Sucrose Gradient Centrifugation	65
<b>III.</b>	<b>Nucleoside Transport Processes of <i>Saccharomyces cerevisiae</i><sup>1</sup></b>	<b>72</b>
III.A	ABSTRACT	73
III.B	INTRODUCTION	75
III.C	RESULTS	78
III.C.i	Sequence comparison of putative nucleoside transport proteins from <i>S. cerevisiae</i>	78
III.C.ii	Disruption of the <i>FUI1</i> and <i>FUN26</i> genes	78
III.C.iii	Cellular resistance to 5-fluorouridine and 5-fluorouracil by yeast with <i>FUI1</i> and <i>FUN26</i> gene disruptions	79
III.C.iv	Uptake of uridine by yeast with <i>FUI1</i> and <i>FUN26</i> gene disruptions	80
III.C.v	Production of recombinant <i>FUN26</i> in <i>Xenopus laevis</i> oocytes	81
III.C.vi	Production of <i>FUN26myc</i> in yeast	83
III.C.vii	<i>FUN26myc</i> is predominantly located in intracellular membranes of yeast	83
III.D	DISCUSSION	85

<b>IV.</b>	<b>Functional expression of mammalian and bacterial concentrative nucleoside transporters in <i>Saccharomyces cerevisiae</i>.</b>	<b>104</b>
IV.A	ABSTRACT	105
IV.B.	INTRODUCTION	106
IV.C.	RESULTS	109
IV.C.ii.	Functional expression of rCNT1 and ΔN31rCNT1 in <i>S. cerevisiae</i>	109
IV.C.iii.	Production of ΔN31rCNT1 and rCNT1 mRNA in <i>S. cerevisiae</i>	110
IV.C.iii.	Functional production of rCNT1 and ΔN31rCNT1 in <i>X. laevis</i> oocytes	111
IV.C.iv.	rCNT1myc, ΔN16rCNT1myc, ΔN23rCNT1myc, and ΔN31rCNT1myc complement a thymidine-transport deficiency in yeast	112
IV.C.v.	hCNT1myc and ΔN23hCNT1myc complement a thymidine-transport deficiency in yeast	113
IV.C.vi.	NUPCmyc complements a thymidine-transport deficiency in yeast	115
IV.C.vii.	Effects of purine and pyrimidine nucleosides on rCNT1myc-, hCNT1myc- and NUPCmyc-dependent thymidine rescue	116
IV.C.viii.	Sequence comparison of known and putative concentrative nucleoside transport proteins	117
IV.C.ix.	The recombinant proteins encoded by open reading frames of <i>H. influenzae</i> (HI0519) and <i>H. pylori</i> (HP1180) complemented a thymidine-transport deficiency in yeast	117
IV.D.	DISCUSSION	119
<b>V.</b>	<b>Functional production of the human equilibrative nucleoside transporter (hENT1) in <i>Saccharomyces cerevisiae</i><sup>1</sup></b>	<b>140</b>
V.A.	ABSTRACT	141
V.B.	INTRODUCTION	143
V.C.	RESULTS	145
V.C.i.	pYhENT1 complementation of a thymidine transport deficiency in yeast	145
V.C.ii.	Production of hENT1 mRNA and protein	146
V.C.iii.	Effects of inhibitors of nucleoside transport on hENT1-dependent thymidine rescue	147
V.C.iv.	Yeast cells with hENT1 exhibit increased cellular uptake of [ <sup>3</sup> H]thymidine	147
V.C.v.	Binding of [ <sup>3</sup> H]NBMPR to hENT1-producing yeast	148
V.C.vi.	Binding of NBMPR to hENT1 in yeast membranes	149
V.C.vii.	Reconstitution of thymidine transport activity into hENT1-containing proteoliposomes	150
V.C.viii.	pYhENT1/N48Q complementation of a deficiency in thymidine transport in yeast	150
V.C.ix.	Binding of [ <sup>3</sup> H]NBMPR to hENT1/N48Q-producing yeast	151
V.C.x.	Dissociation and association of [ <sup>3</sup> H]NBMPR from hENT1-producing and hENT1/N48Q-producing yeast	156
V.C.xi.	Inhibition of binding of [ <sup>3</sup> H]NBMPR to hENT1-producing and hENT1/N48Q-producing yeast by dilazep and dipyridamole	153
V.D.	DISCUSSION	154

<b>VI.</b>	<b>Characterization of the native and recombinant human equilibrative NBMPR-insensitive nucleoside transporter protein (hENT2)</b>	<b>186</b>
VI.A.	ABSTRACT	187
VI.B.	INTRODUCTION	189
VI.C.	RESULTS	192
VI.C.i.	Thymidine uptake in HeLa cells	192
VI.C.ii.	pYhENT2 complementation of a thymidine transport deficiency in yeast	193
VI.C.iii	Production of hENT2 mRNA and protein	194
VI.C.iv.	Yeast cells with hENT2 exhibit increased cellular uptake of [ <sup>3</sup> H]thymidine	195
VI.C.v.	Reconstitution of thymidine transport activity into hENT2-containing proteoliposomes	196
VI.C.vi.	Effects of nucleosides and nucleobases on hENT2-dependent thymidine rescue of <i>S. cerevisiae</i> in the complementation assay	196
VI.C.vii	Effect of inhibitors of nucleoside transport on hENT2-dependent thymidine rescue of <i>S. cerevisiae</i> in the complementation assay	197
VI.C.viii.	Assessment of the importance of N-linked glycosylation for hENT2 function by expression of glycosylation-defective mutants in <i>S. cerevisiae</i>	198
V.C.ix.	Development of an approach for determination of topology landmarks in recombinant hENT2 using N-linked scanning mutagenesis	199
VI.D.	DISCUSSION	202
<b>VII.</b>	<b>General Discussion</b>	<b>226</b>
VII.A	The nucleoside transporter proteins of <i>S.cerevisiae</i>	227
V.II.B	Development of <i>S. cerevisiae</i> as a model expression system	229
V.II.C	Functional expression of hENT1 in <i>S. cerevisiae</i>	231
V.II.D	Functional expression of hENT2 in <i>S. cerevisiae</i> and CHO cells	231
V.II.E	Nucleoside transporter proteins as therapeutic targets	232
<b>VIII.</b>	<b>Bibliography</b>	<b>236</b>

## LIST OF TABLES

<b>Table II-1</b>	<b>Yeast strains used in this study</b>	<b>66</b>
<b>Table II-A</b>	<b>Plasmids used in this study</b>	<b>67</b>
<b>Table II-2B</b>	<b>Plasmids used in this study</b>	<b>68</b>
<b>Table II-2C</b>	<b>Plasmids used in this study</b>	<b>70</b>
<b>Table II-3</b>	<b>Antibodies used in this study</b>	<b>71</b>
<b>Table III-1</b>	<b>Sequence comparisons of members of the “uracil/allantoin” transporter family and ENT family</b>	<b>103</b>
<b>Table IV-1</b>	<b>Functional complementation of a thymidine transport deficiency in yeast by recombinant rCNT1myc, ΔN16rCNT1myc, ΔN23rCNT1myc, and ΔN31rCNT1myc</b>	<b>135</b>
<b>Table IV-2</b>	<b>Inhibition of rCNT1myc-, hCNT1myc-, and NUPCmyc-mediated complementation of a thymidine transport deficiency in yeast</b>	<b>136</b>
<b>Table IV-3</b>	<b>Amino acid identity comparison of members of the CNT family</b>	<b>137</b>
<b>Table IV-4</b>	<b>Functional complementation of a thymidine transport deficiency in yeast by recombinant HI0519 and HP1180</b>	<b>138</b>
<b>Table IV-5</b>	<b>Inhibition of HI0519-mediated complementation of a thymidine transport deficiency in yeast</b>	<b>139</b>
<b>Table V-1</b>	<b>Effect of nucleoside transport inhibitors on hENT1-mediated complementation</b>	<b>184</b>
<b>Table V-2</b>	<b>Effect of nucleoside transport inhibitors on hENT1-mediated complementation</b>	<b>185</b>

-



## LIST OF FIGURES

Figure I-1	Chemical structures of physiologic nucleosides	28
Figure I-2	Chemical structures of inhibitors of equilibrative nucleoside transport	30
Figure I-3	Phylogenetic analysis of known and putative nucleoside transporter proteins	32
Figure I-4	Predicted topology model of hCNT1	36
Figure I-5	Predicted topology model of hENT1	38
Figure III-1	Disruption of the FUI1 and FUN26 gene loci in yeast.	89
Figure III-2	Cellular resistance to 5-fluorouridine and 5-fluorouracil	91
Figure III-3	Loss of uridine transport activity in <i>fui1</i> -disruption mutants and its reconstitution by introduction and over-expression of a FUI1-containing plasmid	93
Figure III-4	Inhibition of FUI1-mediated uridine transport by nucleosides, nucleobases and related substances: identification of candidate permeants and inhibitors	95
Figure III-5	FUN26-mediated uptake of nucleosides in oocytes of <i>X. laevis</i>	98
Figure III-6	Production and subcellular location of recombinant FUN26myc in yeast membranes	101
Figure IV-1	Functional complementation of a thymidine transport deficiency in yeast harbouring pYΔN31rCNT1 but not pYrCNT1	123
Figure IV-2	Production of ΔN31rCNT1 and rCNT1 mRNA yeast	124
Figure IV-3	rCNT1- and ΔN31rCNT1-mediated uptake of uridine	127
Figure IV-4	Functional complementation of a thymidine transport deficiency in yeast by recombinant hCNT1 and ΔN23hCNT1myc	129
Figure IV-5	Functional complementation of a thymidine transport deficiency in yeast by recombinant NUPCmyc	131
Figure IV-6	Production of recombinant NUPCmyc protein	134
Figure V-1	Functional complementation of a thymidine transport deficiency in yeast by recombinant hENT1	160
Figure V-2	Production of hENT1 mRNA and recombinant protein by yeast	162
Figure V-3	Cellular uptake of [ <sup>3</sup> H]thymidine by yeast producing recombinant hENT1	164
Figure V-4	Equilibrium binding of [ <sup>3</sup> H]NBMPr to yeast producing recombinant hENT1 and membranes containing recombinant hENT1	166
Figure V-5	Demonstration of recombinant hENT1 in yeast membranes by reconstitution of thymidine transport activity	170
Figure V-6	Functional complementation of a thymidine transport deficiency in yeast by recombinant hENT1/N48Q	173
Figure V-7	Equilibrium binding of [ <sup>3</sup> H]NBMPr to yeast producing recombinant pYN48Q	175
Figure V-8	Dissociation of [ <sup>3</sup> H]NBMPr from yeast producing either recombinant hENT1 or hENT1/N48Q	177
Figure V-9	Inhibition by dilazep and dipyridamole of [ <sup>3</sup> H]NBMPr binding to yeast producing either recombinant hENT1 or hENT1/N48Q	179
Figure VI-1	Kinetic analysis of <i>ei</i> -mediate transport of thymidine in HeLa cells	207
Figure VI-2	Inhibition of <i>ei</i> -mediated [ <sup>3</sup> H]uridine and [ <sup>3</sup> H]thymidine uptake in HeLa by dilazep and dipyridamole	209
Figure VI-3	Functional complementation of a thymidine transport deficiency in <i>S. cerevisiae</i> by recombinant hENT2	211
Figure VI-4	Production of hENT2 mRNA and recombinant protein by <i>S. cerevisiae</i> .	213
Figure VI-5	Cellular uptake of [ <sup>3</sup> H]thymidine by <i>S. cerevisiae</i> producing	

	<b>recombinant hENT2</b>	<b>216</b>
<b>Figure VI-6</b>	<b>Demonstration of recombinant hENT2 in <i>S. cerevisiae</i> membranes by reconstitution of thymidine transport activity</b>	<b>218</b>
<b>Figure VI-7</b>	<b>Inhibition of hENT2-mediated complementation of a thymidine transport deficiency in <i>S. cerevisiae</i></b>	<b>220</b>
<b>Figure VI-8</b>	<b>Functional complementation of a thymidine transport deficiency in <i>S. cerevisiae</i> by hENT2 glycosylation-defective mutants</b>	<b>222</b>
<b>Figure VI-9</b>	<b>Determination of two topological landmarks in hENT2</b>	<b>224</b>

## ABBREVIATIONS

<i>cif</i>	concentrative, insensitive to NBMPR, formycinB is a permeant
<i>cit</i>	concentrative, insensitive to NBMPR, thymidine is a permeant
<i>cib</i>	concentrative, insensitive to NBMPR, broadly selective
<i>csg</i>	concentrative, sensitive to NBMPR, guanosine is a permeant
<i>cs</i>	concentrative, sensitive to NBMPR
CHO	Chinese hamster ovary
CMM	complete minimal media
CNT	concentrative nucleoside transporter
CNT1	refers to a pyrimidine-nucleoside preferring CNT
CNT2	refers to a purine-nucleoside preferring CNT
CTB	cell transport buffer
EST	expressed sequence tag
<i>ei</i>	equilibrative and insensitive to inhibition by NBMPR
ENT	equilibrative nucleoside transporter
<i>es</i>	equilibrative and sensitive to inhibition by NBMPR
FUN	function unknown now
GAL	galactose
GCG	genetics computer group
GLU	glucose
h	human
IC <sub>50</sub>	inhibitory concentration at which 50 % of the activity is inhibited
K <sub>d</sub>	dissociation constant
K <sub>i</sub>	apparent inhibitory constant
m	mouse

<b>MBM</b>	<b>modified Barth's medium</b>
<b>MTX</b>	<b>methotrexate</b>
<b>NBMPR</b>	<b>nitrobenzylmercaptapurine ribonucleoside (6-[(4-nitrobenzyl)thio]-9-<math>\beta</math>-D-ribofuranosyl purine)</b>
<b>NBTGR</b>	<b>nitrobenzylthioguanosine; 2-amino-6-[(4-nitrobenzyl)thio]-9-(<math>\beta</math>-D-ribofuranosyl)purine</b>
<b>O.D.</b>	<b>optical density</b>
<b>PNGaseF</b>	<b>peptide-N-glycosidase F</b>
<b>PBS</b>	<b>phosphate buffered saline</b>
<b>pk</b>	<b>pig kidney</b>
<b>r</b>	<b>rat</b>
<b>RPMI</b>	<b>Roswell Park Memorial Institute</b>
<b>SAA</b>	<b>sulfanilamide</b>
<b>XTB</b>	<b>Xenopus transport buffer</b>

-

**I.**  
**Introduction**

..

~

## **I. Nucleoside transport proteins**

### **I.A. General introduction**

Nucleoside transport proteins are integral membrane proteins that mediate the uptake and release of physiological and nucleoside drugs used in anti-cancer and anti-viral therapies (reviewed in (1-4)). The permeation of most nucleosides across plasma membranes occurs in a mediated fashion because they are generally highly hydrophilic compounds that do not readily diffuse across lipid bilayers. Nucleosides play an important role in a host of physiologic processes (2-4). The purine nucleoside adenosine influences cardiac and vascular physiology, acts as an anti-inflammatory compound, and neuromodulator (3). Additionally, the salvage of nucleosides is required for the synthesis of nucleic acids in human cells that lack purine biosynthetic pathways, such as enterocytes and bone marrow cells (3,4). The physiologic purine nucleosides adenosine and guanosine and the pyrimidine nucleosides thymidine and uridine have most commonly been used in radioisotope tracer assays to measure nucleoside transport (2); their chemical structures are presented in Figure I-1. Uridine is a substrate of all the mammalian nucleoside transport proteins studied to date (2,4). The physiologic relevance of the apparent universal transportability of uridine remains unclear and perhaps underscores an unknown cellular role of uridine. Once believed to be a universal substrate of nucleoside transport proteins (4), adenosine now appears to have a dual role, acting in some instances as a high-affinity, high-capacity permeant, and in other cases acting as a high-affinity, low capacity (perhaps inhibitory) permeant (2). A number of nucleoside-analog drugs possess both antineoplastic and antiviral activity (reviewed in (1-6)). As is the case with physiologic nucleosides, nucleoside-analog drugs are generally hydrophilic and require mediated transport to cross plasma membranes (via nucleoside transport proteins) to exert cytotoxic effects at intracellular targets (2). There is increasing evidence to suggest that nucleoside transport

proteins of intracellular (organellar) membranes may also play a role in the transport of physiologic nucleosides and nucleoside-analog drugs (7-9).

Seven distinct nucleoside transport processes have been demonstrated in mammalian cells on the basis of substrate specificities, inhibition by diagnostic agents, and mechanisms of transport (1,2,4,5). Historically, the nucleoside transport processes of mammalian cells have been designated by trivial and numerical nomenclatures on the basis of these functional differences (3,4,10,11). A summary of the naming systems for the various human nucleoside transport activities and, where known, the corresponding proteins is presented in Table I-1A,B. The mammalian nucleoside transporters comprise two functionally distinct groups. The equilibrative nucleoside transporters (ENTs) are bidirectional, broadly selective transporters that catalyze the facilitated diffusion of nucleosides down their concentration gradients. The mammalian ENTs have been subdivided on the basis of their sensitivity to nanomolar concentrations of nitrobenzylmercaptapurine ribonucleoside (NBMPR; 6-[(4-nitrobenzyl)thio]-9- $\beta$ -D-ribofuranosyl purine) into *es* (equilibrative-sensitive) and *ei* (equilibrative-insensitive) transporters. The chemical structures of inhibitors of equilibrative nucleoside transporters are presented in Figure I-2. The concentrative nucleoside transporters (CNTs) are Na<sup>+</sup>-dependent symporters that move nucleosides into cells against their concentration gradients and have been given acronyms based on their functional characteristics (*cit*, *cif*, *cib*, *csg*, *cs*) as well as numerical designations (N1-N6) based on the order of discovery. The *cit* (N2, N4), *cif* (N1) and *cib* (N3) transport processes are insensitive to NBMPR and prefer, respectively, either pyrimidine nucleosides, purine nucleosides or both. The *cit* transport process has two subtypes that are distinguished by preferences for either pyrimidine nucleosides alone (N2) or pyrimidine nucleosides and guanosine (N4). The *csg* and *cs* transport processes have been described as NBMPR-sensitive transport processes with broad permeant selectivities.

Since 1994, the proteins responsible for the majority of nucleoside transport processes of mammalian cells have been identified by molecular cloning and functional expression of cDNAs in either oocytes of *Xenopus laevis* (12-20) or cultured cells (21). The mammalian nucleoside transporters identified thus far comprise two structurally unrelated protein families that are known as the CNT and ENT proteins (1-4,6). cDNAs encoding representatives of the two major CNT subfamilies (CNT1, pyrimidine-nucleoside selective; CNT2, purine-nucleoside selective) have been cloned from human, rat, pig and mouse tissues (12,13,15,16,20,22,23). cDNAs encoding representatives of the two ENT subfamilies (ENT1, NBMPR-sensitive; ENT2, NBMPR-insensitive) have been cloned from human and rat tissues (16,18,19,21). The mammalian protein subfamilies identified thus far by molecular cloning and their transport processes are listed in Table I-1A,B.

There has been a rapid increase in the speed of identification of nucleoside transporter cDNAs since the isolation of the first cDNAs encoding representative members of the CNT and ENT families (12,18). Cloning strategies based on sequence similarities and functional screening have identified in excess of 20 nucleoside transporter cDNAs from eukaryotes and prokaryotes. Additionally, homology searches of sequence databases using predicted nucleoside transport protein and/or cDNA sequences have identified a number of structurally related proteins that are candidate nucleoside transporters. It is now apparent that the variability in the properties of the ENTs and CNTs among different cells and species has expanded beyond the scope of their historical trivial and numerical designations. The nucleoside transporter proteins are categorized on the basis of their structural similarity to either CNTs or ENTs, and their molecular and functional properties should be considered individually. A phylogenetic tree of known and putative nucleoside transporter proteins is presented in Figure I-3. The characteristics of the proteins that are known to function as nucleoside transporters are presented in Tables I-2, I-3 and I-4 (mammalian CNTs), Tables I-5 and I-6 (mammalian ENTs) and Tables I-7 and I-8 (bacterial, parasitic and yeast nucleoside transporters).



## **I.B. Mammalian concentrative nucleoside transporters**

### **I.B.i Pyrimidine nucleoside selective CNTs**

#### **I.B.i.a rCNT1**

A marked stimulation of Na<sup>+</sup>-dependent uridine transport was noted in oocytes of *X. laevis* that had been injected with rat jejunum poly(A)<sup>+</sup> RNA (24). A cDNA encoding a protein with this activity, rCNT1, was subsequently identified by functional expression screening of a rat intestinal cDNA library in oocytes of *X. laevis* (12). rCNT1 was predicted to encode a protein of 648 amino acids (72 kDa) possessing 8-14 transmembrane spanning domains (12). The current predicted topology model for the mammalian CNTs is based on recent evidence that suggests the presence of 13 transmembrane spanning domains in rCNT1 (6). Northern and RT-PCR analyses have identified rCNT1 mRNA in a variety of rat tissues including small intestine (11,12), liver (25), and brain (26).

Functional expression of rCNT1 cDNA in oocytes of *X. laevis* (12,13,27) and cultured cell lines (28,29) established that the recombinant transporter accepts thymidine, uridine, cytidine and adenosine but not guanosine or inosine as substrates (Table I-2). Although initial studies, which measured the ability of competing nucleosides to inhibit rCNT1-mediated uridine influx, had identified the purine nucleoside adenosine as a potential substrate of rCNT1 because of its potent inhibition (12), direct measure of rCNT1-mediated [<sup>3</sup>H]adenosine influx subsequently established that adenosine is a relatively poor substrate, acting as a high-affinity (low K<sub>m</sub>), low-capacity (low V<sub>max</sub>) substrate (13,29). These observations led to the conclusion that adenosine is likely to be an inhibitor of rCNT1-mediated pyrimidine nucleoside at physiologic concentrations (< 10 μM). rCNT1 has been shown to mediate the uptake of a variety of pyrimidine nucleoside-analog drugs, including 3'-azido-3'-deoxythymidine (zidovudine) and 2',3'-dideoxycytidine (zalcitabine) (13), 1-(arabinofuranosyl)cytosine (cytarabine) (11), 5-

fluoro-2'-deoxyuridine (floxuridine), 5-iodo-2'-deoxyuridine (herplex;stoxil), and 2',2'-difluorodeoxycytidine (gemcitabine) (29).

#### **I.B.i.b hCNT1**

Two hCNT1 cDNAs were isolated from a human kidney cDNA library by hybridization and RT-PCR based on the rCNT1 cDNA sequence (15). The slight differences in the cDNA sequences between the two cDNAs likely represent RT-PCR induced errors and/or genetic polymorphisms. The cDNAs encode proteins that display similar transport properties when expressed in *X. oocytes*; these proteins will be considered hereafter as a single entity. The proposed topology model of hCNT1, which is based on predictive algorithms and the experimental demonstration that hCNT1 is N-linked glycosylated in the C-terminal region of the protein (6), is presented in Figure I-4.

Functional expression of the hCNT1 cDNA in oocytes of *X. laevis* established that the recombinant transporter is a Na<sup>+</sup>/nucleoside symporter that transports pyrimidine nucleosides (e.g., thymidine, uridine, cytidine) (15). Although adenosine was found to inhibit hCNT1-mediated uridine influx ( $K_i = 50 \mu\text{M}$ ), it was a poor substrate of hCNT1 when adenosine uptake was directly compared to uridine uptake (15). As is the case with rCNT1 (13,29), adenosine appears to act as a high-affinity low-capacity permeant of hCNT1. hCNT1 has also been shown to transport the nucleoside analogs 3'-azido-3'-deoxythymidine (zidovudine), 2',3'-dideoxycytidine (zalcitabine) (15), and 2',3'-difluorodeoxycytidine (gemcitabine) (5). See Table I-3 for a comparison of the kinetics of uptake of recombinant rCNT1 and hCNT1. The hCNT1 gene has been localized to 15q25-26 (15) and its structural organization has been determined (GenBank accession number AH0008469).

#### **I.B.i.c pkCNT1**

A cDNA encoding the pig CNT protein was produced from pig renal cortex by RT-PCR based on the rCNT2 cDNA sequence (22). Functional expression of the cDNA in oocytes of *X. laevis* established that the recombinant transporter (designated pkCNT1) is a

nucleoside/Na<sup>+</sup>-symporter that transports pyrimidine nucleosides (Tables I-2 and I-3). pkCNT1 mediates the uptake of uridine with high affinity ( $K_m = 9.3 \mu\text{M}$ ). Uridine uptake can be inhibited by cytidine, uridine, thymidine, and adenosine (22), an inhibition profile that is consistent with that of a pyrimidine nucleoside preferring, CNT1-type transporter.

The nucleoside analogs 5-iodo-2'-deoxyuridine (herplex;stoxil), 5-fluoro-2'-deoxyuridine (floxuridine) and 3'-azido-3'-deoxythymidine (zidovudine), but not 9-[(2-hydroxyethoxy)methyl]-guanine or 1-( $\beta$ -D-arabinofuranosyl)cytosine (cytarabine), were able to inhibit pkCNT1-mediated uridine uptake and thus are either substrates or inhibitors of pkCNT1 (22).

### **I.B.ii Purine nucleoside selective CNTs**

#### **I.B.ii.a rCNT2**

cDNAs encoding the purine nucleoside selective concentrative transporter of rats were isolated from cDNA libraries from intestine (13) and liver (14) by expression screening in oocytes of *X. laevis*. The two cDNAs that were isolated encode functional transporters, designated rCNT2 (13) and rSPNT1 (14), that differ in predicted protein sequence (intestine rCNT1 versus liver rSPNT1, respectively) at amino acid residues 419 (glycine (13) versus alanine (14)) and 522 (valine (13) versus isoleucine (14)). The recombinant intestinal and liver proteins display similar transport properties when expressed in *X. oocytes* and are, therefore, considered to be physiologically equivalent. Functional expression of the rCNT2 and rSPNT1 cDNAs in oocytes of *X. laevis* (13,14) established that these recombinant proteins are nucleoside/Na<sup>+</sup>-symporters that transport purine nucleosides (e.g., adenosine, guanosine, inosine) and the pyrimidine nucleoside uridine (Table I-4).

#### **I.B.ii.b hCNT2**

hCNT2 was identified in human intestine (17) and SPNT1 in human kidney (20) by RT-PCR amplification and functional expression of their cDNAs in oocytes of *X. laevis*. The two independently isolated cDNA sequences were identical except at position 75,

which is arginine in hCNT1 (17) and serine in SPNT1 (20). The hCNT1/SPNT1 gene has been localized to chromosome 15q15 (17) and 15q13-14 (20). Functional expression of the hCNT2 and SPNT1 cDNAs in oocytes of *X. laevis* (17,20) established that the recombinant transporter is a nucleoside/Na<sup>+</sup>-symporter that transports purine nucleosides (e.g., adenosine, guanosine, inosine) and the pyrimidine nucleoside uridine (Table I-4). The nucleoside analogs 3'-azido-3'-deoxythymidine (zidovudine) and 2',3'-dideoxycytidine (zalcitabine) do not appear to be substrates of hCNT2 (17).

#### **I.B.ii.c mCNT2**

mCNT2 was identified in mouse spleen (23) by RT-PCR amplification based on the rCNT2 cDNA sequence and functional expression of the mCNT2 in COS-1 cells. The structural organization of the mCNT2 gene has been determined (GenBank accession number AF079853), and the gene has been localized to chromosome 2e3 within the mouse genome (23). Functional expression of the mCNT2 cDNA in COS-1 cells by transient transfection established that the recombinant protein is a nucleoside/Na<sup>+</sup>-symporter that transports formycin B, a C-nucleoside analog of inosine. mCNT2-mediated formycin B uptake was inhibited by inosine, adenosine and uridine, but not by cytidine or thymidine, characteristic of members of the purine-nucleoside specific (CNT2) family (Table I-2).

#### **I.B.iii. Functional domains of the mammalian CNT proteins**

The availability of cDNAs encoding structurally related nucleoside transport proteins with distinct functional differences has permitted the exploitation of these differences (e.g., substrate specificity) to identify specialized functional domains of the recombinant proteins. Experimental approaches that involve the generation of chimeric recombinant nucleoside transporters from structurally related proteins has permitted the determination of key amino acid residues involved in substrate specificity for the CNTs (28,30,31).

### **I.B.iii.a Amino acids involved in substrate recognition in the CNTs**

Despite transporting different types of nucleosides, hCNT1 (pyrimidine-nucleoside specific) and hCNT2 (purine-nucleoside specific) share a high degree of amino acid identity (66%). This high identity has facilitated identification of amino acid residues involved in substrate recognition in the human CNTs by allowing production of functional chimeric recombinant proteins hCNT1 and hCNT2 (30). A similar approach has been applied to the pyrimidine-nucleoside and purine-nucleoside specific transporters from rat, rCNT1 and rCNT2 (28,31).

The region of hCNT2 responsible for purine nucleoside recognition was identified by introducing portions of hCNT2 into the corresponding regions of hCNT1 and assessing nucleoside transport mediated by the resulting recombinant chimeras when produced in *X. laevis* oocytes (30). The discussion that follows is based on the topology model that predicts 13 transmembrane spanning domains. Initial experiments revealed that a chimera possessing transmembrane spanning domains 1-6 of hCNT2 (residues 1-302) and the last seven predicted transmembrane spanning domains 7-13 of hCNT1 (residues 303-650) displayed pyrimidine-nucleoside specificity (30). This result suggested that the region of hCNT1 responsible for conferring pyrimidine-nucleoside substrate specificity resides within domains 7-13. Generation of a chimera possessing transmembrane spanning domains 1-9 of hCNT2 together with transmembrane spanning domains 10-13 of hCNT1 displayed purine-nucleoside specificity (30). These results suggested that transmembrane spanning domains 7-9 (residues 303 - 387) contain the determinants of substrate specificity. Residues 303-387 of hCNT1 and hCNT2 share a high degree (85 %) of amino acid identity, suggesting that only a few amino acid residues determine the purine nucleoside and pyrimidine nucleoside specific selectivity of hCNT2 and hCNT1, respectively. An hCNT2-type transporter was generated from hCNT1 by mutating the hCNT1 cDNA such that four hCNT1 amino acid residues were converted to hCNT2

residues at the corresponding positions. The hCNT1 to hCNT2 mutations were S319G, Q320M, S353T and L354V (30).

A similar approach was utilized in the determination of the residues involved in substrate recognition for the rat CNT family members. The transport characteristics of rCNT1 and rCNT2 chimeras revealed that transplantation of residues 297 - 358 of rCNT2 into rCNT1 converted rCNT1 into a purine nucleoside-specific (rCNT2-like) transporter. This result suggested that the determinants of purine nucleoside recognition reside within residues 297 - 358 (putative transmembrane spanning domains 7 and 8) of rCNT2 (28). Transplantation of residues 287 - 330 (putative transmembrane spanning domain 7) of rCNT2 into rCNT1 converted rCNT1 into a broadly specific (purine and pyrimidine nucleoside-specific) transporter (28). These results suggested that amino acids residues 297 - 358 of rCNT1 and rCNT2 possess the determinants of nucleoside recognition. Further studies using site-directed mutagenesis went on to show that conversion of serine 318 of rCNT1 to glycine (the rCNT2 counterpart) converted rCNT1 to a purine nucleoside-specific transporter (31).

### **I.C Mammalian equilibrative nucleoside transporters**

#### **I.C.i. NBMPR-sensitive equilibrative nucleoside transporters**

##### **I.C.i.a hENT1**

The hENT1 cDNA was isolated from a human placental cDNA library using the amino acid sequence obtained from N-terminal sequencing of the purified human erythrocyte *es* transporter (18). The native *es* nucleoside transporter protein from human erythrocytes is a heterogeneously glycosylated protein with an apparent molecular mass of 45-65 kDa (32). The hENT1 cDNA encodes a predicted protein of 465 amino acids (52 kDa) possessing 11 transmembrane spanning domains (Table I-5). The proposed topology model of hENT1, which is based on predictive algorithms, is presented in Figure I-5. The predicted hENT1 protein sequence contains consensus sequence motifs for a number of

posttranslational modifications (e.g., N-linked glycosylation, phosphorylation), the functional significance of which is not known.

Northern analyses established that hENT1 mRNA is found in many different normal human tissues (2,18), and several cancer cell lines (33). Expressed sequence tags (ESTs) derived from hENT1 mRNA from many normal and neoplastic human tissues have been identified in genomic data bases. These findings are consistent with the apparently ubiquitous nature of the hENT1 protein. The hENT1 gene is localized to 6p21.1-p21.2 (34) and its structural organization has been determined (GenBank accession number AF190884).

Functional expression of the hENT1 cDNA in oocytes of *X. laevis* established that the recombinant transporter is both purine nucleoside (adenosine, guanosine, inosine) and pyrimidine nucleoside (thymidine, cytidine, uridine) specific. hENT1 has also been shown to transport the nucleoside analogs 2-chloro-2'-deoxyadenosine, 1-( $\beta$ -D-arabinofuranosyl)cytosine (cladribine), 9- $\beta$ -D-arabinofuranosyl-2-fluoroadenine (fludarabine) and 2',3'-difluorodeoxycytidine (gemcitabine) (18). Each of the classical ENT transport inhibitors (NBMPR, dilazep, dipyridamole) were shown to inhibit hENT1-mediated uridine influx into oocytes of *X. laevis* at low (nM) concentrations (18). The kinetic characteristics of the recombinant equilibrative nucleoside transporters are given in Table I-6.

#### **I.C.i.b rENT1**

The rENT1 cDNA was isolated from a rat jejunum cDNA library by RT-PCR based on the hENT1 cDNA sequence (16). Functional expression of the rENT1 cDNA in oocytes of *X. laevis* established that the recombinant transporter has broad permeant selectivity and accepts pyrimidine (thymidine, cytidine, uridine) and purine (guanosine, inosine, adenosine) nucleosides (Table I-5). Recombinant rENT1 was shown to transport

uridine with  $K_m$  and  $V_{max}$  values of, respectively, 0.15 mM and 18 pmol/oocyte min<sup>-1</sup> (Table I-6). rENT1-mediated uridine influx in oocytes was sensitive ( $IC_{50} = 4.6$  nM) to inhibition by NBMPR (16). In contrast to the human ortholog, rENT1 was insensitive to inhibition by the non-nucleoside analog dipyridamole ( $IC_{50} \geq 1$   $\mu$ M). hENT1 mRNA was detected in rat liver and lung tissues (16).

#### **I.C.ii. NBMPR-insensitive equilibrative nucleoside transporters**

##### **I.C.ii.a hENT2**

The hENT2 cDNA was isolated from human placenta by RT-PCR based on its sequence similarity to hENT1 (19). Its identity was established by functional expression in oocytes of *X. laevis* (19). An independent isolate was obtained by functional expression cloning in a nucleoside transport deficient human leukemia cell line (21). The two independently isolated cDNAs encode identical proteins. Functional expression of the hENT2 cDNA in oocytes of *X. laevis* and the nucleoside transport defective leukemia cell line (CEM/araC) established that recombinant hENT2 has broad selectivity for pyrimidine and purine nucleosides and also accepts the nucleobase hypoxanthine as a permeant (Table I-5) (19,21). hENT2 is relatively insensitive to inhibition by NBMPR and dipyridamole since only high concentrations (10  $\mu$ M) were required to inhibit hENT2-mediated uridine influx by, respectively, 60% and 100% (21).

##### **I.C.ii.b rENT2**

The rENT2 cDNA was isolated from a rat jejunum cDNA library by RT-PCR based on the hENT1 sequence (16). Functional expression of the rENT2 cDNA in oocytes of *X. laevis* established that the recombinant transporter is broadly specific for pyrimidine (thymidine, cytidine, uridine) and purine (guanosine, inosine, adenosine) nucleosides (Table I-5). Recombinant rENT2 was shown to transport uridine with  $K_m$  and  $V_{max}$  values of, respectively, 0.3 mM and 140 pmol/oocyte min<sup>-1</sup> (Table I.L-6). rENT2-mediated uridine influx was relatively insensitive ( $IC_{50} > 1$   $\mu$ M) to inhibition by NBMPR.



### **I.C.iii Functional domains of the mammalian ENT proteins**

#### **I.C.iii.a Region of hENT1 responsible for conferring dipyridamole sensitivity**

The *es* transport processes of human and rat cells are both potently inhibited by NBMPR (3,4). In contrast, the human *es* transport process is potently inhibited by dipyridamole whereas the rat *es* transport process is insensitive to inhibition (3,4). Isolation of the cDNAs encoding the transporter proteins responsible for the human and rat *es* processes, hENT1 and rENT1, respectively, identified two distinct proteins that share a high degree of amino acid identity (78%). Characterization of the transport properties of recombinant hENT1 and rENT1 in *X. laevis* oocytes confirmed the intrinsic difference between the two transporters in sensitivity to inhibition by the non-nucleoside inhibitor dipyridamole. Recombinant hENT1 is potently inhibited by dipyridamole ( $IC_{50} \sim 10$  nM) whereas recombinant rENT1 is insensitive to high concentrations of dipyridamole ( $IC_{50} > 1$   $\mu$ M). The region of hENT1 involved in the interaction with dipyridamole was defined by experiments in which positionally analogous portions of the hENT1 and rENT1 were swapped with each other (35). Transport measurements with recombinant chimeric proteins revealed that the chimera possessing the N-terminal half of hENT1 fused to the C-terminal half of rENT1 was inhibited by dipyridamole, whereas the chimera with the reverse configuration was unaffected. Thus, the region of dipyridamole sensitivity appeared to reside in the N-terminal half of hENT1. Subsequently, experiments involving chimeras with smaller transplanted domains established that putative transmembrane domains 3-6 (residues 100-261) of hENT1 carry the determinants of dipyridamole sensitivity. When transmembrane-spanning domains 3-6 of hENT1 were transplanted into rENT1, the majority of mediated [<sup>3</sup>H]uridine uptake (~75%) was inhibited by dipyridamole. Thus, it was concluded that the region of binding of dipyridamole and perhaps also of NBMPR, is contained within residues 100-261, which are believed to form transmembrane domains 3-6 of hENT1.

## **I.D “Orphan” nucleoside transport processes**

Several sodium dependent nucleoside transport activities have been identified in human cells for which the corresponding cDNAs have not been identified. These concentrative transport processes have been difficult to characterize because they coexist with other nucleoside transport processes (e.g., CNT- or ENT-mediated processes), often confounding interpretation of the transport profiles observed.

A transport process in freshly isolated chronic lymphocytic leukemia cells responsible for the uptake of 2-chloro-2'-deoxyadenosine (cladribine), 2-fluoro-9- $\beta$ -D-arabinosyladenosine (fludarabine) and formycin B was identified as concentrative and sensitive (*cs*) to inhibition by NBMPR (36). The substrate specificity of physiologic nucleosides of the *cs* transport process has not been fully characterized.

A concentrative transport activity that is selective for guanosine and sensitive to inhibition by NBMPR (*csg*) has been described in cultured human NB4 acute promyelocytic leukemia cells (10). When transport was measured in the presence of 1  $\mu$ M NBMPR ( $IC_{50} = 0.7 \pm 0.1$  nM) or in sodium-free transport media (10). *csg*-mediated guanosine transport was reduced to 25% of its original activity. Additionally, *csg*-mediated guanosine transport was inhibited to 50% of its original activity when measured in the presence of 1 mM purine or pyrimidine nucleosides (10). The *csg* transport process appears to be distinct from the *cs* transport process - for example, *cgs* does not transport adenosine whereas *cs* does.

A unique sodium-dependent nucleoside transport process (*cib*) has been identified in the human colon cancer (CaCo) cell line (37). The *cib* transport process appears to accept both purine and pyrimidine nucleosides as permeants and is insensitive to inhibition by NBMPR. The low levels of *cib* activity in CaCo cells have hindered detailed characterization.

## **I.E Nucleoside transporters of parasitic protozoans**

Parasitic protozoa of the genera *Trypanosoma*, *Leishmania*, *Toxoplasma* and *Plasmodium* are responsible for such human diseases as sleeping sickness, leishmaniasis and toxoplasmic encephalitis and malaria (38). These parasitic protozoa are unable to synthesize purines *de novo* and therefore must rely on the salvage of purine nucleosides and nucleobases from the host for survival. The salvage of purine nucleosides from host tissue fluids and plasma often requires unique parasitic transporters that are inserted in the plasma membranes of host cells as well as in plasma membranes of parasitic cells (38). The parasitic purine nucleoside transporters are also responsible for the uptake of a number of anti-parasitic drugs.

### **I.E.i LdNT1 and LdNT2**

*Leishmania donovani* possess two transport processes, one responsible for the uptake of guanosine and inosine and the other for the uptake of adenosine and a variety of pyrimidine nucleosides. The proteins responsible for transport of adenosine and pyrimidine nucleosides (LdNT1.1, LdNT1.2) (39) and guanosine and inosine (LdNT2) (40) have recently been identified by molecular cloning.

#### **I.E.i.a LdNT1**

Two cDNAs encoding closely related nucleoside transport proteins (LdNT1.1 and LdNT1.2) were isolated by functional expression of *L. donovani* genomic DNA in a nucleoside transport-defective strain (TUBA5) of *L. donovani* (39). The LdNT1.1 and LdNT1.2 genes are tandemly linked and encode proteins that differ at only six amino acid positions (the LdNT1.1 to LdNT1.2 protein substitutions are P43S, M107I, T160A, A489E, T490R and Y491H). Both proteins mediated the uptake of adenosine and uridine when produced in TUBA5 cells (Table I-7). Additionally, the LdNT1.2 protein was shown to mediate the uptake of adenosine when LdNT1.2 transcripts were microinjected into oocytes of *X. laevis*. Kinetic analysis of transporter-mediated uridine and adenosine uptake in TUBA5 cells into which the LdNT1.1 and LdNT1.2 cDNAs had been introduced

revealed that the two transporters differ in their substrate affinities. LdNT1.1 exhibited  $K_m$  values for adenosine and uridine uptake of 0.17  $\mu\text{M}$  and 5.6  $\mu\text{M}$ , respectively, whereas LdNT1.2 displayed a  $K_m$  for adenosine and uridine uptake of 0.66  $\mu\text{M}$  and 40  $\mu\text{M}$ , respectively (Table I-8).

#### **I.E.i.b LdNT2**

A cDNA encoding the guanosine-inosine transporter protein was isolated in a nucleoside transport-defective strain (FBD5) of *L. donovani* (40). LdNT2 is a single copy gene that produces major and minor mRNA transcripts of 3 Kb and 5 Kb, respectively. Recombinant LdNT2 produced in FBD5 cells was shown to mediate the uptake of inosine and guanosine with  $K_m$  values of 0.3  $\mu\text{M}$  and 1.7  $\mu\text{M}$ , respectively. LdNT2-mediated inosine uptake was inhibited (96%-44%) by some nucleosides and nucleobases (guanosine, 8-aminoguanosine, 6-thioguanosine, formycin B, 4-thiopurinol riboside and allopurinol riboside), partially (12%-35%) by other nucleosides and nucleobases (xanthosine, uridine, thymidine, hypoxanthine, guanine, xanthine) and not at all (< 1%) by others (adenosine, cytidine, thymine, uracil). LdNT2-mediated inosine uptake was unaffected by high concentrations of NBMPR.

#### **I.E.ii TbAT1 and TbNT2**

*Trypanosoma brucei* possesses two transport processes that are involved in salvage of purine nucleosides and/or nucleobases from the host: P1, which is specific for adenosine and inosine, and P2, which is specific for adenosine and adenine. cDNAs encoding the proteins responsible for the P1 and P2 transport processes (TbNT2 and TbAT1, respectively) have been isolated and functionally expressed (41,42). Both proteins are members of the ENT family of proteins (Table I-7).

##### **I.E.ii.a TbAT1**

The TbAT1 cDNA was isolated by functional expression in *S. cerevisiae* from a cDNA library from a bloodstream form of *Trypanosoma brucei* (41). TbAT1 has 25%

identity with hENT1. Expression of TbAT1 cDNA in *S. cerevisiae* was shown to stimulate uptake of adenosine ( $K_m = 2.2 \mu\text{M}$ , Table I-8) that was inhibited by adenine but not by inosine, hypoxanthine, guanosine, uridine or uracil. TbAT1-mediated adenosine uptake was also inhibited by trypanocides including melaminophenyl arsenicals and isometamidium. Expression of the TbAT1 cDNA in *S. cerevisiae* conferred sensitivity of yeast to melarsen oxide (41). Thus TbAT1 exhibits an inhibition profile that is consistent with the limited substrate selectivity and inhibitor sensitivity of the P2 transport process. A variant of the TbAT1 cDNA from a drug-resistant form of *T. brucei* was isolated and found to differ at 10 nucleotide positions that would result in 6 amino acid substitutions (L71V, L380P, A178T, G181E, D239G and N286S), converting TbAT1 to TbAT1'. When expressed in *S. cerevisiae*, LdNT1' was not able to stimulate adenosine uptake nor confer sensitivity to melarsen oxide (41).

#### **I.E.ii.b TbNT2**

The TbNT2 cDNA was isolated by hybridization cloning and RT-PCR using a cDNA library from a blood form of *T. brucei* (42). TbNT2 shares 22% amino acid identity with hENT1. Functional expression of the TbNT2 cDNA in oocytes of *X. laevis* established that the recombinant transporter accepts adenosine ( $K_m = 0.99 \mu\text{M}$ ), inosine ( $K_m = 1.18 \mu\text{M}$ ) and guanosine as permeants (Tables I-7, I-8) (42). LdNT2-mediated adenosine uptake in oocytes was reduced by adenosine, inosine, guanosine, 8-aminoguanosine, 6-thioguanosine, allopurinol riboside, thioribopurinol riboside, 2,4-dinitrophenyl, carbonylcyanide-4-(trifluoromethoxy)phenylhydrazone but not by adenine, guanine, xanthine, uracil, thymidine, uridine, thymidine or allopurinol (42). This inhibition profile is consistent with the P1 transport process and is distinct from that of any of the known mammalian ENT proteins. It is not known if the mammalian ENT inhibitors (dilazep, dipyridamole, NBMPR) have an effect on TbNT2. The observation that 2,4-dinitrophenol and carbonylcyanide-4-(trifluoromethoxy)phenylhydrazone inhibited TbNT2-mediated transport activity in oocytes suggests that TbNT2 may be a proton/nucleoside

symporter (42). Southern analysis of *T. brucei* genomic DNA suggests the presence of a family of LdNT2-related genes that may be clustered together within the genome (42).

### **I.E.iii TgAT**

*Toxoplasma gondii* possess two transport processes that are involved in purine salvage routes: a process that transports adenosine and a process that transports inosine and is inhibited by formycin B and hypoxanthine but not by adenosine, adenine, uridine or thymidine (43). The protein (TgAT) that is responsible for adenosine transport has been identified by molecular cloning (44).

The TgAT cDNA was isolated by a functional screen using insertional mutagenesis of the *T. gondii* genomic DNA (44). TgAT shares 22% amino acid identity with hENT1. Functional expression of the TgAT cDNA in oocytes of *X. laevis* established that the recombinant transporter has moderate affinity for adenosine ( $K_m = 114 \mu\text{M}$ , Table I-8). TgAT-mediated adenosine uptake in oocytes was reduced completely by adenosine, inosine, guanosine, formycin B and allopurinol riboside and partially (50%-80%) by hypoxanthine and guanine, whereas adenine had no effect. TgAT-mediated adenosine uptake was inhibited completely by dipyridamole (1  $\mu\text{M}$ ) and partially (80%) by NBMPR (1  $\mu\text{M}$ ). Mutation of the TgAT gene locus resulted in the elimination of adenosine uptake in *T. gondii* tachyzoites, suggesting that TgAT is the sole adenosine transporter in *T. gondii* (44).

### **I.E.iv PfNT1 and PfENT1**

A nucleoside transporter protein of broad selectivity has recently been independently identified in *Plasmodium falciparum* by two groups using a functional genomics approach (45,46). The cDNAs predict a protein termed PfNT1 by Carter *et al.* (45) and PfENT1 by Parker *et al.* (46). The predicted proteins differ by only a single amino acid at position 385; PfNT1 has a phenylalanine residue (45) whereas PfENT1 has a leucine residue (46). The Plasmodium transporters share approximately 36% and 31% amino acid identity with hENT1 and hENT2, respectively. Functional expression of the

PfNT1 and PfENT1 cDNAs in oocytes of *X. laevis* indicated that the two recombinant transporters differed substantially with respect to their affinities for adenosine, abilities to transport nucleobases and sensitivities to inhibitors of mammalian ENTs (Table 8).

Direct measurements of uptake of radiolabeled permeants established that recombinant PfENT1 transported a variety of nucleosides (uridine, thymidine, cytidine, adenosine, guanosine, inosine), nucleoside analog drugs (zidovudine, zalcitabine, didanosine, fludarabine, cladribine, gemcitabine) and nucleobases (uracil, thymine, cytosine, adenine, guanosine, hypoxanthine) (46). PfENT1 exhibited moderate affinities for adenine ( $K_m$ , 320  $\mu$ M) and hypoxanthine ( $K_m$ , 410  $\mu$ M). In contrast, recombinant PfNT1 evidently lacks the capacity for nucleobase transport since uptake of radiolabeled adenosine was unaffected by a variety of purine and pyrimidine nucleobases (45). PfNT1 exhibited high-affinity adenosine transport ( $K_m$ , 13.2  $\mu$ M) and adenosine uptake was reduced substantially (55%-88%) by a variety of purine and pyrimidine nucleosides (45). The two recombinant transporters differed in the sensitivities to classic inhibitors of mammalian ENTs in that PfENT1-mediated transport activity was unaffected by either dipyrnidamole or NBMPR (46) whereas PfNT1-mediated transport activity was reduced partially (85%) by 10  $\mu$ M dipyrnidamole (45). PfENT1 activity was unaffected by pH (46).

#### **I.F. Nucleoside transporters of yeast**

##### **I.F.i *Candida albicans***

The yeast *Candida albicans* is a commensal organism that is increasingly found to be an opportunistic pathogen in immunocompromised individuals. *C. albicans* possesses both purine nucleoside specific and pyrimidine nucleoside specific transport activities. The precise substrate specificities of the *C. albicans* transporters has been controversial (47-49). However, the recent cloning of a cDNA encoding a purine nucleoside specific *C. albicans* transporter (NUP, nucleoside permease) has permitted the determination of its substrate specificity (Tables I-7 and I-8).

The NUP gene was isolated from a *C. albicans* genomic DNA library by phenotypic complementation of an adenosine transport deficiency in *S. cerevisiae* (50). NUP is a predicted protein that shares limited amino acid identity (20%) with NUPG, a bacterial nucleoside transporter (see section I.H). Functional expression of the NUP gene in *S. cerevisiae* established that the recombinant transporter mediated the uptake of adenosine and guanosine (50). NUP-mediated adenosine uptake in *S. cerevisiae* was reduced by adenosine and guanosine but not by thymidine, uridine or cytidine. NUP-mediated adenosine transport was inhibited completely by dipyrnidamole (200  $\mu$ M) and partially (75%) by NBMPR (20  $\mu$ M) (50).

#### **I.E.ii Saccharomyces cerevisiae**

The uptake of nutrients into the yeast *Saccharomyces cerevisiae* is a critical first step in meeting the cellular requirements for survival under rapidly changing conditions (51). The transport of nutrients into *S. cerevisiae* involves multiple transport systems, often with overlapping or redundant substrate specificities, whose activities are regulated by a variety of external (e.g., environmental supply of nutrients) and internal (e.g., growth state) cues (51). Some of the earliest examples in which transport systems were genetically identified in yeast include those systems that are responsible for the uptake of purines and pyrimidine nucleobases and nucleosides (52,53). The availability of the complete genomic sequencing of *S. cerevisiae* has permitted computer-assisted classification of known and potential transport proteins (54,55). Sequence analysis of several predicted transport proteins identified sequence identities with nucleobase and allantoin transporter, resulting in the formation of a single family of permeases, the "uracil/allantoin" permease family (54,55). One of these (FUI1) has been implicated in transport of uridine by genetic experiments (56). Sequence analysis also identified a reading frame encoding a protein of unknown function (FUN26) and sequence similarity to members of the ENT family (18). Current understanding of nucleobase transport in *S. cerevisiae* is greater than for nucleoside



transport. During the course of the current work considerable progress has been made in obtaining a biochemical understanding of the nucleobase transporters FUR4 and FCY2.

### **I.G Nucleobase transport processes of *S. cerevisiae*.**

The nucleobase transporters of *S. cerevisiae* consist of the uracil permease, FUR4, and the purine-cytosine permease, FCY2. FUR4, which is predicted to have 633 amino acids (71.7 kDa) with 10-12 transmembrane spanning domains and long hydrophilic N- and C-terminal tails (57), mediates the uptake of uracil (58). A *fur4* mutant was found to be strongly resistant to the nucleobase analog 5-fluorouracil and weakly resistant to 5-fluorouridine (53), suggesting that FUR4 transports 5-fluorouracil and, to a lesser extent, its cognate ribonucleoside. Analysis of post-translational modifications of FUR4 indicated that it does not undergo glycosylation or proteolytic processing (59) and does undergo phosphorylation on serine residues after arrival at the plasma membrane (60). FUR4 follows the secretory pathway to the plasma membrane and is subsequently degraded in the vacuole (61); the signal for degradation is ubiquitination of R248 of the FUR4 protein (62). A charged residue in predicted transmembrane-spanning domain 4 (K272) appears to be involved in binding and translocation of uracil (63,64). Spontaneous (63) and site-directed (64) mutations in FUR4 (K272E) resulted in increased  $K_m$  and  $K_d$  values for uracil transport and binding, respectively, suggesting that K272 plays a role in permeant binding and translocation. The level of uracil in the growth medium appears to play a role in regulation of the transporter (65) such that yeast decrease the amount of FUR4 in the plasma membrane during conditions in which uracil is present in abundance (65).

FCY2 mediates transport of adenine, guanine, hypoxanthine and cytosine across the yeast plasma membrane (66). Cytosine uptake displays saturation kinetics (67) with  $K_m$  and  $V_{max}$  values that are dependent on the proton concentration (68). FCY2 is predicted to have 533 amino acids (58 kDa) with 10-12 transmembrane spanning domains and long hydrophilic N- and C-terminal tails. There are consensus sequences for post-translational modifications, including N-linked glycosylation and phosphorylation; FCY2 does not

undergo glycosylation (69) but is phosphorylated on serine residues (70). Cytosine uptake is inhibited by 2,4-dinitrophenol, NaN<sub>3</sub>, and chlorohexidine, suggesting that a membrane ATPase is involved in coupling of FCY2-mediated transport to ATP hydrolysis (67). FCY2 activity is pH dependent (range between pH 2.5 and pH 6.5) (71), with optimum activity at pH 5.0 (72).

#### **I.H Nucleoside transport processes of *S. cerevisiae*.**

Relatively little is known about the nucleoside transport processes of yeast, and the nucleoside transport protein(s) of *S. cerevisiae* have not been unambiguously identified. The open reading frame encoding the FUI1 protein has been suggested to encode a uridine permease (56). The FUI1 locus was originally identified as a mutant with increased resistance to the cytotoxic nucleoside analog 5-fluorouridine (53). The FUI1 gene is present on yeast chromosome 2. FUI1 is a predicted protein of 639 amino acids (72 kDa) with 10 transmembrane-spanning domains. It has a variety of posttranslational modification sites, including eight consensus sites for N-linked glycosylation and three consensus sites for protein kinase A phosphorylation, the functional significance of which is not known. FUI1, a member of the "uracil/allantoin" family, has high amino acid similarity, 70% and 69% respectively, with FUR4 (uracil permease) and DAL4 (allantoin permease). FUI1 is not an essential protein as a *fui1* knockout yeast strain was found to be viable (56). However, the *fui1*-disruption mutant was resistant to the cytotoxic effects of 5-fluorouridine (56), suggesting that FUI1 may be a uridine permease. Although loss of cytotoxicity to 5-fluorouridine is suggestive of a uridine-specific transport process, the same phenotype might be observed if FUI1 played a role in the anabolism of 5-fluorouridine. For example, the uridine kinase URK1 from *S. cerevisiae* was initially identified by loss of cytotoxicity to 5-fluorouridine when the URK1 gene was deleted (73). Direct measure of FUI1-mediated uridine transport is required to establish that FUI1 has uridine transport activity. Although FUI1 shares a high degree of amino acid similarity

with *DAL4*, it does not complement a *dal4*-mutant for growth on allantoin as a sole nitrogen source (56).

Database analysis of the *S. cerevisiae* genome indicated that the protein encoded by the yeast open reading frame YAL022c, termed FUN26 (function unknown now 26), shares limited amino acid identity (18%) with hENT1 and hENT2 (18,19), leading to the suggestion that FUN26 may function as a nucleoside transporter protein (18). FUN26 does not share sequence similarity with other yeast proteins. FUN26 is predicted to have 517 amino acids (58.3 kDa) with 11 transmembrane-spanning domains; FUN26 is not an essential protein since disruption of the gene (YAL022c) was not lethal (74). No phenotype has been associated with elimination of the FUN26 gene.

## **I.I Bacterial nucleoside transporters**

### **I.I.i NUPC and NUPG**

*Escherichia coli* possesses two structurally unrelated nucleoside transport systems *nupC* and *nupG* (75), which are located at 50 and 63.4 minutes, respectively, on the *E. coli* chromosome (76). NUPC is structurally related to members of the CNT family, sharing 27% amino acid identity with rCNT1 and hCNT1, and has been shown to be membrane associated (75), consistent with its proposed role as a nucleoside transport protein. NUPG (76) has limited sequence identity (~ 20%) with the *C. albicans* nucleoside transport protein NUP, see section I.E.1. NUPC and NUPG both transport a broad range of nucleosides and were initially distinguished by the ability of NUPG, but not NUPC, to transport guanosine and deoxyguanosine (75,76). Recombinant NUPC has been produced and functionally characterized in oocytes of *X. laevis* and shown to accept pyrimidine nucleosides (i.e., thymidine, uridine, cytidine, Table I-7) in a proton-dependent fashion (77). NUPC-mediated uridine transport in oocytes was inhibited by adenosine, suggesting that adenosine also interacts with recombinant NUPC (77). Despite the similar permeant selectivities of the NUPC and NUPG proteins, they do not share any sequence similarities. The two transport systems also differ in their genetic regulation; *nupC* is regulated by the

*cytR* gene whereas *nupG* is regulated by both the *cytR* and *deo* genes (78). Both genes are subject to catabolite repression by the cAMP-CRP system (75).

## **I.J Expression systems for analysis of recombinant nucleoside transporters**

Examination of a protein outside of its native cellular context is often advantageous because it allows the protein of interest to be studied "in isolation" of confounding host cell influences. However, the production of recombinant polytopic membrane proteins in heterologous expression systems can be problematic, and frequently only low amounts of recombinant protein are produced. A variety of model expression systems have been utilized with varying degrees of success for membrane proteins; these include oocytes of *X. laevis*, cultured mammalian cells and the yeast *S. cerevisiae*.

### **I.J.i Oocytes of *X. laevis***

Oocytes of *X. laevis* have been used to functionally produce several membrane transport proteins: the human Na<sup>+</sup>-glucose cotransporter, hSGLT-1 (79,80); the mouse anion exchange proteins, AE1 and AE2 (81); the rat organic cation transporter OCT2 (82); the mammalian glucose transporters GLUT4 (83), GLUT1 and GLUT3 (84); the cystic fibrosis transmembrane conductance regulator CFTR (85); and the rat kidney Na<sup>+</sup>/HCO<sub>3</sub><sup>-</sup> cotransporter, rkNBC (86). Oocytes of *X. laevis* have also been used to functionally express cDNAs encoding nucleoside transporters of the CNT and ENT families (12-18,20,27,28,31,87). This approach was used to identify a CNT activity from rat jejunum (24) and subsequently to isolate the first cDNA encoding a mammalian nucleoside transporter, rCNT1 (12). For kinetic characterization of recombinant nucleoside transport proteins, *X. laevis* oocytes are considered the "gold standard" because of their low background (oocytes lack endogenous nucleoside transport activity), large size and high reproducibility. They are well suited for studies of the effects of changes in primary structure (e.g., site-directed mutagenesis, production of chimeras) on function and have been used to identify amino acid residues involved in permeant (30,31,87) and inhibitor

(35) binding. A limitation of the oocyte expression system is low throughput, which limits the quantities of recombinant transporter that can be produced.

#### **I.J.ii Cultured mammalian cells**

Cultured cell lines have been used as model expression systems for functional production of a number of transporter proteins. Among these are: the Na-Ca<sup>+</sup>K exchanger, NCKX1 (88); the rat norepinephrine transporter, rNET (89); the glucose transporter GLUT3 (90); and the anion exchanger protein AE1 (91-93). Transient and stable transfection of cultured mammalian cells have also been used to functionally express cDNAs encoding nucleoside transporter proteins (21,29,94,95), with the first example being the transient transfection of the rCNT1 cDNA into the simian kidney cell line COS-1 (29) in a study of kinetic characteristics of recombinant rCNT1. The substrate specificity of rCNT2 (94) and hCNT2 (96) have been studied in the human cervical carcinoma cell line HeLa by transient transfection of the cDNAs in this human cell line. Additionally, the hENT2 cDNA was cloned by functional expression in a nucleoside transport-defective variant of the human leukemic cell line CEM (21). Stable transfectants that produce functional nucleoside transporter proteins have also been derived: rCNT1 in mouse leukemia L1210 cells (95), hCNT2 and hCNT1 in human leukemic CEM cells (Lang, T., Young, J.D. and Cass, C.E. unpublished results) and hENT1 and hENT2 in cultured pig kidney cells (97). The limitations of these model systems include: (i) the typically low levels of transient (10-30%) and stable (< 0.001%) transfection efficiencies, (ii) the inability to easily produce large amounts of recombinant transporter protein, and (iii) the high cost of maintaining tissue culture materials and facilities.

#### **I.J.iii *S. cerevisiae***

Although the yeast *S. cerevisiae* is a frequently used expression system for cytosolic proteins, only a few membrane transporter proteins have been successfully produced in recombinant form in yeast. These include: the Band 3 anion exchanger protein (AE1) (98), the multidrug resistance proteins *mdr1* and *mdr3* (99) and the cystic fibrosis

transmembrane conductance regulator (CFTR) (100). Yeast have a number of advantages as a model functional expression system: (i) established genetic and molecular methodologies (101), (ii) the ability to rapidly produce large amounts culture at low cost, (iii) the ease of functional analysis of recombinant proteins, and (iv) the availability of the complete genome sequence of *S. cerevisiae*. These features have allowed genome-wide analysis of *S. cerevisiae* genes through (i) characterization of the genome by gene-deletion and parallel analysis (102), (ii) identification of cell cycle-regulated genes (103), and (iii) the examination of the temporal program of gene expression accompanying the metabolic shift from fermentation to respiration (104). No other model expression system exists with such a detailed understanding of the host's physiologic and biochemical processes.

A cloning strategy, based on the absence of thymidine transport activity in yeast and, (ii) pharmacologic blockade of dTMP synthesis to isolate nucleoside transporter cDNAs by functional expression in *S. cerevisiae* has been devised (105,106). Inhibition of *de novo* production of dTMP from dUMP by exposure to methotrexate (MTX) and sulfanilamide (SAA) prevents cell growth (105,106), which can not normally be restored by the addition of thymidine because of the absence of a mechanism for mediated uptake of thymidine (52,53). It was predicted that introduction of a nucleoside transporter cDNA into yeast would complement growth under the selective conditions of MTX and SAA if thymidine was present in the growth medium. Thus, a functional selection strategy was developed to screen cDNA libraries in a yeast expression plasmid for clones capable of complementing cell growth on the basis of their ability to confer the capacity for inward transport of thymidine across the yeast plasma membrane (105,106) in a yeast strain that also has thymidine kinase (by introduction of a thymidine-kinase expressing plasmid). This approach identified two truncated membrane proteins that allowed yeast to import extracellular thymidine and thus grow under the selective conditions imposed (105,106). These proteins (MTP and ND4) are associated with organellar membranes (lysosomes and

mitochondria, respectively) and their recombinant full-length forms exhibit little, if any, nucleoside transport activity when produced in oocytes (105) or yeast (106).

### **I.K Objectives of the study**

It was hypothesized that the yeast *S. cerevisiae* could be developed as a model expression system to produce recombinant nucleoside transporter proteins for investigation of relationships between protein structure and function. The specific objectives of this work were to:

1. Characterize the nucleoside transport processes of *S. cerevisiae*.
2. Develop methods to functionally express nucleoside transport protein cDNAs in *S. cerevisiae*.
3. Examine the interaction of inhibitors of nucleoside transport with hENT1 and a glycosylation-defective mutant (hENT1/N48Q) in *S. cerevisiae*.
4. Functionally express and characterize hENT2 in *S. cerevisiae*.

**Figure I-1 Chemical structures of physiologic nucleosides**

The chemical structures of two purine nucleosides (adenosine, guanosine) and three pyrimidine nucleosides (uridine, cytidine, thymidine) are presented.

- 3 -

1

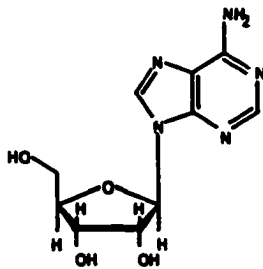
.



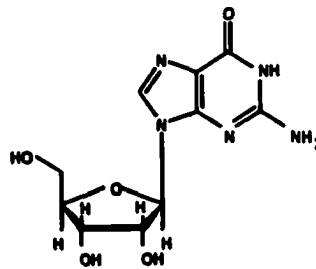
**Figure I-1**

**Chemical structures of physiologic nucleosides**

**Purine nucleosides**

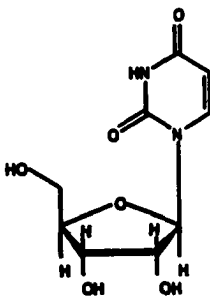


**adenosine**

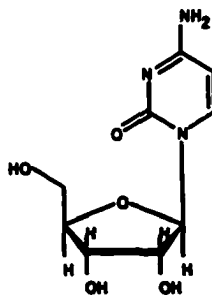


**guanosine**

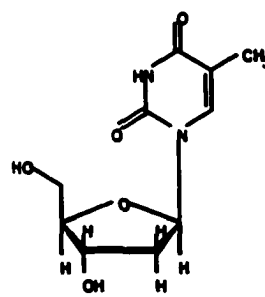
**Pyrimidine nucleosides**



**uridine**



**cytidine**



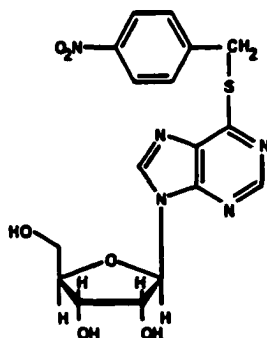
**thymidine**

**Figure I-2 Chemical structures of inhibitors of equilibrative nucleoside transport**

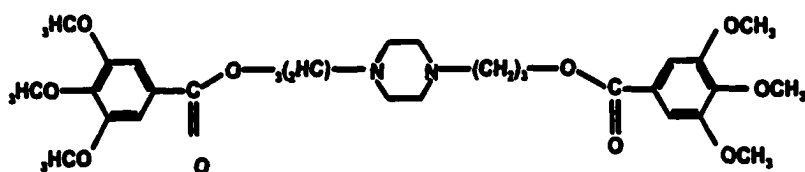
The chemical structures of three equilibrative nucleoside transport inhibitors (NBMPR; 6-[(4-nitrobenzyl)thio]-9- $\beta$ -D-ribofuranosyl purine, dilazep, dipyridamole) are presented.

**Figure I-2**

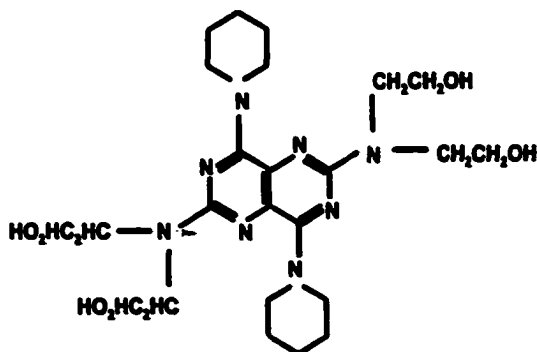
**Chemical structures of inhibitors of  
equilibrative nucleoside transport**



**NBMPR**



**dilazep**



**dipyridamole**

**Figure I -3 Phylogenetic analysis of known and putative nucleoside transporter proteins**

A phylogenetic tree of known and putative nucleoside transporter proteins was constructed using "Pileup" and "Growtree" software from GCG (Genetics Computer Group, Madison, WI, U.S.A.). In the list that follows, the proteins for which there is experimental evidence of either direct (i.e., flux analysis) or indirect nature (i.e., loss of uptake by genetic deletion) are in bold type. GenBank accession numbers are underlined.

**Panel A: *the CNT family*: rCNT1, U10279; hCNT1, U62967; pkCNT1, AF009673; rCNT1, U25055; mCNT2, AF079853; hCNT2, AF036109; hfCNT, AF132298; F27E11.1, AF016413; F27E11.2, AF016413; HI0519, U32734; HP1180, AE000623; yeiM, AE000305; yeiJ, AE000305; nupC (*E. coli*), X74825; yxjA, Z99124.1; nupC (*B. subtilis*), X82174; yutK, Z99120. Panel B: *the ENT family*: LdNT1.2, AF041473; LdNT1.1, AF065311.1; TbAT1, AF152369.1; TbAT1', AF152370.1; LdNT2, AF245276; TbNT2, AF153409.1; TgAT, AF061580; PfENT1, AAF221844; PfNT1, AF221122; F36H2.2, Z81078; FUN26, AAC04935.1; ZK809.4, Z68303.1; K09A9.3, Z79601.1; F16H11.3, U55376.1; K02E11.1, Z77665.1; mENT2, AF257190; rENT2, AF015305; hENT2, AF034102; hENT1, AF190884; rENT1, AF015304, mENT1.1, AF257188; mENT1.2, AF257189. Panel C: *the uracil/allantoin permease family*: THI10, U19027; YOR071c, Z74979; YOR192c, Z75100; DAL4, Z38061; FUR4, Z35890; FUI1, Z35803.**

Not shown are two nucleoside transporters that are not members of known nucleoside transporter families. NUP, AF016246; nupG, X06174; tpt1, L11576.

**Figure I-3 A**

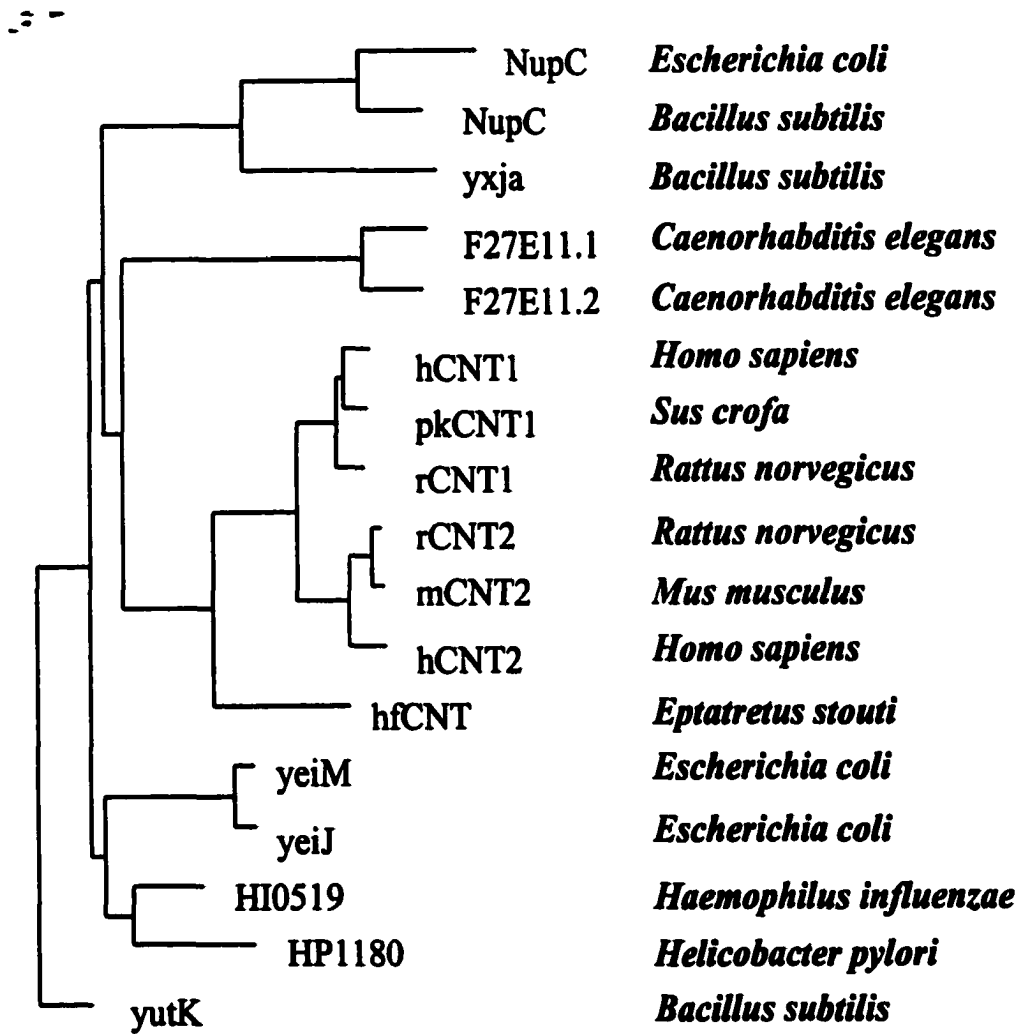


**Figure I-3 B**

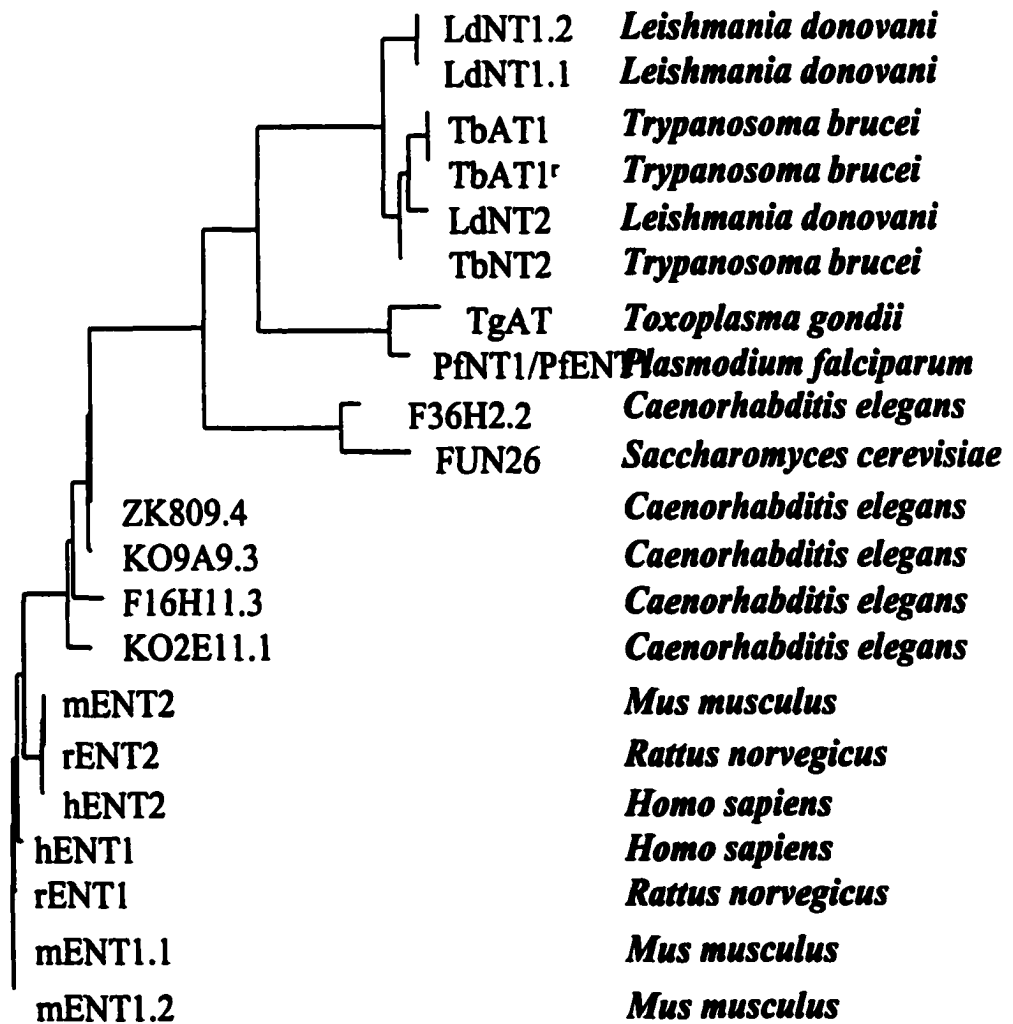
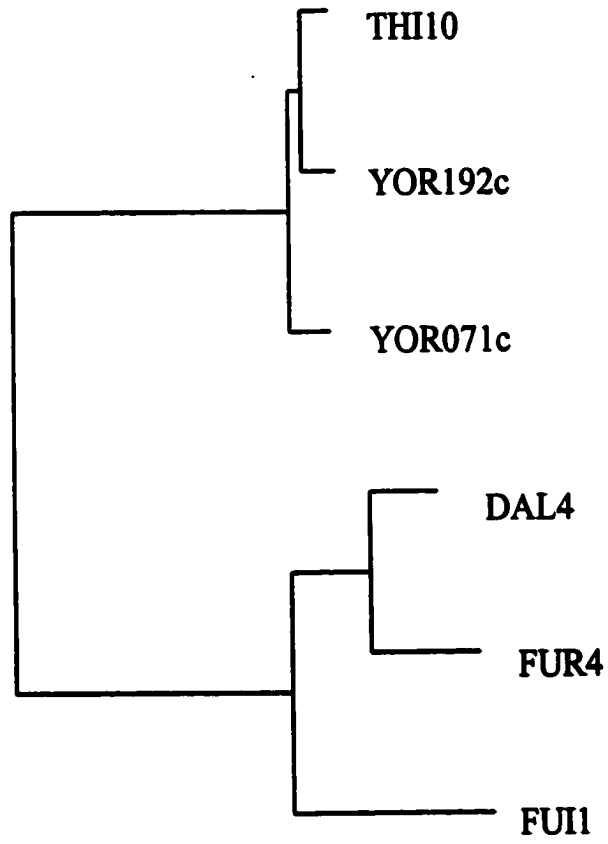


**Figure I-3 C**



## **NOTE TO USERS**

**Page(s) missing in number only; text follows. Page(s) were microfilmed as received.**

**35**

**This reproduction is the best copy available.**

**UMI**



**Figure I-4 Predicted topology model of hCNT1**

The current topology model of hCNT1 is based on the prediction of 13 transmembrane spanning domains (6). Individual amino acid residues are indicated by the circled single-letter abbreviations and the predicted N-linked glycosylation consensus sites are indicated by (\*). The substrate binding domain identified by Loewen *et al.*(30) is also indicated.

**Figure I-4**

## Predicted topology model of hCNT1

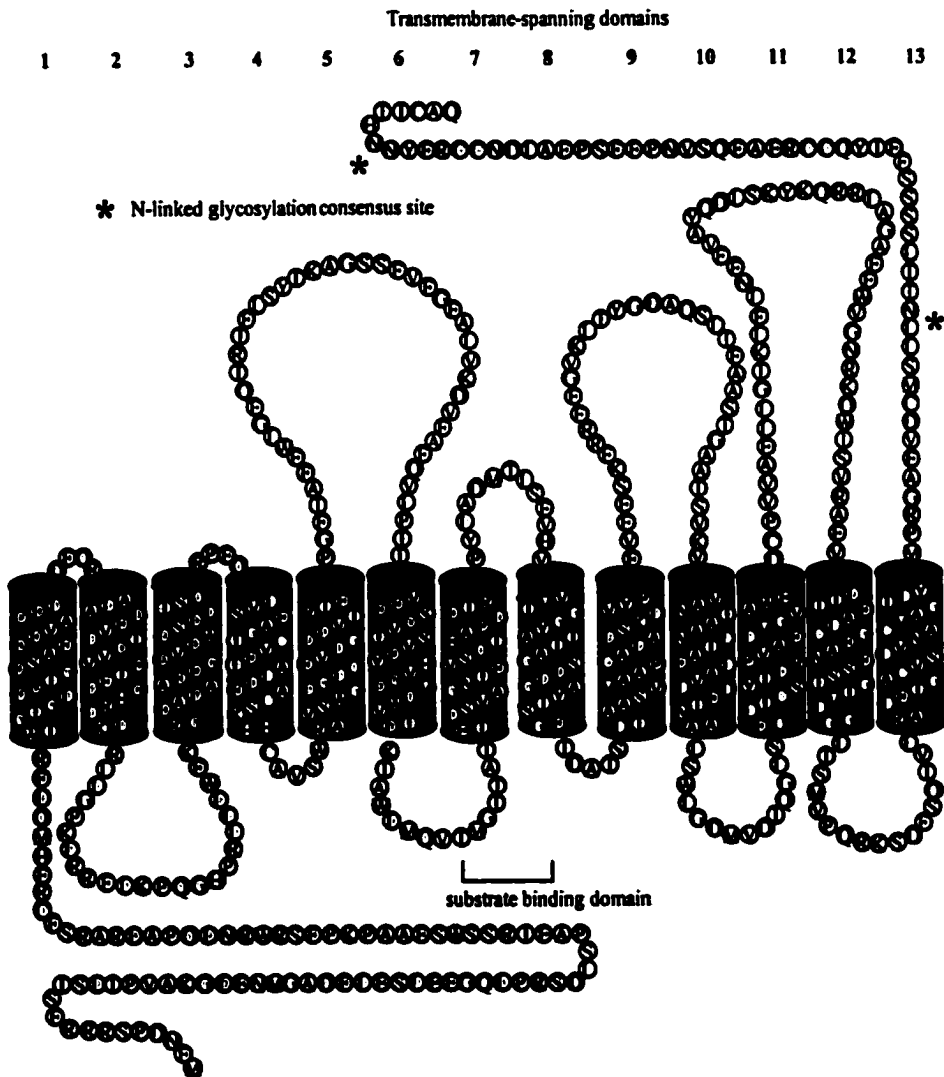


### **Figure I-5 Predicted topology model of hENT1**

The current topology model of hENT1 is based on the prediction of 11 transmembrane spanning domains (18). Individual amino acid residues are indicated by the circled single-letter abbreviations and the predicted N-linked glycosylation consensus sites are indicated by (\*). The dipyridamole binding domains identified by Sundarum *et al.*(35) are also indicated.

**Figure I-5**

## Predicted topology model of hENT1

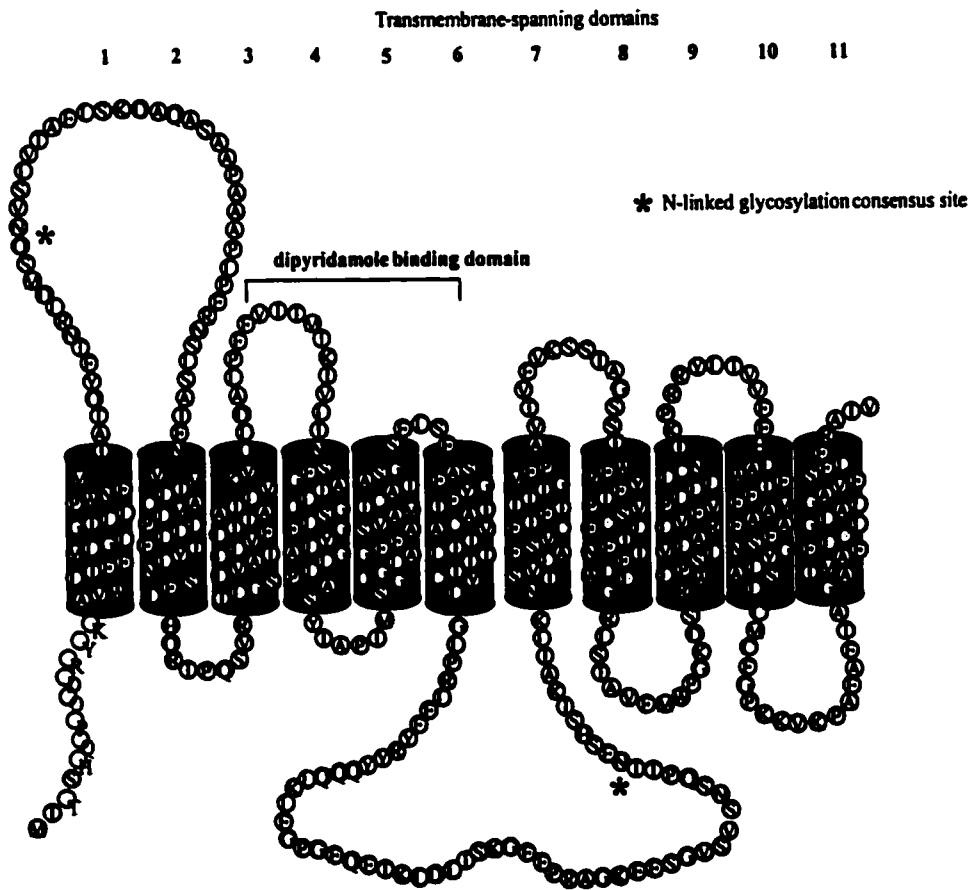


**Table 1-1A Concentrative nucleoside transport processes of human cells**

<b>Trivial name</b>	<b>Numerical designation</b>	<b>Permeant selectivity</b>	<b>Transporter protein</b>	<b>References</b>
<i>cif</i>	N1	purine nucleosides, uridine	hCNT2	(17,20)
<i>cit</i>	N2	pyrimidine nucleosides	hCNT1	(15)
<i>cit</i>	N4	pyrimidine nucleosides, adenosine, guanosine	n.d. <sup>1</sup>	(169,170)
<i>cib</i>	N3	purine and pyrimidine nucleosides	n.d. <sup>1</sup>	(37)
<i>cs</i>	N5	2-chloro-2'-deoxyadenosine 2-fluoro-9-β-D-arabinosyladenosine formycin B	n.d. <sup>1</sup>	(36)
<i>csg</i>	N6	guanosine	n.d. <sup>1</sup>	(10)

<sup>1</sup> not determined

**Table. I-1B Equilibrative nucleoside transport processes of human cells**

<b>Trivial name</b>	<b>Numerical designation</b>	<b>Permeant selectivity</b>	<b>Transporter protein</b>	<b>References</b>
<i>es</i>	n.a. <sup>1</sup>	purine and pyrimidine nucleosides	hENT1	(18)
<i>ei</i>	n.a. <sup>1</sup>	purine and pyrimidine nucleosides	hENT2	(19,21)

<sup>1</sup> not applicable

**Table. I-2 Characteristics of mammalian proteins of the concentrative nucleoside transporter (CNT) family**

<b>Transporter</b>	<b>Number of residues</b>	<b>kDa</b>	<b>TMs<sup>1</sup></b>	<b>Permeant selectivity</b>	<b>Known tissue distribution</b>	<b>References</b>
<i>Rattus norvegicus</i>						
rCNT1	648	71	8-14	pyrimidine nucleosides	jejunum, intestine, kidney	(6,11,12,24-26,28,29)
rCNT2	659	71	14	purine nucleosides, uridine	liver, heart, spleen, jejunum	(13,14,26)
<i>Homo sapiens</i>						
hCNT1	650	71	14	pyrimidine nucleosides	kidney	(15)
hCNT2	658	72	14	purine nucleosides, uridine	kidney, intestine, heart, liver	(17,20)
<i>Sus scrofa</i>						
pkCNT	647	71	14	pyrimidine nucleosides	intestine, kidney	(22)
<i>Mus musculus</i>						
mCNT2	660	72	11	purine nucleosides	spleen	(23)

<sup>1</sup> number of transmembrane spanning domains predicted in the references (cited here) that described the initial isolation and characterization of the cDNA.

**Table. I-3 Kinetic characteristics of recombinant CNT1 proteins**

<b>Transporter</b>	<b>Permeant</b>	<b>K<sub>m</sub><sup>1</sup></b> ( $\mu$ M)	<b>V<sub>max</sub><sup>1</sup></b> (pmol/oocyte/min)	<b>V<sub>max</sub>/K<sub>m</sub></b>	<b>Reference</b>
<b>rCNT1</b>	uridine	37	21	0.57	(13)
	adenosine	26	0.07	0.003	(13)
	3'-azido-3'-deoxythymidine	490	24	0.049	(27)
	2',3'-dideoxycytidine	510	19	0.039	(27)
<b>hCNT1</b>	uridine	45	26	0.58	(15)
	gemcitabine	24	5.8	0.24	(5)
<b>pkCNT1</b>	uridine	8.6	4.9	0.57	(22)

<sup>1</sup> all kinetic data were obtained from studies of the [<sup>3</sup>H]nucleoside influx into oocytes



**Table. I-4 Kinetic characteristics of recombinant CNT2 proteins**

<b>Transporter</b>	<b>Permeant</b>	<b>K<sub>m</sub><sup>1</sup></b> <b>(μM)</b>	<b>V<sub>max</sub><sup>1</sup></b> <b>(pmol/oocyte/min)</b>	<b>V<sub>max</sub>/K<sub>m</sub></b>	<b>Reference</b>
<b>rCNT2</b>	<b>uridine</b>	<b>31</b>	<b>0.86</b>	<b>0.03</b>	<b>(17)</b>
	<b>adenosine</b>	<b>14</b>	<b>0.9</b>	<b>0.06</b>	<b>(17)</b>
	<b>adenosine</b>	<b>6</b>	<b>0.46</b>	<b>0.08</b>	<b>(14)</b>
<b>hCNT2</b>	<b>uridine</b>	<b>40</b>	<b>0.74</b>	<b>0.02</b>	<b>(17)</b>
	<b>adenosine</b>	<b>8</b>	<b>0.49</b>	<b>0.06</b>	<b>(17)</b>
	<b>uridine</b>	<b>80</b>	<b>0.53</b>	<b>0.007</b>	<b>(20)</b>
	<b>inosine</b>	<b>5</b>	<b>0.19</b>	<b>0.04</b>	<b>(20)</b>
	<b>gemcitabine</b>	<b>n.t.<sup>2</sup></b>	<b>n.t.<sup>1</sup></b>	<b>n.t.<sup>2</sup></b>	<b>(5)</b>

<sup>1</sup> all kinetic data were obtained from studies of the [<sup>3</sup>H]nucleoside influx into oocytes

<sup>2</sup> no transport of [<sup>3</sup>H]gemcitabine detected

**Table. I-5 Characteristics of mammalian proteins of the equilibrative nucleoside transporter (ENT)<sup>1</sup> family**

<b>Transporter</b>	<b>Number of residues</b>	<b>kDa</b>	<b>TMs<sup>1</sup></b>	<b>Permeant selectivity</b>	<b>Known tissue distribution</b>	<b>Reference</b>
<i>Homo sapiens</i>						
<b>hENT1</b>	465	52	11	pyrimidine and purine nucleosides	ubiquitous	(2,18,33)
<b>hENT2</b>	465	52	11	pyrimidine and purine, nucleosides, hypoxanthine	heart, kidney, skeletal muscle, thymus, prostate	(19,21)
<i>Rattus norvegicus</i>						
<b>rENT1</b>	475	52	11	pyrimidine and purine nucleosides	jejunum	(16)
<b>rENT2</b>	456	52	11	pyrimidine and purine nucleosides	intestine, brain (hippocampus, cortex, striatum, cerebellum)	(16,171)

<sup>1</sup> number of transmembrane spanning domains predicted in the references (cited here) that described the initial isolation and characterization of the cDNA.

**Table I-6 Kinetic characteristics of recombinant ENT proteins**

<b>Transporter</b>	<b>Permeant</b>	<b>K<sub>m</sub><sup>1</sup></b> <b>(μM)</b>	<b>V<sub>max</sub><sup>1</sup></b> <b>(pmol/oocyte/min)</b>	<b>V<sub>max</sub>/K<sub>m</sub></b>	<b>Inhibition by:</b> <b>NBMPR, dil<sup>2</sup>, dip<sup>3</sup></b> <b>K<sub>i</sub> (nM)</b>	<b>Reference</b>
<b>hENT1</b>	<b>uridine</b>	<b>240</b>	<b>3.6</b>	<b>0.015</b>	<b>2, 57, 134</b>	<b>(18)</b>
	<b>gemcitabine</b>	<b>160</b>	<b>1.5</b>	<b>0.02</b>	<b>n.d.<sup>4</sup></b>	<b>(5)</b>
<b>hENT2</b>	<b>uridine</b>	<b>200</b>	<b>6.4</b>	<b>0.032</b>	<b>n.d.<sup>4</sup></b>	<b>(18)</b>
	<b>gemcitabine</b>	<b>740</b>	<b>43</b>	<b>0.059</b>	<b>n.d.<sup>4</sup></b>	<b>(5)</b>
<b>rENT1</b>	<b>uridine</b>	<b>150</b>	<b>18</b>	<b>0.12</b>	<b>2, 1000, 1000</b>	<b>(16)</b>
<b>rENT2</b>	<b>uridine</b>	<b>300</b>	<b>14</b>	<b>0.05</b>	<b>n.d.<sup>4</sup></b>	<b>(16)</b>

<sup>1</sup> all kinetic data were obtained from studies of [<sup>3</sup>H]nucleoside influx into oocytes

<sup>2</sup> dilazep

<sup>3</sup> dipyridamole

<sup>4</sup> not determined

**Table 1-7 Characteristics of nucleoside transporter proteins of lower organisms**

<b>Transporter</b>	<b>Number of residues</b>	<b>kDa</b>	<b>TMs<sup>1</sup></b>	<b>Permeant selectivity</b>	<b>References</b>
<i>Escherichia coli</i>					
<b>NUPC</b>	<b>400</b>	<b>43</b>	<b>10</b>	<b>pyrimidine nucleosides</b>	<b>(75,77)</b>
<b>NUPG</b>	<b>418</b>	<b>43</b>	<b>10</b>	<b>pyrimidine nucleosides, inosine, guanosine, deoxyguanosine</b>	<b>(76)</b>
<i>Candida albicans</i>					
<b>NUP</b>	<b>407</b>	<b>44</b>	<b>8-12</b>	<b>adenosine, guanosine</b>	<b>(50)</b>
<i>Leishmania donovani</i>					
<b>LdNT1.1/1.2</b>	<b>491</b>	<b>54</b>	<b>11</b>	<b>adenosine</b>	<b>(39)</b>
<i>Trypanosoma brucei</i>					
<b>TbAT1</b>	<b>463</b>	<b>51</b>	<b>10</b>	<b>adenosine, adenine</b>	<b>(41)</b>
<b>TbNT2</b>	<b>464</b>	<b>52</b>	<b>11</b>	<b>adenosine, inosine, guanosine</b>	<b>(42)</b>
<i>Toxoplasma gondii</i>					
<b>TgAT</b>	<b>462</b>	<b>51</b>	<b>11</b>	<b>adenosine</b>	<b>(47)</b>

**Table I-8 Kinetic characteristics of recombinant nucleoside transporter proteins of lower organisms**

<b>Transporter</b>	<b>Permeant</b>	<b><math>K_m^1</math> (<math>\mu</math>M)</b>	<b>Reference</b>
<b>LdNT1.1</b>	<b>uridine</b>	<b>5.6</b>	<b>(39)</b>
	<b>adenosine</b>	<b>0.17</b>	<b>(39)</b>
<b>LdNT1.2</b>	<b>uridine</b>	<b>40</b>	<b>(39)</b>
	<b>adenosine</b>	<b>0.66</b>	<b>(39)</b>
<b>TbAT1</b>	<b>adenosine</b>	<b>2.2</b>	<b>(41)</b>
<b>TbNT2</b>	<b>adenosine</b>	<b>0.99</b>	<b>(42)</b>
	<b>inosine</b>	<b>1.18</b>	<b>(42)</b>
<b>TgAT</b>	<b>adenosine</b>	<b>114</b>	<b>(44)</b>

<sup>1</sup> All kinetic data except for that of TbAT1 were obtained from studies of the [<sup>3</sup>H]nucleoside influx into oocytes. Kinetic data for TbAT1 was established from [<sup>3</sup>H]nucleoside influx into *S. cerevisiae*.

..

## **II.**

### **Materials and methods**

·

### **II.A.i Yeast Strains, media and plasmids**

KY114 (MAT $\alpha$ , gal, ura3-52, trp1, lys2, ade2, his d2000) was the parental yeast strain used throughout these studies (105). PCR-mediated one-step gene-disruption yeast mutants (fui1::TRP, fun26::HIS) were generated from KY114 by the method of Baudin (107). The yeast strains used are presented in Table II-1.

Yeast were maintained at 30°C in complete minimal medium (CMM) containing 0.67% yeast nitrogen base (Difco, Detroit, MI, USA), amino acids as required to maintain auxotrophic selection, and either 2% (w/v) glucose (CMM/GLU) or 2% (w/v) galactose (CMM/GAL). Yeast growth in liquid culture was monitored by measuring the absorbance (optical density) of cultures at 600 nm (OD<sub>600</sub>). Agar plates contained CMM with various supplements and 2% (w/v) agar (Difco). Transformations of the yeast/*Escherichia coli* shuttle vector pYES2 (Invitrogen, Carlsbad, CA, USA) and its derivatives into yeast were performed using a standard lithium acetate method (108).

All plasmids were propagated in the *E. coli* strain TOP10F' (Invitrogen) and maintained in Luria broth with ampicillin (50 µg/ml) at 37°C. Details of plasmid construction are provided below; the plasmids used are listed in Tables II-2 A-C. Plasmid DNA was prepared using an alkaline/lysis method (101,109) or using Qiagen columns (Qiagen, Mississauga, ON) according to manufacturer's instructions. PCR amplifications and cDNA cloning were performed by standard methods (101,109). The fidelity of all cDNA constructs was confirmed by sequencing the cDNA inserts and the regions of the plasmids that included the cloning sites. DNA sequencing was performed by fluorescent-dideoxy cycle sequencing using an automated 310 Genetic Analyzer and Autoassembler software (PE Biosystems, Foster City, CA.).

### **II.A.ii Plasmid construction in Chapter III**

The FUI1 open reading frame was inserted into the yeast expression vector pYES2 to generate pYFUI1 using the primers (restriction sites underlined) 5'FUI1sacI (5'-GCT

**GAG CTC ATG CCG GTA TCT GAT TCT GG-3'**) and **3'FUI1sphI** (**5'-GCA GCA TGC TTA GAT ATA TCG TAT CTT TTC ATA GC-3'**). The FUN26 open reading frame was inserted into pYES2 to generate pYFUN26 using the primers (restriction sites underlined) **5'FUNkpnI** (**5'-GCT GGT ACC ATG AGT ACT AGT GCG GAC ACT G-3'**) and **3'FUNsphI** (**5'- GCA GCA TGC CTA CCT GAT AAT AAA GTC AAT TAT G-3'**).

A version of FUN26 with the c-myc immunoeptope at its C-terminus was engineered to allow detection of the recombinant protein by immunoblotting. pYFUN26myc was generated using the primers (restriction sites underlined) **5'FUNkpnI** and **3'FUNmyc** (**5'-GCA GCA TGC CTA CAA GTC CTC TTC AGA AAT GAG CTT TTG CTC CCT GAT AAT AAA GTC AAT TAT GAA G-3'**).

The FUN26 gene-disruption plasmid pYFUN26-HIS3 was generated by subcloning the blunted-HIS3(BamHI) fragment from pJJ215 into the blunted XhoI/PstI sites of pYFUN26. The FUI1 gene-disruption plasmid was generated by subcloning the blunted TRP1(BglII) fragment from pAS5 (110) into the blunted BglII/AflI sites of pYFUI1. Chromosomal DNA from KY114, prepared as described previously (101), was used as the template for all PCR amplification reactions.

For functionai expression of FUN26 and FUI1 mRNA in oocytes of *Xenopus laevis*, the FUN26 and FUI1 open reading frames were subcloned into the *Xenopus* oocyte expression vector pSP64T (111) immediately down-stream of the *Xenopus*  $\beta$ -globin 5' untranslated region and immediately upstream of the *Xenopus*  $\beta$ -globin 3' untranslated region, generating pGFUN26 and pGFUI1, respectively.

The plasmids first used in Chapter III are listed in Table II-2A.

#### **II.A.iii Plasmid construction in Chapter IV**

Primers complementary to the 5' and 3' ends of hCNT1 (from *H. sapiens*), rCNT1 (from *R. norvinigus*), NUPC (from *E. coli*) and the open reading frames HI0159 (from *H. influenzae*) and HP1180 (from *H. pylori*) were designed for PCR amplification. The



templates for PCR reactions were pQQH1 (12), p11.3 (15), pG3 (77) for rCNT1, hCNT1 and NUPC, respectively. Chromosomal DNA from *H. influenzae* and *H. pylori* were the templates for isolation of HI0519 and HP1180, respectively. Unique *KpnI* and *SphI* restriction sites were introduced into the 5' and 3' primers, respectively, to permit directional cloning into pYES2 (restriction sites are underlined).

For rCNT1 the 5' primers were: 5'-rcnt1 (5'-GCT GGT ACC ATG GCA GAC AAC ACA CAG AGG -3'), 5'-rΔN16 (5'- GCT GGT ACC ATG GCC CAC GGC CTG GAG -3'), 5'-rΔN23 (5'- GCT GGT ACC ATG GGG GCA GAA TTC CTG GAA AG -3'), 5'-rΔN31 (5'-GCT GGT ACC ATG GAG GAA GGC CGA CTC CC -3'); the 3' primer, which introduced the c-myc (EQLISEEDL) epitope, was 3'-rcnt1myc (5' GCA GCA TGC CTA CAA GTC CTG TTC AGA TAT GAG CTT TTG CTC TGT GCA GAC TGT GTG GTT GTA AAA TC-3').

For hCNT1 the 5' primers were: 5'hcnt1 (5'- GCT GGT ACC ATG GAG AAC GAC CCC TCG AGA C-3'), 5'hΔN23 (5'-GCT GGT ACC ATG GGG GCT GAT TTC TTG GAA AGC-3'); the 3' primer, which introduced the c-myc epitope, was 3'hcnt1myc (5'-GCA GCA TGC TCA CAA GTC CTC TTC AGA AAT GAG CTT TTG CTC CTG TGC GCA GAT CGT GTG GTT G-3').

For NUPC the 5' primer was 5'-nupc (5'- GCT GGT ACC ATG GAC CGC GTC CTT CAT TTT G -3') and the 3' primer (introducing the c-myc epitope) was 3'-nupcmyc (5'- GCA GCA TGC TTA CAA GTC CTC TTC AGA AAT GAG CTT TTG CTC CAG CAC CAG TGC TGC CAT TGA CGC -3').

For HI0519 the 5' primer was 5'hi (5'-GCT GGT ACC ATG ATG GTG TTA AGC AGC ATT TTG-3') and the 3' primer was 3'hi (5'-GCA GCA TGC CTA AAG TGC TGC AGC ACC TAA GCC G-3').

For HP1180 the 5' primer was 5'hp (5'-GCT GGT ACC ATG ATT TTT AGC TCT CTT TTT AG-3') and the 3' primer was 3'hp (5'-GCA GCA TGC TCA ATG AGC GTT TAG CCC TAT G-3').

The plasmids generated (primer combinations are in parentheses) were: pYrCNT1-myc (5'*rcnt1*/3'*rcnt1*myc), pYΔN16rCNT1myc (rΔN16/3'*rcnt1*myc), pYΔN23rCNT1myc (5'-rΔN23/3'-cNT1myc), pYΔN31CNT1myc (5'-rΔN31/3'-cNT1myc), pYhCNT1 (5'*hcnt1*/3'*hcnt1*myc), pYΔN23hCNT1myc (5'hΔN23/3'*hcnt1*myc), pYNUPC-myc (5'-*nupc*/3'-*nupc*myc), pYHI0519 (5'*hi*/3'*hi*), and pYHP1180 (5'hp/3'hp).

The plasmids first used in Chapter IV are listed in Table II-2B.

#### II.A.iv Plasmid construction in Chapter V

The hENT1 cDNA was inserted into the pYES2 yeast expression vector under control of the inducible Gal1 promoter. The resulting plasmid (pYhENT1) was produced using the cDNA encoding hENT1 (18) as the template for amplification by PCR and the following 5' *KpnI* and 3' *SphI*-containing primers (restriction sites underlined): 5'-GCT GGT ACC ATG ACA ACC AGT CAC CCT C-3' and 5'-GCA GCA TGC CAC AAT TGC CCG GAA-3'. pYN48Q is a plasmid containing a mutant construct in which Asn-48 of hENT1 had been changed to Gln by site-directed mutagenesis (M. Sundaram, S. Y. M. Yao, E. Chomey, C. E. Cass, S. A. Baldwin and J. D. Young) and was obtained by PCR amplification of the N48Q coding region using 5' *KpnI* and 3' *SphI*.

The plasmids first used in Chapter V are listed in Table II-2B.

#### II.A.v Plasmid construction in Chapter VI

The hENT2 cDNA was inserted into the pYES2 yeast expression vector containing the inducible Gal1 promoter, generating pYhENT2. pYhENT2 was produced using the cDNA encoding hENT2 (19) as the template for PCR amplification and the following primers (restriction sites underlined): 5' *KpnI*, 5'-GCT GGT ACC ATG GCC CGA GGA GAC GC C-3' and 3' *SphI*, 5'-GCA GCA TGC GAG CAG CGC CTT GAA G-3'. The

hENT2 cDNA was cloned immediately downstream, and thus under the control of the GalI promoter. An immunotagged version of hENT2 that carried the c-myc immunopeptide at its C-terminus (pYhENT2myc) was generated using the 5'KpnI primer and the 3'myc primer (5'-GCA TCA TGC TCA CAG ATC CTC TTC TGA GAT GAG TTT TTG TTC GAG CAG CGC CTT GAA GAG G-3').

Site-directed mutagenesis of the hENT2 cDNA was performed using the Altered Sites II *in vitro* Mutagenesis System according to the manufacturer's instructions (Promega, Madison, WI). Conversion of Asn-48 and Asn-57 to Gln residues was performed using the N48/57Q primer (5'-GGC CGG GGC CGG CCA GCG ACA AGC CGG ATC CTG AGC ACC CAG CAC ACG GGT CCC G-3') to generate pYN48/57Q. Conversion of Asn-225 to Gln was performed using the N225Q primer (5'-GCT ACT ACC TGG CCC AGA AAT CAT CCC AGG-3') to generate pYN225Q. Conversion of Asn-48, Asn-57 and Asn-225 to Gln was performed using the N48/57Q and N225Q primers, to generate pYnull. The glycosylation-defective hENT2 mutants were engineered to possess the c-myc epitope at their N-termini to generate pYN48/57Qmyc, pYN225Qmyc and pYnullmyc using standard techniques (101). The cDNAs encoding hENT2 and the hENT2 glycosylation-defective mutants were cloned into the mammalian expression vector pcDNA3 (Invitrogen) to generate pchENT2myc, pcN48/57Qmyc, pcN225Qmyc, and pcnullmyc for use in transient transfection experiments in CHO cells.

The plasmids first used in Chapter VI are listed in Table II-2C.

## **II.B. Phenotypic complementation assay**

The complementation assay used to detect the presence of functional nucleoside transporters was based on the ability of an introduced cDNA to rescue thymidine transport-defective yeast from drug-induced  $\delta$ TMP starvation when cultured in the presence of exogenously supplied thymidine (105,112). In brief, yeast cells grown in CMM/GLU were harvested and transferred to CMM/GAL and, after a growth-period of 8-10 h, were transferred to plates with either CMM/GLU or CMM/GAL that also contained

sulphanilamide (SAA) at 6 mg/ml and methotrexate (MTX) at 50 µg/ml (CMM/GLU/MTX/SAA and CMM/GAL/MTX/SAA, respectively) in the absence or presence of varied concentrations of thymidine. The extreme concentrations of thymidine (0 and 1 mM thymidine) served as negative and positive controls, respectively, in that the absence of thymidine prevented survival whereas its presence at high concentrations permitted survival (by the entry of thymidine into yeast by passive diffusion). Previous studies (105,106) have shown that test concentrations of  $\leq 200$  µM thymidine are suitable to detect introduced cDNAs that encode nucleoside transporter proteins with thymidine transport activity that are inserted into plasma membranes. Plates were incubated at 30°C for 3.5-4.5 days and then assessed for colony formation. In some cases, the plating media were supplemented with test compounds for an assessment of their ability to prevent complementation.

## II.C. Cell culture

Human carcinoma (HeLa) and Chinese hamster ovary cells (CHO), originally obtained by Dr. C. E. Cass from the American Type Culture Collection (Rockville, MD), were maintained in the absence of antibiotics in RPMI (Roswell Park Memorial Institute) 1640 or F12 (HAM's) media (Gibco/BRL Life Technologies), respectively, that was supplemented with 10% calf serum. Stock cultures were incubated at 37°C in a humidified atmosphere of 5% CO<sub>2</sub> and air, and were subcultured every 4-6 days by trypsinization. Cell concentrations were determined by electronic particle counting (Model Z2, Coulter Electronics, Hialeah, FL), and cultures were established at cultured to  $1 \times 10^4$  cells/ml. Stock cultures were normally passaged for  $\leq 30$  generations after which they were discarded and new stock culture were initiated from low-passage, mycoplasma-free, frozen cells stored in liquid nitrogen.

Transient transfection of CHO cells was performed using DOSPER Liposomal Transformation Reagent according to the manufacturer's instructions (Boehringer Mannheim, Laval, PQ). Briefly, actively proliferating cultures were seeded in 100-mm

tissue culture plates ( $2 \times 10^6$  cells/plate) the day prior to transfection and allowed to grow at 37°C for 24 hr. On the day of the transfection, the culture growth media was replaced with fresh growth media and the DOSPER/cDNA mixture (12 µg of cDNA per plate) was added drop-wise to the cells. Transfected cells were incubated for 6 h at 37°C after which the transfection media was replaced with fresh growth media. After an additional 24 h at 37°C, the transfected cultures were trypsinized, pooled and washed by centrifugation at room temperature with PBS. The resulting transfected cells were used for preparation of total membranes by the procedure described in section II.F. Cell culture and transfection were carried out by Mrs. D. Mowles (University of Alberta).

#### **II.D. RNA isolation and Northern analysis**

Total RNA was isolated from proliferating yeast by the hot acid/phenol method (101). RNA (10 µg) was resolved electrophoretically on a denaturing 1.0% (w/v) agarose/formaldehyde gel and transferred by upward capillary transfer (101) to Hybond-N membranes (Amersham, Oakville, ON). <sup>32</sup>P-Probes were prepared by random-priming labeling of a cDNA fragment with the use of a T7 Quick Prime Kit according to the manufacturer's instructions (Pharmacia, Dorval, PQ). Hybond-N membranes were incubated with <sup>32</sup>P-probes in ExpressHyb hybridization solution according to the manufacturer's instructions (Clontech, Palo Alto, CA). The Hybond-N membranes were washed twice at room temperature in 0.2% (w/v) SDS, 2XSSC (2xSSC; 0.3M NaCl, 0.03 M Na<sub>3</sub>-citrate) and twice at 42°C in the same solution, after which the hybridization complexes were detected by autoradiography (101).

#### **II.E. Preparation of yeast membranes**

Yeast cells were grown to an OD<sub>600</sub> of 0.8-1.5. Cells were (i) collected by centrifugation (500 x g, 5 min, room temperature), (ii) washed by centrifugation (500 x g, 5 min, room temperature) three times with yeast breaking buffer (0.2 mM EDTA, 0.2 mM dithiothreitol, 10 mM Tris-HCl, pH 7.5) containing protease inhibitors (Complete Protease Inhibitors; Boehringer Mannheim), and (iii) lysed by vortex-mixing in the presence of glass

beads (425-600  $\mu\text{M}$ ; Sigma, Mississauga, ON) for 15 min at 4°C. Unbroken cells and glass beads were removed from lysates by centrifugation (500 x g, 5 min, 4°C) and membrane fractions were obtained from the resulting lysates by centrifugation (100000 x g, 60 min, 4°C). The membrane preparations were either used immediately or frozen at -80°C.

## **II.F. Preparation of CHO membranes**

Transiently transfected CHO cells were harvested by trypsinization and washed twice in phosphate-buffered saline (PBS: 137 mM NaCl, 5.5 mM KCl, 1 mM  $\text{Na}_2\text{HPO}_4$ , 1 mM  $\text{KH}_2\text{PO}_4$ , pH 7.4). The resulting cell pellets were resuspended in 5 volumes of cell homogenization buffer (1 mM  $\text{ZnCl}_2$ , 10 mM Tris-HCl, pH 7.4, 0.5 mM dithiothreitol, 0.3 mM phenylmethylsulfonyl fluoride) containing protease inhibitors (Complete Protease Inhibitors) and lysed (10 s, 4°C) by polytron homogenization (Brinkmann Instruments, Mississauga, ON). Unbroken cells were removed by centrifugation (850 x g, 10 min, 4°C), and membranes were collected by centrifugation (27200 x g, 30 min, 4°C). Membrane pellets were resuspended in cell homogenization buffer with 9.25% (w/v) sucrose and subjected to centrifugation (27200 x g, 30 min, 4°C). The resulting membrane preparations were resuspended in cell homogenization buffer with 9.25% (w/v) sucrose and either used immediately or frozen at -80°C.

## **II.G. Protein determination**

A variety of methods exist for the determination of protein content of biological samples. Protein concentrations for Chapters III and VI were determined by the Bradford assay using BioRad Reagent (Bio-Rad Technologies, CloneTech, Palo Alto, CA). Protein concentrations for Chapters IV and V were determined using a modified Lowry assay (113).

### **II.G.i. Modified Lowry assay**

Protein concentrations in Chapters IV and V were determined using a modified Lowry assay (113). Briefly, a protein sample was adjusted to a volume of 150  $\mu\text{l}$  to which

was added 500  $\mu$ l Solution C (Solution C, 100 parts Solution A to 1 part Solution B; Solution A, 2% (w/v)  $\text{Na}_2\text{CO}_3$ , 0.4% (w/v) Na-tartrate, 1% (w/v) SDS; Solution B, 4%  $\text{CuSO}_4$ ) and incubated at room temperature for 10 min. To this was added 50  $\mu$ l Solution D (Solution D, Phenol Reagent, 2N Folin-Ciocalteu) mixed 1 to 1 with distilled water, which was allowed to incubated at room temperature for 45 min. The absorbance of the sample was measured at 750 nm and the protein concentration of the sample was determined from a standard curve prepared using bovine serum albumin.

#### **II.G.ii Bradford assay**

Protein concentrations for Chapters III and VI were determined by the Bradford assay using BioRad reagent. Briefly, a protein sample was adjusted to a final volume of 800  $\mu$ l and 200  $\mu$ l BioRad Reagent added and incubated at room temperature for 5 min. The absorbance of the sample was measured at 595 nm and the protein concentration of the sample was inferred from a standard curve prepared using bovine serum albumin.

#### **II.H. Peptide-N-Glycosidase F treatment of proteins from membranes of transfected CHO cells**

Removal of N-linked glycans from glycoproteins within membrane preparations from transiently transfected CHO cells (prepared as described above, II.F) was carried out using peptide-N-glycosidase F (PNGaseF) treatment according to the manufacturer's instructions (Oxford GlycoSciences, Bedford, Ma), with the following modifications. CHO membrane preparations (15  $\mu$ g in cell homogenization buffer, see section II.F.) were incubated in denaturation buffer (20 mM sodium phosphate, pH 7.5, 50 mM EDTA, 0.02% (w/v) sodium azide, 0.5% (w/v) SDS, 5.0% (v/v)  $\beta$ -mercaptoethanol) for 1 h at 37°C. Octylglucoside (6% (w/v)) was then added to the denatured membrane samples in a 5-fold excess over SDS. Buffer (20 mM sodium phosphate, pH 7.5, 50 mM EDTA, 0.02% (w/v) sodium azide) with or without PNGaseF (1 unit) was added to the solubilized membrane samples, which were then incubated at 37°C, 18-24 hr. Protein samples were either used immediately or frozen at -80°C.

## **II.I. Electrophoresis and immunoblotting**

SDS-polyacrylamide gel (12%) electrophoresis was performed (114) with membrane samples that had been solubilized in urea, after which proteins were transferred by semi-dry blotting (400 mA, 1 hr, Tyler Electronics, Edmonton, AB) to polyvinylidene fluoride membranes (Immobilon-P, Millipore, Bedford, MA). The resulting membranes were subjected to the following treatments at 4°C: (i) incubation (5-24 hr) in TTBS (0.2% Tween 20, 0.137 mM NaCl, 20 mM Tris-HCl, pH 7.5) containing 5% (w/v) skim milk powder, (ii) incubation (3-24 hr) in TTBS with primary antibodies and 1% (w/v) skim milk powder (iii) brief incubation with TTBS, (iv) incubation (1-3 hr) with TTBS containing horseradish peroxidase-conjugated anti-rabbit secondary antibodies and 1 % (w/v) skim milk powder, (v) brief incubation with TTBS, and (vi) detection by enhanced chemiluminescence (ECL; Amersham) and autoradiography according to the manufacturer's instructions.

The antibodies and their sources are listed in Table I-3.

## **II.J. Nucleoside uptake**

### **II.J.i. *S. cerevisiae***

The uptake of [<sup>3</sup>H]labeled nucleosides ([methyl-<sup>3</sup>H]thymidine, 84 Ci/mmol; [5-<sup>3</sup>H]uridine, 15 Ci/mmol; Moravek Biochemicals, Brea, CA) by actively proliferating yeast was measured at room temperature by the "oil stop" method as described for cultured cells (112,115), with the following modifications. Yeast were grown to an OD<sub>600</sub> of 0.8-1.5, collected by centrifugation (500 x g, 5 min, room temperature), washed by centrifugation (500 x g, 5 min, room temperature) three times with fresh growth media, and resuspended in fresh growth media to an OD<sub>600</sub> of 2. Uptake was initiated by the rapid addition of media-containing [<sup>3</sup>H]nucleoside to yeast cultures. Triplicate 200-μl portions of the cultures were removed at regular time intervals and uptake reactions were terminated by centrifugation (12000 x g, 2 min, room temperature) through 200 μL of transport oil (a mixture of 75% 550 silicon oil and 15% light paraffin oil; specific gravity, 1.03 g/ml) in



individual microfuge tubes. The layer of media above the transport oil and the transport oil were removed from individual tubes by aspiration and the exposed cell pellets were solubilized with 0.5 ml 5% (v/v) Triton X-100. The solubilized material was transferred to scintillation vials and mixed with 5-ml scintillation fluid (EcoLite, ICN, Costa Mesa, CA) for determination of radioactive content by scintillation counting.

For determination of initial rates of [<sup>3</sup>H]nucleoside uptake (i.e., transport rates), yeast that had been grown and prepared as described above for uptake studies were resuspended in fresh growth media to an OD<sub>600</sub> of 4. Uptake reactions were conducted at room temperature and were initiated by rapid addition of yeast suspensions in growth media (100 μl) to growth media that contained [<sup>3</sup>H]nucleoside at twice the concentration to be tested (100 μl) layered on top of transport oil (200 μl) in a microfuge tube. Uptake reactions were terminated and the radioactive content of resulting yeast pellets were determined as described above for uptake assays.

#### **II.J.ii. HeLa cells**

Transport of [<sup>3</sup>H]nucleosides into HeLa cells was determined at room temperature as described before (116). Briefly, actively proliferating HeLa cells were plated in 60 x 15 mm tissue culture plates (Falcon, Becton Dickinson, Franklin Lake, NJ) at a densities of  $6 \times 10^6 - 10^7$  cells/plate. Following two days of incubation at 37°C, growth media was removed and cells were washed twice in cell transport buffer (CTB; 3 mM K<sub>2</sub>HPO<sub>4</sub>, 5 mM glucose, 130 mM NaCl, 1.8 mM CaCl<sub>2</sub>, 1 mM MgCl<sub>2</sub>, 20 mM Tris-HCl, pH 7.4) prior to use. Uptake reactions were initiated by the addition of CTB that contained [<sup>3</sup>H]nucleoside (1.5 ml/plate) to the cells. Uptake reactions were terminated at timed intervals by aspiration of the [<sup>3</sup>H]nucleoside containing CTB and gentle washing (three times) with ice-cold CTB. The amount of [<sup>3</sup>H]nucleoside associated with cells at "zero time" was determined by incubation of cells in CTB that contained 10<sup>4</sup>-fold excess non-radioactive permeant followed by rapid (1-2 sec) measurement of [<sup>3</sup>H]nucleoside uptake. Cells were solubilized with 1 ml of 5% (v/v) Triton X-100, transferred to scintillation vials and mixed with 5 ml

of EcoLite for the determination of radioactive content of cells by scintillation counting. Inhibition of [<sup>3</sup>H]nucleoside uptake was determined by incubating cultures with graded concentrations of test compounds in CTB 15 min prior to measurement of uptake rates in the presence of the same concentration of test compound. The concentration of test compound that inhibited uptake rates by 50% (IC<sub>50</sub> value) was determined from semilog concentration-effect relationship curves of the transport data using GraphPad PRISM v 2.0 software. The apparent inhibitory constants (K<sub>i</sub> values) were calculated by the method of Cheng and Prusoff (117) from the observed IC<sub>50</sub> values. The transport experiments in HeLa cells were conducted by Mrs. D. Mowles (University of Alberta).

### II.J.iii. *X. laevis* oocytes

*In vitro* synthesized transcripts were prepared from plasmids (SP6 or T7 MEGAscript Kit Ambion, Austin, TX) in water and injected into mature stage IV oocytes of *X. laevis* as described previously (24). A parallel set of oocytes were injected with water alone for determination of basal uptake rates. Injected oocytes were incubated for 3 days at 18°C in modified Barth's medium (MBM: 88 mM NaCl, 1 mM KCl, 0.33 mM Ca(NO<sub>3</sub>)<sub>2</sub>, 0.41 CaCl<sub>2</sub>, 0.82 mM MgSO<sub>4</sub>, 2.4 mM NaHCO<sub>3</sub>, 2.5 mM Na/pyruvate, 0.1 mg/ml penicillin, 0.1 mg/ml gentamycin sulphate, 10 mM HEPES, pH 7.5). MBM was changed daily and oocytes were washed once in *Xenopus* Transport Buffer (XTB, 100 mM NaCl, 2mM KCl, 1 mM CaCl<sub>2</sub>, 1 mM MgCl<sub>2</sub>, 10 mM HEPES, pH 7.5) prior to use in uptake assays.

Uptake of [<sup>3</sup>H]nucleosides by oocytes was measured by conventional tracer techniques (24). Briefly, uptake reactions were initiated by the addition of 0.2 ml [<sup>3</sup>H]nucleoside-containing XTB to 8-12 oocytes. For experiments with NBMPR, dilazep or dipyridamole, oocytes were incubated for 30 min in XTB that contained inhibitor before the addition of XTB that contained [<sup>3</sup>H]nucleoside at the same concentration of inhibitor. Uptake was terminated by aspiration of the [<sup>3</sup>H]nucleoside-containing XTB, followed by six washes with ice-cold XTB. Individual oocytes were transferred to scintillation vials and

solubilized in 0.5 ml 5% (w/v) SDS, after which 5 ml of EcoLite was added to each vial for determination of oocyte-associated [<sup>3</sup>H]nucleoside by scintillation counting. These experiments were performed in collaboration with Dr. S. Yao (University of Alberta) who prepared the oocytes and conducted the transport experiments (with the exception of those transport experiments presented in Chapter IV).

## **II.K. [<sup>3</sup>H]NBMPR binding**

Intact yeast cells or membranes prepared from yeast as described above were assessed for their ability to bind [<sup>3</sup>H]NBMPR by a filtration assay described previously (7,118,119), with the following modifications. Yeast cells with pYhENT1, pYN48Q, or pYES2 were grown in CMM/GAL/MTX/SAA containing 40 μM thymidine (pYhENT1, pYN48Q) or 1 mM thymidine (pYES2) to an OD<sub>600</sub> of 0.8-1.5. Cells were washed by centrifugation (500xg, 5 min, room temperature) three times in binding buffer (100 mM KCl, 1 mM CaCl<sub>2</sub>, 0.1 MgCl<sub>2</sub>, 10 mM TRIS-HCl, pH 7.4) and resuspended in binding buffer to an OD<sub>600</sub> of 2. Duplicate samples (approximately 15 and 20 μg of protein per assay for yeast cells and membranes, respectively) were incubated at 22°C for 40 min with graded concentrations of [<sup>3</sup>H]NBMPR (0.12-24 nM) in binding buffer in the absence or presence of 10 μM dilazep (Sigma). Yeast cells or membranes were collected on Whatman GF/B filters (Whatman, Springfield, Mill, KY) under vacuum and the filters were washed four times with binding buffer. Individual filters were placed in scintillation vials with 10 ml of EcoLite and the radioactivity associated with the filters was measured by scintillation counting. The amount of [<sup>3</sup>H]NBMPR that bound specifically to yeast cells or membranes was calculated from the difference between the amount of [<sup>3</sup>H]NBMPR that bound in the absence of 10 μM dilazep and the amount that bound in its presence. Dilazep has previously been shown to competitively inhibit binding of NBMPR to the *es* transport protein and thus was used for assessment of non-specific NBMPR binding (120,121).

The inhibition of [<sup>3</sup>H]NBMPR binding by dilazep or dipyrindamole was measured by first incubating assay mixtures for 10 min at room temperature with graded

concentrations of dilazep or dipyridamole before the addition of [<sup>3</sup>H]NBMPR. The apparent inhibition constants ( $K_i$  values) were calculated by the method of Cheng and Prusoff from the observed  $IC_{50}$  values (117).

#### **II.L. Kinetics of dissociation and association of [<sup>3</sup>H]NBMPR**

Intact yeast cells with pYhENT1 or pYN48Q (grown in CMM/GAL/MTX/SAA with 40  $\mu$ M thymidine) were incubated with 2.5 nM [<sup>3</sup>H]NBMPR in binding buffer for 40 min at 22°C. The dissociation process was initiated by the introduction of a 10<sup>4</sup>-fold excess of unlabelled NBMPR such that dissociated [<sup>3</sup>H]NBMPR molecules were diluted by unlabelled NBMPR, thereby preventing reassociation of [<sup>3</sup>H]NBMPR. Portions of the assay mixtures were removed at regular intervals and yeast cells were collected on Whatman GF/B filters under vacuum. Individual filters were washed twice with binding buffer and placed in scintillation vials with 10 ml of EcoLite, after which the radioactive content of individual filters was measured by scintillation counting. The association process was assessed by the addition of 2.5 nM [<sup>3</sup>H]NBMPR to yeast cells. Portions of the assay mixtures were removed at regular time intervals and yeast cells were collected on Whatman GF/B filters under vacuum as described for the dissociation process. The dissociation and association rate constants were calculated using a non-linear one-phase exponential dissociation and association equation using GraphPad PRISM software, respectively. Kinetic experiments were performed in collaboration with Dr. R. Mani (University of Alberta).

#### **II.M. Reconstitution of hENT1 and hENT2-mediated thymidine transport into proteoliposomes**

Reconstitution of functional recombinant hENT1 or hENT2 into proteoliposomes was performed by an adaptation of a procedure used previously for the reconstitution of the es transporter from mammalian cells (119,122,123). Membranes prepared from yeast cells with pYhENT1 or pYhENT2 (grown in CMM/GAL/MTX/SAA with 40  $\mu$ M thymidine) were solubilized in binding buffer containing 1.0% (w/v) octylglucoside

(Sigma) and 0.15% (w/v) asolectin for 1 h at 4°C with mixing. Solubilized membranes (200 µg/ml protein) were supplemented with sonicated lipids (Avanti Polar Lipids, Alabaster, AL) consisting of phosphatidylcholine (bovine brain), cholesterol, phosphatidylethanolamine (egg) and phosphatidylserine (bovine brain) at a molar ratio of 33:33:26:8 and a trace amount (10<sup>5</sup> dpm./ml) of [<sup>14</sup>C]cholesteryl oleate (Amersham) to allow quantitation of the lipid content of proteoliposomes. The removal of octylglucoside and formation of proteoliposomes was performed by gel filtration (Sephadex G-50 medium, 1.5-cm x 38-cm column) of the lipid/protein/detergent mixtures at a flow rate of 1 ml/min. Proteoliposomes were collected in the void volume and were either used immediately or frozen in ethanol/solid CO<sub>2</sub> and stored at -80°C.

The uptake of [<sup>3</sup>H]thymidine into proteoliposomes (at 4°C) was initiated by the addition of 100-µl portions of proteoliposome suspension (approximately 5 µg of protein, with or without inhibitors) to 25 µl of binding buffer that contained [<sup>3</sup>H]thymidine. Uptake was terminated by centrifuging the proteoliposome mixture through Sephadex G-50 fine minicolumns (Fisher Scientific 1 ml disposable plastic syringe) equilibrated with a mixture of transport inhibitors (10 mM adenosine, 10 µM dipyrindamole and 10 µM nitrobenzylthioguanosine (NBTGR; nitrobenzylthioguanosine; 2-amino-6-[(4-nitrobenzyl)thio]-9-(β-D-ribofuranosyl)purine)) in binding buffer. The eluate was collected and the <sup>14</sup>C and <sup>3</sup>H contents were determined by scintillation counting. Results were normalized using [<sup>14</sup>C]cholesteryl oleate as an internal standard to quantify the lipid content of proteoliposomes. Mediated uptake of [<sup>3</sup>H]thymidine was calculated from the difference between total uptake and non-mediated uptake, which was measured in the presence of 10 mM adenosine, 10 µM dipyrindamole and 10 µM NBTGR. The sensitivity of [<sup>3</sup>H]thymidine uptake to inhibition by NBMPR was determined by incubating proteoliposomes for 10 min with graded concentrations of NBMPR in binding buffer prior to the initiation of [<sup>3</sup>H]thymidine uptake. Reconstitution experiments with hENT1 and hENT2 were performed in collaboration with Dr. R. Mani (University of Alberta).

## **II.N Sucrose Gradient Centrifugation**

**Yeast membranes prepared as described above (section II.E) were fractionated on a 20% (w/v) to 53% (w/v) continuous sucrose gradient (prepared in yeast breaking buffer) by centrifugation (98,124). Briefly, yeast membranes were layered atop a 10% (w/v) to 53% (w/v) sucrose gradient followed by centrifugation (150 000 x g , 18 h, 4°C). One-ml portions of the gradient were removed and further subjected to centrifugation (60 min, 180 000, 4°C). Pelleted membranes were immediately subjected to electrophoresis and immunoblotting as described in section II.I.**

**Table II-1 Yeast strains used in this study**

<b>Strain</b>	<b>Genotype</b>	<b>Reference</b>
KY114 <sup>1</sup>	MAT $\alpha$ , gal, ura3-52, trp1, lys2, ade2, his d2000	(105)
fui1::TRP	MAT $\alpha$ , gal, ura3-52, trp1, lys2, ade2, his d2000, $\Delta$ fui1::TRP1	this study
fun26::HIS	MAT $\alpha$ , gal, ura3-52, trp1, lys2, ade2, his d2000, $\Delta$ fun26::HIS3	this study

<sup>1</sup> KY114 is auxotrophic for the following nucleobase and amino acids (genetic markers are in parentheses): uracil (ura3-52), tryptophan (trp1), lysine (lys2), and histidine (his d2000). KY114 was a generous gift of Dr. M. Ellison, Department of Biochemistry, University of Alberta.

**Table II-A Plasmids used in this study**

---

<b>Plasmid</b>	<b>Features</b>	<b>Reference and/or origin</b>
<b>Plasmids first used in Chapter III</b>		
pYES2	yeast expression vector	Invitrogen
pYFUI1	FUI1 gene under control of GAL1 promoter in pYES2	this study
pYFUN26	FUN26 gene under control of GAL1 promoter in pYES2	this study
pYFUN26myc	immunotagged (c-myc) FUN26 in pYES2	this study
pAS5	possesses TRP1 selectable marker	Dr. B. Lemire <sup>1</sup> (110)
pJJ215	possesses HIS3 selectable marker	Dr. B. Lemire <sup>1</sup>
pSPG4T	<i>Xenopus laevis</i> expression vector	Dr. J. Young <sup>2</sup> (111)
pGFUN26	FUN26 gene in pSPG4T	this study
pGFUI1	FUI1 gene in pSPG4T	this study

---

<sup>1</sup> a generous gift of Dr. B. Lemire, University of Alberta, Edmonton, AB.

<sup>2</sup> a generous gift of Dr. J. D. Young, University of Alberta, Edmonton, AB.



**Table II-2B Plasmids used in this study**

<b>Plasmid</b>	<b>Features</b>	<b>Reference and/or origin</b>
<b>Plasmids first dused in Chapter IV</b>		
pDH01	thymidine kinase cDNA from <i>H. simplex</i> under control of CUP1 promoter in YEp96	(105,106)
pQQH1 (12)	rCNT1 cDNA in pGEM3	Dr. J. Young <sup>1</sup>
pYrCNT1	rCNT1 in pYES2	this study
pYrCNT1myc	immunotagged (c-myc) rCNT1 in pYES2	this study
pYΔN16rCNT1mycr	CNT1 lacking the N-terminal 16 amino acids in pYES2	this study
pYΔN23rCNT1myc	rCNT1 lacking the N-terminal 23 amino acids in pYES2	this study
pYΔN31rCNT1myc	rCNT1 lacking the N-terminal 31 amino acidss in pYES2	this study
p11.3 (15)	hCNT1 cDNA in pGEM3	Dr. J. Young <sup>1</sup>
pYhCNT1myc	immunotagged (c-myc) hCNT1 in pYES2	this study
pYΔN23hCNT1myc	hCNT1lacking the N-terminal 23 amino acids in pYES2	this study
pG3 (77)	NUPC gene in pGEM3	Dr. J. Young <sup>1</sup>
pYNUPCmyc	immunotagged (c-myc) NUPC in pYES2	this study
<b>Plasmids first used in Chapter V</b>		
pYhENT1	hENT1 cDNA under control of GAL1 promoter in pYES2	this study
pYN48Q	N48Q cDNA under control of GAL1 promoter in pYES2	this study

<sup>1</sup> a generous gift of Dr. J. D. Young, University of Alberta, Edmonton, AB.

..

~

**Table II-2C                      Plasmids used in this study**

<b>Plasmid</b>	<b>Features</b>	<b>Reference and/or origin</b>
<b>Plasmids first used in Chapter VI</b>		
pYhENT2	hENT2 cDNA under control of GAL1 promoter in pYES2	this study
pYhENT2myc	immunotagged (c-myc) of hENT2 in pYES2	this study
pYN48/57Qmyc	immunotagged (c-myc) hENT2myc (N48/57Q)0 in pYES2	this study
pYN225Qmyc	immunotagged (c-myc) hENT2myc (N225Q) in pYES2	this study
pYnullmyc	immunotagged (c-myc) hENT2myc (N48Q, N57Q, N225Q) in pYES2	this study
pcDNA3	mammalian expression vector	Invitrogen
pchENT2myc	immunotagged (c-myc) hENT2 in pcDNA3	this study
pcN48/57Qmyc	immunotagged (c-myc) N48/57Q mutant of hENT2 in pcDNA3	this study
pcN225Qmyc	immunotagged (c-myc) N225Q mutant of hENT2 in pcDNA3	this study
pcnullmyc	immunotagged (c-myc) hENT2myc (N48Q, N57Q, N225Q) in pcDNA3	this study

**Table II-3 Antibodies used in this study**

<b>Antibody</b>	<b>Species</b>	<b>Target</b>	<b>Source</b>
<b>Primary Antibodies</b>			
9E10	mouse	<i>c-myc</i> epitope (EQLISEEDL)	BaBCo
$\alpha$ -PMA1 (125)	rabbit	plasma membrane ATPase (PMA1)	Dr. L. Fliegel <sup>1</sup>
$\alpha$ -PEP12 (126)	rabbit	PEP12 protein (endosomal marker)	Dr. D. Hogue <sup>2</sup>
$\alpha$ -hENT1	rabbit	SKGEEPRAGKEESGVSNS	Dr. S. Baldwin <sup>3</sup>
$\alpha$ -hENT2	rabbit	residues 213 – 290 of hENT2	Dr. C. Cass <sup>4</sup>
<b>Secondary Antibodies</b>			
$\alpha$ -mouse-HRP <sup>5</sup>	goat	mouse IgG	JacksonLabs
$\alpha$ -rabbit-HRP <sup>5</sup>	goat	rabbit IgG	JacksonLabs

1. A generous gift of Dr. L. Fliegel, Department of Biochemistry, University of Alberta, Edmonton, AB.
2. A generous gift of Dr. D. L. Hogue, B.C Cancer Research Center, University of British Columbia, Vancouver, BC.
3. A generous gift of Dr. S. A. Baldwin, School of Biochemistry and Molecular Biology, University of Leeds, Leeds, U.K.
4. Antibodies developed by Mr. M. Cabrita, Department of Biochemistry, University of Alberta, Edmonton, AB, against a fusion polypeptide (unpublished results).
5. horse-radish peroxidase

### **III.**

## **Nucleoside Transport Processes of *Saccharomyces cerevisiae*<sup>1</sup>**

<sup>1</sup>*(A version of this chapter has been reported previously (127))*

### III.A ABSTRACT

The proteins involved in membrane transport of nucleosides in the yeast *Saccharomyces cerevisiae* had not been characterized when this work was initiated. This chapter describes studies of two structurally unrelated membrane proteins with features that suggested their involvement in nucleoside transport processes of yeast: FUI1, an apparent member of the uracil/allantoin family of yeast permeases that was identified genetically as a putative uridine transporter, and FUN26, a predicted protein of unknown function with sequence similarity to members of the equilibrative nucleoside transporter (ENT) family. Disruption of *fui1*, the gene encoding the FUI1 protein, conferred resistance to 5-fluorouridine and eliminated the capacity for inwardly directed transport of extracellular [<sup>3</sup>H]uridine; these characteristics were reversed by over-expression of the FUI1 cDNA in the *fui1*-disruption mutant. In contrast, influx of [<sup>3</sup>H]uridine was unaffected either by disruption of the FUN26 gene (YAL022c) in uridine-transport competent yeast or by over-expression of the FUN26 cDNA in *fui1*-disruption mutants. These results indicated that inwardly directed transport of extracellular uridine into yeast was mediated by FUI1 and not by FUN26. FUI1 exhibited high-affinity transport of uridine ( $K_m$ ,  $22 \pm 3 \mu\text{M}$ ) and the pattern of inhibition by non-radioactive test compounds indicated high selectivity for uridine since only partial, or no, inhibition was observed in the presence of high concentrations ( $\geq 1 \text{ mM}$ ) of (i) thymidine, 2'-deoxyuridine, 2'-deoxy-5-fluorouridine and 2'-deoxy-5-bromouridine, (ii) uracil, 5-fluorouracil, thymine, thiamine and allantoin, or (iii) selected purine nucleobases and nucleosides (i.e., guanosine, adenosine, inosine, cytidine, hypoxanthine, thymine, ribose). Production of recombinant FUN26 in oocytes of *X. laevis* stimulated inward fluxes of [<sup>3</sup>H]uridine, [<sup>3</sup>H]adenosine and [<sup>3</sup>H]cytidine. FUN26-mediated [<sup>3</sup>H]uridine transport in oocytes was independent of pH and insensitive to the classic ENT inhibitors dilazep, dipyrindamole and NBMPR. Recombinant FUN26 tagged with the c-myc immunoeptope also exhibited transport activity in oocytes. When yeast membranes containing recombinant FUN26myc were fractionated by continuous

sucrose gradient centrifugation, immunoblotting of gradient fractions with antibodies against the c-myc epitope indicated that the epitope-tagged protein was present primarily in intracellular membranes. Taken together, these results suggested that nucleoside transport processes in *S. cerevisiae* are mediated by at least two proteins with different functional characteristics. FUI1, a member of the uracil/allantoin family, imports uridine across cell-surface membranes and has high selectivity for uracil-containing ribonucleosides. FUN26, a member of the ENT family, mediates passage of pyrimidine and purine nucleosides across intracellular membranes and has broad permeant selectivity.

### III.B INTRODUCTION

Among the earliest examples of transport systems genetically identified in *S. cerevisiae* were those responsible for the uptake of purine and pyrimidine nucleosides and nucleobases (52,53). While a great deal is now known about the proteins (FUR4, FCY2) responsible for nucleobase transport in *S. cerevisiae*, there is, as yet, little information about the proteins responsible for nucleoside transport. The import of 0.1 mM uridine across the cell surface has been demonstrated in *S. cerevisiae*, however, this transport process has not been kinetically characterized (53).

A nucleoside-specific vacuolar transport process with selectivity for adenosine and guanosine has been identified in *S. cerevisiae* (128). Direct measure of [<sup>14</sup>C]adenosine and [<sup>14</sup>C]guanosine transport into isolated yeast vacuoles defined the kinetics of uptake with  $K_m$  values of 0.15 mM and 0.63 mM, respectively (128). The uptake of adenosine by vacuoles appeared to be dependent on the growth state of the yeast with variations in adenosine uptake rates that suggested a cell-cycle dependence of the transport process. The uptake of 0.6 mM adenosine into vacuoles was inhibited by S-adenosyl-L-methionine (0.25 mM, 100%), S-adenosyl-L-homocysteine (2.5 mM, 20%) and adenine (2.5 mM, 25%) but not inosine (2.5 mM), guanosine (2.5 mM), hypoxanthine (2.5 mM) or AMP (5 mM) (128). S-adenosyl-L-methionine was a competitive inhibitor of adenosine uptake into vacuoles (128). Together, these experiments suggested that yeast vacuoles possess at least two nucleoside transport processes, one preferring adenosine and S-adenosyl-L-methionine and the other preferring guanosine. These data could also be explained by a single nucleoside transporter, since the test concentration of guanosine (2.5 mM) for inhibition of adenosine transport was not much greater than the  $K_m$  value (0.63 mM) for guanosine transport. The molecular identity of the vacuolar transport process(es) has not, as yet, been identified (128).



Database analysis of the *S. cerevisiae* genome indicated that the protein encoded by the yeast open reading frame YAL022c, termed FUN26 (function unknown now 26), shares limited amino acid identity (18%) with hENT1 and hENT2 (18,19), leading to the suggestion that FUN26 may function as a nucleoside transporter protein (18). FUN26, which was identified as a result of the sequencing of chromosome 1 of *S. cerevisiae* (74), does not share sequence similarity with other yeast proteins. It is predicted to have 517 amino acids (58.3 kDa) with 11 transmembrane-spanning domains, a large hydrophilic N-terminal tail (76 amino acids) and two large hydrophilic regions between transmembrane-spanning domains 1 and 2 (19 amino acids) and 6 and 7 (78 amino acids). FUN26 is not an essential protein since disruption of the gene (YAL022c) was not lethal (74).

FUI1 is a yeast protein unrelated to FUN26 that has also recently been suggested to be a putative nucleoside transporter (56). The locus encoding FUI1, which is on chromosome 2, was originally identified from a mutant with increased resistance to the cytotoxic nucleoside analog 5-fluorouridine (53). FUI1 is predicted to be a protein of 639 amino acids (72 kDa) with 10 transmembrane-spanning domains. The resistance to 5-fluorouridine of the *fui1*-disruption mutant led to the suggestion that FUI1 is a uridine transporter (56). Computer-assisted classification placed FUI1 in the "uracil/allantoin" permease family (54,55) since it shares 70% and 69% amino acid similarity with FUR4 (uracil permease) and DAL4 (allantoin permease), respectively. There is, as yet, no direct evidence that FUI1 encodes a membrane transporter with selectivity for uridine and/or uracil.

The work described in this chapter was undertaken to characterize the transport of uridine and other nucleosides in *S. cerevisiae*. The identification of similarities between FUN26 and FUI1 with, respectively, members of the ENT and uracil/allantoin transporter families pointed to FUN26 and FUI1 as candidate nucleoside transporter proteins. Specifically, the aims of the work described in this chapter were to determine if FUI1 or

FUN26 encode proteins with nucleoside transport activity and, if so, to characterize their transport characteristics.

The involvement of FUN26 and FUI1 in the import of extracellular uridine was assessed by analysis of the effects of disruption of the FUN26 and FUI1 genes (YAL022c, *fui1*) by insertional mutagenesis and reintroduction of the intact coding sequences in the pYES2 yeast expression vector. Toxicities of 5-fluorouridine and 5-fluorouracil were examined in plating studies because these drugs were used in the isolation of the *fui1* mutant that led to the suggestion that FUI1 is a uridine transporter. Uptake of extracellular [<sup>3</sup>H]uridine alone and in the presence of high concentrations ( $\geq 1$  mM) of a variety of nucleosides and nucleobases was examined to assess the role of the recombinant proteins in the transport of uridine across yeast plasma membranes. FUI1 exhibited high affinity and selectivity for uridine and was shown to be the protein primarily responsible for inwardly directed transport of uridine into *S. cerevisiae*. Expression of the FUN26 cDNA failed to confer uridine transport capability on yeast with the YAL022c/*fui1* gene disruptions. It was also tested in oocytes of *X. laevis*, because of the proven effectiveness of the latter system in the identification of nucleoside transporter proteins (12-16,18,19). The inability to detect native or recombinant FUN26-mediated uridine uptake activity in yeast suggested that FUN26 may not reside at the yeast cell surface. To determine if FUN26 localizes to internal membranes, the protein was tagged with the c-myc immunopeptide and yeast membrane fractions were prepared by continuous sucrose gradient centrifugation and analyzed for the presence of recombinant FUN26myc by immunoblotting.

### **III.C RESULTS**

#### **III.C.i Sequence comparison of putative nucleoside transport proteins from *S. cerevisiae***

FUI1, which was identified genetically as a uridine transporter (53,56), has high amino acid sequence identity with members of the "uracil/allantoin" permease family of *S. cerevisiae* (54,55). A sequence comparison of members of the uracil/allantoin permease family is presented in Table III-1A. The high degree of sequence identity with DAL4 (allantoin permease, 56%), FUR4 (uracil permease, 55%), THI10 (thiamine permease, 29%) and two open reading frames that encode putative thiamine permeases suggested a functional relationship between FUI1 and the uracil/allantoin permeases.

FUN26, the protein of unknown function predicted from the YAL022c open reading frame, has 15-18% amino acid sequence identity with the human and rat members of the ENT family. A sequence comparison of selected members of the ENT family is presented in Table III-1B. This limited sequence identity, which was first noted when the hENT1 cDNA was cloned (18), raised the possibility that FUN26 encodes a transporter of *S. cerevisiae* with selectivity for nucleosides and/or related compounds.

#### **III.C.ii Disruption of the FUI1 and FUN26 genes**

The gene loci for FUI1 and FUN26 were disrupted by insertional mutagenesis to allow determination of their functional characteristics independently of each other, taking advantage of the TRP1/HIS3<sup>-</sup> phenotype of the KY114 yeast strain (Figure III-1). The TRP1 sequence, which encodes phosphoribosyl-anthranilate isomerase [EC 5.3.1.24], was inserted within the FUI1 coding sequence, the resulting *fui1::TRP1* disruption fragment was introduced into KY114, and mutant yeast were selected in media that lacked tryptophan. Similarly, the HIS3 sequence, which encodes imidazoleglycerolphosphate dehydratase [EC 4.2.1.19], was inserted within the FUN26 coding sequence, the resulting *fun26::HIS3* disruption fragment was introduced into KY114, and mutant yeast were

selected in media that lacked histidine. The FUI1 and FUN26 gene disruption strategies are illustrated in Figures III-1A and III-1B, respectively. PCR analysis of yeast chromosomal DNA prepared from either the parental strain or the TRP1<sup>+</sup> and HIS3<sup>+</sup> transformants confirmed disruption of the FUI1 and FUN26 loci, respectively (Figure III-3C).

### **III.C.iii Cellular resistance to 5-fluorouridine and 5-fluorouracil by yeast with FUI1 and FUN26 gene disruptions**

Yeast are sensitive to both 5-fluorouridine and 5-fluorouracil cytotoxicity (53) and disruption of a gene encoding a cell-surface transport protein that mediates uptake of either of these drugs would be expected to impart resistance to the drug. The experiments of Figure III-2 were undertaken to determine if disruption of the FUI1 or FUN26 genes and/or reintroduction of the cognate coding sequence on an expression plasmid altered sensitivity to either 5-fluorouridine or 5-fluorouracil. In the experiments with 5-fluorouridine (Figure III-2A), cultures of the parental (FUI1<sup>+</sup>, FUN26<sup>+</sup>) strain or the *fun26*-disruption mutant failed to grow when plated on solid medium that contained graded concentrations of 5-fluorouridine at concentrations  $\geq 10 \mu\text{M}$ . In contrast, growth of the *fui1*-disruption mutant was observed at the highest (1 mM) concentration of 5-fluorouridine tested. When the *fui1*-disruption mutant was transformed with pYFUI1 and grown under inducing conditions, the resulting transformants exhibited even greater sensitivity to 5-fluorouridine than the parental (FUI1<sup>+</sup>, FUN26<sup>+</sup>) strain, whereas when the KY114 parental strain was transformed with pYFUN26 and grown under inducing conditions, the sensitivity to 5-fluorouridine was unchanged. When similar plating experiments were undertaken with 5-fluorouracil, identical sensitivities were observed for all yeast strains and transformants (Figure III-2B). Taken together, the results of Figure III-2 suggested a role, presumably involving inwardly directed transport across the plasma membrane, for FUI1, but not for FUN26, in 5-fluorouridine toxicity and no role for either FUI1 or FUN26 in 5-fluorouracil toxicity.

#### **III.C.iv Uptake of uridine by yeast with FUI1 and FUN26 gene disruptions**

To determine if the differences in 5-fluorouridine sensitivity observed in the experiments of Figure III-3 were related to uridine-transport capacity, uptake of 1  $\mu\text{M}$  [ $^3\text{H}$ ]uridine was measured into cells of the parental strain (FUI1<sup>+</sup>, FUN26<sup>+</sup>) and the *fui1*- and *fun26*-disruption mutants (Figure III-3A). Uptake of uridine by cells of the *fui1*-disruption mutant was absent whereas uptake by cells of the *fun26*-disruption mutant was the same as that seen by cells of the parental (FUI1<sup>+</sup>, FUN26<sup>+</sup>) strain. These results were consistent with the conclusion that FUI1, and not FUN26, was responsible for the uridine transport activity observed in the parental (FUI1<sup>+</sup>, FUN26<sup>+</sup>) strain.

In the experiments of figures III-3B and III-3C, the ability of recombinant FUI1 or FUN26 to reconstitute uridine-transport activity in the *fui1*-disruption mutant was assessed by measuring the uptake of 1  $\mu\text{M}$  [ $^3\text{H}$ ]uridine into mutant cells transformed with either pYFUI1 or pYFUN26 and grown under inducing conditions. Uptake of [ $^3\text{H}$ ]uridine was stimulated in pYFUI1-containing yeast and this uptake was eliminated in the presence of a great excess (10 mM) of non-radioactive uridine (Figure III-3B). In contrast, reconstitution of uridine uptake activity was not observed when pYFUN26 was introduced into the *fui1*-disruption mutant (Figure III-3C). These results indicated that production of recombinant FUI1, but not FUN26, in the recipient mutant cells restored the capacity for cellular uptake of uridine.

The linearity of uridine uptake time courses observed when the FUI1 cDNA was expressed in the *fui1*-disruption mutant in the experiments of Figure III-3B allowed measurement of initial rates of uptake, which are required for kinetic characterization of uridine transport. In the experiments of Figure III-3D, the *fui1*-disruption mutant harbouring pYFUI1 was grown under inducing conditions and the initial rates of uptake were determined over a range of [ $^3\text{H}$ ]uridine concentrations. Uridine transport was

saturable with  $K_m$  and  $V_{max}$  values (mean  $\pm$  SD), respectively, of  $22 \pm 3 \mu\text{M}$  and  $3500 \pm 240 \text{ pmol/mg protein/s}$ .

Detailed structure-activity studies were undertaken to identify compounds that inhibited FUI1-mediated uridine transport activity and were therefore candidate permeants of FUI1. In the experiments of Figure III-4 the transport of  $1 \mu\text{M}$  [ $^3\text{H}$ ]uridine was measured in the absence or presence of high concentrations of (i) nucleosides, nucleobases and ribose, (ii) uridine and uridine analogs (iii) substrates of the "uracil/allantoin" family of yeast permeases, or (iv) ENT transport inhibitors. The results of Figure III-4A demonstrated that FUI1-mediated [ $^3\text{H}$ ]uridine uptake was inhibited completely by uridine, an indication that uptake was occurring in a mediated process. FUI1-mediated uptake was inhibited partially by uracil, 5-fluorouracil and thymine, but not by ribose or the other nucleosides (i.e., guanosine, adenosine, inosine, cytidine, thymidine) or nucleobases (i.e., thymine, hypoxanthine) tested. The results of Figure III-4B demonstrated that FUI1-mediated [ $^3\text{H}$ ]uridine uptake was inhibited strongly by uridine analogs (5-fluorouridine = 2'-deoxyuridine = 5-fluoro-5'-deoxyuridine) and to a lesser extent by other uridine analogs (5-fluoro-2'-deoxyuridine = 5-bromo-2'-deoxyuridine = 5-methyluridine = 5-iodouridine). Although high concentrations of uracil inhibited FUI1-mediated transport partially (Figure III-4A), the other substrates (allantoin, thiamine) of the uracil/allantoin permease were without effect when tested at 10 mM (Figure III-4C). Similarly, FUI1-mediated transport was not inhibited by dilazep, dipyridamole or NBMPR (Figure III-4C), the "classic" inhibitors of the mammalian ENT family of proteins (2,14). Together, the experiments of Figure III-4 demonstrated that FUI1 is a uridine-selective transporter with (i) preferences for uridine over uracil and the ribosyl over the deoxyribosyl moiety of uridine, and (ii) a low tolerance for modification of the 5-position of the base.

### **III.C.v Production of recombinant FUN26 in *Xenopus laevis* oocytes**

The sequence similarity of FUN26 to the ENT proteins of mammalian cells (20%) suggested that FUN26 might be a nucleoside transporter (18), despite the failure to

demonstrate FUN26-mediated uptake of uridine in yeast. Since it was possible that FUN26 was not functional in yeast under the conditions of the experiments of Figure III-5, recombinant FUN26 was produced and tested in oocytes of *X. laevis* using established procedures for functional expression of ENT proteins (16,18). In the experiments of Figure III-5A, the uptake of 20  $\mu\text{M}$  [ $^3\text{H}$ ]nucleoside or [ $^3\text{H}$ ]nucleobase was measured over 60 min in oocytes that had been injected with either FUN26 transcripts in water or water alone. FUN26 expression stimulated the uptake of [ $^3\text{H}$ ]cytidine, [ $^3\text{H}$ ]adenosine and [ $^3\text{H}$ ]uridine 6-9 fold and of [ $^3\text{H}$ ]thymidine and [ $^3\text{H}$ ]inosine only modestly (~2 fold) above that of water-injected oocytes. Expression of FUN26 had no effect on the uptake of [ $^3\text{H}$ ]hypoxanthine or [ $^3\text{H}$ ]uracil.

The activities of the yeast nucleobase transport proteins (FUR4, FCY2), which are nucleobase/proton symporters of plasma membranes, are dependent on proton concentration (63,68). To determine if FUN26 transport activity was dependent on symport of protons, the pH sensitivity of FUN26-mediated uridine uptake in *X. laevis* oocytes was examined in the experiments of Figure III-5B. The uptake of 20  $\mu\text{M}$  [ $^3\text{H}$ ]uridine from transport buffer at pH values of 5.5 to 7.5 was measured over 30 min into oocytes that had been injected three days earlier with either FUN26 transcripts in water or water alone. Uridine uptake by the FUN26-producing oocytes was the same at the tested pH values, indicating that the transport activity of FUN26, like that of the mammalian ENTs, was not pH dependent.

The effects of ENT transport inhibitors (NBMPR, dilazep and dipyridamole) on FUN26-mediated uridine transport in *X. laevis* oocytes were examined in the experiments of Figure III-5C. The uptake of 20  $\mu\text{M}$  [ $^3\text{H}$ ]uridine by FUN26-producing or non-producing oocytes was measured in transport buffer alone or in transport buffer that also contained NBMPR, dilazep or dipyridamole. Uridine uptake by the FUN26-producing oocytes was unaffected by 10  $\mu\text{M}$  NBMPR, dipyridamole or dilazep, suggesting that these inhibitors do not interact with FUN26.

### **III.C.vi Production of FUN26myc in yeast**

The transport characteristics of recombinant FUN26 produced in *X. laevis* oocytes indicated that FUN26 has nucleoside transport activity. However, cell surface FUN26-mediated uridine transport activity was not detected in yeast using indirect (plating assays) or direct ( $^3\text{H}$ ]uridine transport) methods in either loss-of-function (*fun26*-disruption mutant) or gain-of-function (pYFUN26-harboured yeast) experiments. To address the biological role of FUN26 in yeast, an immunotagged (c-myc) version of FUN26 was generated (FUN26myc) to enable cellular localization of the recombinant protein. Membranes that were prepared from yeast harbouring either pYFUN26myc or pYES2, and that had been grown under inducing conditions (CMM/GAL) were solubilized, electrophoresed and subjected to immunoblotting with anti-c-myc monoclonal antibodies (Figure III-6A). Immunoreactive material that migrated with mobility (55 kDa) similar to that expected of FUN26 (58.3 kDa) was detected in membranes of pYFUN26myc-containing yeast (lane 2) and was not present in membranes of pYES2-containing yeast (lane 1). These results, which demonstrated the presence of the recombinant protein in yeast membranes, raised the possibility that FUN26myc (and therefore also FUN26) may reside in intracellular membranes. Addition of the c-myc epitope did not affect the function of the protein since production of recombinant FUN26myc in *X. laevis* oocytes stimulated  $^3\text{H}$ ]uridine uptake ( $5.8 \pm 0.8$  pmol uridine/oocyte/60 min).

### **III.C.vii FUN26myc is predominantly located in intracellular membranes of yeast**

The presence of recombinant FUN26myc in yeast membranes, combined with the absence of detectable FUN26-transport activity in intact yeast, suggested a role for FUN26 in intracellular membranes. The cellular location of recombinant FUN26myc was assessed by density-gradient fractionation and immunoblotting. Membranes from yeast (KY114) harbouring pYFUN26myc and grown in inducing (CMM/GAL) conditions were prepared and subjected to continuous sucrose gradient (20% (w/w) - 53% (w/w)) centrifugation.



Gradient fractions were subjected SDS-PAGE and immunoblotting (Figure III-6B) using antibodies against (i) the c-myc epitope (to detect FUN26myc), (ii) PMA1 (a yeast plasma membrane resident protein) (125) and PEP12 (an intracellular, prevacuolar membrane resident protein) (126). The plasma membrane marker (PMA1) was distributed throughout the sucrose gradient as described previously for yeast (98,124) and the intracellular membrane marker (PEP12) was distributed in greatest abundance in just two or three fractions. Recombinant FUN26myc, which was detected with anti-c-myc antibodies, displayed a distribution pattern that closely resembled that of PEP12, suggesting that recombinant FUN26myc was predominantly present in intracellular membranes.

### III.D DISCUSSION

Cytotoxicity of nucleoside analogs has been used by others as a functional screen to identify nucleoside transport processes in *S. cerevisiae* (53,56). While these assays provided indirect evidence of the nucleoside transport activity of FUI1, unequivocal demonstration of its role as a cell-surface nucleoside transporter by direct measure of nucleoside fluxes was not provided.

Sequence comparisons identified an open reading frame (YBL042c) that is predicted to encode a protein (FUI1) that belongs to the uracil/allantoin permease family (54,55). The experiments of Figure III-2 established that disruption of the FUI1-gene locus leads to increased resistance to the cytotoxic nucleoside analog 5-fluorouridine (56), suggesting that the FUI1 protein may be involved in the cellular uptake of uridine and uridine analogs. Overexpression of recombinant FUI1 increased the sensitivity of yeast to 5-fluorouridine, a result that was consistent with FUI1 involvement in cell-surface uptake of 5-fluorouridine or in the subsequent anabolism of 5-fluorouridine. Its functional role was directly assessed in the experiments of Figure III-3 in which FUI1 was shown to encode a cell-surface uridine transporter by several criteria: (i) disruption of the FUI1 gene abrogated [<sup>3</sup>H]uridine transport, (ii) overexpression of the FUI1 cDNA in the *fui1*-disruption mutant restored [<sup>3</sup>H]uridine uptake to levels greater than those observed in the parental strain, and (iii) FUI1-mediated [<sup>3</sup>H]uridine uptake was a saturable process that conformed to Michaelis-Menten kinetics ( $K_m = 22 \pm 3 \mu\text{M}$ ;  $V_{max} = 3500 \pm 35 \text{ pmol/mg protein/s}$ ). Together, these experiments established that the FUI1 gene encodes a nucleoside transport protein with a high affinity for uridine.

Candidate permeants and/or inhibitors of FUI1 were identified by assessing FUI1-mediated [<sup>3</sup>H]uridine transport in the absence or presence of a high concentration of the test compound. The capacity to inhibit [<sup>3</sup>H]uridine transport was indicative of either substrate or inhibitor activity for the transporter and therefore provided information about the relative

affinities of FUI1 for various nucleoside derivatives. FUI1 was shown to: (i) prefer uridine over uracil, (ii) prefer a hydroxyl group on the 2'-position of the ribosyl over the deoxyribosyl moiety, and (iii) have a low tolerance for substitutions (F-, Br-, CH<sub>3</sub>-, I-) at the 5-position of the base. FUI1-mediated [<sup>3</sup>H]uridine transport was not inhibited by purine nucleosides, hypoxanthine or ribose, indicating little, if any, interaction of these compounds with FUI1. FUI1 also lacked sensitivity to inhibition by NBMPR, dilazep, and dipyridamole. Although FUI1 shares high sequence identity with other members of the uracil/allantoin permease family, it evidently has minimal overlapping substrate selectivities with other family members since FUI1-mediated uridine uptake was not inhibited by allantoin or thiamine and was only modestly inhibited (~30%) by a high concentration (10 mM) of uracil.

Analysis of the *S. cerevisiae* genomic databases identified the open reading frame YAL022c (FUN26) as encoding a protein that resembles members of the ENT family of membrane proteins (18). The limited sequence identity of FUN26 with members of the ENT family (e.g., 18% identity with hENT1 and hENT2) suggested that there might be conservation of function between FUN26 and ENT family members. Recombinant nucleoside transport proteins from a variety of organisms have been functionally expressed in oocytes of *X. laevis* (12,15,16,18,19). Since FUN26 transport activity was not detected in yeast, *X. laevis* oocytes were used for functional expression of FUN26 transcripts to determine if the FUN26 protein has nucleoside transport activity. Recombinant FUN26 protein mediated transport of adenosine, cytidine, uridine and to a lesser extent, inosine and thymidine, whereas the nucleobases, uracil and hypoxanthine, were not transported. FUN26-mediated uridine transport activity was independent of pH, a feature characteristic of mammalian ENT family members. FUN26-mediated transport activity was not inhibited by NBMPR, dilazep or dipyridamole suggesting that these inhibitors do not interact with FUN26.

Disruption of the FUN26 gene locus did not alter cell-surface uridine transport activity even though recombinant FUN26 exhibited uridine transport activity when produced in *X. laevis* oocytes. The apparent lack of FUN26-mediated cellular uptake of uridine suggested that recombinant FUN26 was either (i) not produced in yeast harbouring pYFUN26 and grown under inducing conditions, or that (ii) recombinant FUN26 was produced but not present at the cell surface. Immunoblotting of yeast membranes prepared from pYFUN26myc-containing yeast that were grown under inducing (CMM/GAL) conditions demonstrated that recombinant FUN26myc was membrane associated. Fractionation and immunoblotting of yeast membranes containing FUN26myc demonstrated that FUN26myc was not present in plasma membranes but rather co-localized predominantly with a marker of late endosomes (PEP12). Thus, it appeared that FUN26 nucleoside transport activity was not detected at the cell surface because FUN26 resides in membranes of late endosomes and, as such, may include vacuolar membranes.

In *S. cerevisiae*, the vacuole serves the role of, and has long been considered to be identical to, the mammalian lysosome (129). In yeast the vacuole serves as the site of degradation of macromolecules, and a variety of integral membrane proteins of the vacuolar membrane are responsible for the uptake and release of vacuolar contents. Transport processes that have been previously identified in yeast vacuoles include those for amino acids (130,131), phosphate (132), calcium (133), glutathione conjugates (134) and nucleosides (128). Direct measure of <sup>14</sup>C-nucleoside transport in vacuoles isolated from *S. cerevisiae* has identified nucleoside transport process(es) involved in the uptake and release of adenosine and guanosine (128).

Similarly, the nucleoside transport activity of human lysosomes resembles that of an ENT protein. Adenosine transport activity in purified lysosomes occurs via a mediated process ( $K_m = 9$  mM) that is independent of pH and sensitive to inhibition by the ENT transport inhibitors NBMPR and dipyrindamole (8). Additionally, adenosine transport by the ENT-like lysosomal transporter is inhibited by competing purine and pyrimidine

nucleosides (8), suggestive of a nucleoside transport protein with broad substrate specificity.

In conclusion, these results suggest that FUI1 and FUN26 mediate cell-surface and intracellular nucleoside transport, respectively, in *S. cerevisiae*. Functional analysis of the FUI1 gene product in *S. cerevisiae* indicated that FUI1 is highly selective for uridine and thus may serve as the predominant salvage route of extracellular uridine. Functional expression of FUN26 transcripts in oocytes of *X. laevis* indicated that the FUN26 protein has nucleoside transport activity of broad specificity with a preference for adenosine, cytidine and uridine. However, FUN26 gene disruption and overexpression had no detectable effect on import of extracellular uridine, in marked contrast to FUI gene disruption and overexpression. Recombinant FUN26 co-localized predominantly with a marker of late endosomes, PEP12, suggesting that the FUN26 protein plays a functional role in intracellular membranes. A prime candidate is the yeast vacuolar membrane, which is known to possess nucleoside transport activity. Analysis of all known genes in *S. cerevisiae* for their expression during the cell cycle has determined that FUN26 mRNA is most abundant during M-phase (103). Thus, a possible role of FUN26 is the vacuolar release of nucleosides (*e.g.*, adenosine, uridine, cytidine) produced by vacuolar catabolism of nucleic acids during the period of rapid RNA and DNA synthesis leading up to cell division.

**Figure III-1 Disruption of the FUI1 and FUN26 gene loci in yeast.**

The PCR-mediated one-step gene disruption strategy is shown for FUI1 (Panel A) and FUN26 (Panel B). The PCR-mediated gene disruption methods were as described in Chapter II, section II.A.i. The *open bars* denote the cDNA coding regions and the *hatched bars* denote the selection markers; the expected size of the disruption constructs is denoted below each diagram. Panel C shows PCR confirmation of FUN26::HIS3 and FUI1::TRP1 gene-disruptions. PCR reactions using yeast chromosomal DNA (parental and mutant) or plasmid from the disruption constructs as the templates in combination with the FUN26-specific primers (5'FUNkpnI/3'FUNsphI) (lanes 1-4) or the FUI1-specific primers (5'FUI1sacI/3'FUI1sphI) (lanes 5-8) were conducted as described in Chapter II, section II.A.i. The templates were as follows: lane 1, KY114; lane 2, FUN26::HIS3 disruption plasmid; lane 3, candidate FUN26:HIS3 mutant; lane 4, water control; lane 5, KY114; lane 6, FUI1::TRP1 disruption plasmid; lane 7 candidate FUI1::TRP1 mutant; lane 8, water control. A 10- $\mu$ l portion of the PCR reaction was resolved on a 1% agarose gel, and the positions of DNA standards are denoted on the left (bases).

**Figure III-1**

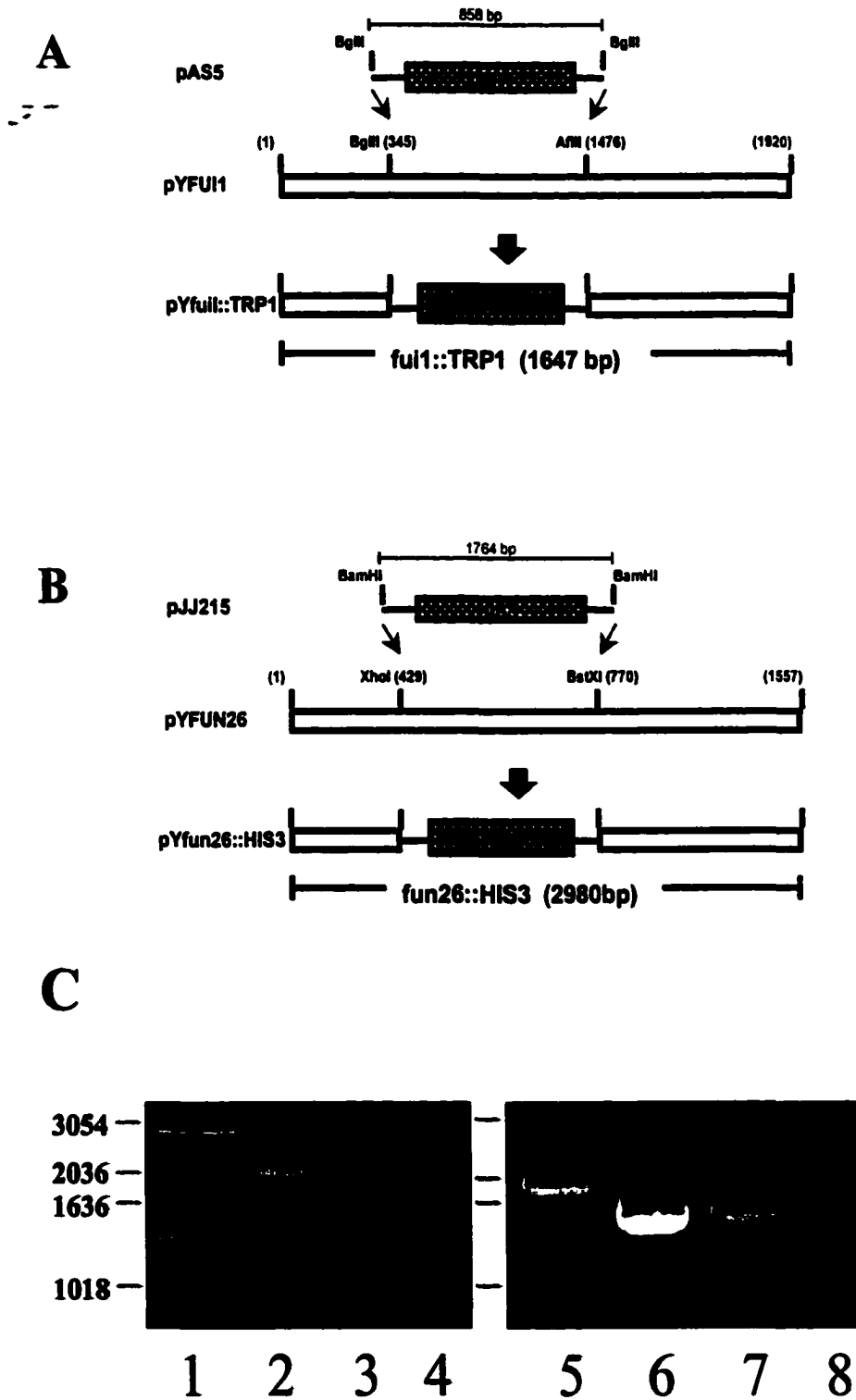


### **Figure III-2 Cellular resistance to 5-fluorouridine and 5-fluorouracil**

The parental (FUN26<sup>+</sup>, FUI1<sup>+</sup>) yeast strain (KY114, lane 1), the *fun26*- and *fui1*-disruption mutants (*fui1*::TRP1, lane 2; *fun26*::HIS3, lane 3), the *fui1*-disruption mutant transformed with the pYFUI1 plasmid (lane 4) and the parental strain (FUN26<sup>+</sup>, FUI1<sup>+</sup>) strain transformed with pYFUN26 (lane 5) were grown in CMM/GAL medium and re-suspended in CMM/GAL to OD<sub>600</sub> values of 1.0, 0.1, 0.01, or 0.001. Ten- $\mu$ l portions of the diluted cultures were plated on solid media possessing graded concentrations (0-1000  $\mu$ M) of 5-fluorouridine (Panel A) or 5-fluorouracil (Panel B) and cell growth on plates was assessed after 2.5 days at 30°C.



## Figure III-2

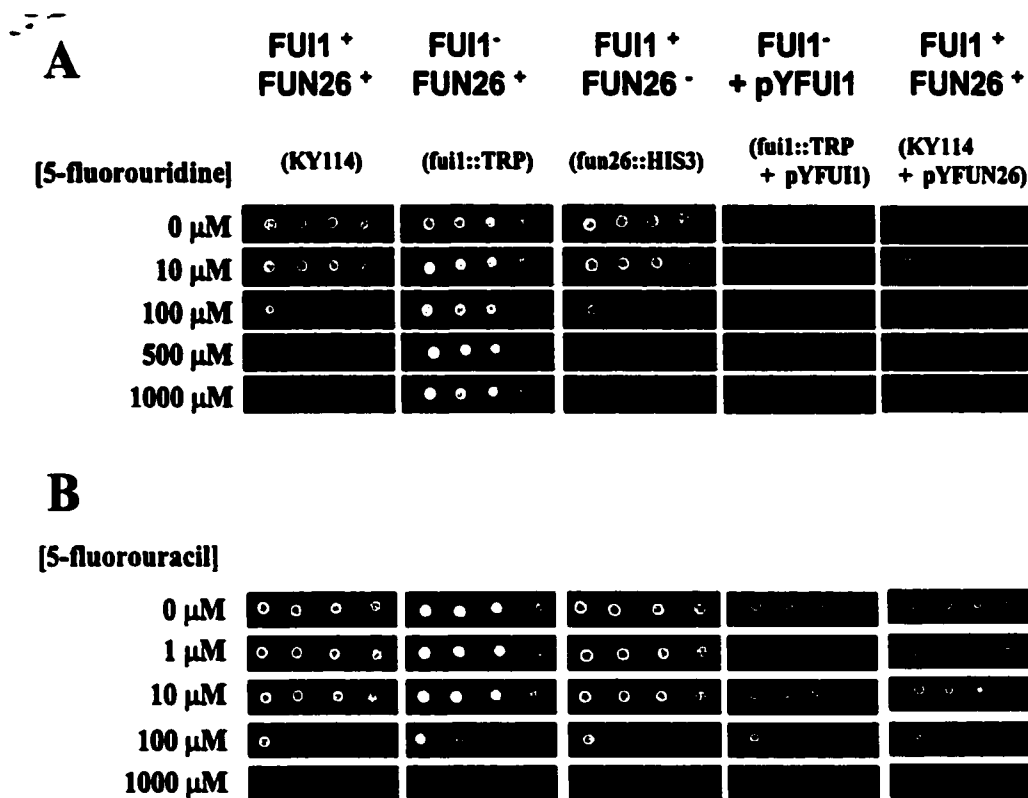


**Figure III-3      Loss of uridine transport activity in *fui1*-disruption mutants and its reconstitution by introduction and over-expression of a FUI1-containing plasmid**

**Panel A:** *A comparison of uptake by parental yeast and the *fui1*- and *fun26*-disruption mutants.* The uptake of 1  $\mu\text{M}$  [ $^3\text{H}$ ]uridine was measured as a function of time into KY114 (-■-), *fui1*::TRP1 (-▼-) or *fun26*::HIS3 (-▲-), yeast grown in CMM/GLU medium as described in Chapter II, section II.J.i. **Panel B:** *Reconstitution of transport in *fui1*-disruption mutants by FUI1 expression.* The uptake of 1  $\mu\text{M}$  [ $^3\text{H}$ ]uridine was measured as a function of time in the absence (-■-) or presence (-▲-) of 10 mM non-radioactive uridine into *fui1*::TRP/pYFUI1 yeast that had been grown in CMM/GAL medium. **Panel C:** *Failure of expression of the FUN26 coding sequence to reconstitute transport in *fui1*-disruption mutants.* The uptake of 1  $\mu\text{M}$  [ $^3\text{H}$ ]uridine was measured as a function of time into KY114 (-■-), *fui1*::TRP1/pYFUN26 (-▼-), or *fui1*::TRP1/pYES2 (-▲-) yeast grown in CMM/GAL medium. **Panel D:** *Saturability of FUI1-mediated uridine transport.* Initial rates of [ $^3\text{H}$ ]uridine uptake were determined into *fui1*::TRP1/pYFUI1 grown in CMM/GAL as shown in Panel B. The rate of FUI1-mediated uptake is presented as a function of the uridine concentration tested. Initial rates of uptake were determined from the slopes of linear portions of uridine uptake time courses over short (0-9 s) time periods. Results are means  $\pm$  S.D. of triplicate determinations. Error bars are not shown where values were smaller than those represented by the symbols. Representative experiments are shown; three separate experiments yielded similar results.

**Figure III-3**

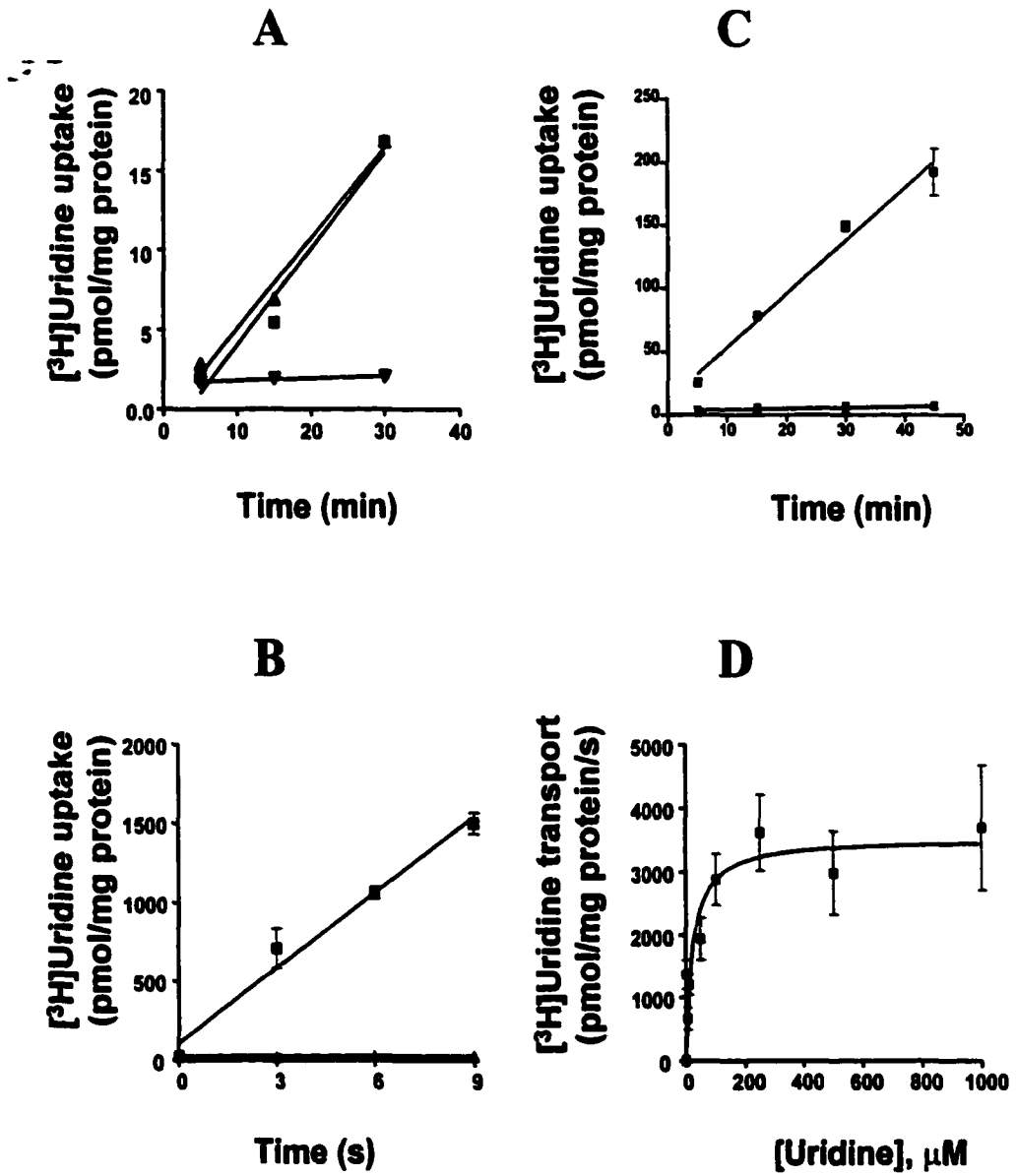


**Figure III-4 Inhibition of FUI1-mediated uridine transport by nucleosides, nucleobases and related substances: identification of candidate permeants and inhibitors**

The uptake of 1  $\mu\text{M}$  [ $^3\text{H}$ ]uridine was measured as described in Chapter II, II.J.i, 9s after addition of the radioactive tracer solution into *fui1::TRP/pYFUI1* yeast (grown in CMM/GAL) that were first incubated for 20 min in the absence (alone) or presence of: **(Panel A)** nucleosides, nucleobases and ribose; **(Panel B)** uridine and uridine analogs or **(Panel C)** thiamine, allantoin or various ENT transport inhibitors. Results are means  $\pm$  SEM of individual experiments (3 samples per condition) that were performed 3-20 times (the number of individual experiments performed is presented in parentheses).

**Figure III-4**

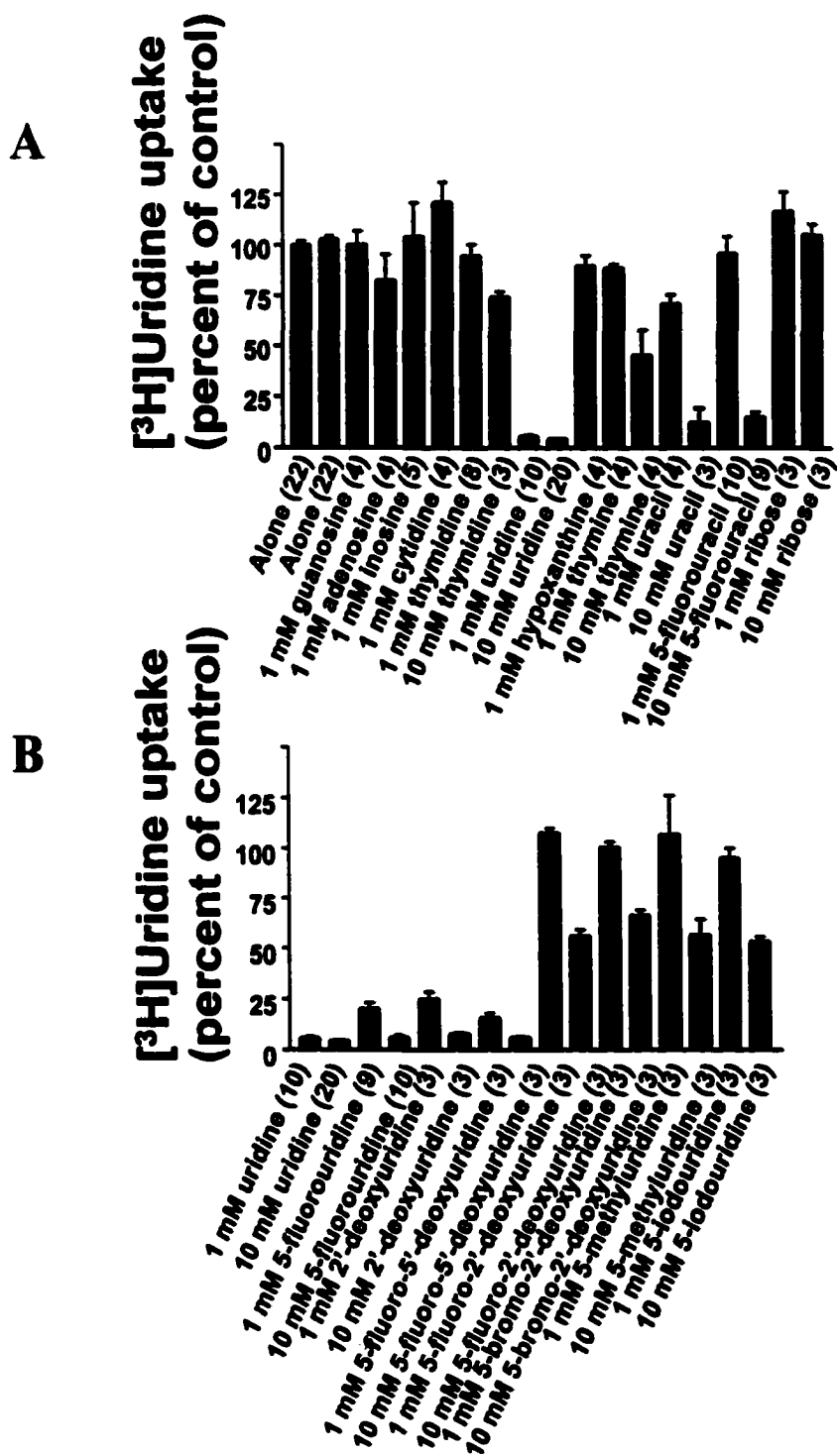


**Figure III-4**

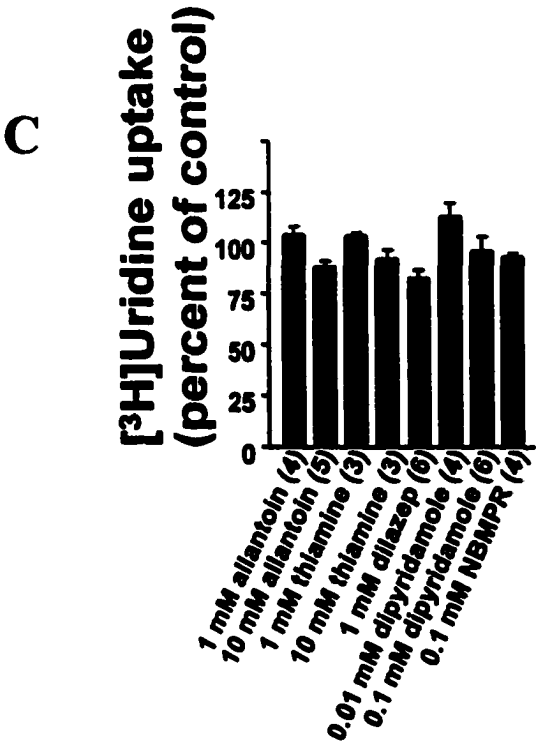


**Figure III-5**      **FUN26-mediated uptake of nucleosides in oocytes of *X. laevis***

Oocytes were injected with water alone (*open bars*) or with water containing RNA transcripts for FUN26 (*closed bar*), as described in Chapter II, section II.J.iii. After incubation for 3 days, the uptake of 20  $\mu\text{M}$  [ $^3\text{H}$ ]nucleoside or [ $^3\text{H}$ ]nucleobase (as indicated) was measured (60 min, 20°C). Rates of uptake represent the mean ( $\pm$  S.D.) of 8-10 oocytes. Representative experiments are shown, three separate experiments yielded similar results. **(Panel A) FUN26-mediated [ $^3\text{H}$ ]nucleoside and [ $^3\text{H}$ ]nucleobase transport.** The uptake of 20  $\mu\text{M}$  [ $^3\text{H}$ ]nucleoside or [ $^3\text{H}$ ]nucleobase (as indicated) was measured (60 min, 20°C). **(Panel B) pH dependence of FUN26-mediated transport.** The uptake of 20  $\mu\text{M}$  [ $^3\text{H}$ ]uridine was measured (30 min, 20°C) into oocytes injected with water alone (*open bars*) or with water that contained RNA transcripts for FUN26 (*closed bars*) in transport medium at pH 5.5 or 7.5 (as indicated). **(Panel C) Effects of ENT Inhibitors on FUN26-mediated transport.** The uptake of 20  $\mu\text{M}$  [ $^3\text{H}$ ]uridine was measured (60 min, 20°C) into oocytes injected with water alone (*open bar*) or with water that contained FUN26 transcript (*closed bar*) with or without NBMPPR, dilazep or dipyridamole (as indicated).

**Figure III-5**

**A**

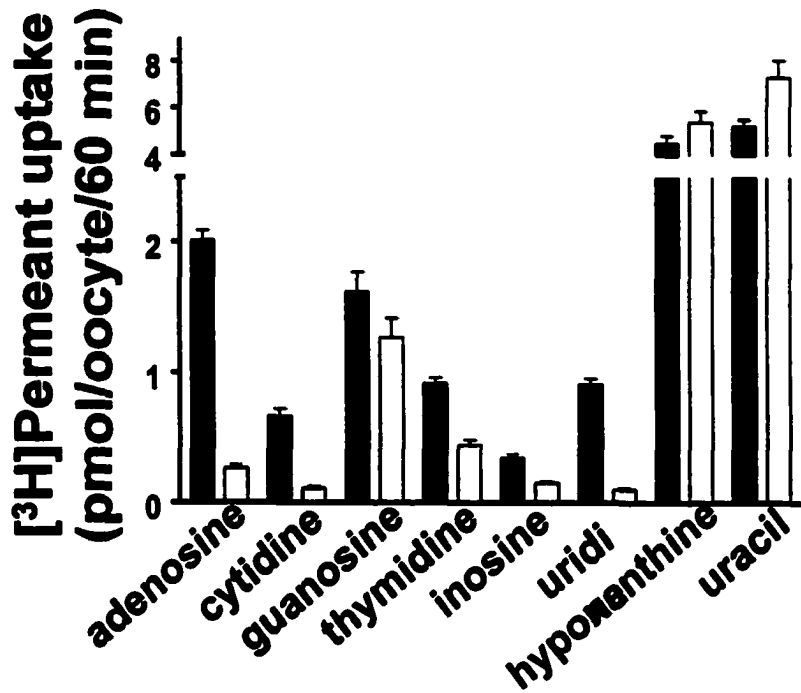




**Figure III-5**

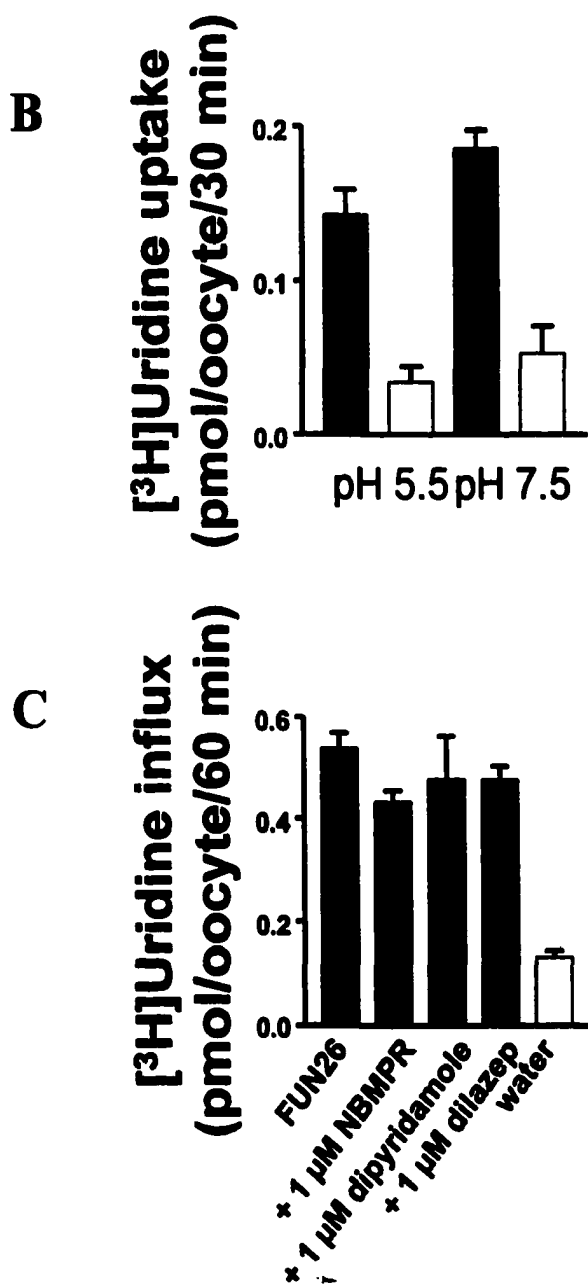


**Figure III-6      Production and subcellular location of recombinant FUN26myc in yeast membranes**

**(Panel A)** Membranes (20  $\mu$ g), prepared as described in Chapter II, section II.E, from yeast with pYES2 (lane 1) or pYFUN26myc (lane 2), grown in CMM/GAL medium, were subjected to immunoblotting with the 9E10 anti-c-myc monoclonal antibodies. The positions of the molecular mass markers are indicated at the left. **(Panel B)** Yeast membranes possessing recombinant FUN26myc were subjected to fractionation by continuous sucrose gradient centrifugation as described in Chapter II, section II.N. The membranes from 1-ml portions of the gradient were subjected to immunoblotting using: (i) the 9E10 anti-c-myc monoclonal antibody (to detect FUN26myc), (ii) anti-PMA1 (plasma membrane ATPase) polyclonal antibodies (plasma membrane specific) (125), (iii) anti-pep12 polyclonal antibodies (prevacuolar membrane specific) (126). The fraction numbers (2-13) correspond to the sequential fractions from the top of the gradient (2) to the bottom of the gradient (13). Two separate experiments yielded similar results, and those from one are shown.

**Figure III-6**

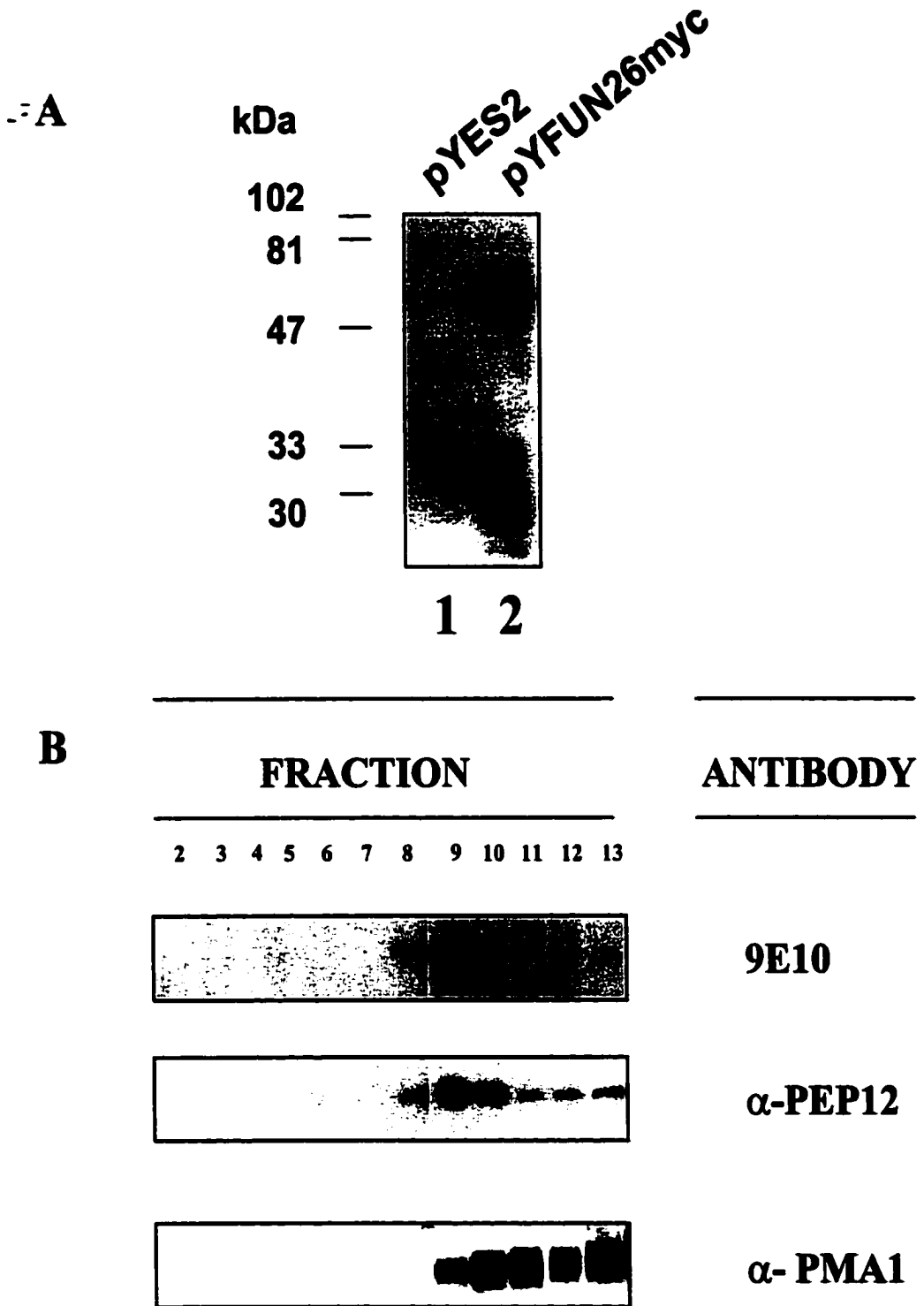


**Table III-1 Sequence comparisons of members of the “uracil/allantoin” transporter family and ENT family**

A comparison matrix of amino acid identity is presented for members of the uracil/allantoin transporter family (Table 1A) and members of the equilibrative nucleoside transporter family (Table 1B). Comparison were performed using “Bestfit” software from GCG (genetics computer group).

**Table 1A**

	<b>THI10</b>	<b>YOR192c</b>	<b>YOR071c</b>	<b>FUR4</b>	<b>DAL4</b>	<b>FUI1</b>
<b>THI10</b>	100					
<b>YOR192c</b>	87	100				
<b>YOR071c</b>	84	82	100			
<b>FUR4</b>	29	28	30	100		
<b>DAL4</b>	30	30	31	70	100	
<b>FUI1</b>	29	29	28	55	56	100

**Table 1B**

	<b>hENT1</b>	<b>rENT1</b>	<b>hENT2</b>	<b>rENT2</b>	<b>FUN26</b>
<b>hENT1</b>	100				
<b>rENT1</b>	87	100			
<b>hENT2</b>	50	51	100		
<b>rENT2</b>	50	49	88	100	
<b>FUN26</b>	18	15	18	16	100

#### **IV.**

### **Functional expression of mammalian and bacterial concentrative nucleoside transporters in *Saccharomyces cerevisiae*.**

#### **IV.A ABSTRACT**

Described here is the use of the yeast *S. cerevisiae* to study recombinant concentrative nucleoside transport proteins. A selection strategy in *S. cerevisiae* was utilized based on the ability of an expressed nucleoside transporter cDNA to mediate the uptake of thymidine under selective conditions which deplete the yeasts' endogenous thymidylate pools. It was shown that the pyrimidine-nucleoside specific concentrative transporters from rat (rCNT1), human (hCNT1) and *Escherichia coli* (NUPC) were able to complement the imposed thymidylate depletion. Using purine and pyrimidine nucleosides to inhibit transporter-mediated rescue of yeast, the apparent substrate selectivities of the three nucleoside transporters were shown to include pyrimidine nucleosides (cytidine, uridine) and adenosine, but not other purine nucleosides (guanosine, inosine). It was found that N-terminally truncated versions of rCNT1 and hCNT1 (lacking up to 31 amino acids) also produced functional transporters able to complement the thymidine transport deficiency in yeast. In addition, open reading frames from *Haemophilus influenzae* (HI0519) and *Helicobacter pylori* (HP1180), identified from database searching for rCNT1 orthologs, were shown to encode nucleoside transporter proteins by their ability to complement the imposed thymidine depletion of the selection strategy. The HI0519 reading frame was shown to encode a protein with an apparently broad substrate specificity which included both purine and pyrimidine nucleosides. This work represents the development of a new model system for the functional expression of nucleoside transporter proteins. Characterization of members of the CNT family with known substrate specificity facilitated the validation of this model expression system that was used to identify two previously unknown and uncharacterized nucleoside transporter proteins.

## **IV.B. INTRODUCTION**

Production of heterologous recombinant proteins in the yeast *S. cerevisiae* has proven to be a powerful approach to study membrane proteins from different organisms. When this work was initiated only a few mammalian membrane transport proteins had been functionally expressed in *S. cerevisiae* including the Band 3 anion exchange protein (AE1) (98), the multidrug resistance proteins *mdr1* and *mdr3* (99) and the cystic fibrosis transmembrane conductance regulator (CFTR) (100). The goal of the work described in this chapter was to develop *S. cerevisiae* as a model expression system to permit characterization of recombinant nucleoside transporter proteins. *S. cerevisiae* lacks an endogenous cell surface thymidine-specific nucleoside transport process (52) and so are well suited for uptake experiments which measure the acquisition of thymidine transport capability. This has the advantage of allowing introduction of a known cDNA species into yeast possessing a thymidine-transport null background, and the ability to examine mutant nucleoside transport proteins generated by site directed mutagenesis of the wild-type cDNA. Finally, development of yeast as a model expression system for nucleoside transporter proteins would permit the characterization of unknown or putative nucleoside transporter proteins, identified as a result of completed and ongoing genomic sequencing projects.

The cloning strategy to isolate nucleoside transporter cDNAs by functional expression in *S. cerevisiae* devised by Hogue *et al.* (105,106) was used as the basis for development of the yeast expression system (see Chapter I, I.K.iii). Briefly, inhibition of *de novo* production of dTMP from dUMP by exposure to methotrexate (MTX) and sulfanilamide (SAA) prevents growth of *S. cerevisiae* by "thymidylate starvation" (105,106). Cell growth can not normally be restored by the addition of exogenous thymidine as yeast lack the capacity for thymidine salvage; yeast lack mechanisms for the transport of thymidine across the plasma membrane and for phosphorylation of thymidine

to dTMP (52,53). Thus, it was predicted that introduction of a nucleoside transporter cDNA into yeast made competent for thymidine phosphorylation would complement growth under the selective conditions of MTX and SAA if a source of extracellular thymidine was provided. A functional selection strategy was developed to screen cDNA libraries for clones capable of complementing cell growth on the basis of their ability to confer the capacity for inward transport of thymidine across the yeast plasma membrane (105,106) in a yeast strain that also contained a thymidine-kinase expression plasmid. This approach identified a truncated version of a highly conserved (> 98% identity in humans and mice) membrane protein of mice that allowed yeast to grow under the selective conditions imposed by importing thymidine (105). This novel protein (MTP) has subsequently been shown, when produced in full-length form in yeast, to confer resistance to nucleobase analogs, antibiotics, anthracyclines, ionophores, and steroid hormones and reside in vacuolar membranes (135).

A cDNA encoding the pyrimidine nucleoside-specific nucleoside transporter protein from rat intestine (rCNT1) was isolated in 1994 by Huang *et al.* by functional cloning using oocytes of *X. laevis* as a model system (12). Although a cDNA encoding a candidate nucleoside transporter protein had been reported earlier (136), its capacity for nucleoside transport was never established, making rCNT1 the first mammalian nucleoside transporter to be identified by molecular cloning. The human ortholog, hCNT1, was subsequently identified by PCR-based molecular cloning and functional characterization in oocytes of *X. laevis* (15). A pyrimidine nucleoside-specific transporter from *E. coli* (NUPC), which had been previously identified genetically (75) was also functionally produced and characterized in the *X. laevis* model expression system (77). Since thymidine is a permeant of rCNT1, hCNT1 and NUPC, their expression in yeast was predicted to mediate the inward transport of thymidine, thereby allowing cell survival under the selective conditions imposed by MTX and SAA. These previously characterized nucleoside transporters, therefore, served



as the basis from which to develop *S. cerevisiae* as a model expression system for nucleoside transporters.

Analysis of genomic databases identified numerous CNT orthologs among a variety of species (see Chapter 1, Figure I.3). Open reading frames from *H. pylori* (HP1180) (137) and *H. influenzae* (HI0519) (138) are predicted to encode proteins with sequence limited identity to known purine and pyrimidine-nucleoside and purine-nucleoside specific CNT family members (see Figure IV.F-1). HP1180 and HI0519 are predicted to encode proteins of, respectively, 418 (44 kDa) and 417 (44 kDa) amino acids, possessing 8-13 transmembrane spanning domains. It is not known if the structural conservation is reflected in functional conservation, nor have similarity searches permitted a prediction of substrate specificity of these putative CNT family members. The MTX/SAA selection strategy was used to explore the potential nucleoside transport activities of the proteins encoded by the open reading frames from *H. influenzae* (HI0519) and *H. pylori* (HP1180).

## **IV.C. RESULTS**

### **IV.C.ii. Functional expression of rCNT1 and $\Delta$ N31rCNT1 in *S. cerevisiae***

The ability of recombinant rCNT1 to complement the thymidine transport-defective phenotype of *S. cerevisiae* was first assessed by plating pYrCNT1-containing yeast under the MTX/SAA selective conditions. There was no growth, except in the plates made with media that contained 1000  $\mu$ M thymidine (Figure IV-1). rCNT1 does not possess a recognized targeting leader sequence in the N-terminal portion of its inferred amino acid sequence. In addition, it has a large number of charged residues in the N-terminal portion preceding the first predicted transmembrane domain that may have impaired the targeting of the recombinant protein in yeast. To circumvent some of the influence of the N-terminal sequence, a portion of the 5'-coding region of the rCNT1 cDNA was deleted to remove the initiating methionine and immediate downstream N-terminal amino acid sequence such that translation would initiate at the methionine at position 32 in the rCNT1 amino acid sequence. This deletion also had the effect of bringing the initiating methionine codon (Met-32) much closer to the GAL1 promoter. The results of the experiments of Figure IV-1 established that the truncated rCNT1 construct (rCNT1 $\Delta$ N31) complemented the thymidine transport-defective phenotype in the presence of 100  $\mu$ M thymidine when grown under inducing conditions (i.e., in galactose containing media), but not when grown under non-inducing conditions (i.e., in glucose-containing media). There was no colony growth in the absence of thymidine and normal growth was observed in the presence of 1000  $\mu$ M thymidine (a concentration that will enter cells by passive diffusion) (Figure IV-1). Thus, the removal of the N-terminal 31 amino acid residues or the increased proximity of the initiating methionine to the GAL1 promoters (or both) resulted in the production of functionally active rCNT1.

#### **IV.C.iii. Production of $\Delta$ N31rCNT1 and rCNT1 mRNA in *S. cerevisiae***

The ability of pY $\Delta$ N31rCNT1, but not pYrCNT1, to rescue yeast subjected to thymidylate starvation suggested that  $\Delta$ N31rCNT1, but not rCNT1, was expressed in yeast. Northern analysis was performed using RNA samples prepared from yeast cells with either pY $\Delta$ N31rCNT1, pYrCNT1 or pYES2 that were cultured (i) in CMM/GLU (transcription repressive, non-selective conditions) or (ii) in CMM/GAL (transcription inducing, non-selective conditions). This analysis determined that mRNA corresponding to both  $\Delta$ N31rCNT1 or rCNT1 was present, respectively, in pY $\Delta$ N31rCNT1-containing and pYrCNT1-containing yeast, but not in pYES2-containing yeast (Figure IV-2). A single band of ~1900 nucleotides was detected in pY $\Delta$ N31rCNT1-containing and pYrCNT1-containing yeast grown in either medium with galactose (CMM/GAL) or medium with glucose (CMM/GLU). No signal was present in the pYES2-containing cells under any of the experimental conditions. These results, which demonstrated the presence of rCNT1 and  $\Delta$ N31rCNT1 mRNA in cells with, respectively, pY $\Delta$ N31rCNT1 and pYrCNT1, also indicated the transcription of the cDNAs when grown in the presence of either glucose or galactose. Finally, these results suggested that the inability of rCNT1 to complement the imposed thymidine-transport deficiency in the complementation assay was due to problems at the level of translation of the rCNT1 transcript.

#### **IV.C.iii. Functional production of rCNT1 and $\Delta$ N31rCNT1 in *X. laevis* oocytes**

To confirm that the N-terminally truncated protein,  $\Delta$ N31rCNT1, encoded a functional nucleoside transporter, recombinant rCNT1 and  $\Delta$ N31rCNT1 were produced and tested in oocytes of *X. laevis* using established procedures for functional expression of CNT proteins (12,24). In the experiments of Figure IV-3, the uptake of 10  $\mu$ M [<sup>3</sup>H]uridine was measured over 30 min in oocytes that had been injected with  $\Delta$ N31rCNT1 in water, rCNT1 transcripts in water or water alone. Transport measurements were carried out in Xenopus Transport Buffer (XTB, section II.J.iii) that contained graded concentration of sodium (NaCl concentrations were 100 mM, 2 mM or 0 mM) to confirm that  $\Delta$ N31rCNT1 retained its sodium-dependent transport activity. rCNT1 stimulated the uptake of [<sup>3</sup>H]uridine above that of water-injected oocytes when assayed in XTB that contained 100 mM NaCl. Uridine uptake was reduced when measured in XTB containing 2 mM NaCl, and transport was reduced to background levels in the absence of NaCl.  $\Delta$ N31rCNT1 was also shown to stimulate the uptake of [<sup>3</sup>H]uridine above that of water-injected oocytes in XTB that contained 100 mM NaCl, although at levels reduced compared to rCNT1. Similarly,  $\Delta$ N31rCNT1 uridine transport activity was reduced when measured in XTB containing 2 mM NaCl, and was eliminated in the absence of NaCl. Together, these results confirmed the observation of the complementation assay indicating that  $\Delta$ N31rCNT1 is a functional nucleoside transporter protein. Furthermore, these results determined that  $\Delta$ N31rCNT1 retained sodium-dependence for transport.

#### **IV.C.iv. rCNT1myc, $\Delta$ N16rCNT1myc, $\Delta$ N23rCNT1myc, and $\Delta$ N31rCNT1myc complement a thymidine-transport deficiency in yeast**

To determine the importance of the N-terminal portion in production of functional transporter, a series of mutants were engineered that relied on initiation of translation from either the first predicted methionine residue or from each of several downstream methionine residues. In each instance the c-myc immunoeptope was added to the C-terminus of rCNT1 to enable immunodetection of the recombinant proteins. To ensure close promoter proximity of the initiating methionine, the cDNA sequences encoding each initiating methionine were cloned into the KpnI restriction site of the pYES2 vector, approximately 20 base-pairs downstream of the GAL1 promoter.

The experiments shown in Table IV-1 established that expression of the pYrCNT1myc cDNA rescued yeast from drug-imposed depletion of dTMP. Additionally, these experiments established that the truncated versions of rCNT1 ( $\Delta$ N16rCNT1myc,  $\Delta$ N23rCNT1myc and  $\Delta$ N31rCNT1myc), which relied on methionine residues downstream (methionine residues 17, 24 and 32, respectively) of the first predicted methionine for translation of initiation, also rescued yeast from drug-imposed depletion of dTMP. Yeast cells with pYrCNT1myc, pY $\Delta$ N16rCNT1myc, pY $\Delta$ N23rCNT1myc, pY $\Delta$ N31rCNT1myc or pYES2 were grown under conditions of thymidylate starvation in the presence of either galactose (inducer) or glucose (repressor) with various concentrations of thymidine. None were able to form colonies in thymidine-free medium whereas all did so in the presence of 1 mM thymidine, a concentration that allowed sufficient uptake by diffusion to support growth and therefore served as a positive control for growth. pYrCNT1myc-containing and truncated pYrCNT1myc-containing yeast also formed colonies in the presence of 100  $\mu$ M thymidine but only when plated on medium that was supplemented with galactose, the inducer required for efficient transcription of the cDNA insert in the pYES2 vector. In

contrast, there was no growth when yeast containing either of these plasmids were plated on medium with MTX/SAA that was supplemented with glucose, the repressor used to block transcription of the rCNT1 insert. These results indicated that expression of the cDNA encoding rCNT1myc was required to complement the growth arrest imposed by thymidylate starvation and were consistent with the acquisition of thymidine-transport capability resulting from growth in the presence of the inducer (galactose). Additionally, these results indicated that rCNT1myc retained the ability to transport thymidine when translation of initiation occurred via alternate downstream methionines, thereby resulting in truncated versions of rCNT1.

rCNT1myc-mediated complementation indicated that the recombinant protein was present at the yeast cell surface. However, when total yeast membranes were prepared from pYrCNT1myc containing cells (grown under selective conditions) and subjected to SDS-PAGE and immunoblotting with the anti-c-myc antibody the recombinant protein was not detected. This may have be due to low levels of recombinant protein production that were sufficient to permit thymidine to enter the yeast over the course of the experiment (3.5 d) but were not of sufficient quantity to visualize by immunoblotting.

#### **IV.C.v. hCNT1myc and $\Delta$ N23hCNT1myc complement a thymidine-transport deficiency in yeast**

The human pyrimidine nucleoside-specific concentrative transporter protein, hCNT1, was isolated by RT-PCR and hybridization cloning based on the rCNT1 sequence (15). hCNT1 was the second nucleoside transporter protein cDNA to become available and was tested for its ability to complement the thymidine transport deficiency of yeast. Additionally, to determine if a truncated version of hCNT1, which relied on downstream Met codon for initiation of translation, produced a functional transporter an hCNT1 mutant was engineered which relied on initiation of translation from the codon encoding Met-32. The cDNA sequences encoding each initiating methionine were cloned into the KpnI restriction site of the pYES2 vector, approximately 20 base pairs downstream of the GAL1

promoter. In each instance the c-myc epitope was added to the C-terminus of hCNT1 and  $\Delta$ N23hCNT1 generating hCNT1myc and  $\Delta$ N23hCNT1myc, respectively.

The experiments shown in Figure IV-4 established that expression of the hCNT1myc cDNA rescued yeast from drug-imposed depletion of dTMP. Additionally, these experiments established that the truncated version of hCNT1 ( $\Delta$ N23hCNT1myc), which relied on the codon for methionine-24 for initiation of translation, also rescued yeast from drug-imposed depletion of dTMP. Yeast cells with pYhCNT1myc, pY $\Delta$ N23hCNT1myc or pYES2 were grown under conditions of thymidylate starvation in the presence of either galactose (inducer) or glucose (repressor) with various concentrations of thymidine. None were able to form colonies in thymidine-free medium whereas all did so in the presence of 1 mM thymidine, the positive control for growth. pYhCNT1myc-containing and pY $\Delta$ N23hCNT1myc-containing yeast also formed colonies in the presence of 100  $\mu$ M thymidine but only when plated on medium that was supplemented with galactose, the inducer required for efficient transcription of the cDNA insert in the pYES2 vector. In contrast, there was no growth when yeast containing either of these plasmids were plated on medium with MTX/SAA that was supplemented with glucose, the repressor used to block transcription of the hCNT1 insert. These results indicated that expression of the cDNA encoding hCNT1myc was required to complement the growth arrest imposed by thymidylate starvation and were consistent with the acquisition of thymidine-transport capability resulting from growth in the presence of the inducer (galactose). Additionally, these results indicated that hCNT1myc retained the ability to transport thymidine when translation of initiation occurred via an alternate downstream methionine (Met-24) thereby resulting in a truncated version of hCNT1.

hCNT1myc-mediated complementation indicated that the recombinant protein was present at the yeast cell surface. However, as was the case with rCNT1myc, when total

yeast membranes were prepared from pYhCNT1myc containing cells (grown under selective conditions) and subjected to SDS-PAGE and immunoblotting with the anti-c-myc antibody the recombinant protein was not detected. This may have been due to low levels of recombinant protein production that were sufficient to permit thymidine to enter the yeast over the course of the experiment (4.5 d) but were not of sufficient quantity to visualize by immunoblotting.

#### **IV.C.vi. NUPCmyc complements a thymidine-transport deficiency in yeast**

NUPC was the first bacterial CNT family member to be identified (75) and has been characterized in the *X. laevis* oocyte expression system (77). The ability of a bacterial nucleoside transporter protein, NUPC, to be functionally produced in yeast was next examined. As was done with rCNT1 and hCNT1, the c-myc immunopeptide was added to the C-terminus of NUPC to enable immunodetection of the recombinant protein. The cDNA sequence encoding the initiating methionine was cloned into the KpnI restriction site of the pYES2 vector, approximately 20 base pairs downstream of the GAL1 promoter.

The experiments shown in Figure IV-5 established that expression of the NUPCmyc cDNA rescued yeast from drug-imposed depletion of dTMP. Yeast cells with pYNUPCmyc or pYES2 were grown under conditions of thymidylate starvation in the presence of either galactose (inducer) or glucose (repressor) with various concentrations of thymidine. None were able to form colonies in thymidine-free medium were as both did so in the presence of 1 mM thymidine, the positive control for growth. pYNUPCmyc-containing yeast also formed colonies in the presence of 100  $\mu$ M thymidine but only when plated on medium that was supplemented with galactose, the inducer required for efficient transcription of the cDNA insert in the pYES2 vector. In contrast, there was no growth when yeast containing either of these plasmids were plated on medium with MTX/SAA that was supplemented with glucose, the repressor used to block transcription of the NUPC insert. These results indicated that expression of the cDNA encoding the bacterial



nucleoside transporter protein, NUPC, was required to complement the growth arrest imposed by thymidylate starvation and were consistent with the acquisition of thymidine-transport capability resulting from growth in the presence of the inducer (galactose).

NUPCmyc-mediated complementation indicated that the recombinant protein was present at the yeast cell surface. Immunoblotting was performed to confirm the presence of recombinant NUPCmyc protein in pYNUPCmyc-containing yeast (Figure IV-6). Yeast cells with either pYNUPCmyc or pYES2 were subjected to thymidylate starvation in the presence of galactose (inducing conditions) and thymidine (40  $\mu$ M or 1 mM respectively) that permitted the yeast (pYNUPCmyc-containing or pYES2-containing) to grow at approximately the same rates. Immunoblotting of yeast membranes with anti-c-myc monoclonal antibodies demonstrated the presence of immunoreactive material in membranes of pYNUPCmyc-containing yeast that was not present in membranes of pYES2-containing yeast. The predominant immunoreactive species was observed as a band of 40 kDa. The predicted molecular mass of NUPC is 43 kDa.

#### **IV.C.vii. Effects of purine and pyrimidine nucleosides on rCNT1myc-, hCNT1myc- and NUPCmyc-dependent thymidine rescue**

The substrate specificities of rCNT1myc, hCNT1myc and NUPCmyc were examined in the experiments of Table IV-2 by assessing the effect of the presence of purine and pyrimidine nucleosides in the growth medium used in the complementation assay. The ability of a test compound to inhibit transporter-dependent thymidine growth would be indicative of either a substrate or inhibitor of the transporter. High concentrations of the pyrimidine nucleosides uridine and cytidine and the purine nucleoside adenosine completely inhibited rCNT1myc-, hCNT1myc-, and NUPCmyc-mediated complementation, guanosine and inosine had no effect. These data indicated that the apparent substrate specificities of recombinant rCNT1myc, hCNT1myc and NUPCmyc included pyrimidine nucleosides and adenosine. When the non-nucleoside transport inhibitors dilazep and

dipyridamole were added to the growth medium, there was no effect on colony formation compared to media that lacked the non-nucleoside inhibitors.

#### **IV.C.viii. Sequence comparison of known and putative concentrative nucleoside transport proteins**

The sequences of cDNAs encoding rCNT1, hCNT1 and NUPC were used in database analysis (e.g., BLAST searches) to identify orthologs and paralogs of the CNT family. The phylogenetic tree presented in Chapter 1 (Figure I-3) depicts relationships among known (possessing nucleoside transport activity) and putative (possessing sequence similarities and of unknown function) CNT family members among eukaryotes and prokaryotes. CNT-like sequences were found in a variety of mammalian (e.g., *H. sapiens*, *R. norvegicus*) and bacterial (e.g., *E. coli*, *H. pylori*, *H. influenzae*) species. An amino acid identity comparison matrix of the CNT family members examined in this Chapter is presented in Table IV-3. The high degree of sequence conservation among the mammalian and bacterial transporters and the open reading frames from *H. pylori* and *H. influenzae* suggested these open reading frames may encode functional members of the CNT family.

#### **IV.C.ix. The recombinant proteins encoded by open reading frames of *H. influenzae* (HI0519) and *H. pylori* (HP1180) complemented a thymidine-transport deficiency in yeast**

The open reading frames HI0519 (from *H. influenzae*) and HP1180 (from *H. pylori*) possess sequence similarities that place them within the CNT family. The complementation assay was used to determine if the proteins encoded by HI0519 and HP1180 possessed nucleoside transport activity.

The cDNA sequence encoding the initiating methionine for HI0519 and HP1180 was cloned into the KpnI restriction site of the pYES2 expression vector, approximately 20 base pairs downstream of the GAL1 promoter. The experiments of Table IV-4 established that expression of the HI0519 and HP1180 cDNAs rescued yeast from drug-imposed depletion of dTMP. Yeast cells with pYHP1180, pYHI0519 or pYES2 were grown under

conditions of thymidylate starvation in the presence of either galactose (inducer) or glucose (repressor) with various concentrations of thymidine. None were able to form colonies in thymidine-free medium whereas all did in the presence of 1 mM thymidine, the positive control for growth. pYHI0519-containing and pYHP1180-containing yeast also formed colonies in the presence of 100  $\mu$ M thymidine but only when plated on medium that was supplemented with galactose, the inducer required for efficient transcription of the cDNA insert in the pYES2 vector. In contrast, there was no growth when yeast containing either of these plasmids were plated on medium with MTX/SAA that was supplemented with glucose, the repressor used to block transcription of the cDNA insert. These results indicated that expression of the cDNAs encoding HP1180 or HI0519 were required to complement the growth arrest imposed by thymidylate starvation and were consistent with the acquisition of thymidine-transport capability resulting from growth in the presence of the inducer (galactose).

The apparent substrate specificity of HI0519 was examined in the experiments of Table IV-5 by determining the effect of the presence of purine and pyrimidine nucleosides in the growth medium used in the complementation assay. High concentrations of pyrimidine nucleosides (uridine, cytidine) and purine nucleosides (adenosine, guanosine, inosine) completely inhibited HI0519-mediated complementation. These data suggested that recombinant HI0519 was apparently selective for both purine and pyrimidine nucleosides.

#### **IV.D. DISCUSSION**

Oocytes of *X. laevis* have been used to both isolate and express cDNAs encoding nucleoside transport proteins (12-16,18,19), and more recently, the nucleoside transport encoding cDNAs have been functionally expressed in transiently transfected cultured mammalian cell lines (21,29). However, both of these expression systems have technical and cost considerations that make the development of an alternate system desirable. The ease of manipulation and established molecular techniques (101) make *S. cerevisiae* an attractive system in which to study recombinant membrane proteins. We describe here the use of *S. cerevisiae* as a model expression system to study human, rat and bacterial CNTs.

We took advantage of a thymidine transport deficiency in *S. cerevisiae* to be used as the basis of a selection strategy in which yeast were rescued from dTMP starvation (imposed by treatment MTX and SAA), when cultured in the presence of exogenously supplied thymidine and possessing a functionally active nucleoside transport protein at the cell surface. In this work, it was found that the full-length nucleoside transport proteins rCNT1, hCNT1 and NUPC were able to complement the thymidine transport-defective phenotype in yeast. Functional production of these proteins was dependent on the close proximity of the cDNA encoding the initiating methionine to the promoter (GAL1) found within the expression vector. Initial efforts to express rCNT1 in yeast indicated that yeast harbouring pYhCNT1 were unable to complement the imposed dTMP deficiency; however, yeast harbouring a deleted version of rCNT1 (pYΔN31rCNT1), which relied on initiation of translation from methionine 32 within the rCNT1 open reading frame, was able to complement cell growth. These results indicated that functional expression of rCNT1 was dependent on either (i) removal of the N-terminal 31 amino acid residues of the recombinant protein, (ii) bringing the cDNA encoding the initiating methionine in close proximity to the GAL1 promoter or (iii) both. The questions of the influence of charged residues or promoter proximity were resolved by subjecting either full-length or truncated

version of rCNT1 and hCNT1 (missing up to the first 31 amino acid residues) to dTMP starvation in the presence of thymidine in the complementation assay. In each instance the mutant version of the nucleoside transporter cDNA was cloned into the KpnI restriction site of the pYES2 vector, which is immediately 3' (within ~ 20 base pairs) to the GAL1 promoter. The ability of all the versions of rCNT1 and hCNT1 (both full-length and truncated) to complement the nucleoside transport-defective phenotype, indicated that recombinant nucleoside transport proteins were produced and some fraction was correctly targeted to the yeast cell surface, allowing the yeast to take up extracellular thymidine.

rCNT1, hCNT1 and NUPC are integral membrane proteins and thus was expected to be present in membrane fractions of yeast expressing the respective plasmid. Immunoblotting of yeast membranes with the anti-c-myc monoclonal antibody demonstrated the presence of immunoreactive protein in pYNUPCmyc-containing yeast but not in pYES2-expressing yeast. The predominant immunoreactive species exhibited an apparent molecular mass of 40 kDa and thus corresponded to NUPC, the predicted molecular mass of NUPC is 43 kDa. The inability to visualize recombinant rCNT1myc and hCNT1myc likely reflected the low abundance of these proteins that was sufficient to complement the imposed dTMP deficiency in yeast over the course of the assay, yet sufficiently low to prevent detection by immunoblotting.

We examined the substrate specificity of recombinant rCNT1myc, hCNT1myc and NUPCmyc by testing the ability of other nucleosides to block thymidine rescue of the growth inhibition imposed by MTX and SAA in the complementation assay. It was found that pYrCNT1-, pYhCNT1-, and NUPCmyc-containing yeast failed to grow in the presence of high concentrations of uridine, cytidine or adenosine whereas growth was unaffected by guanosine or inosine. These findings suggested that thymidine, uridine, cytosine and adenosine were substrates of these transporters, whereas guanosine and inosine were not. These findings are consistent with previous studies that showed the substrates of rCNT1, hCNT1, and NUPC to include pyrimidine nucleosides (thymidine,

uridine, cytidine) and the purine nucleoside adenosine to be a high-affinity low-capacity substrate of these nucleoside transport proteins (12,15,29). The two inhibitors of equilibrative nucleoside transport processes, dilazep and dipyridamole, had no effect on the growth of the nucleoside transporter-containing yeast.

Analysis of microbial genome databases identified the open reading frames HI0519 (from *H. influenzae*) and HP1180 from (*H. pylori*) as encoding proteins that are structural members of the CNT family. The limited sequence identity of HI0519 and HP1180 with purine nucleoside and pyrimidine nucleoside-specific members of the CNT family suggested that there might be conservation of function between HI0519, HP1180 and CNT family members. Therefore, the complementation assay in *S. cerevisiae* was used to determine if the HI0519 and HP1180 recombinant proteins possessed nucleoside transport activity. Both pYHI0519 and pYHP1180 were able to complement the imposed dTMP starvation in yeast indicative of the capacity for the inward transport of thymidine of both transporters. The substrate specificity of recombinant HI0519 was examined by assessing the ability of other nucleosides to block transporter-mediated rescue of the growth inhibition imposed by MTX and SAA in the complementation assay. pYHI0519-containing yeast failed to grow in the presence of high concentrations of uridine, cytidine, adenosine, guanosine and inosine. These findings suggested that the pyrimidine and purine nucleosides tested were substrates of HP1180. Thus, HI0519 appeared to encode a unique member of the CNT family that is not strictly pyrimidine or purine specific, but rather a novel broadly specific CNT protein.

In conclusion, we have developed the yeast *S. cerevisiae* as a model expression system to functionally express nucleoside transporter proteins. The pyrimidine nucleoside-specific CNT proteins examined (rCNT1, hCNT1, NUPC) were all functionally expressed in yeast with a substrate specificity that was consistent with that previously reported (12,15,29,75). Furthermore, it was determined that truncated versions of rCNT1 and hCNT1 (lacking upto 32 amino acid residues) possessed nucleoside transport activity.

Having demonstrated the efficacy of the yeast model system we were able to assess the ability of the CNT related proteins encoded by HI0519 and HP1180 from *H. influenzae* and *H. pylori*, respectively, to complement cell growth using the MTX/SAA selection strategy. Both HI0519 and HP1180 were found to encode previously unidentified nucleoside transporter proteins. Furthermore, HI0519 was found to possess novel activity; in contrast to known members of the CNT family which are either purine or pyrimidine nucleoside specific. Recombinant HI0519 was found to be broadly specific to both purine and pyrimidine nucleosides.

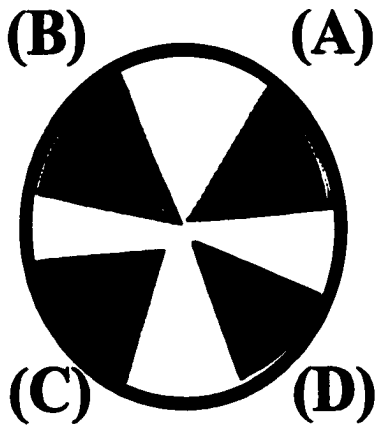
**Figure IV-1      Functional complementation of a thymidine transport deficiency in yeast harbouring pY $\Delta$ N31rCNT1 but not pYrCNT1**

Yeast cells containing either pYES2, pYrCNT1 or pY $\Delta$ N31rCNT1 were streaked on CMM/GAL/MTX/SAA (gal) medium (inducing conditions, thymidylate starvation) that contained 0  $\mu$ M thymidine (A), 1 mM thymidine (B) or 100  $\mu$ M thymidine (C). Yeast cells were also streaked on CMM/GLU/MTX/SAA (glu) medium (repressive conditions, thymidylate starvation) that contained 100  $\mu$ M thymidine (D). Growth on plates was assessed after 3.5 days. Three separate experiments, one of which is presented, yielded similar results.

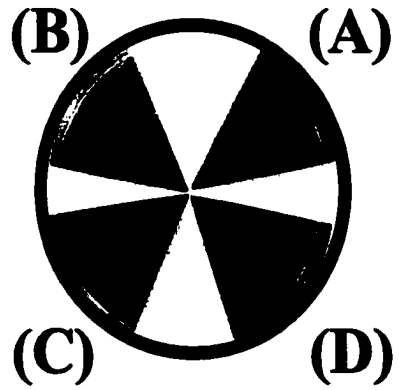


# Figure IV-1

**pYES2**



**pYrCNT1**



**pY $\Delta$ N31rCNT1**

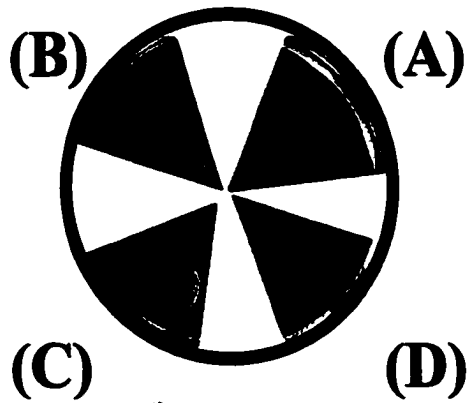


**Figure IV-2 Production of  $\Delta$ N31rCNT1 and rCNT1 mRNA yeast**

Total RNA from yeast with pYES2 (lanes 1,2), pYrCNT1 (lanes 3,4), or pY $\Delta$ N31rCNT1 (lanes 5,6), prepared as described in Chapter II, section II.D, was subjected to Northern analysis with a <sup>32</sup>P-labelled rCNT1 cDNA fragment (nt 1-1941) and then detected by autoradiography. Growth conditions were as follows: CMM/GLU medium (lanes 2,4,6) or CMM/GAL (lanes 1,3,5) as indicated.

**Figure IV-2**

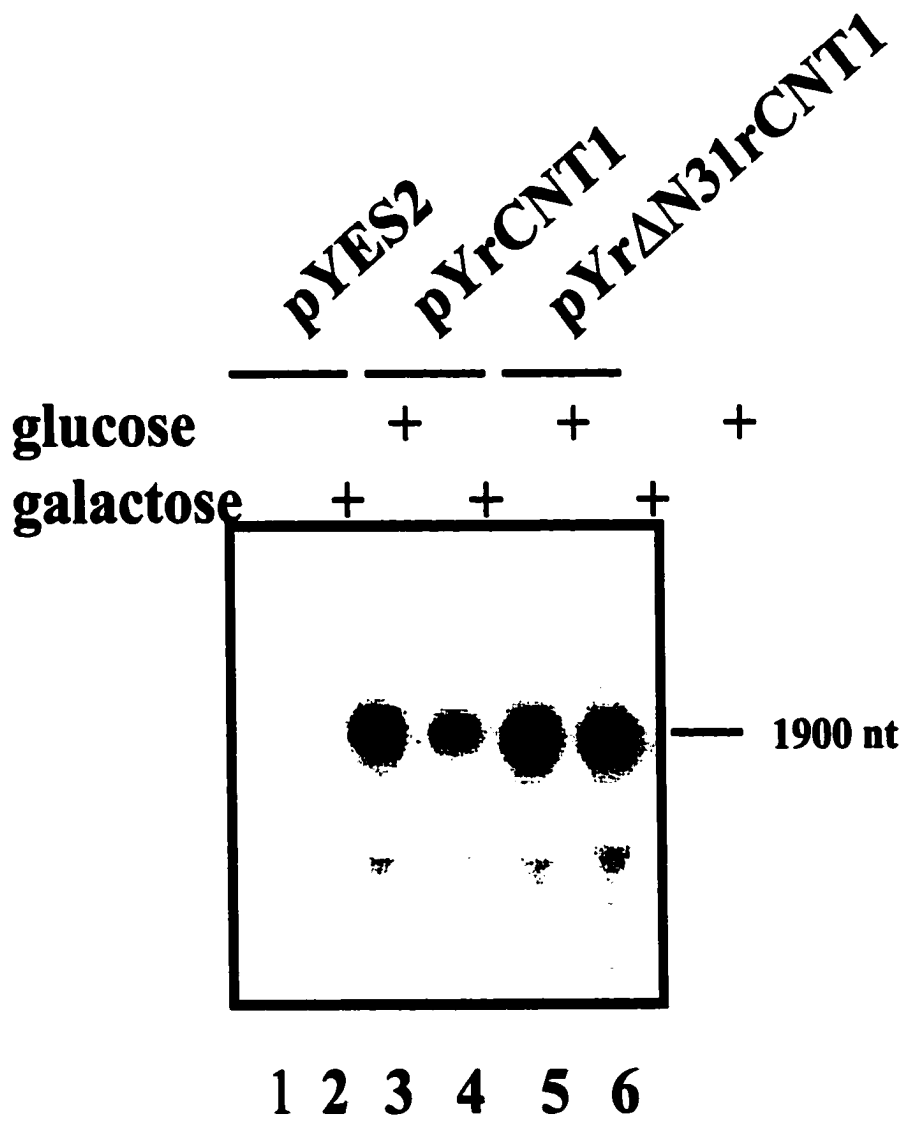


**Figure IV-3 rCNT1- and  $\Delta$ N31rCNT1-mediated uptake of uridine**

Oocytes were injected with water alone (*open bar*) or with water containing mRNA transcripts for rCNT1 (*closed bar*) or  $\Delta$ N31rCNT1 (*hatched bar*), as described in the Chapter II, section II.J.iii. After incubation for 3 days, the uptake of 10  $\mu$ M [ $^3$ H]uridine was measured (30 min, 20°C) into oocytes assayed in the presence of graded concentrations of NaCl (as indicated). The radioactive accumulation of [ $^3$ H]uridine was determined by scintillation counting of individual oocytes. Each point represents the mean $\pm$ S.D. of 8-10 oocytes. Two separate experiments, one of which is presented, yielded similar results.

1

.

**Figure IV-3**

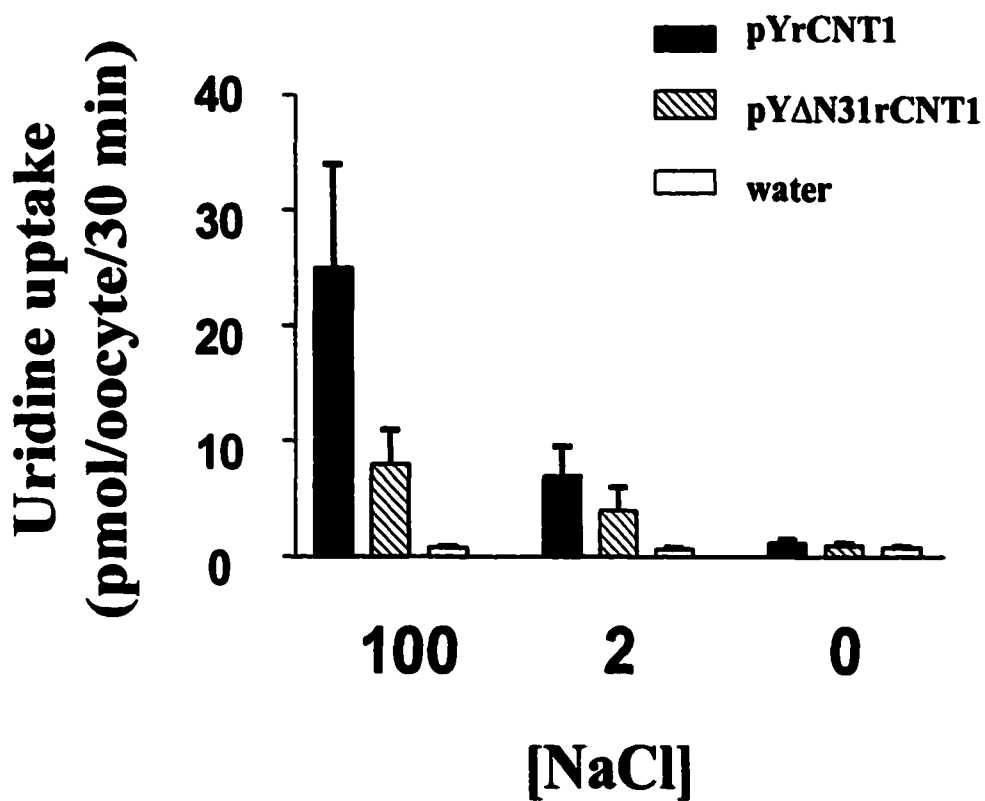


**Figure IV-4      Functional complementation of a thymidine transport deficiency in yeast by recombinant hCNT1 and  $\Delta$ N23hCNT1myc**

Yeast cells containing pYES2, pYhCNT1myc or pY $\Delta$ N23hCNT1myc were streaked on solid CMM/GAL/MTX/SAA medium (inducing conditions, thymidylate starvation) that contained 0  $\mu$ M thymidine (A), 1 mM thymidine (B) or 100  $\mu$ M thymidine (C). Yeast cells were also streaked on CMM/GLU/MTX/SAA medium (repressive conditions, thymidylate starvation) that contained 100  $\mu$ M thymidine (D). Growth on plates was assessed after 4.5 days. Three separate experiments, one of which is presented, yielded similar results.

## Figure IV-4

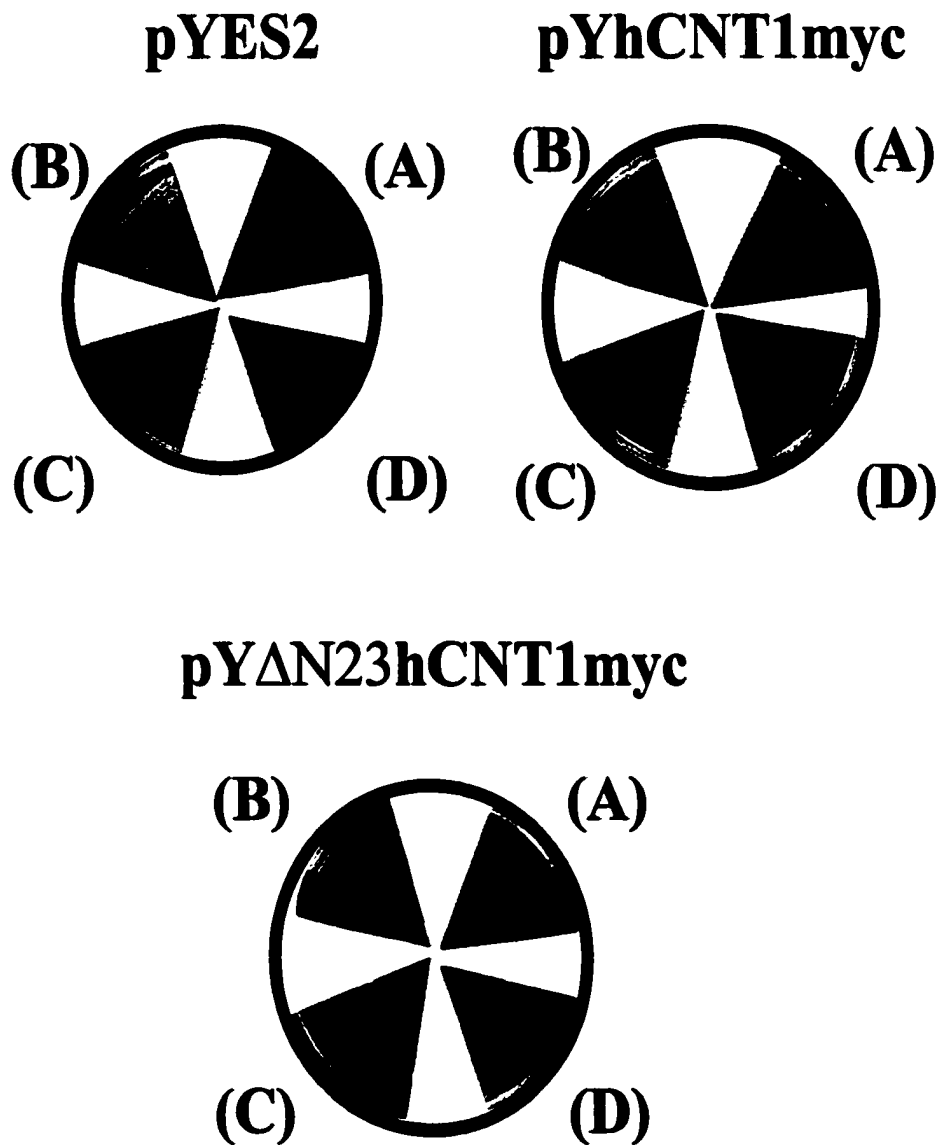


**Figure IV-5      Functional complementation of a thymidine transport deficiency in yeast by recombinant NUPCmyc**

Yeast cells containing either pYES2 or pYNUPCmyc were streaked on CMM/GAL/MTX/SAA medium (inducing conditions, thymidylate starvation) that contained 0  $\mu$ M thymidine (A), 1 mM thymidine (B) or 100  $\mu$ M thymidine (C). Yeast cells were also streaked on CMM/GLU/MTX/SAA medium (repressive conditions, thymidylate starvation) that contained 100  $\mu$ M thymidine (D). Growth on plates was assessed after 3.5 days. Three separate experiments, one of which is presented, yielded similar results.



# Figure IV-5

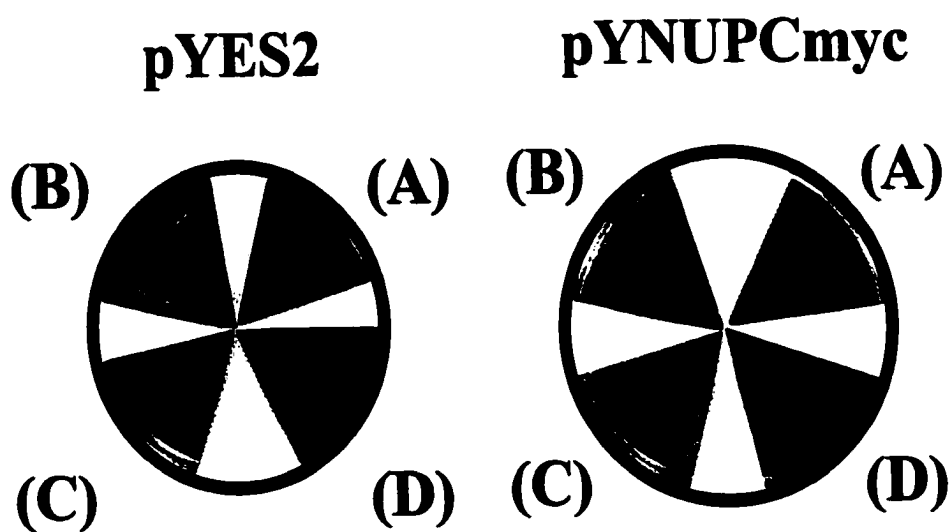


**Figure IV-6      Production of recombinant NUPCmyc protein**

Membranes, prepared as described in Chapter II, section II.E, from yeast with pYES2 (lane 1) or pYNUPCmyc (lane 2) grown in CMM/GAL/MTX/SAA medium that contained 1 mM or 40  $\mu$ M thymidine respectively, were subjected to immunoblotting with the 9E10 anti-c-myc monoclonal antibody. The positions of molecular mass markers are indicated to the left of the figure.

**Figure IV-6**

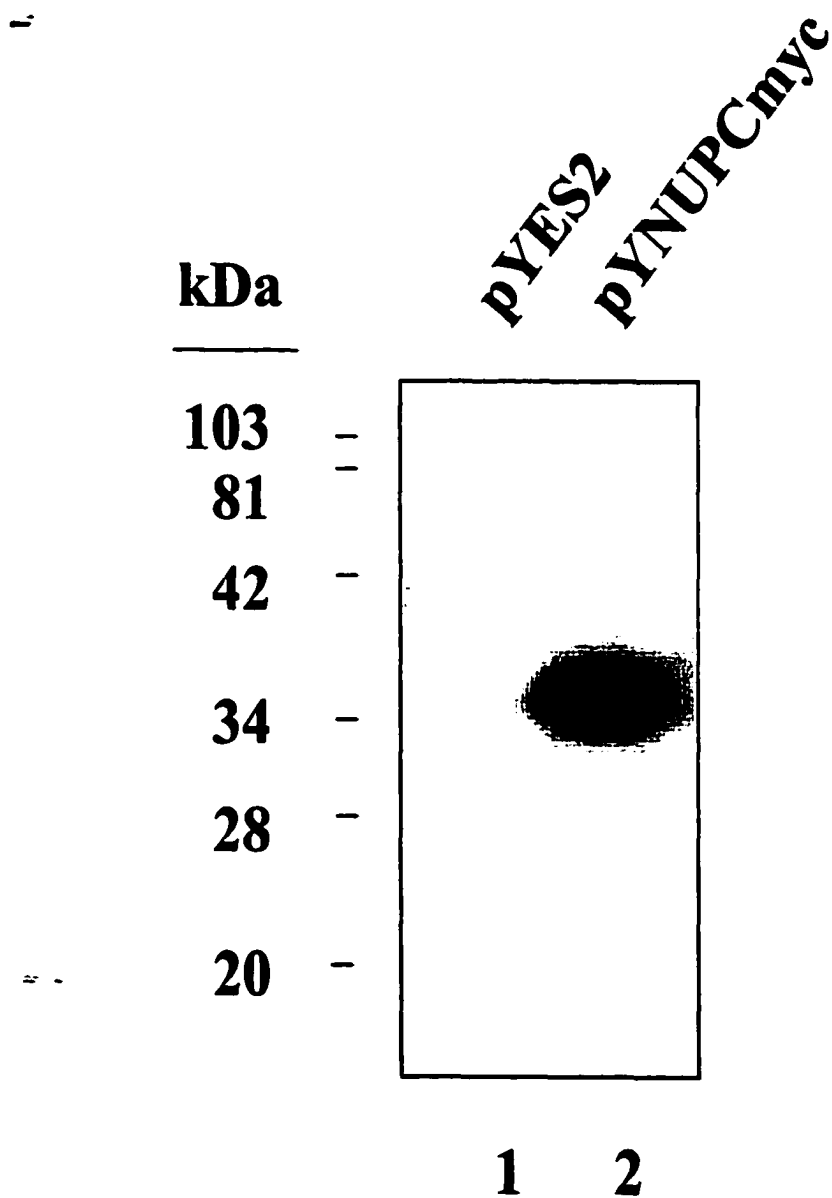


**Table IV-1**

	<b>Thymidine (<math>\mu</math>M)</b>					
	<b>0 <math>\mu</math>M</b>		<b>1000 <math>\mu</math>M</b>		<b>100 <math>\mu</math>M</b>	
	<b>gal</b>	<b>glu</b>	<b>gal</b>	<b>glu</b>	<b>gal</b>	<b>glu</b>
<b>pYES2</b>	-	-	+	+	-	-
<b>pYrCNT1myc</b>	-	-	+	+	+	-
<b>pY<math>\Delta</math>N16rCNT1myc</b>	-	-	+	+	+	-
<b>pY<math>\Delta</math>N24rCNT1myc</b>	-	-	+	+	+	-
<b>pY<math>\Delta</math>N31rCNT1myc</b>	-	-	+	+	+	-

**Table IV-1 Functional complementation of a thymidine transport deficiency in yeast by recombinant rCNT1myc,  $\Delta$ N16rCNT1myc,  $\Delta$ N23rCNT1myc, and  $\Delta$ N31rCNT1myc**

Yeast cells containing either pYES2, pYrCNT1myc, pY $\Delta$ N16rCNT1myc, pY $\Delta$ N23rCNT1myc or pY $\Delta$ N31rCNT1myc were streaked on CMM/GAL/MTX/SAA (gal) medium (inducing conditions, thymidylate starvation) that contained 0  $\mu$ M thymidine, 1 mM thymidine or 100  $\mu$ M thymidine. Yeast cells were also streaked on CMM/GLU/MTX/SAA (glu) medium (repressive conditions, thymidylate starvation). Growth on plates was assessed after 3.5 days, "+" denotes growth, "-" denotes the absence of growth. Three separate experiments yielded similar results.

**Table IV-2**

	<u>pYES2</u>	<u>pYrCNT1myc</u>	<u>pYhCNT1myc</u>	<u>pYNUPCmyc</u>
<b>alone</b>	-	+	+	+
<b>uridine</b>	-	-	-	-
<b>cytidine</b>	-	-	-	-
<b>adenosine</b>	-	-	-	-
<b>guanosine</b>	-	+	+	+
<b>inosine</b>	-	+	+	+
<b>dilazep</b>	-	+	+	+
<b>dipyridamole</b>	-	+	+	+

**Table IV-2 Inhibition of rCNT1myc-, hCNT1myc-, and NUPCmyc-mediated complementation of a thymidine transport deficiency in yeast**

Yeast cells containing either pYES2, pYrCNT1myc, pYhCNT1myc or pYNUPCmyc were streaked on CMM/GAL/MTX/SAA medium (inducing conditions, thymidylate starvation) that contained 0  $\mu$ M thymidine, 1 mM thymidine or 100  $\mu$ M thymidine, alone, or that contained a competing test compound at 1 mM (indicated on left). Growth on plates was assessed after 3.5 days, "+" denotes growth, "-" denotes the absence of growth. Growth of yeast at the test concentration (100  $\mu$ M) is presented. Growth on media that contained 0  $\mu$ M and 1000  $\mu$ M was the same as was observed previously for pYrCNT1myc (Figure IV-1), pYhCNT1myc (Figure IV-4) and pYNUPCmyc (Figure IV-5). Three separate experiments yielded similar results.

**Table IV-3 Amino acid identity comparison of members of the CNT family**  
 A comparison matrix of amino acid identity is presented for members of the concentrative nucleoside transporter family. Comparisons were performed using "Bestfit" software from GCG.

	<b>rCNT1</b>	<b>hCNT1</b>	<b>NUPC</b>	<b>HI0519</b>	<b>HP1180</b>
<b>rCNT1</b>	100				
<b>hCNT1</b>	86	100			
<b>NUPC</b>	37	37	100		
<b>HI0519</b>	38	39	31	100	
<b>HP1180</b>	38	36	29	58	100

**Table IV-4**

	<b>Thymidine (<math>\mu\text{M}</math>)</b>					
	<b>0 <math>\mu\text{M}</math></b>		<b>1000 <math>\mu\text{M}</math></b>		<b>100 <math>\mu\text{M}</math></b>	
	<b>gal</b>	<b>glu</b>	<b>gal</b>	<b>glu</b>	<b>gal</b>	<b>glu</b>
<b>pYES2</b>	-	-	+	+	-	-
<b>pYHI0519</b>	-	-	+	+	+	-
<b>pYHP1180</b>	-	-	+	+	+	-

**Table IV-4 Functional complementation of a thymidine transport deficiency in yeast by recombinant HI0519 and HP1180**

Yeast cells containing either pYES2, pYHI0519 or pYHP1180 were streaked on CMM/GAL/MTX/SAA medium (inducing conditions, thymidylate starvation) that contained 0  $\mu\text{M}$  thymidine, 1 mM thymidine or 100  $\mu\text{M}$  thymidine. Yeast cells were also streaked on CMM/GLU/MTX/SAA (glu) medium (repressive conditions, thymidylate starvation). Growth on plates was assessed after 3.5 days, "+" denotes growth, "-" denotes the absence of growth. Three separate experiments yielded similar results.

**Table IV-5**

---

	<b><u>pYES2</u></b>	<b><u>pYHI0519</u></b>
<b>alone</b>	-	+
<b>uridine</b>	-	-
<b>cytidine</b>	-	-
<b>adenosine</b>	-	-
<b>guanosine</b>	-	-
<b>inosine</b>	-	-

---

**Table IV-5 Inhibition of HI0519-mediated complementation of a thymidine transport deficiency in yeast**

Yeast cells containing either pYES2 or pYHI0519 were streaked on CMM/GAL/MTX/SAA medium (inducing conditions, thymidylate starvation) that contained 0  $\mu$ M thymidine, 1 mM thymidine or 100  $\mu$ M thymidine, alone, or that contained a competing test compound at 1 mM (indicated on left). Growth on plates was assessed after 3.5 days, "+" denotes growth, "-" denotes the absence of growth. Growth of yeast at the test thymidine concentration (100  $\mu$ M) is presented. Growth on media that contained 0  $\mu$ M and 1000  $\mu$ M was the same as was observed previously for pYHI0519 (Table IV-4). Three separate experiments yielded identical results.



**V.**

**Functional production of the human equilibrative nucleoside transporter  
(hENT1) in *Saccharomyces cerevisiae*<sup>1</sup>**

<sup>1</sup>*(A version of this chapter has been reported previously (139))*

## V.A. ABSTRACT

In the previous chapter concentrative nucleoside transporter proteins from human, rat and *E. coli* were functionally expressed in *S. cerevisiae*. Development of *S. cerevisiae* as a model expression system provided the platform from which to further exploit the yeast expression system to characterize recombinant nucleoside transporter proteins. Recombinant human equilibrative nucleoside transporter (hENT1) was produced in *S. cerevisiae*, thereby allowing the development of methods to compare the binding of inhibitors of equilibrative nucleoside transport to wild-type hENT1 and a N-glycosylation-defective mutant of hENT1. Equilibrium binding of [<sup>3</sup>H]NBMPR to hENT1-producing yeast revealed a single class of high-affinity sites that were shown to be in membrane fractions by (i) equilibrium binding (means ± S.D.) of [<sup>3</sup>H]NBMPR to intact yeast ( $K_d$ ,  $1.2 \pm 0.2$  nM;  $B_{max}$ ,  $5.0 \pm 0.5$  pmol/mg of protein) and membranes ( $K_d$ ,  $0.7 \pm 0.2$  nM;  $B_{max}$ ,  $6.5 \pm 1$  pmol/mg of protein), and (ii) reconstitution of hENT1-mediated [<sup>3</sup>H]thymidine transport into proteoliposomes that was potently inhibited by NBMPR. Dilazep and dipyridamole inhibited NBMPR binding to hENT1 with  $IC_{50}$  values of  $130 \pm 10$  and  $380 \pm 20$  nM respectively. The role of N-linked glycosylation in the interaction of NBMPR with hENT1 was examined by quantification of binding of [<sup>3</sup>H]NBMPR to yeast producing either wild-type hENT1 or a glycosylation-defective mutant (hENT1/N48Q) in which Asn-48 was converted into Gln. The  $K_d$  for binding of NBMPR to hENT1/N48Q was  $10.5 \pm 1.6$  nM, indicating that the replacement of an Asn residue with Gln decreased the affinity of hENT1 for NBMPR. The decreased affinity of hENT1/N48Q for NBMPR was due to an increased rate of dissociation ( $k_{off}$ ) and a decreased rate of association ( $k_{on}$ ) of specifically bound [<sup>3</sup>H]NBMPR; the values for hENT1-producing and hENT1/N48Q-producing yeast were, respectively,  $0.14 \pm 0.02$  and  $0.36 \pm 0.05$  min<sup>-1</sup> for  $k_{off}$  and  $1.2 \times 10^8$  and  $0.40 \times 10^8$  M<sup>-1</sup>min<sup>-1</sup> for  $k_{on}$ . These results indicated that the conservative conversion of an Asn

**residue into Gln at position 48 of hENT1 and/or the loss of N-linked glycosylation capability altered the binding characteristics of the transporter for NBMPR.**

## **V.B. INTRODUCTION**

The human *es* cDNA (hENT1) was isolated from a human placental cDNA library using amino acid sequence obtained from N-terminal sequencing of the purified human erythrocyte *es* transporter (18). hENT1 is predicted to encode a protein of 456 amino acid residues with a molecular mass of 50.2 kDa, three potential N-linked glycosylation sites and 11 transmembrane domains (18). The predicted topology of hENT1 assumes a single N-linked glycosylation site, which was thought to be in the large extracellular loop between the first two transmembrane domains from the N terminus (18) on the basis of an earlier demonstration that the *es* transporter of human erythrocytes is glycosylated very close to one end of the protein (140). The assignment of Asn-48 as the site of the N-linked glycosylation of hENT1 was confirmed by an analysis of the electrophoretic mobility of recombinant hENT1 in which the Asn was replaced with Gln (M. Sundaram, S.Y.M. Yao, E. Chomey, C.E. Cass, S.A. Baldwin and J.D. Young, unpublished work). The role of N-linked glycosylation in the biosynthetic processing and function of hENT1 is not known. The perturbation of N-linked glycosylation of membrane proteins in a murine cell line that possesses three nucleoside transport processes produced complex changes in uridine transport kinetics but had little, if any, effect on the abundance or apparent affinity of the *es* transporter for NBMPR (112,140).

The experiments of chapter IV demonstrated that cDNAs encoding the concentrative nucleoside transporters can be expressed in the yeast *S. cerevisiae* using the phenotypic complementation assay (105,106) in which the growth of a yeast strain that is deficient in thymidine transport is assessed under selection conditions that prevent the production of dTMP. The work described in this chapter was undertaken to determine if the cDNA encoding hENT1 could be similarly expressed and, if so, to develop methods for analysis of interaction of hENT1 with permeants and inhibitors. Described here is the demonstration of the functional expression of hENT1 cDNA in *S. cerevisiae* by the

following criteria: (i) survival of yeast under the selection conditions, (ii) the presence of hENT1 mRNA and protein in yeast, (iii) mediated uptake of thymidine by intact yeast and proteoliposomes reconstituted from detergent-solubilized membranes, (iv) the inhibition of thymidine uptake by NBMPR, and (v) the high-affinity binding of NBMPR to intact yeast and yeast membranes. The role of N-linked glycosylation in hENT1 function was examined by comparing the equilibrium binding of [<sup>3</sup>H]NBMPR to yeast producing either wild-type hENT1 or a mutant in which Asn-48 was converted into Gln (hENT1/N48Q). hENT1/N48Q exhibited a decreased affinity for NBMPR relative to that of hENT1, which was due to an increase in the dissociation rate and a decrease in the association rate. The apparent affinities of hENT1/N48Q for dipyridamole and dilazep, which were examined by assessing their relative abilities to inhibit the binding of [<sup>3</sup>H]NBMPR under equilibrium conditions, increased relative to that of hENT1. The results, which demonstrated the production of recombinant hENT1 in yeast in quantities sufficient for analysis of the equilibrium binding and dissociation kinetics of the prototypic inhibitor (NBMPR) of *es*-mediated transport in mammalian cells, support earlier conclusions that the transport inhibitors (NBMPR, dipyridamole, and dilazep) bind to the *es* transport protein at or near the nucleoside recognition site.

## **V.C. RESULTS**

### **V.C.i. pYhENT1 complementation of a thymidine transport deficiency in yeast**

The results of Chapter IV suggested that introduction of a nucleoside transporter cDNA in close proximity to the GAL1 promoter, found within the pYES2 expression vector, may be an important factor in the functional expression of the introduced cDNA. The hENT1 cDNA was cloned into pYES2 vector in the same position (6 base pairs downstream of the GAL1 promoter in the KpnI and SphI restriction sites) as was used successfully for the CNTs in Chapter IV. The experiments shown in Figure V-1 established that expression of the hENT1 cDNA rescued yeast from drug-imposed depletion of dTMP. Yeast cells with pYhENT1 or pYES2 were grown under conditions of thymidylate starvation in the presence of either galactose (inducer) or glucose (repressor) with various concentrations of thymidine. pYES2-containing and pYhENT1-containing yeast were unable to form colonies in thymidine-free medium (Figure V-1A) but did so in the presence of 1 mM thymidine (Figure V-1B). pYhENT1-containing yeast also formed colonies in the presence of 10  $\mu$ M thymidine but only when plated on medium that was supplemented with galactose, the inducer required for efficient transcription of the cDNA insert in the pYES2 vector (Figure V-1C). There was no growth when pYhENT1-containing yeast cells were plated on medium with MTX/SAA that was supplemented with glucose, the repressor used to block transcription of the hENT1 insert (Figure V-1D). These results indicated that expression of the cDNA encoding hENT1 was required to complement the growth arrest imposed by thymidylate starvation and were consistent with the acquisition of thymidine-transport capability resulting from growth in the presence of the inducer (galactose).

### **V.C.ii. Production of hENT1 mRNA and protein**

The ability of pYhENT1 to rescue yeast subjected to thymidylate starvation implied expression of the hENT1 cDNA insert. Northern analysis was performed to demonstrate that mRNA corresponding to hENT1 cDNA was present in pYhENT1-containing yeast but not in pYES2-containing yeast (Figure V-2A). RNA samples were prepared from yeast cells with either pYhENT1 or pYES2 that were cultured (i) in the presence of drugs in conditions under which extracellular thymidine could be salvaged for growth (CMM/GAL/MTX/SAA plus 40  $\mu$ M or 1 mM thymidine, respectively) or (ii) in the absence of drugs under conditions that either induced or repressed transcription of the cDNA insert. A single band of 1650 nt was detected in pYhENT1-containing yeast grown in medium with galactose and to a smaller extent in pYhENT1-containing yeast grown in medium with glucose. No signal was present in the pYES2-containing cells under any of the experimental conditions. These results, which demonstrated the presence of hENT1 mRNA in cells with pYhENT1, indicated enhanced transcription of hENT1 cDNA by activation of the Gal1 promoter.

Immunoblotting was performed to confirm the presence of recombinant hENT1 protein in pYhENT1-containing yeast (Figure V-2B). Yeast cells that had been transformed with either pYhENT1 or pYES2 were subjected to thymidylate starvation in the presence of galactose (inducing conditions) and either 40  $\mu$ M or 1 mM thymidine, respectively; that cultures were established under conditions that permitted the pYhENT1-containing and pYES2-containing yeast to grow at approximately the same rates. Immunoblotting with anti-hENT1 polyclonal antibodies directed against a synthetic peptide epitope (hENT1 residues 254-272) demonstrated the presence of immunoreactive material in membranes of pYhENT1-containing yeast that was not present in membranes of pYES2-containing yeast. The predominant immunoreactive species was observed as a broad band of 40-45 kDa; two minor immunoreactive species of 80 and 120 kDa were also observed. The predicted molecular mass of non-glycosylated hENT1 is 50.2 kDa.

### **V.C.iii. Effects of inhibitors of nucleoside transport on hENT1-dependent thymidine rescue**

NBMPR, dilazep and dipyridamole are potent inhibitors of the native *es*-transport process and have been used as pharmacological probes in the identification of *es*-mediated processes (1,3). hENT1-dependent complementation in yeast was assessed in the presence of inhibitor concentrations known to block activity of the *es*-mediated processes (Table V-1). None of the inhibitors blocked colony formation by either pYES2-containing or pYhENT1-containing yeast in the presence of a high concentration (1 mM) of thymidine, indicating the ability of yeast to survive if provided with a usable source of thymidine. The ability of the inhibitors to block thymidine rescue of pYhENT1-containing yeast at low thymidine concentrations indicated that recombinant hENT1 had retained its ability to recognize and be inhibited by NBMPR, dilazep and dipyridamole.

### **V.C.iv. Yeast cells with hENT1 exhibit increased cellular uptake of [<sup>3</sup>H]thymidine**

Results of the complementation assay indicated acquisition of thymidine transport capability in yeast producing recombinant hENT1, suggesting that it should be possible to also directly measure cellular uptake of [<sup>3</sup>H]thymidine. The uptake of 1.0 μM [<sup>3</sup>H]thymidine was measured in yeast with either pYhENT1 or pYES2 that had been cultured in MTX/SAA-containing medium with the inducer and a thymidine supplement (40 μM or 1 mM respectively) to allow growth (Figure V-3). Thymidine uptake by pYhENT1-containing yeast was greater than that by pYES2-containing yeast (Figure V-3, Panel A) and was inhibited by the addition of an excess of unlabeled thymidine (Figure V-3, Panel B). These results indicated that the expression of pYhENT1 was accompanied by acquisition of the capacity for cellular uptake of thymidine by a process that was mediated since it could be eliminated by isotope dilution. The addition of any one of the three *es* transport inhibitors (NBMPR, dilazep or dipyridamole) decreased thymidine uptake by pYhENT1-containing yeast to levels only slightly above those observed with pYES2-



containing yeast (Figure V-3, Panel B). The inhibitor-sensitive nature of thymidine uptake was a further indication that pYhENT1-containing yeast, when grown in the presence of galactose, produced functional recombinant hENT1.

#### **V.C.v. Binding of [<sup>3</sup>H]NBMPR to hENT1-producing yeast**

Equilibrium binding studies with human erythrocytes and membrane vesicles have yielded values for binding-site numbers ( $B_{max}$ ) and affinities ( $K_d$ ) that represent the interaction of [<sup>3</sup>H]NBMPR with the *es* transporter protein (4), now known to be hENT1 (1,18). Equilibrium binding of [<sup>3</sup>H]NBMPR to pYhENT1-containing yeast was examined under conditions similar to those used previously in studies with mammalian cells (112). Yeast cells were incubated with 8.0 nM [<sup>3</sup>H]NBMPR alone or in the presence of 10  $\mu$ M dilazep, a tight-binding competitive inhibitor of *es*-mediated transport that is commonly used to distinguish between specific and non-specific binding of NBMPR to the nucleoside recognition site of the transporter (120,121). Equilibrium was reached within 20-30 min of exposure of pYhENT1-containing yeast to [<sup>3</sup>H]NBMPR (Figure V-4A). In subsequent binding experiments, cells (or membrane vesicles) were incubated with [<sup>3</sup>H]NBMPR for 40 min to ensure equilibrium between free and bound ligand.

The presence of high levels of dilazep-sensitive binding of [<sup>3</sup>H]NBMPR to pYhENT1-containing yeast, when grown under inducing conditions, suggested that it would be possible to use equilibrium binding of [<sup>3</sup>H]NBMPR to quantify the functional recombinant transporter in yeast. Studies with the purified *es* transporter of human erythrocytes (32) suggested that high-affinity binding ( $K_d < 1.0$  nM) of NBMPR to the transporter (a heterogeneously glycosylated polypeptide of 45-65 kDa) occurred with a 1:1 stoichiometry. In the experiment shown in Figure V-4B, equilibrium binding was determined at graded concentrations (0.12-24 nM) of [<sup>3</sup>H]NBMPR with intact pYhENT1-containing or pYES2-containing yeast cells that were grown in liquid cultures in medium with MTX/SAA, galactose and either 40  $\mu$ M (pYhENT1) or 1 mM (pYES2) thymidine. The amount of [<sup>3</sup>H]NBMPR specifically bound was determined by conducting binding

assays in the presence and absence of excess dilazep. Dilazep-sensitive binding of [<sup>3</sup>H]NBMPR to pYhENT1-containing yeast was saturable with mean values ( $\pm$ S.D.) of three independent experiments for  $B_{\max}$  and  $K_d$ , respectively,  $5.0 \pm 0.5$  pmol/mg of protein and  $1.2 \pm 0.2$  nM. Binding data fit best to a one-site binding model (using GraphPad v 2.0 software) suggesting that NBMPR interacted with a single class of high-affinity binding sites. There was no [<sup>3</sup>H]NBMPR binding to yeast with pYES2. These results demonstrated that the expression of pYhENT1 in yeast was accompanied by the acquisition of NBMPR-binding activity, evidently the consequence of functionally active, recombinant hENT1. The affinity of recombinant protein for NBMPR was similar to that of the native *es* transporters of erythrocytes and cultured cells (3,4). Assuming a 1:1 stoichiometry between NBMPR binding and recombinant hENT1, there were approximately  $10^4$  functionally active molecules per cell.

#### **V.C.vi. Binding of NBMPR to hENT1 in yeast membranes**

Experiments were undertaken to confirm that the binding of NBMPR to pYhENT1-containing yeast represented interaction with the membrane-associated recombinant hENT1 (Figure V-4C). Crude membranes, isolated from cells grown under inducing conditions, were incubated with graded concentrations of [<sup>3</sup>H]NBMPR in the absence or presence of excess dilazep for the detection of non-specific binding. A Scatchard analysis of the dilazep-sensitive (i.e., specific) component of binding indicated a single class of NBMPR binding sites with mean values ( $\pm$  S.D.) of three separate experiments for  $B_{\max}$  and  $K_d$ , respectively, of  $6.5 \pm 1.0$  pmol/mg protein and  $0.7 \pm 0.2$  nM. Binding data fit best to a one-site binding model (using GraphPad v 2.0 software) suggesting that NBMPR interacted with a single class of high-affinity binding sites. These results demonstrated that membranes prepared from pYhENT1-containing yeast possessed high-affinity NBMPR-binding sites, consistent with the conclusion that a large proportion of the NBMPR-binding sites were membrane associated.

### **V.C.vii                    Reconstitution of thymidine transport activity into hENT1-containing proteoliposomes**

The experiments of Figure V-5A and V-5B were undertaken to determine whether membrane-associated recombinant hENT1 could be solubilized and functionally reconstituted into proteoliposomes. Membranes prepared from pYhENT1-containing yeast cells that were grown in the presence of galactose (inducing conditions) were solubilized with octylglucoside, and exogenously supplied lipids were used to prepare proteoliposomes by a procedure used previously to reconstitute native *es* transporter from human and mouse cells (119,122,123). The time course of uptake of 20  $\mu$ M [ $^3$ H]thymidine (Figure V-5A) was determined into proteoliposomes alone (total uptake) or in the presence of a mixture of nucleoside transport inhibitors (non-mediated uptake). These results demonstrated functional reconstitution of thymidine-transport activity from membranes of pYhENT1-expressing yeast. The differences between the calculated initial rates of total and non-mediated uptake were used to calculate the initial rate of transport (7 pmol/s per mg reconstituted protein).

To confirm that recombinant hENT1 reconstituted into proteoliposomes retained its sensitivity to NBMPR, the concentration-effect relationship of the inhibition of [ $^3$ H]thymidine uptake into proteoliposomes by NBMPR was determined (Figure V-5B) and yielded an  $IC_{50}$  value of 5.5 nM. Thus, the sensitivity of thymidine transport mediated by recombinant hENT1 in proteoliposomes to inhibition by NBMPR was similar to that previously observed with erythrocytes and cultured cell lines (33,116,123).

### **V.C.viii.    pYhENT1/N48Q complementation of a deficiency in thymidine transport in yeast**

hENT1 is predicted to contain a single N-linked glycosylation site in the large extracellular loop between transmembrane domains 1 and 2 at Asn-48 (18). The role of N-linked glycosylation in the biosynthetic processing and function of hENT1 is not known. A cDNA in which the N-linked glycosylation site of hENT1 (Asn-48) was converted to

Gln by site directed mutagenesis (M. Sundaram, S.Y.M. Yao, E. Chomey, C.E. Cass, and S.A. Baldwin and J.D. Young, unpublished work) was cloned into the pYES2 expression vector to generate pYN48Q, which was then functionally expressed in yeast. When yeast cells with either pYN48Q or pYES2 were exposed to MTX/SAA in the presence of galactose (inducer) or glucose (repressor), both types of transformants formed colonies in the presence of 1 mM thymidine (Figure V-6B) and neither formed colonies in thymidine-free medium (Figure V-6A). Colonies were also formed by pYN48Q-containing yeast, but not by pYES2-containing yeast, in the presence of galactose and 10  $\mu$ M thymidine (Figure V-6C), whereas none were observed in the presence of glucose and 10  $\mu$ M thymidine (Figure V-6D). Yeast cells with pYN48Q or pYES2 were also tested under inducing conditions in medium containing MTX/SAA and either 10  $\mu$ M or 1000  $\mu$ M thymidine alone or with 1  $\mu$ M NBMPR, 10  $\mu$ M dilazep or 10  $\mu$ M dipyridamole (Table V-2). Colonies were formed by both types of transformants in 1000  $\mu$ M thymidine in both the absence and presence of the transport inhibitors, whereas, colonies were observed when pYN48Q-containing yeast cells were plated in medium containing 10  $\mu$ M thymidine and none were observed in the presence of the inhibitors. These results demonstrated that the expression of pYN48Q cDNA in yeast complemented the growth arrest imposed by thymidylate starvation by enabling thymidine rescue by a process that was blocked by the *es* inhibitors. Thus, glycosylation at Asn-48 was not required for production of functional, inhibitor-sensitive, hENT1 in yeast.

#### **V.C.ix. Binding of [<sup>3</sup>H]NBMPR to hENT1/N48Q-producing yeast**

The ability of pYN48Q, which encodes a hENT1 variant lacking the capacity for N-glycosylation, to complement the thymidine-transport defect of yeast phenotypically under selection conditions (see Figure V-6) suggested that functionally active hENT1/N48Q was produced and processed to the plasma membrane. Equilibrium binding of [<sup>3</sup>H]NBMPR to pYN48Q-containing yeast was examined (Figure V-7) under conditions identical to those used in earlier studies with pYhENT1-containing yeast (see Section V.C.v). NBMPR

binding was saturable, with mean values ( $\pm$  S.D.) of six separate experiments for  $K_d$  and  $B_{max}$ , respectively, of  $10.5 \pm 1.6$  nM and  $15.0 \pm 1$  pmol/mg of protein. Binding data fit best to a one-site binding model (using GraphPad v 2.0 software) suggesting that NBMPR interacted with a single class of high-affinity binding sites. The 10-fold increase in the  $K_d$  values observed for yeast producing the "mutant" protein, relative to those for yeast with the "wild-type" protein, suggested that the conversion of Asn to Gln induced a structural change in the vicinity of the NBMPR-binding site that lowered the affinity for NBMPR. The 3-fold increase in  $B_{max}$  values in hENT1/N48Q-producing yeast, relative to those of hENT1-producing yeast, suggested that the quantity of functionally active (with respect to NBMPR binding) mutant hENT1 was greater than that observed with the wild-type hENT1.

#### **V.C.x. Dissociation and association of [ $^3$ H]NBMPR from hENT1-producing and hENT1/N48Q-producing yeast**

The rates of dissociation of [ $^3$ H]NBMPR from intact pYhENT1-containing and pYN48Q-containing yeast (grown under selective conditions) were determined (Figure V-8) to investigate the basis of the decreased affinity of [ $^3$ H]NBMPR for hENT1/N48Q. The apparent dissociation rate constants (mean values  $\pm$  S.D. for three separate experiments) for yeast producing either recombinant hENT1 or recombinant hENT1/N48Q were  $0.14 \pm 0.02$  and  $0.36 \pm 0.05$  min $^{-1}$  respectively. It therefore seems that the conformational changes resulting from the conversion of Asn-48 into Gln and/or the absence of the N-linked oligosaccharide led to an accelerated dissociation of [ $^3$ H]NBMPR from its binding site. Such a difference in the dissociation rates could result in weaker binding of NBMPR by recombinant hENT1/N48Q than by recombinant hENT1. This conformational change was also reflected in changes in the apparent association rate constants.  $K_{on}$  values (means for two experiments) of hENT1 and hENT1/N48Q were determined as  $1.2 \times 10^8$  and  $0.4 \times 10^8$  M $^{-1}$  min $^{-1}$  respectively.

**V.C.xi. Inhibition of binding of [<sup>3</sup>H]NBMPR to hENT1-producing and hENT1/N48Q-producing yeast by dilazep and dipyridamole**

Dilazep and dipyridamole are potent inhibitors of NBMPR binding to mammalian cells, and their inhibition of *es*-mediated transport activity has been attributed to their interaction with sites that are the same as, or overlap with, NBMPR-binding sites (118,120,121). The experiments of Figure V-9 were undertaken to determine if the conversion of Asn-48 into Gln also altered interaction of hENT1 with dilazep and/or dipyridamole. The apparent relative affinities of dilazep and dipyridamole for recombinant hENT1 and hENT1/N48Q were compared by assessing their abilities to inhibit the binding of [<sup>3</sup>H]NBMPR to pYhENT1-containing and pYN48Q-containing yeast. Dilazep and dipyridamole decreased [<sup>3</sup>H]NBMPR binding to pYhENT1-containing yeast with IC<sub>50</sub> values (mean ± S.D. for three separate experiments) of 130 ± 10 and 380 ± 20 nM respectively, and to pYN48Q-containing yeast with IC<sub>50</sub> values (means ± S.D. for three separate experiments) of 50 ± 5 and 230 ± 3 nM, respectively. The apparent K<sub>i</sub> values, estimated by the method of Cheng and Prusoff (117), for the inhibition of NBMPR binding to hENT1-producing and hENT1/N48Q-producing yeast were, respectively, 90 and 30 nM for dilazep and 260 and 150 nM for dipyridamole. These results indicated that the conversion of Asn-48 into Gln in hENT1 resulted in a conformational changes that evidently increased the apparent affinity of the *es* transporter for dilazep and dipyridamole.

## V.D. DISCUSSION

The availability of cDNAs encoding the ENT proteins of rat and human cells has allowed detailed kinetic studies of the recombinant transporters in oocytes of *X. laevis* oocytes to be performed (16,18). Cultured cells have also been used for the functional expression of hENT2 (21). However, these heterologous expression systems have not produced sufficient quantities of recombinant protein to permit a detailed analysis of the physical characteristics of the recombinant transporter proteins. Reported here is the first demonstration of functional expression of wild-type and mutant hENT1 cDNA in yeast. Although equilibrium binding analysis with [<sup>3</sup>H]NBMPR has been used extensively for quantification of the *es* transporter in cells and membrane preparations, multiple *es* transporter isoforms with similar affinities for NBMPR would appear as a single transporter type in equilibrium binding studies. The functional expression of the hENT1 cDNA in yeast permitted a detailed analysis of the binding of NBMPR to the recombinant transporter proteins in an *es*-null background, and identified differences in binding affinities between the wild-type and N-glycosylation-defective mutant transporter proteins.

Yeast cells lack the capacity for mediated uptake of extracellular thymidine (52), a feature that permits the expression of nucleoside transporter cDNAs by imposing a drug selection (MTX, SAA) that results in the depletion of thymidylate and in cell death, unless a mechanism for salvage of extracellular thymidine is present and functional in the recipient yeast (105,106). The expression of hENT1 cDNA in yeast subjected to thymidylate starvation could enable growth of yeast if exogenous thymidine was supplied to the growth medium. Northern analysis confirmed that (i) hENT1 mRNA was present in pYhENT1-containing yeast but not pYES2-containing yeast, and (ii) greater quantities of hENT1 mRNA were present in pYhENT1-containing yeast grown in the presence of galactose (inducing conditions for the expression plasmid) than in yeast grown in the presence of glucose (repressive conditions for the expression plasmid). Inhibition of transport by

nanomolar concentrations of NBMPR, dilazep or dipyridamole is diagnostic of the *es* transport process of mammalian cells (1,3,14), and thymidine rescue of pYhENT1-expressing yeast from thymidylate starvation was blocked by addition of excess (1 or 10  $\mu$ M) NBMPR, dilazep or dipyridamole to the growth medium. pYhENT1-containing yeast, but not pYES2-containing yeast, accumulated radioactivity during 20-min incubations with [ $^3$ H]thymidine; this uptake was shown to occur in a mediated fashion and to be inhibited by NBMPR, dilazep and dipyridamole.

hENT1 is an integral membrane protein and thus was expected to be present in membrane fractions of pYhENT1-expressing yeast. Immunoblotting of yeast membranes with hENT1-specific polyclonal antibodies (directed against a synthetic peptide corresponding to residues 254-272) demonstrated the presence of immunoreactive protein in pYhENT1-expressing yeast but not in pYES2-expressing yeast. The predominant immunoreactive species exhibited an apparent molecular mass of 40-45 kDa and thus corresponded to the hENT1 monomer; the predicted molecular mass of non-glycosylated hENT1 is 50.2 kDa. The larger minor reactive species of 80 and 120 kDa were probably hENT1 dimers and trimers, respectively. The native *es* transporter, recognized by photoaffinity labeling with [ $^3$ H]NBMPR, migrates during SDS-PAGE with a wide range of mobilities (42-60 kDa) among different species and cell types (3,4). These differences in apparent molecular mass have been attributed to variable degrees of N-linked glycosylation (33,112,116,140,141).

A further demonstration that recombinant hENT1 was located primarily in yeast membranes came from results of studies of equilibrium binding of [ $^3$ H]NBMPR with membrane preparations from pYhENT1-containing yeast. Crude membranes from pYhENT1-containing yeast that had been grown under inducing conditions exhibited high-affinity binding of NBMPR with  $K_d$  and  $B_{max}$  values ( $\pm$  S.D.), respectively, of  $0.7 \pm 0.2$  nM and  $6.5 \pm 1.0$  pmol/mg. NBMPR bound to both pYhENT1-expressing yeast and yeast membranes derived therefrom with  $K_d$  values similar to those found for the *es* transporters



of a variety of mammalian cell types (4). The number of NBMPR-binding sites observed in pYhENT1-expressing yeast was similar to the values reported (142) for human erythrocytes (approximately  $10^4$  sites per cell), suggesting, since NBMPR binds to the *es* transporter protein with an apparent stoichiometry of 1:1 (32), that there were approximately  $10^4$  functionally active hENT1 molecules per cell. Although the *es* transporter protein of human erythrocytes has been purified to homogeneity by immunoaffinity chromatography, the quantities obtained were small (32). The level of hENT1 production in yeast opens the way for use of the yeast expression system for the production of recombinant hENT1 protein for purification.

NBMPR binding to the *es* transporter occurs at the exofacial surface (143,144) and its binding site is believed to be the same as, or to overlap with, the nucleoside recognition site for permeation (144,145). Examination of NBMPR binding to the N-glycosylation-defective mutant hENT1/N48Q revealed a decrease to one-tenth, relative to hENT1, in the affinity of the recombinant protein for NBMPR. The decreased affinities were shown to be due in part to increased rates of dissociation because  $k_{off}$  values of specifically bound [ $^3$ H]NBMPR from hENT1-producing and hENT1/N48Q-producing yeast were 0.14 and 0.36  $\text{min}^{-1}$  respectively. The decreased affinities were also due to changes in the rates of NBMPR association since  $k_{on}$  values were  $1.2 \times 10^8$  and  $0.40 \times 10^8 \text{ M}^{-1} \text{ min}^{-1}$ , respectively, for hENT1-producing and hENT1/N48Q-producing yeast.

The decreased affinity of hENT1 for NBMPR after the alteration of Asn-48 implicates this residue, and/or the N-glycosylated oligosaccharide, in the binding of NBMPR to hENT1. The region of hENT1 involved in the binding of dipyridamole has recently been explored by experiments in which portions of the human and rat *es* transporters (hENT1, rENT1) were swapped with each other, thereby exploiting the intrinsic differences in dipyridamole sensitivity between the two transporters (35). The characteristics of the resulting hENT1/rENT1 chimeras indicated that the region responsible for sensitivity to dipyridamole (and therefore also to NBMPR) is contained within the N-

terminal half of hENT1, primarily in transmembrane domains 3-6 (residues 100-261). The results of the present study suggested that the region N-terminal to the third transmembrane domain, most probably the large extracellular loop connecting the first and second transmembrane domains, may also contribute to the formation of the nucleoside recognition site of hENT1. Alternatively, replacement of N48 to Q may have long range perturbing effects on the protein and influence the NBMPR binding region from a distance. It has previously been suggested that NBMPR covalently attaches to hENT1 in the N-terminal half of the protein, within 15 kDa of the N-glycosylation site (140).

When examined under equilibrium conditions, dilazep and dipyridamole competitively inhibit NBMPR binding to the *es* transporter of human erythrocytes and other cell types. They are therefore thought to interact, like NBMPR, at or near the nucleoside recognition site at the exofacial surface of the transporter (118,120,121,144,146). The ability of dilazep and dipyridamole to interact with recombinant hENT1 was demonstrated by assessing the binding of NBMPR to hENT1-producing yeast in the presence of graded concentrations of either of the two *es* inhibitors. Dilazep and dipyridamole inhibited the binding of NBMPR with  $IC_{50}$  values (means  $\pm$  S.D.) of  $130 \pm 10$  and  $380 \pm 20$  nM, which yielded apparent inhibitory constants ( $K_i$ ) for dilazep and dipyridamole of 90 and 260 nM, respectively. These values are similar to those observed elsewhere in studies with native *es* transporters (1,3,14,122). The  $IC_{50}$  values for inhibition of binding of NBMPR to hENT1/N48Q-producing yeast by dilazep and dipyridamole were used to calculate apparent  $K_i$  values of 30 and 150 nM, respectively. These results suggested that the conversion of Asn-48 to Gln resulted in conformational differences between hENT1 and hENT1/N48Q that increased the affinity of the latter for both dilazep and dipyridamole.

The abundance of recombinant hENT1 in pYhENT1-expressing membranes provided a source of recombinant hENT1 for reconstitution into proteoliposomes, thereby permitting a direct demonstration of hENT1-dependent transport activity. Reconstituted proteoliposomes, prepared from hENT1-producing yeast, exhibited a mediated uptake of

thymidine that was inhibited by NBMPR ( $IC_{50}$  5.5 nM) at concentrations similar to those seen previously (116) with intact BeWo cells ( $IC_{50}$  1.6 nM), which have recently been shown by reverse-transcriptase-mediated PCR to express the hENT1 gene (7). Native *es* transporters have previously been solubilized from mammalian cells and reconstituted into proteoliposomes (119,122,123,147), although in several of these studies the cells also contained other nucleoside transporters. The reconstitution of recombinant hENT1 from yeast membranes into proteoliposomes has advantages because of the absence of endogenous thymidine-transporting and NBMPR-binding activities and because of the opportunities presented through recombinant DNA techniques for modification of the hENT1 amino acid sequence.

In conclusion, *S. cerevisiae* has proved to be a useful model system in which to study recombinant hENT1. Phenotypic complementation of thymidylate starvation indicated that hENT1 cDNA was functionally expressed in yeast and exhibited the expected sensitivity to inhibition by NBMPR, dilazep and dipyridamole. Northern analysis and immunoblotting confirmed the production of hENT1 mRNA and recombinant protein, respectively, in pYhENT1-containing yeast grown in medium that contained an inducer (galactose) for expression of the cDNA insert. Recombinant hENT1 was produced at modest levels in intact yeast and was shown to be present in yeast membranes. Equilibrium binding analysis demonstrated site-specific interaction of NBMPR with the nucleoside recognition site on recombinant hENT1 and provided a means of evaluating the effects of dilazep and dipyridamole on NBMPR binding. The conservative conversion of Asn-48 to Gln, with the consequent loss of N-linked glycosylation capability, decreased the affinity of hENT1 for NBMPR and increased its affinity for dilazep and dipyridamole, suggesting that Asn-48 and/or the N-linked oligosaccharide, influences the structure(s) of the nucleoside and inhibitor recognition site(s) of hENT1. Finally, recombinant hENT1 retained its ability to transport thymidine after solubilization with octylglucoside and

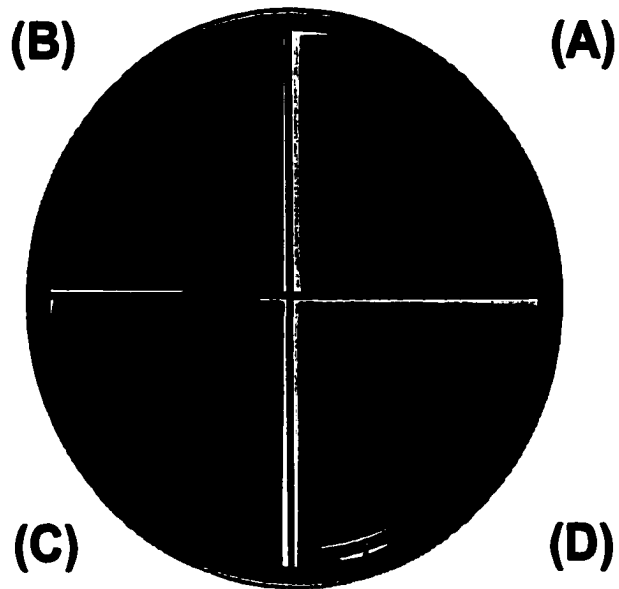
**reconstitution into proteoliposomes, opening the door to use of the yeast expression system for the production of transport-competent recombinant hENT1 for protein purification.**

**Figure V-1      Functional complementation of a thymidine transport deficiency in yeast by recombinant hENT1**

Yeast cells containing either pYES2 or pYhENT1 were streaked on solid CMM/GAL/MTX/SAA medium (inducing conditions, thymidylate starvation) that contained 0  $\mu$ M thymidine (A), 1 mM thymidine (B) or 10  $\mu$ M thymidine (C) as described in Chapter II, section II.B. Yeast cells were also streaked on CMM/GLU/MTX/SAA medium (repressive conditions, thymidylate starvation) that contained 10  $\mu$ M thymidine (D). Growth on plates was visualized after 3.5 days. Three separate experiments, one of which is shown, yielded similar results.

**Figure V-1**

**pYES2**



**pYhENT1**

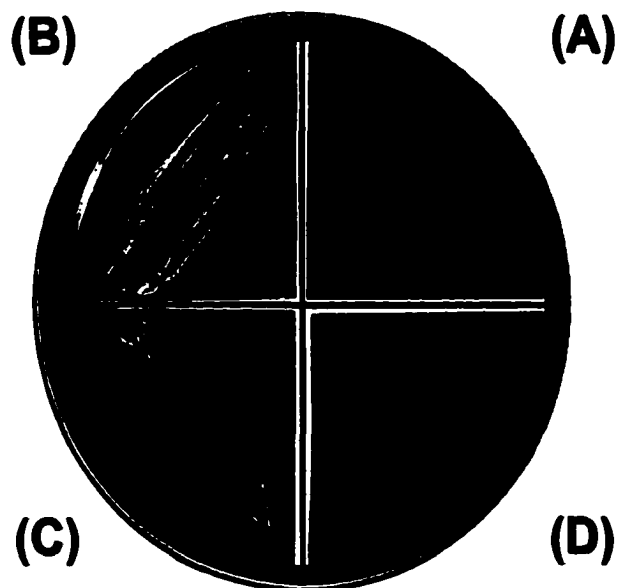
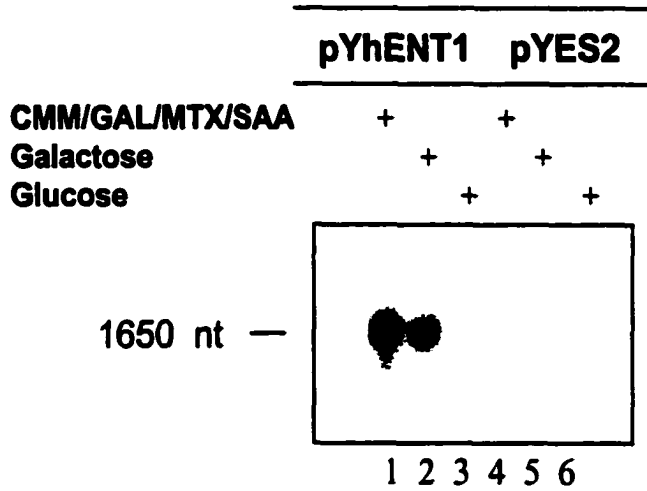


**Figure V-2            Production of hENT1 mRNA and recombinant protein by yeast**

**Panel A.** Total RNA from yeast transformed with pYhENT1 (lanes 1-3) or pYES2 (lanes 4-6) was subjected to Northern analysis with <sup>32</sup>P-labelled hENT1 cDNA fragment (nt 1-648) and then detected by autoradiography, as described in Chapter II, section II.D. Growth conditions were as follows: CMM/GAL/MTX/SAA medium that contained either 40 μM thymidine (lane 1) or 1 mM thymidine (lane 4); CMM/GAL medium (lanes 2 and 5); CMM/GLU medium (lanes 3 and 6). **Panel B.** Membranes, prepared as described in Chapter II, section II.E, from yeast with pYES2 (lane 1) or pYhENT1 (lane 2) grown in CMM/GAL/MTX/SAA medium that contained 1 mM or 40 μM thymidine respectively, were subjected to immunoblotting with hENT1-specific polyclonal antibodies as described in Chapter II, section II.I. The positions of molecular mass markers are indicated (in kDa) at the left.

# Figure V-2

(A)



(B)

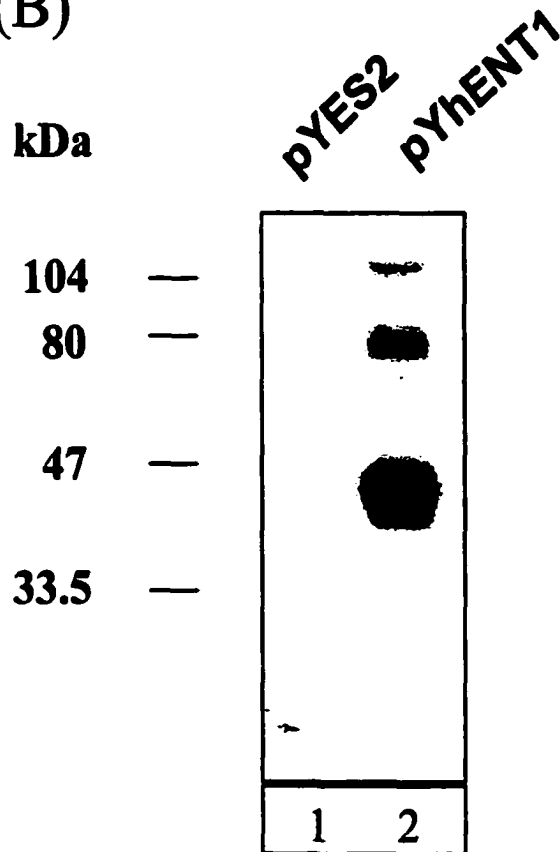




**Figure V-3 Cellular uptake of [<sup>3</sup>H]thymidine by yeast producing recombinant hENT1**

**Panel A.** The uptake of 1.0  $\mu\text{M}$  [<sup>3</sup>H]thymidine was measured, as described in Chapter II, section II.J.i, into yeast transformed with pYhENT2 (-■-) or pYES2 (-▲-) grown in CMM/GAL/MTX/SAA medium (inducing conditions) that contained respectively 40  $\mu\text{M}$  or 1 mM thymidine. **Panel B.** Yeast cells with pYhENT1 or pYES2 were grown as described for panel A. Cells were incubated for 20 min with 1.0  $\mu\text{M}$  [<sup>3</sup>H]thymidine alone (100% of uptake) or in the presence of either 10 mM thymidine, 1  $\mu\text{M}$  NBMPR, 10  $\mu\text{M}$  dilazep or 10  $\mu\text{M}$  dipyridamole after which cell-associated radioactivity was measured as described in Chapter II, section II.J.i. The “background” quantity of [<sup>3</sup>H]thymidine adsorption on pYES2-containing yeast was subtracted from the “stimulated” quantity observed for pYhENT1-containing yeast. Results are means  $\pm$  S.D. for triplicate determinations of the cellular content of thymidine equivalents (i.e., thymidine and its metabolites). Error bars are not shown where values were smaller than that represented by the symbols. Two separate experiments, one of which is shown, gave similar results.

-

.

**Figure V-3**

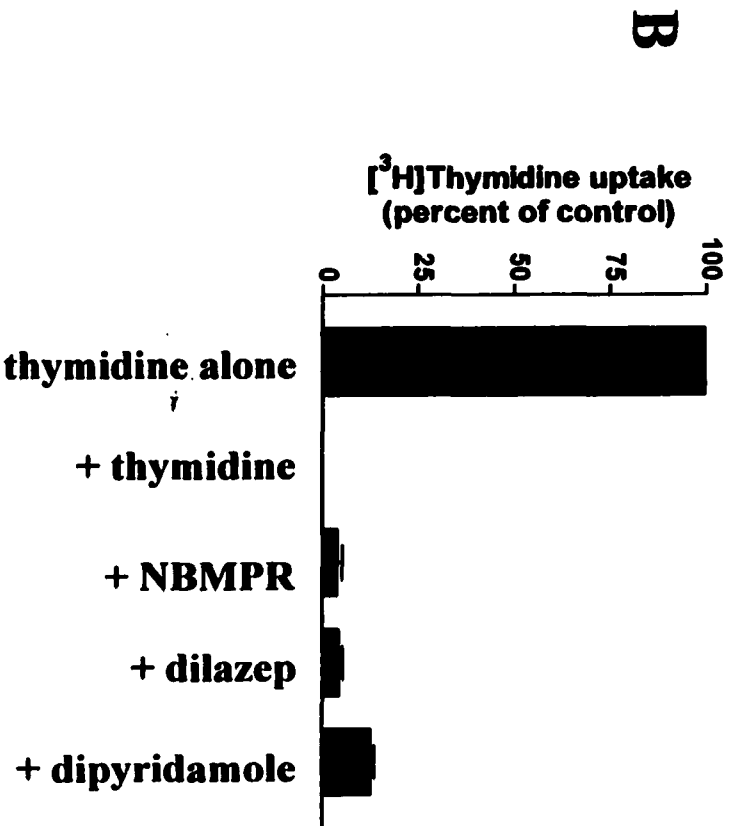
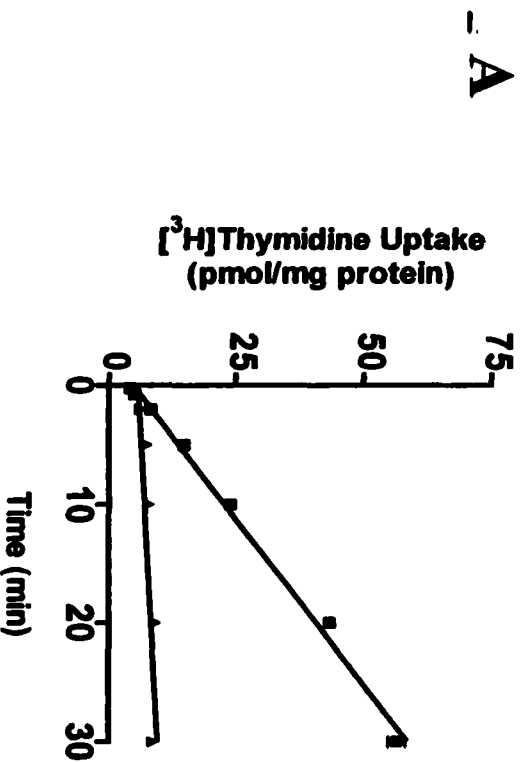


**Figure V-4      Equilibrium binding of [<sup>3</sup>H]NBMPR to yeast producing recombinant hENT1 and membranes containing recombinant hENT1**

**Panel A:** Time course of [<sup>3</sup>H]NBMPR binding (8 nM) to yeast transformed with pYhENT1 and grown in CMM/GAL/MTX/SAA media (inducing conditions) that contained 40  $\mu$ M thymidine was determined as described in Chapter II, section II.K. Each point is the average of duplicate determinations (individual values differed from the value shown by  $\leq 10\%$ ). Two experiments, one of which is shown, gave similar results. **Panel B:** Equilibrium binding of [<sup>3</sup>H]NBMPR (0.12 nM - 24 nM) to yeast transformed with pYhENT1 (-■-) or pYES2 (-●-) and grown in CMM/GAL/MTX/SAA medium (inducing conditions) that contained 40  $\mu$ M or 1 mM thymidine, respectively, was determined as described in Chapter II, section II.K. Results are presented as the amounts of specifically bound [<sup>3</sup>H]NBMPR as a function of free [<sup>3</sup>H]NBMPR. Each point is the average of duplicate determinations (individual values differed from the value shown by  $\leq 11\%$ ). Three experiments, one of which is shown, gave similar results, yielding (means  $\pm$  S.D) values for  $B_{max}$  and  $K_d$  of , respectively,  $5.0 \pm 0.5$  pmol/mg of protein and  $1.2 \pm 0.2$  nM. **Inset to Panel A:** Scatchard analysis of specific binding of [<sup>3</sup>H]NBMPR to pYhENT1-containing yeast. **Panel C:** Equilibrium binding of [<sup>3</sup>H]NBMPR (0.12 - 24 nM) was determined with membranes prepared as described in Chapter II, section II.E, from yeast transformed with pYhENT1 and grown in CMM/GAL/MTX/SAA media that contained 40  $\mu$ M thymidine. The amount of [<sup>3</sup>H]NBMPR that specifically bound is presented as a function of free [<sup>3</sup>H]NBMPR. Each point is the average of duplicate determinations; individual values differed from the value shown by  $\leq 8\%$ . Three experiments, one of which is shown, gave similar results with  $B_{max}$  and  $K_d$  values (means  $\pm$  S.D.) of  $6.5 \pm 1.0$  pmol/mg protein and  $0.7 \pm 0.2$  nM, respectively. **Inset to Panel A:** Scatchard analysis of specific [<sup>3</sup>H]NBMPR binding to hENT1-containing yeast membranes.

# Figure V-4 A

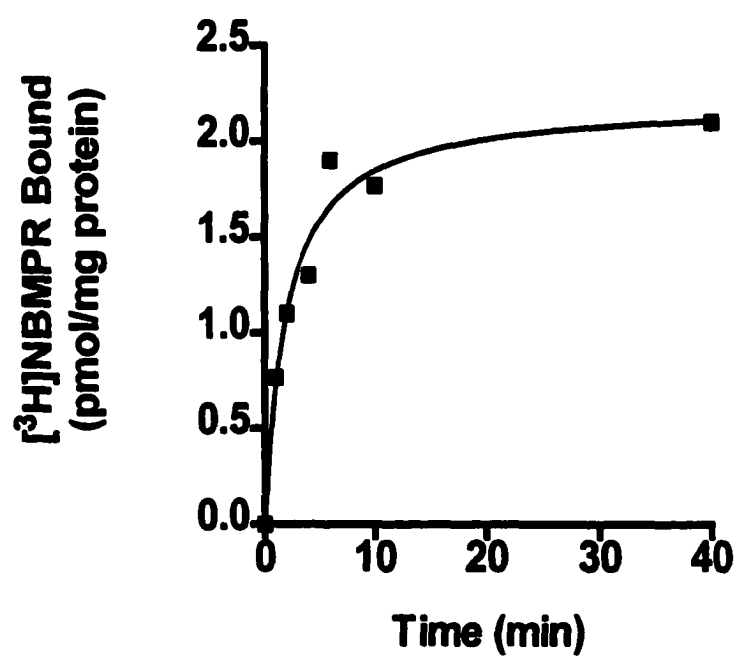


**Figure V-4 B**

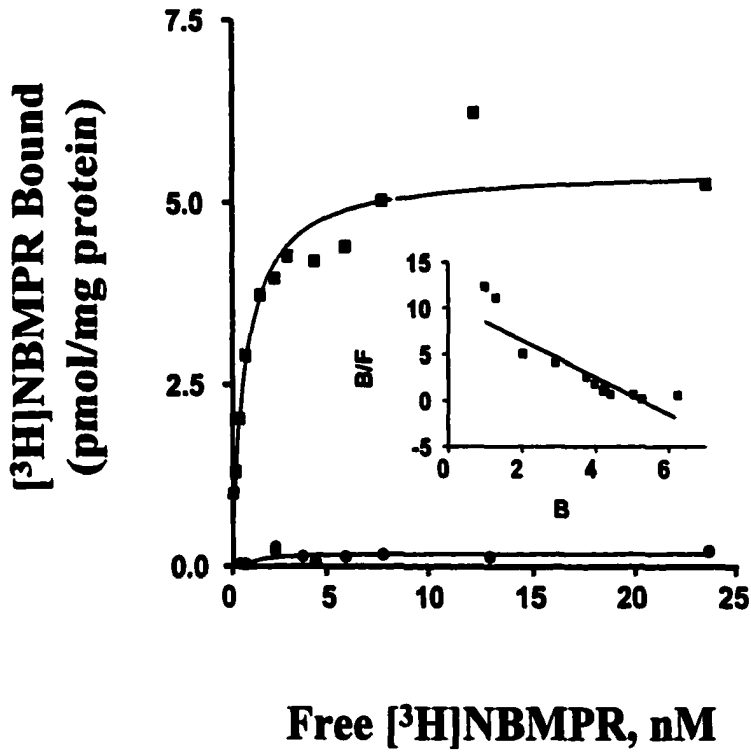


**Figure V-4 C**

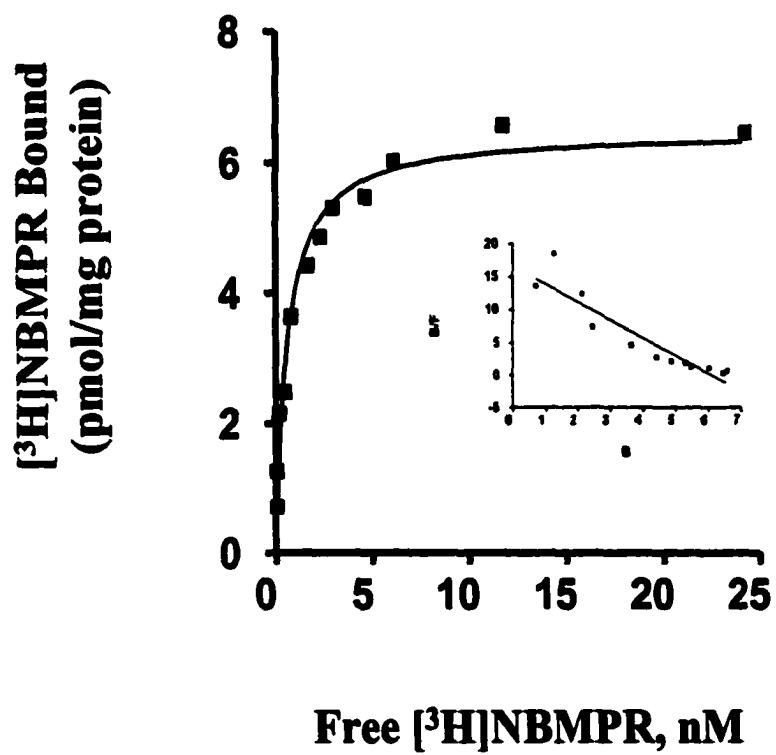


**Figure V-5 Demonstration of recombinant hENT1 in yeast membranes by reconstitution of thymidine transport activity**

**Panel A:** Crude membranes prepared from yeast with pYhENT1, as described for Figure V-2, were solubilized with octylglucoside and reconstituted into liposomes. The uptake of 20  $\mu\text{M}$  [ $^3\text{H}$ ]thymidine was measured for the indicated timed intervals in the absence (-■-, total uptake) or presence (-▲-, non-mediated uptake) of a mixture of transport inhibitors (10 mM adenosine, 10  $\mu\text{M}$  dipyridamole and 10  $\mu\text{M}$  NBTGR). hENT1-mediated uptake of [ $^3\text{H}$ ]thymidine (-▼-) was determined by subtracting the total uptake from the non-mediated uptake. Each point is the average of duplicate determinations (individual values differed from the values shown by  $\leq 8\%$ ). Two experiments, one of which is shown, gave similar results, yielding an average initial rate of thymidine uptake of 7 pmol/s per mg of protein. **Panel B:** hENT1-containing liposomes were prepared as described for Panel A and then incubated with NBMPR (0.0375 nM - 12.5  $\mu\text{M}$ ) for 10 min after which uptake of 20  $\mu\text{M}$  [ $^3\text{H}$ ]thymidine was measured for 20 sec (as described for Panel A) in the presence of the same concentrations of NBMPR. Results are presented as the relative amounts of hENT1-mediated [ $^3\text{H}$ ]thymidine uptake as a function of the concentration of NBMPR. hENT1-mediated [ $^3\text{H}$ ]thymidine uptake in the absence of NBMPR was taken as 100 % uptake. Each point is the average of duplicate determinations (individual values differed from the values shown by  $\leq 9\%$ ). Two experiments, one of which is shown, gave similar results, yielding an average  $\text{IC}_{50}$  of 5.5 nM for the inhibition of thymidine uptake by NBMPR.

-

**Figure V-5 A**

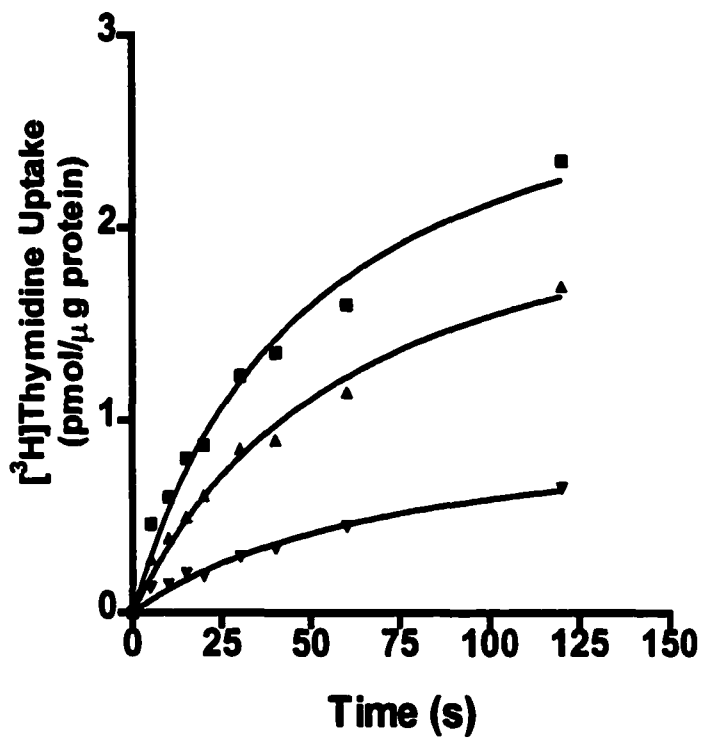




# Figure V-5 B

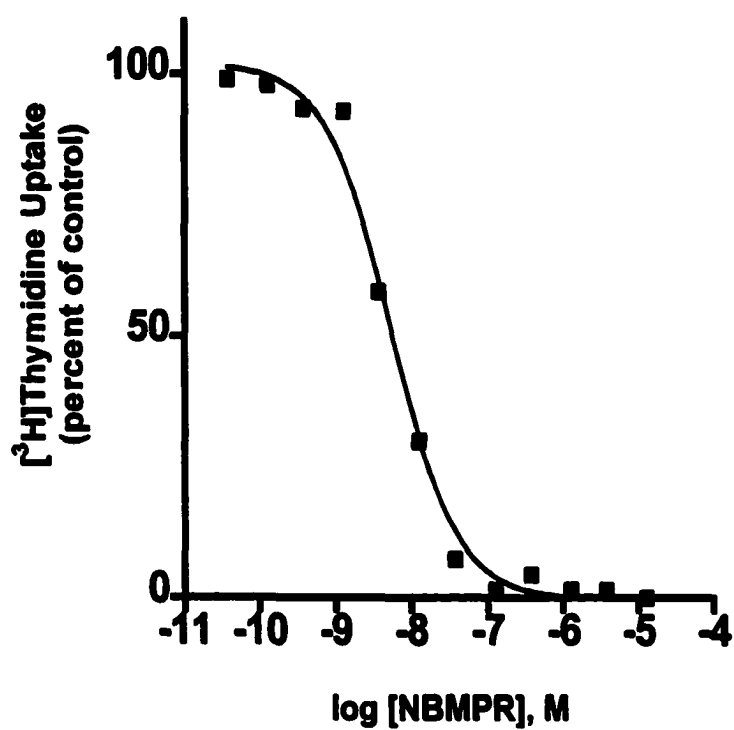
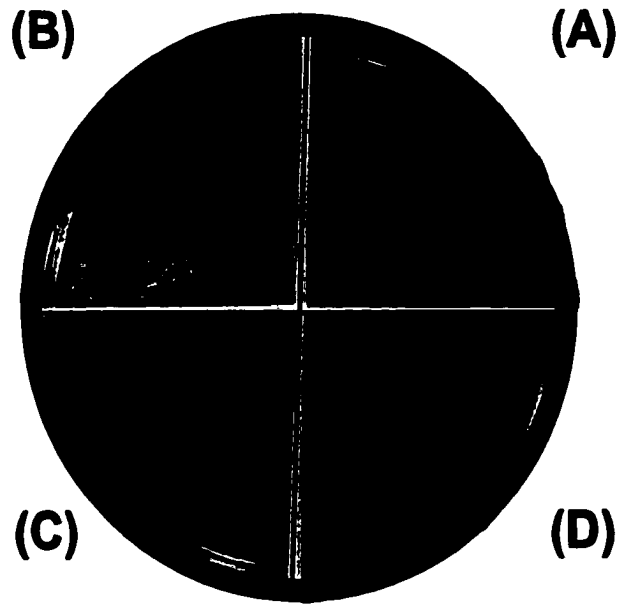


**Figure V-6      Functional complementation of a thymidine transport deficiency in yeast by recombinant hENT1/N48Q**

Yeast cells containing either pYES2 or pYN48Q were streaked on solid CMM/GAL/MTX/SAA medium (inducing conditions, thymidylate starvation) that contained 0  $\mu$ M thymidine (A), 1 mM thymidine (B) or 10  $\mu$ M thymidine (C) as described in Chapter II, section II.B. Yeast cells were also streaked on CMM/GLU/MTX/SAA medium (repressive conditions, thymidylate starvation) that contained 10  $\mu$ M thymidine (D). Growth on plates was visualized after 3.5 days. Three separate experiments, one of which is shown, yielded similar results.

**Figure V-6**

**pYES2**



**pYhENT1/N48Q**

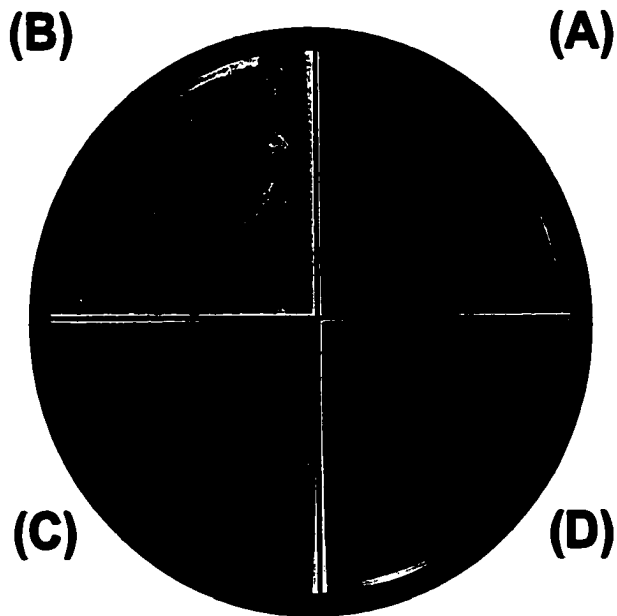


**Figure V-7      Equilibrium binding of [<sup>3</sup>H]NBMPR to yeast producing recombinant pYN48Q**

Equilibrium binding of [<sup>3</sup>H]NBMPR (0.12 nM - 24 nM) to yeast transformed with pYN48Q and grown in CMM/GAL/MTX/SAA medium (inducing conditions) that contained 40 μM thymidine was measured as described in Chapter II, section II.K, and in the legend of Figure V-4. Results are presented as the amounts of specifically bound [<sup>3</sup>H]NBMPR as a function of free [<sup>3</sup>H]NBMPR. Each point is the average of duplicate determinations (individual values differed from the value shown by ≤ 13%). Six experiments, one of which is shown, gave similar results yielding values (means ± S.D.) for B<sub>max</sub> and K<sub>d</sub> of, respectively, 15 ± 1.1 pmol/mg of protein and 10.5 ± 1.6 nM. *Inset.* Scatchard analysis of specific binding of [<sup>3</sup>H]NBMPR to pYN48Q-containing yeast.

-

.

**Figure V-7**

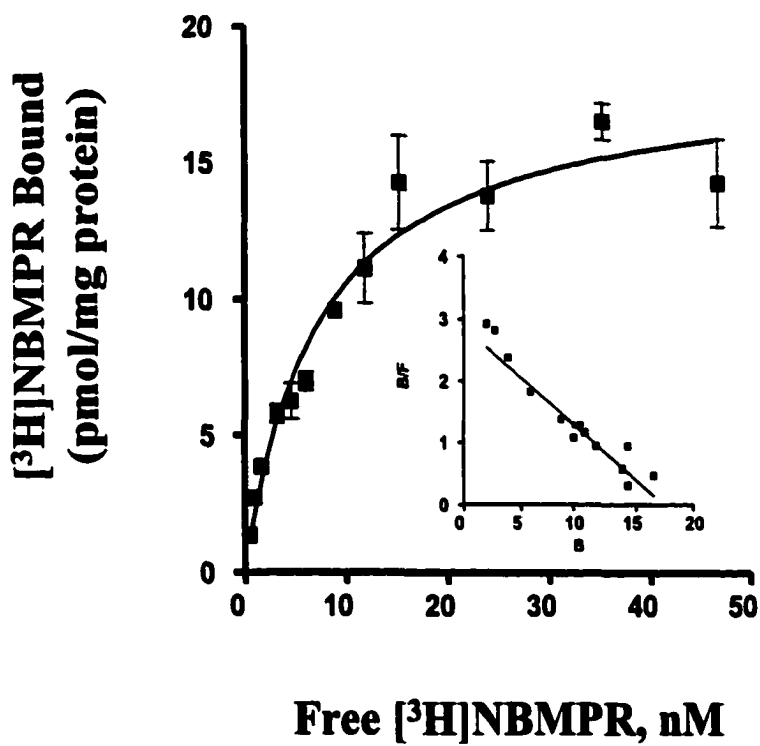


**Figure V-8      Dissociation of [<sup>3</sup>H]NBMPR from yeast producing either recombinant hENT1 or hENT1/N48Q**

Yeast cells transformed with pYhENT1 (-■-) or pYN48Q (-▲-) and grown in CMM/GAL/MTX/SAA medium containing 40 μM thymidine, as described in Chapter II, section II.L, were incubated at 22°C in the presence of 2.5 nM [<sup>3</sup>H]NBMPR and allowed to reach equilibrium. Excess (5 μM) unlabelled NBMPR was then added to the cells and the amount of [<sup>3</sup>H]NBMPR that remained bound was measured at the times indicated. Specific binding of [<sup>3</sup>H]NBMPR is shown as a function of time. Values for dissociation rate constants were estimated with a non-linear one-phase exponential decay equation using GraphPad PRISM v 2.0 software. Each point is the average of duplicate determinations; individual values differed from the value shown by ≤ 6% (pYhENT1) or ≤ 5% (pYN48Q). Three experiments, one of which is shown, gave similar results for the apparent rate of dissociation for hENT1 and N48Q, yielding values (means ± S.D.) of 0.14 ± 0.02 and 0.36 ± 0.05 min<sup>-1</sup> respectively.

**Figure V-8**

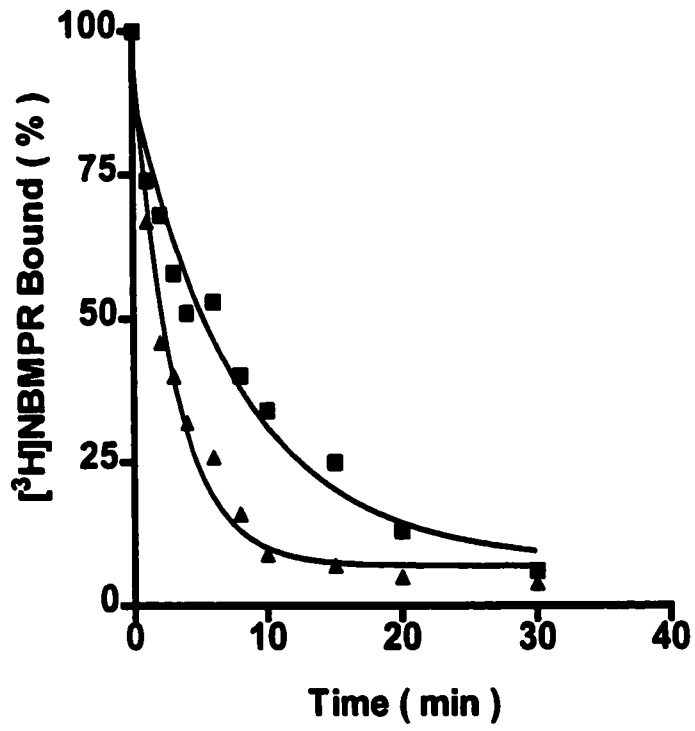


**Figure V-9      Inhibition by dilazep and dipyridamole of [<sup>3</sup>H]NBMPR binding to yeast producing either recombinant hENT1 or hENT1/N48Q**

Yeast cells transformed with pYhENT1 or pYN48Q were grown in CMM/GAL/MTX/SAA medium that contained 40  $\mu$ M thymidine as described in Chapter II, section II.K. The pYhENT1-containing yeast cells were incubated with 0.5 nM [<sup>3</sup>H]NBMPR alone or together with graded concentrations (0.125- 10  $\mu$ M) of either dilazep (A) or dipyridamole (B); the pYN48Q-containing yeast cells were incubated with 6 nM [<sup>3</sup>H]NBMPR alone or with graded concentrations of dilazep (C) or dipyridamole (D). The concentrations of [<sup>3</sup>H]NBMPR differed between pYhENT1-containing and pYN48Q-containing yeast because of the differences in  $K_d$  values for NBMPR binding. Results are presented as the percentages of [<sup>3</sup>H]NBMPR bound as a function of the logarithm of the concentration of dilazep or dipyridamole. The amount of [<sup>3</sup>H]NBMPR that bound in the absence of additives was taken as 100% binding. Each point is the average of duplicate determinations; individual values differed from the value shown by  $\leq 12$  %. Three experiments, one of which is shown for each inhibitor, gave similar results, yielding  $IC_{50}$  values (means  $\pm$  S.D.) for dilazep and dipyridamole inhibition of NBMPR binding to hENT1 of  $130 \pm 10$  and  $380 \pm 20$  nM respectively, and to hENT1/N48Q of  $50 \pm 5$  and  $230 \pm 3$  nM. respectively .



**Figure V-9 A**

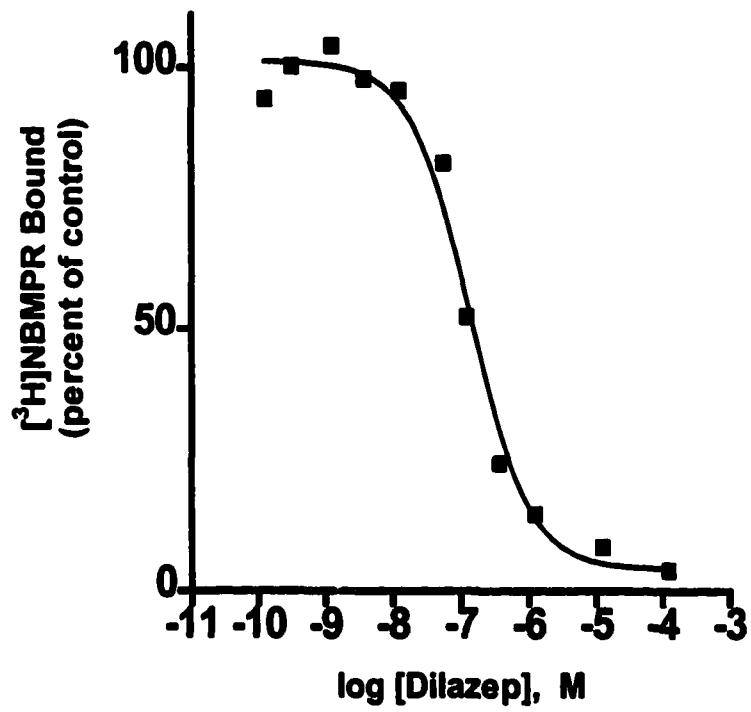


# Figure V-9 B

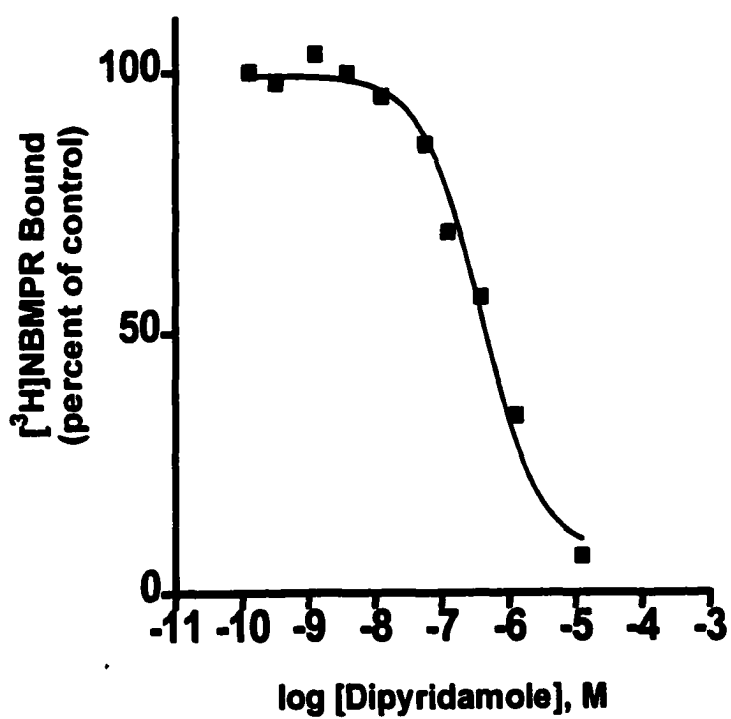


# Figure V-9 C

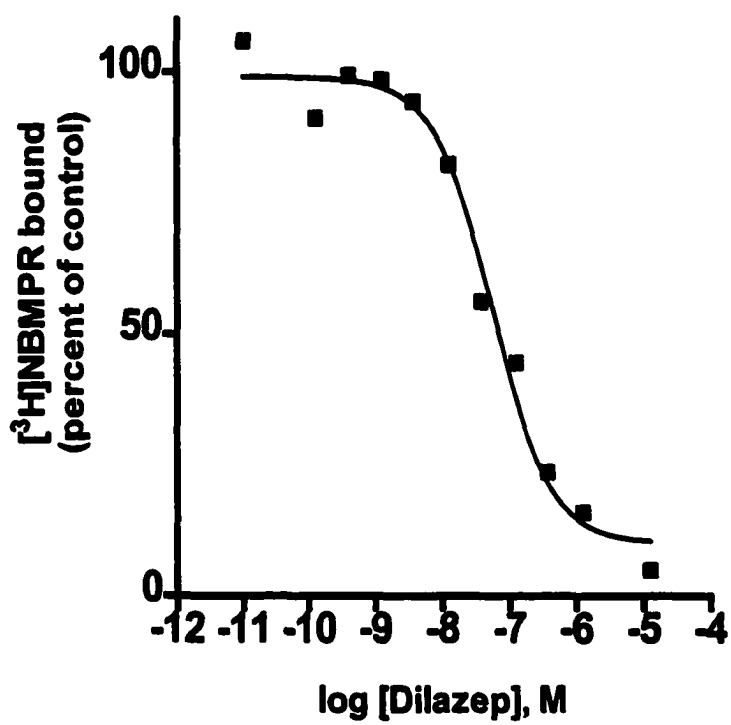


**Figure V-9 D**

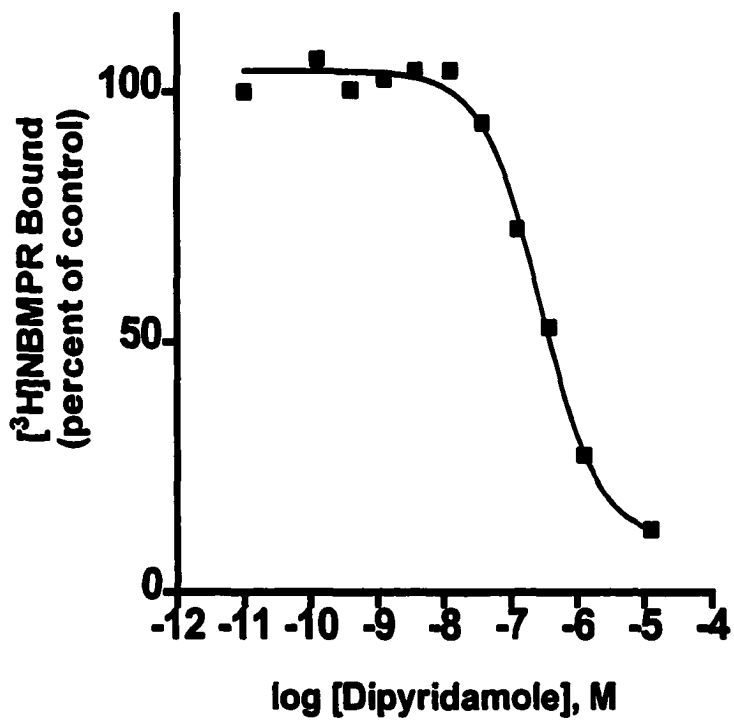


**Table V-1 Effect of nucleoside transport inhibitors on hENT1-mediated complementation**

Yeast cells transformed with either pYES2 or pYhENT1, grown in CMM/GAL medium, were streaked on solid CMM/GAL/MTX/SAA medium (inducing conditions, thymidylate starvation) that contained 0  $\mu\text{M}$  thymidine, 1 mM thymidine or 10  $\mu\text{M}$  thymidine as described in Chapter II, section II.B, and one the three inhibitors at the concentration indicated. Growth on plates was visualized after 3.5 days. Growth comparable to that found in the presence of 1000  $\mu\text{M}$  thymidine is denoted as (+) and the complete absence of growth is denoted as (-). Three separate experiments yielded similar results.

Inhibitor	pYES2			pYhENT1		
	Thymidine ( $\mu\text{M}$ )					
	0	10	1000	0	10	1000
none	-	-	+	-	+	+
1 $\mu\text{M}$ NBMPR	-	-	+	-	-	+
10 $\mu\text{M}$ dilazep	-	-	+	-	-	+
10 $\mu\text{M}$ dipyridamole	-	-	+	-	-	+

**Table V-2            Effect of nucleoside transport inhibitors on hENT1-mediated complementation**

Yeast cells transformed with either pYES2 or pYN48Q, grown in CMM/GAL medium, were streaked on solid CMM/GAL/MTX/SAA medium (inducing conditions, thymidylate starvation) that contained 0  $\mu$ M thymidine, 1 mM thymidine or 10  $\mu$ M thymidine as described in Chapter II, section II.B, and one the three inhibitors at the concentration indicated. Growth on plates was visualized after 3.5 days. Growth comparable to that found in the presence of 1000  $\mu$ M thymidine is denoted as (+) and the complete absence of growth is denoted as (-). Three separate experiments yielded similar results.

Inhibitor	pYES2			pYN48Q		
	Thymidine ( $\mu$ M)					
	0	10	1000	0	10	1000
none	-	-	+	-	+	+
1 $\mu$ M NBMPR	-	-	+	-	-	+
10 $\mu$ M dilazep	-	-	+	-	-	+
10 $\mu$ M dipyridamole	-	-	+	-	-	+

## **VI.**

### **Characterization of the native and recombinant human equilibrative NBMPR-insensitive nucleoside transporter protein (hENT2)**

-

-

## VI.A. ABSTRACT

The human equilibrative nitrobenzylmercaptapurine ribonucleoside (NBMPR)-insensitive transporter (*ei*) has been found to co-exist with other nucleoside transport processes in all cell types studied to date, making its characterization difficult. Additionally, the *ei* transport process usually represent the minority (10-30%) of the total nucleoside transport activity, further confounding analysis of this transporter. Dilazep and dipyridamole are well-established non-nucleoside inhibitors of *es* nucleoside transport processes that block hENT1-mediated transport at nanomolar concentrations. When this work was initiated, the sensitivity of the *ei* nucleoside transport process to dilazep and dipyridamole had not been quantified. The objective of this work was to examine the sensitivity of the *ei* nucleoside transport process to dilazep and dipyridamole, using cultured HeLa cells to study inhibitor sensitivity of the native *ei* process, and the yeast nucleoside transport expression system to study determinants of inhibitor sensitivity. Dilazep and dipyridamole were shown to be less potent inhibitors of the *ei* process and displayed  $IC_{50}$  values for thymidine uptake of  $4.1 \pm 1.3 \mu\text{M}$  and  $0.09 \pm 0.03 \mu\text{M}$ , respectively, and for uridine uptake of  $2.9 \pm 0.8 \mu\text{M}$  and  $0.23 \pm 0.13 \mu\text{M}$ , respectively. The hENT2 cDNA was inserted into the yeast expression vector pYES2 to create pYhENT2 and functional production of recombinant hENT2 was demonstrated in *S. cerevisiae* using a selection strategy based on the ability of the introduced transporter protein to rescue yeast from thymidylate starvation by enabling salvage of extracellular thymidine. Recombinant hENT2 was able to complement the imposed thymidine depletion, indicating hENT2-mediated transport of thymidine into the recipient cells. hENT2 was shown to be present in yeast plasma membranes as determined by direct measure of rates of uptake of [<sup>3</sup>H]thymidine into (i) hENT2-producing yeast, and (ii) proteoliposomes reconstituted from the hENT2-containing yeast membranes. Purine and pyrimidine nucleosides were tested for their ability to inhibit hENT2-mediated rescue of



yeast under the selection conditions to assess the apparent substrate selectivities of hENT2. Adenosine, uridine, inosine and to a lesser extent hypoxanthine and thymidine, inhibited hENT2-mediated complementation. Dipyridamole, but not NBMPR or dilazep, inhibited hENT2-mediated complementation, demonstrating that the yeast nucleoside transport expression system can be used to study determinants of dipyridamole interaction with hENT2. Glycosylation mutants of hENT2 were produced by site-directed mutagenesis of the cDNA sequence encoding asparagine residues 48, 57 and 225 to the codon encoding glutamine. These results demonstrated that the predicted loop region between transmembrane spanning domains 1 and 2 was extracellular, since a mutant version of hENT2 lacking asparagine residues 48 and 57 (contained within this loop region) did not undergo glycosylation. The predicted loop region between transmembrane spanning domains 6 and 7 was intracellular since a mutant lacking asparagine 225 (contained within this loop region) could be glycosylated.

## **NOTE TO USERS**

**Page(s) not included in the original manuscript and are unavailable from the author or university. The manuscript was microfilmed as received.**

**189**

**This reproduction is the best copy available.**

**UMI**

mediated nucleoside transport in mammalian cells (16,19,21), the kinetic characteristics of the *ei* transport process and the basis of interaction of the non-nucleoside analogs dilazep and dipyridamole with hENT2 remain poorly understood. Described here are studies with HeLa cells in which (i) the kinetic parameters for thymidine transport were determined for the NBMPR-insensitive process, and (ii) the ability of dilazep and dipyridamole to block *ei*-mediated nucleoside transport was quantified by determining concentration-effect relationships for dilazep and dipyridamole-dependent inhibition of NBMPR-insensitive thymidine and uridine transport. It was previously shown that cDNAs encoding nucleoside transporter proteins can be expressed in *S. cerevisiae* by assessing the growth of a yeast strain that is deficient in thymidine transport under selection conditions that prevent the production of dTMP *de novo* (Chapter IV, V and (139)). Thus, experiments were undertaken to establish that recombinant hENT2 could be functionally produced in *S. cerevisiae* as a first step in the development of an approach to study the determinants of hENT2 interaction of the non-nucleoside transport inhibitors. Demonstrated here is the functional expression of hENT2 cDNA in *S. cerevisiae* by the following criteria: (i) the survival of yeast under the selection conditions, (ii) the presence of hENT2 mRNA and protein in yeast, and (iii) the mediated uptake of thymidine by intact hENT2-containing yeast and proteoliposomes reconstituted from detergent-solubilized membranes. The apparent substrate specificity of hENT2 for both purine and pyrimidine nucleosides and nucleobases was assessed by testing their ability to inhibit phenotypic complementation of the thymidine transport deficiency. Similarly, the effects of NBMPR, dilazep and dipyridamole on the transport activity of recombinant hENT2 were assessed by testing the ability of high concentrations to inhibit phenotypic complementation of the thymidine transport deficiency in yeast subjected to thymidylate starvation. Elimination of the N-linked glycosylation site of the *es* transporter by conversion of N48 to Q did not eliminate its ability to function as a transporter but did alter its sensitivity to inhibition by dilazep and dipyridamole (Chapter V). The role of N-linked glycosylation of hENT2 was examined by

**comparing phenotypic complementation in yeast producing wild type hENT2 with that of mutants in which the predicted N-linked glycosylation sites were eliminated by conversion of N to Q at positions 48, 57 and/or 225. Finally, the hENT2-glycosylation mutants were used to determine the topological orientation of two landmark regions within hENT2.**

## VI.C. RESULTS

### VI.C.i. Thymidine uptake in HeLa cells

HeLa cells functionally possess both the equilibrative NBMPR-sensitive (*es*) and equilibrative NBMPR-insensitive (*ei*) nucleoside transport processes (116). However, because the *ei*-mediated transport component represents the minority of total transport activity it has been difficult to kinetically characterize. To permit the measurement of kinetics of *ei* (HeLa)-mediated nucleoside uptake, the *es*-component of nucleoside transport was pharmacologically blocked with the potent *es*-inhibitor NBMPR (100 nM), to permit examination of *ei*-mediated transport in isolation. Previous studies of thymidine transport in HeLa cells (116) have established that *es*-mediated transport is completely blocked when cells are exposed to 100 nM NBMPR, a concentration that is well in excess of that needed to saturate the inhibitory sites (now known to be associated with hENT1) with high affinity for NBMPR. The experiments of Figure VI-1 established the kinetics of *ei*-mediated [<sup>3</sup>H]thymidine uptake. Initial rates of [<sup>3</sup>H]thymidine uptake are presented as a function of the concentration of [<sup>3</sup>H]thymidine used. Thymidine uptake conformed to Michaelis-Menten kinetics and two independent experiments, one of which is shown in Figure VI-1, yielded mean  $K_m$  and  $V_{max}$  values, respectively, of 355  $\mu$ M and 5.7 pmol/10<sup>6</sup> cells/s.

The human *es* transport protein is potently inhibited by the nucleoside analog NBMPR as well as by the structurally distinct coronary vasodilators dilazep and dipyridamole (4). While it is well established that the *ei* process of human cells is inhibited by dilazep and dipyridamole, the concentration dependence of these inhibitors has not been well defined. The experiments of Figure VI-2 were undertaken to quantify the relative abilities of dilazep (panels A,C) and dipyridamole (panels B,D) to inhibit *ei*-mediated [<sup>3</sup>H]uridine uptake (panels A,B) and [<sup>3</sup>H]thymidine uptake (panel C,D). For both nucleosides dipyridamole was a more potent inhibitor of *ei*-mediated transport activity than dilazep. The mean  $IC_{50}$  values ( $\pm$  S.D.) from three separate experiments, one of which is

shown in Figure VI-2, for inhibition of uridine uptake by dilazep or dipyridamole, respectively, were  $2.9 \pm 0.8 \mu\text{M}$  and  $0.23 \pm 0.13 \mu\text{M}$  and for [ $^3\text{H}$ ]thymidine uptake were  $4.1 \pm 1.3 \mu\text{M}$  and  $0.09 \pm 0.03 \mu\text{M}$ .

#### **VI.C.ii. pYhENT2 complementation of a thymidine transport deficiency in yeast**

Pharmacologic blockade of the *es* transport process permitted partial characterization of the *ei* transport process in HeLa cells. However, the functional production of recombinant *ei* (hENT2) in a model expression system that otherwise lacked the capacity to transport the nucleoside permeant under study would simplify the characterization of hENT2 and would enable studies of site-directed mutants of hENT2. Additionally, site-directed hENT2-mutants could readily be examined in such a model expression system. To expand the work initiated with the native hENT2 of HeLa cells, the yeast nucleoside transporter expression system was used to study recombinant hENT2.

In previous work (Chapters IV and V) functional production of a recombinant nucleoside transporter occurred when the cDNA inserts were cloned in the KpnI and SphI sites of the pYES2 expression vector. In so doing, the codon encoding the initiating methionine was in close proximity to (within ~ 20 base pairs) the GAL1 promoter. The hENT2 cDNA was cloned into the KpnI and SphI sites of the pYES2 expression vector, generating pYhENT2. The experiments of Figure VI-3 were undertaken to determine if expression of the hENT2 cDNA could rescue yeast from drug-imposed depletion of dTMP. Yeast cells with pYhENT2 or pYES2 were grown under conditions of thymidylate starvation in the presence of either galactose (inducer) or glucose (repressor) with various concentrations of thymidine. pYES2-containing and pYhENT2-containing yeast were unable to form colonies in thymidine-free medium (Figure VI-3A) but did so in the presence of 1 mM thymidine (Figure VI-3B); these conditions were shown in earlier experiments (Chapter IV section IV.C.ii) to control for the selection conditions (thymidine-free medium) and for colony-forming ability through diffusional uptake (1 mM thymidine).

pYhENT2-containing yeast also formed colonies in the presence of 10  $\mu$ M thymidine but only when plated on MTX/SAA medium that was supplemented with galactose, the inducer required for efficient transcription of the cDNA insert in the pYES2 vector (Figure VI-3C). There was no growth when pYhENT2-containing yeast cells were plated on medium with MTX/SAA that was supplemented with glucose, the repressor used to block transcription of the hENT2 insert (Figure VI-3D). The expression of the cDNA encoding hENT2 was required to complement the growth arrest imposed by thymidylate starvation, a result that was consistent with the acquisition of thymidine-transport capability.

### **VI.C.iii Production of hENT2 mRNA and protein**

Northern analysis was performed to determine if mRNA corresponding to hENT2 cDNA was present in pYhENT2-containing yeast (Figure VI-4A). RNA samples were prepared from yeast cells (with either pYhENT2 or pYES2) that were cultured (i) in the presence of the selecting drugs under conditions that extracellular thymidine could be salvaged for growth (CMM/GAL/MTX/SAA with either 40  $\mu$ M or 1 mM thymidine respectively) or (ii) in the absence of the selecting drugs under conditions that either induced (galactose-containing medium) or repressed (glucose-containing medium) transcription of the cDNA insert. A single band of 1650 nt was detected in pYhENT2-containing yeast grown in MTX/SAA medium with galactose and to a somewhat lesser extent in yeast grown in CMM/GAL medium. No signal was present in pYhENT2-containing yeast grown in CMM/GLU or in pYES2-containing yeast under any of the experimental conditions. These results, which demonstrated the presence of hENT2 mRNA in cells with pYhENT2, indicated enhanced transcription of hENT2 cDNA by activation of the Gal1 promoter.

Immunoblotting was performed to confirm the presence of recombinant hENT2myc protein in pYhENT2myc-containing yeast (Figure VI-4B). When these studies were initiated hENT2-specific antibodies were not available. The hENT2 cDNA was engineered to possess the cDNA sequence encoding the c-myc immunopeptide at the 3' end of the

hENT2 cDNA (corresponding to the C-terminus of the resulting recombinant protein). During the course of this work, polyclonal antibodies directed against a fusion polypeptide that contained the putative cytosolic loop of hENT2 (residues 213 – 290) became available (M. Cabrita *et al.* unpublished results). Yeast cells with either pYhENT2myc or pYES2 were subjected to thymidylate starvation in the presence of galactose (inducing conditions) and either 40  $\mu$ M or 1 mM thymidine, respectively; these conditions permitted the pYhENT2myc-containing and pYES2-containing yeast to grow at approximately the same rates. Immunoblotting with c-myc monoclonal antibodies or anti-hENT2 polyclonal antibodies (as indicated) demonstrated the presence of immunoreactive material in membranes of pYhENT2myc-containing yeast that was not present in membranes of pYES2-containing yeast. The predominant immunoreactive species was observed as a band of 49 kDa. The predicted molecular mass of non-glycosylated hENT2myc is 50.2 kDa. Immunoblotting with the anti-hENT2 polyclonal antibodies demonstrated the presence of immunoreactive material in membranes of pYhENT2myc-containing yeast that was not present in membranes of pYES2-containing yeast. The anti-hENT2 polyclonal antibodies displayed fewer (if any) cross-reactive material than the anti c-myc monoclonal antibodies and appeared to react with higher affinity to hENT2myc. Therefore the anti-hENT2 polyclonal antibodies were used for the remainder of the studies.

#### **VI.C.iv. Yeast cells with hENT2 exhibit increased cellular uptake of [<sup>3</sup>H]thymidine**

To determine if the phenotypic complementation observed in pYhENT2-containing yeast was due to acquisition of thymidine transport activity, thymidine uptake experiments were conducted with yeast transformed with either pYhENT2 or pYES2. The uptake of 1.0  $\mu$ M [<sup>3</sup>H]thymidine was measured into yeast with either pYhENT2 or pYES2 that had been cultured in MTX/SAA-containing medium with the inducer and either 40  $\mu$ M or 1 mM thymidine, respectively (Figure VI-5). Thymidine uptake by pYhENT2-containing yeast was greater than that by pYES2-containing yeast. These results indicated that the



expression of pYhENT2 was accompanied by the acquisition of the capacity for cellular uptake of thymidine providing a further indication that pYhENT2-containing yeast, when grown in the presence of galactose, produced functional recombinant hENT2.

#### **VI.C.v. Reconstitution of thymidine transport activity into hENT2-containing proteoliposomes**

The experiments of Figure VI-6 were undertaken to demonstrate the presence of membrane-associated recombinant hENT2 by solubilization and functional reconstitution into proteoliposomes. Membranes prepared from pYhENT2-containing yeast cells that were grown under inducing conditions were solubilized with octylglucoside. Exogenously supplied lipids were used to prepare proteoliposomes by a procedure used previously to reconstitute native *es* transporter from human and mouse cells (119,122,123). The time course of uptake of 20  $\mu$ M [<sup>3</sup>H]thymidine (Figure VI-6) was determined into proteoliposomes in the absence of additives or in the presence of a mixture of nucleoside transport inhibitors to determine non-mediated uptake. The differences between the calculated initial rates of uptake were used to calculate the initial rate of inhibitable transport of thymidine (20 pmol/s per mg of reconstituted protein). These results, which demonstrated the functional reconstitution of thymidine transport activity from membranes of pYhENT2-expressing yeast, established that the introduced transport activity was mediated since it could be inhibited by compounds (adenosine, dipyridamole) known to block *ei* transport.

#### **VI.C.vi. Effects of nucleosides and nucleobases on hENT2-dependent thymidine rescue of *S. cerevisiae* in the complementation assay**

The apparent substrate specificity of hENT2 was examined in the experiments of Figure VI-7 by determining the effects of purine and pyrimidine nucleosides and nucleobases on colony formation in the yeast complementation assay. The ability of a test compound to inhibit hENT2-dependent colony formation under selective conditions would be indicative of either a hENT2 substrate or inhibitor. High concentrations of the

nucleosides inosine, uridine, and adenosine completely inhibited hENT2-mediated complementation whereas cytidine and guanosine had only minor inhibitory effects. High concentrations of the nucleobases hypoxanthine and thymine, but not of adenine, uracil or cytosine, also inhibited hENT2-mediated complementation, although not to the same extent as inosine, uridine and adenosine. These data indicated that hENT2 has the capacity to interact with a broad spectrum of purine and pyrimidine nucleosides and nucleobases and was consistent with the observed broad permeant selectivity of the native *ei* process. The observation that hENT2-mediated complementation was inhibited by thymine was unexpected.

#### **VI.C.vii Effect of inhibitors of nucleoside transport on hENT2-dependent thymidine rescue of *S. cerevisiae* in the complementation assay**

NBMPR, dilazep and dipyridamole have been used as pharmacological probes to distinguish between the *es* and *ei* transport processes in a variety of mammalian cell types (1,3). In the experiments of section VI.D.i the sensitivity of the native *ei*-transport process in HeLa cells to inhibition by dipyridamole and dilazep was examined, and dipyridamole was found to inhibit the *ei* transport process to a greater extent than dilazep. hENT2-dependent complementation in yeast subjected to thymidylate starvation was assessed in the presence of the ENT inhibitors in the experiments of Figure VI-7. High concentrations of dipyridamole (100  $\mu$ M) but not dilazep (100  $\mu$ M) or NBMPR (10  $\mu$ M) were shown to inhibit hENT2-dependent colony formation. The ability of dipyridamole to block the thymidine rescue of pYhENT2-containing yeast at low thymidine concentrations indicated the production of recombinant hENT2 that was able to recognize and be inhibited by dipyridamole, but not by dilazep and NBMPR.

#### **VI.C.viii. Assessment of the importance of N-linked glycosylation for hENT2 function by expression of glycosylation-defective mutants in *S. cerevisiae***

The addition of oligosaccharides to asparagine residues (N-linked glycosylation) occurs co-translationally during the synthesis of proteins. N-linked glycosylation occurs in the lumen of the endoplasmic reticulum on asparagine residues possessing the consensus sequence N-X-S/T, where X is any amino acid other than P. A survey of membrane glycoproteins has found that N-linked glycosylation consensus sites are generally (i) spaced at least 10 residues from a transmembrane-spanning domain, (ii) in a loop that is at least 30 residues in length (149). N-linked glycosylation appears to play a role in the proper folding of newly synthesized proteins and may act in the maintenance of quality control during protein synthesis (150). However, N-linked glycosylation of recombinant membrane transport proteins is not necessarily an essential process, and there are a variety of examples in which mutant proteins that lack N-linked glycosylation sites have been functionally produced in expression systems, including the hENT1 glycosylation-defective mutant hENT1/N48Q (described in Chapter VI and (139)).

hENT2 is predicted to contain three N-linked glycosylation sites: two in the loop between transmembrane domains 1 and 2 at N48 and N57 and one in the loop between transmembrane domains 6 and 7 at N225 (19,21). The role of N-linked glycosylation in the biosynthetic processing and function of hENT2 is not known. cDNAs in which the N-linked glycosylation sites of hENT2myc were converted to Q by site-directed mutagenesis were cloned into the KpnI and SphI sites of the pYES2 expression vector (pYN48/57Qmyc, pYN225Qmyc and pYnullmyc) and then functionally expressed in yeast. When yeast cells with the cDNAs encoding the glycosylation defective hENT2-mutants or pYES2 were exposed to MTX/SAA in the presence of galactose (inducer) or glucose (repressor), pYN48/57Qmyc-, pYN225Qmyc- and pYnullmyc-containing yeast formed colonies in the presence of 1 mM thymidine but not in thymidine-free medium (Figure VI-

8). Colonies were also formed by pYN48/57Qmyc-, pYN225Qmyc- and pYnullmyc-containing yeast in the presence of galactose and 50 and 100  $\mu$ M thymidine, whereas none were observed in pYES2-containing yeast (Figure VI-8). Thus the expression of pYN48/57Qmyc, pYN225Qmyc and pYnullmyc cDNAs in yeast complemented the growth arrest imposed by thymidylate starvation. These results indicated that the glycosylation-defective mutants had retained their capacity for thymidine transport and demonstrated that glycosylation was not required for production of functional hENT2 in yeast.

**V.C.ix. Development of an approach for determination of topology landmarks in recombinant hENT2 using N-linked scanning mutagenesis**

At the time of this study was undertaken, there was no experimental verification of the hENT2 topology model proposed by Griffiths *et al.* (19). N-Linked scanning mutagenesis was selected as an approach to identify topological landmarks within recombinant hENT2. This method takes advantage of natural biosynthetic processing mechanisms in which only those N-linked glycosylation consensus sites (N-X-S/T) that are exposed to the lumen of the endoplasmic reticulum are glycosylated and would therefore correspond to extracellularly exposed regions when the membrane protein is present at the cell surface. Glycosylated and non-glycosylated proteins can be distinguished by differences in mobility during SDS-PAGE analysis and immunoblotting. Thus, elimination of endogenous N-linked glycosylation sites within recombinant membrane proteins and/or the selective introduction of individual consensus sites can serve as a general strategy to map the topology of membrane proteins. N-linked scanning mutagenesis has been used to assess the topology of a variety of integral membrane transporter proteins (151-155). An important consideration when undertaking topology studies is that the mutant proteins generated should retain their function, an indication that the protein has undergone "normal" folding and processing. The hENT2 glycosylation mutants (hENT2/N48,57Qmyc; hENT2/N225Qmyc; hENT2/nullmyc) examined in the previous section (VI.D.vii.) were functional, and thus properly folded.

The cDNAs in which the N-linked glycosylation sites of hENT2myc were converted to Q by site-directed mutagenesis were cloned into the mammalian expression vector pCDNA3 (pcN48/57Qmyc, pcN225Qmyc and pcnullmyc) and transiently transfected into Chinese hamster ovary (CHO) cells. The CHO cell line was chosen because this cell line has been used frequently by others as the host for transient transfections of heterologous cDNAs (156-158). Total membranes were prepared from transfected CHO cells and subjected to treatment with Peptide N-glycosidase F (PNGaseF) for removal of N-linked glycans. The resulting deglycosylated membrane samples, as well as “mock” treated samples (prepared identically with the exclusion of PNGaseF), were subjected to SDS-PAGE and immunoblotting with anti-hENT2 polyclonal antibodies (Figure VI-9). These results indicated that pchENT2myc-containing cells produced an immunoreactive species (lane 1) that decreased in size when treated with PNGaseF (lane 2). Elimination of both the N-glycosylation sites contained within the predicted loop region between transmembrane spanning domains 1 and 2 (pcN48/57Qmyc, possessing an intact site at N225) resulted in the production of an immunoreactive species that corresponded to the deglycosylated form of hENT2 (compare untreated and PNGaseF treated samples in lanes 3 and 4, respectively, with the PNGaseF-treated pchENT2myc sample in lane2). These data, which suggested that either N48 and/or N57 was glycosylated, established that the loop region between transmembrane spanning domains 1 and 2 was extracellular. Elimination of the N-linked glycosylation site at N225Q (pcN225Qmyc, possessing intact sites at N48 and N57) resulted in an immunoreactive species (lane 5) that corresponded to fully glycosylated hENT2myc in untreated samples (lane 1). This immunoreactive material decreased in size when treated with PNGaseF (lane 6) and corresponded to deglycosylated hENT2myc in PNGaseF treated sample (lane 2). These data, which suggested that N225 was not glycosylated, established that the loop region between transmembrane spanning domains 6 and 7 was intracellular.

BLANK.

## **VI.D. DISCUSSION**

The availability of cDNAs encoding the ENT proteins from rat and human cells has allowed detailed kinetic studies of the recombinant transporters in oocytes of *Xenopus oocytes* to be performed (16,18). Cultured cells have also been used for the functional expression of hENT2 (21,97). However, these heterologous expression systems have not produced sufficient quantities of recombinant protein to permit a detailed analysis of the physical characteristics of the transporters. Several integral membrane proteins have been introduced into the yeast *S. cerevisiae* with the production of substantial quantities of functional recombinant proteins (98,99,159,160). The production of recombinant hENT2 in yeast of sufficient quantity for purification and physical characterization remains a long term goal. The production of hENT2 in yeast described here was, however, sufficient for functional studies of recombinant hENT2.

HeLa cells possess two distinct components of nucleoside transport that differ in their sensitivities to inhibition by NBMPR, the *es* and *ei* transport processes (148). The *es* transport process represents the majority (70-80%) of total transport in proliferating HeLa cultures (116) and thus is better understood than the *ei* transport process, even though HeLa cells were the source of one of the recently cloned hENT2 cDNAs (21). The isolation of cDNAs encoding hENT2 (19,21), together with the recent development of hENT2-specific antibodies (Cabrita, M. *et al.* unpublished results) has facilitated examination of transporter characteristics. Experiments were undertaken to further characterize the transport properties of the native *ei*-transport process of HeLa cells. Determination of the kinetics of thymidine transport of the native *ei* process of HeLa cells was achieved by pharmacologic blockade of the *es* transport process by inclusion of 100 nM NBMPR in transport medium, thereby permitting examination of the *ei* transport process in isolation. The *ei*-mediated uptake of thymidine conformed to Michaelis-Menten kinetics with  $K_m$  and  $V_{max}$  values of 355  $\mu$ M and 5.34 pmol/10<sup>6</sup> cells/s, respectively.

The *es* transport process of human cells is inhibited by nanomolar concentrations of NBMPR, dilazep and dipyridamole (19,21). While the *ei* process of human cells has been shown to be resistant to relatively high ( $\geq 1 \mu\text{M}$ ) concentrations of NBMPR, its sensitivities to dilazep and dipyridamole have not been fully characterized. The concentration-effect relationships for inhibition of *ei*-mediated transport of [ $^3\text{H}$ ]uridine and [ $^3\text{H}$ ]thymidine in HeLa cells by dilazep and dipyridamole indicated that the *ei* transport process was more sensitive to inhibition by dipyridamole than by dilazep. These data suggested that hENT1 and hENT2 share structural determinants that confer sensitivity to dipyridamole.

While pharmacologic blockade of the *es* process of HeLa cells permitted functional examination of the *ei* process, introduction of recombinant hENT2 into a transport-deficient eukaryotic model system would facilitate functional studies of the *ei* transport process. The yeast nucleoside transport expression system, described in Chapter IV, was used for production of recombinant hENT2. It was demonstrated that expression of the hENT2 cDNA in yeast subjected to thymidylate starvation enabled growth when exogenous thymidine was present in the growth medium. Northern analysis confirmed that (i) hENT2 mRNA was present in pYhENT2-containing yeast but not in pYES2-containing yeast, and (ii) hENT2 mRNA was present in pYhENT1-containing yeast grown in the presence of galactose (inducing conditions) but was absent in yeast grown in the presence of glucose (repressive conditions).

To compare the ability of NBMPR, dilazep and dipyridamole to inhibit the native and recombinant hENT2, the sensitivity of recombinant hENT2 to inhibition by these ENT inhibitors was assessed using the complementation assay. Thymidine rescue of pYhENT2-expressing yeast from thymidylate starvation was blocked by addition of 100  $\mu\text{M}$  dipyridamole but unaffected by the addition of 100  $\mu\text{M}$  dilazep and 10  $\mu\text{M}$  NBMPR to the growth medium. These data suggested that recombinant hENT2 was sensitive to dipyridamole. The inability of dilazep and NBMPR to prevent hENT2-mediated growth at



micromolar concentrations indicated operation of hENT2 at levels sufficient to sustain growth over the course (3.5 days) of the experiment. The absence of an effect with dilazep was unexpected, given its ability to inhibit *ei* transport in HeLa cells, and raised the possibility of degradation of dilazep during the experiment. Direct measure of hENT2-mediated thymidine uptake, in the presence or absence of the ENT inhibitors, will be required to better define the ability of dipyridamole, dilazep and NBMPR to inhibit recombinant hENT2.

Domain swapping experiments designed to explore the intrinsic difference in sensitivity to inhibition by dipyridamole between the human and rat *es* transporters (hENT1 and rENT1) have established that the determinants for dipyridamole sensitivity reside in the N-terminal half of hENT1, with the majority of dipyridamole sensitivity associated with transmembrane spanning domains 2-6 (35). hENT1 and hENT2 share high amino acid identity (50%) and it is likely that the hENT2 structural determinants for dipyridamole sensitivity are similar to (or the same as) those of hENT1. Thus, site-directed mutagenesis of the hENT2 cDNA within predicted transmembrane spanning domains 2-6 may allow determination of the residues involved in the interaction of dipyridamole with hENT2.

hENT2 is an integral membrane protein and thus was expected to be present in membrane fractions of pYhENT2-expressing yeast. Immunoblotting of yeast membranes with the 9E10 anti-c-myc monoclonal antibody, and anti-hENT2 polyclonal antibodies, demonstrated the presence of immunoreactive protein in pYhENT2myc-expressing yeast but not in pYES2-expressing yeast. The predominant immunoreactive species exhibited an apparent molecular mass of 49 kDa and thus corresponded to the hENT2 monomer because the predicted molecular mass of non-glycosylated hENT1 is 50.2 kDa.

The apparent substrate specificity of hENT2 was determined by inhibition experiments in which the ability of a purine or pyrimidine nucleoside to inhibit hENT2-mediated thymidine complementation was assessed. Compounds that inhibited hENT2-mediated complementation would be indicative of either substrates or inhibitors of the

transporter. Adenosine, uridine and inosine were shown to completely inhibit hENT2-mediated complementation whereas cytidine and guanosine had little effect. The nucleobases hypoxanthine and thymine were found to partially inhibit hENT2-mediated complementation. The finding that thymine also inhibited hENT2-mediated complementation was unexpected and suggested that this nucleobase may be a substrate of hENT2. Together, these data suggested a role of hENT2 in the uptake of nucleosides and nucleobases. The presence of both hENT1 and hENT2 in the same cell type has raised the question as to the physiological necessity for two apparently broadly specific nucleoside transport proteins. The results of the complementation assay indicated that the substrate specificity of hENT2 was distinct from that of hENT1 and suggested distinct cellular roles of each transporter in cell types possessing both transporters.

hENT2 possesses three consensus sites for N-linked glycosylation at predicted residues N48, N57 and N225. The functional significance of these consensus sites and the role of N-linked glycosylation in the proper functioning of hENT2 is not known. The functional expression of hENT2 glycosylation mutants (lacking one, two or all three consensus glycosylation sites) in *S. cerevisiae* established that glycosylation is not necessary for the production of functional hENT2.

N-linked mutagenesis of recombinant hENT2 established two topological landmarks in hENT2. The loop region between predicted transmembrane spanning domains 1 and 2 was shown to be glycosylated, at either residue N48 or N57 (or both residues), indicating that this loop region was exposed to the lumen of the endoplasmic reticulum during biosynthesis and therefore was present to the extracellular side of the plasma membrane. Because the first loop region was extracellular it is probable that the N-terminus of the protein was intracellular. It was shown that the loop region between transmembrane domains 6 and 7 was not glycosylated at residue N225 and was therefore intracellular. Together these data support the predicted topology model of hENT2

suggested by predictive algorithms (18,21). Continued studies will be required to further define the topology of hENT2.

The abundance of recombinant hENT2 in pYhENT2-expressing membranes provided a source of recombinant hENT2 for reconstitution into proteoliposomes, thereby permitting a direct demonstration of hENT2-dependent transport activity. Reconstituted proteoliposomes, prepared from hENT2-producing yeast, exhibited a mediated uptake of thymidine ( $20 \pm 2$  pmol/s per mg of reconstituted protein). Native *ei* transporters have previously been solubilized from Ehrlich ascites tumor cell plasma membranes and reconstituted into proteoliposomes (122) although in these studies the proteoliposomes also contained the *es* transporter. The reconstitution of recombinant hENT2 from yeast membranes into proteoliposomes has advantages because of the absence of endogenous thymidine-transporting activities and because of the opportunities presented through recombinant DNA techniques for modification of the hENT2 amino acid sequence.

**Figure VI-1      Kinetic analysis of *ei*-mediate transport of thymidine in HeLa cells**

The uptake of graded concentrations of [<sup>3</sup>H]thymidine into proliferating HeLa cells was measured. Initial rates of [<sup>3</sup>H]thymidine uptake were determined into HeLa cells in which the *es* component of transport had been pharmacologically blocked with 100 nM NBMPR as described in Chapter II, section II.J.ii. The rate of *ei*-mediated transport is presented as a function of the substrate concentration tested. Results are means ± S.D. for triplicate determinations of the cellular [<sup>3</sup>H]nucleoside content. Two experiments, one of which is shown, gave similar results, yielding mean values for  $K_m$  and  $V_{max}$  for thymidine uptake of 355 μM and 5.7 pmol/10<sup>6</sup> cells/s, respectively.

# Figure VI-1

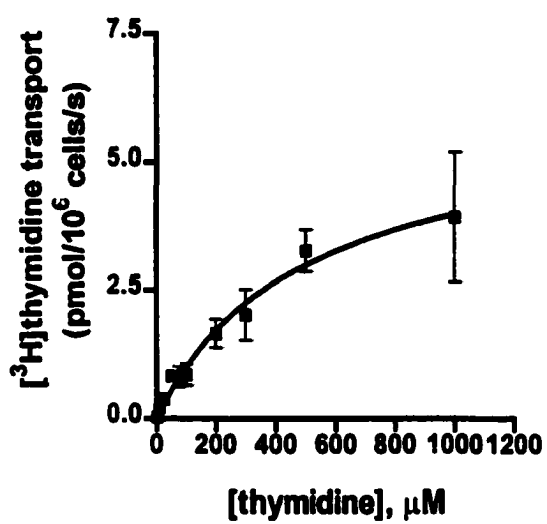


**Figure VI-2      Inhibition of *ei*-mediated [<sup>3</sup>H]uridine and [<sup>3</sup>H]thymidine uptake in HeLa by dilazep and dipyridamole**

The rates of *ei*-mediated transport of 100 μM [<sup>3</sup>H]uridine (Panels A and B) and 100 μM [<sup>3</sup>H]thymidine (Panels C and D) were determined as described in the legend of Figure VI-1 by measuring initial rates of uptake in cells treated (for 15 min before and also during uptake reactions) with 100 nM NBMPR (to block *es*-mediated transport). Uptake reactions were conducted at 22°C in the absence or presence of graded concentrations of dilazep (Panel A and C) or dipyridamole (Panel B and D) as described in Chapter II, section II.J.ii. Results are presented as the percentage of rates observed in the presence of various concentrations of inhibitor relative to the rates observed in the absence of inhibitors. Uptake in the absence of dilazep or dipyridamole is considered 100% uptake. Results are means (± S.D.) for triplicate determinations of the rates of uptake. Three experiments, one of which is shown, gave similar results, yielding mean (±S.D.) IC<sub>50</sub> values for dilazep and dipyridamole inhibition of [<sup>3</sup>H]uridine uptake of 2.9 ± 0.8 μM and 0.23 ± 0.13 μM respectively, and [<sup>3</sup>H]thymidine uptake of 4.1 ± 1.3 μM and 0.09 ± 0.03 μM respectively. IC<sub>50</sub> values were inferred from the sigmoidal dose-response curve using PRISM GraphPad V 2.0 software.

1

.

# Figure VI-2

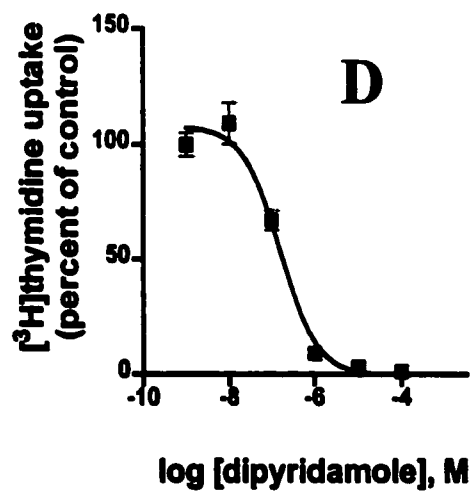
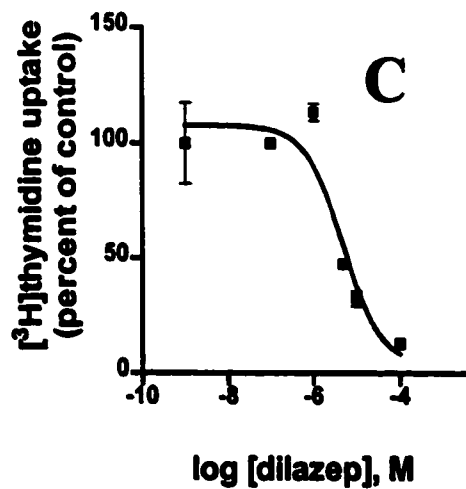
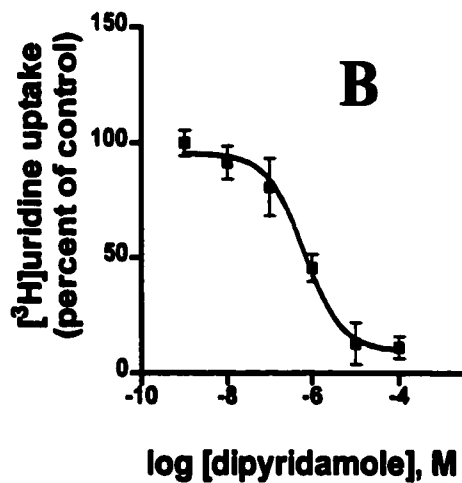
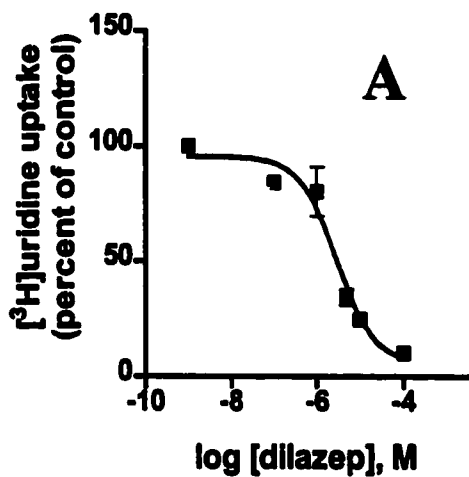


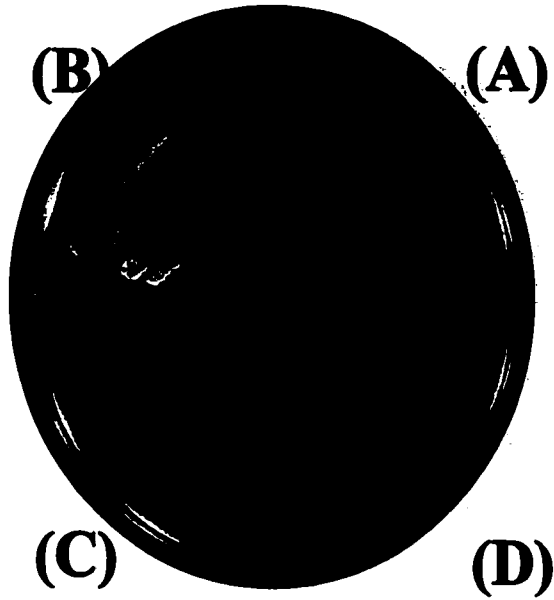
**Figure VI-3      Functional complementation of a thymidine transport deficiency in *S. cerevisiae* by recombinant hENT2**

Yeast cells containing either pYES2 or pYhENT2 were streaked on CMM/GAL/MTX/SAA solid medium (inducing conditions, thymidylate starvation) that contained either 0  $\mu$ M thymidine (A), 1 mM thymidine (B) or 10  $\mu$ M thymidine (C) as described in Chapter II, section II.B. Yeast cells were also streaked on CMM/GLU/MTX/SAA medium (repressive conditions, thymidylate starvation) that contained 10  $\mu$ M thymidine (D). Growth on plates was visualized after 3.5 days. Three separate experiments, one of which is shown, yielded similar results.



**Figure VI-3**

**pYES2**



**pYhENT2**

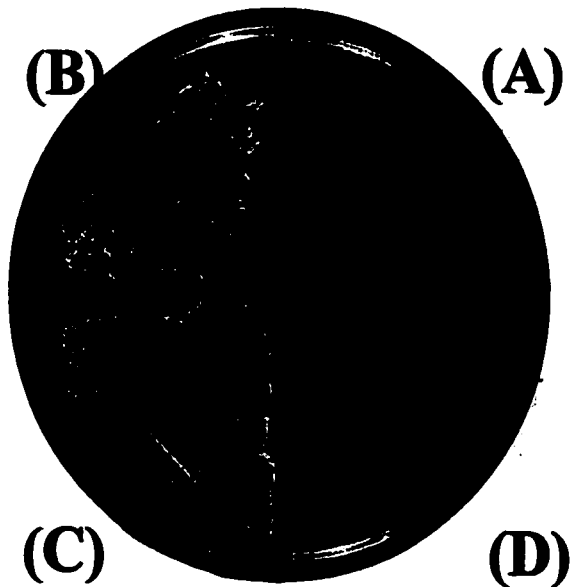


**Figure VI-4      Production of hENT2 mRNA and recombinant protein by *S. cerevisiae*.**

**Panel A.** Total RNA from yeast with pYhENT2 (lanes 1-3) or pYES2 (lanes 4-6) was prepared from proliferating yeast (section II.D) and subjected to Northern analysis with a <sup>32</sup>P-labelled hENT2 cDNA fragment (nucleotides 1-718) and then detected by autoradiography, as described in Chapter II, section II.D. Yeast growth conditions were as follows: CMM/GAL/MTX/SAA medium that contained either 40 μM thymidine (lane 3) or 1 mM thymidine (lane 6); CMM/GAL medium (lanes 2 and 5); CMM/GLU medium (lanes 1 and 4). **Panel B.** Membranes, prepared as described in Chapter II, section II.E, from yeast with pYES2 (lane 1) or pYhENT2myc (lane 2) grown in CMM/GAL/MTX/SAA medium that contained 1 mM or 40 μM thymidine respectively, were subjected to immunoblotting with the 9E10 anti-c-myc monoclonal antibodies or anti-hENT2 polyclonal antibodies (as indicated). The positions of molecular mass markers are indicated (in kDa) at the left.

-

.

# Figure VI-4A

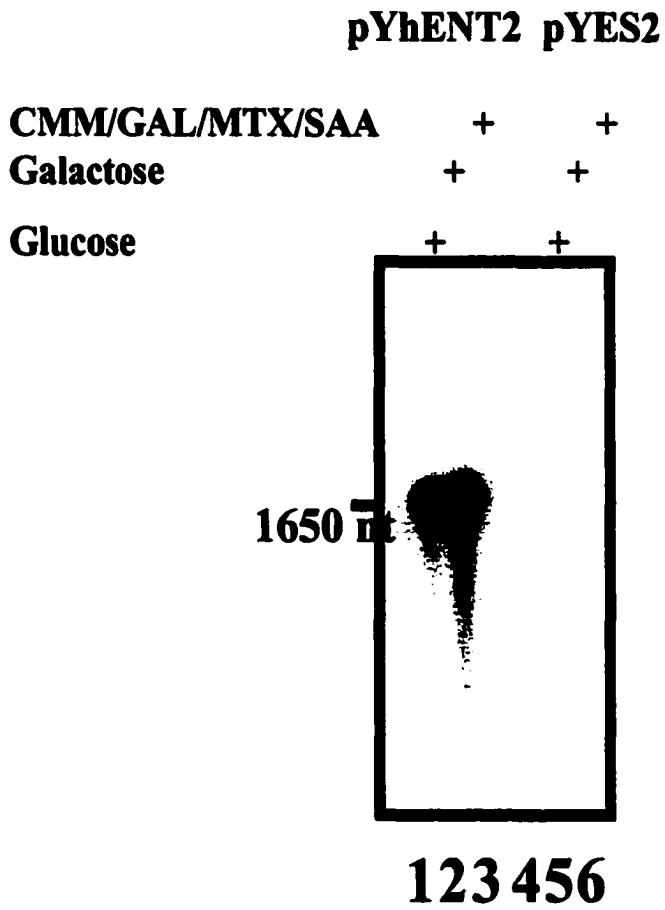


**Figure VI-4 B**

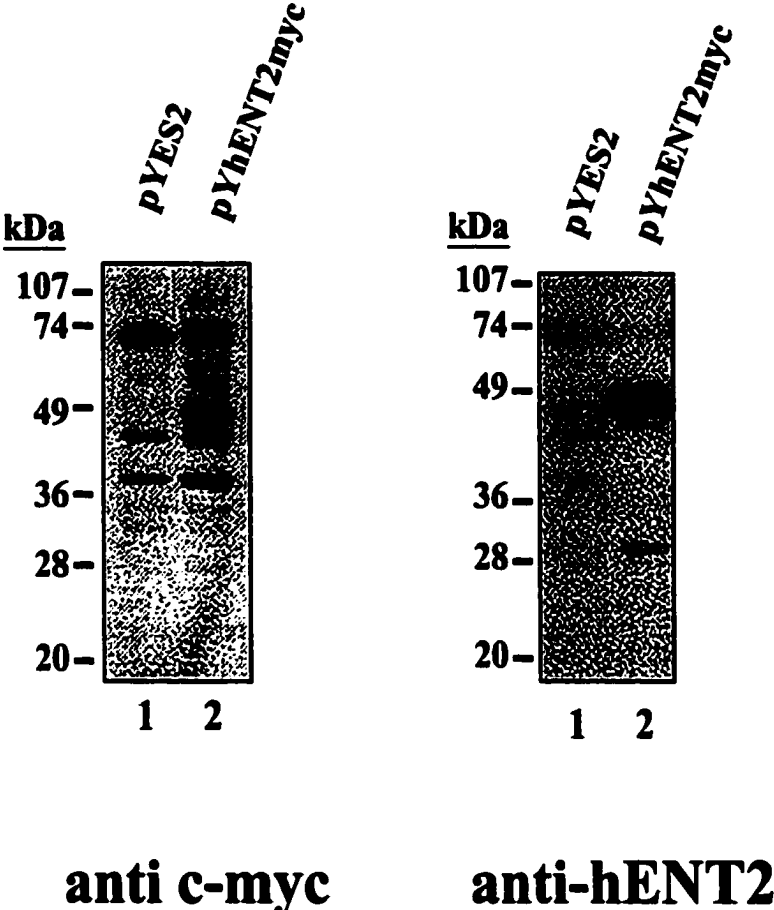


**Figure VI-5 Cellular uptake of [<sup>3</sup>H]thymidine by *S. cerevisiae* producing recombinant hENT2**

Yeast transformed with pYhENT2 or pYES2 were grown in CMM/GAL/MTX/SAA medium (inducing conditions) that contained respectively 40 μM or 1 mM thymidine. The uptake of 1.0 μM [<sup>3</sup>H]thymidine into proliferating yeast, as a function of time, was measured as described in Chapter II, Section II.J.i. Results are means (± S.D.) for triplicate determinations of the cellular content of thymidine. Error bars are not shown where values were smaller than that represented by the symbols. Two separate experiments, one of which is shown, gave similar results.

1

.

**Figure VI-5**

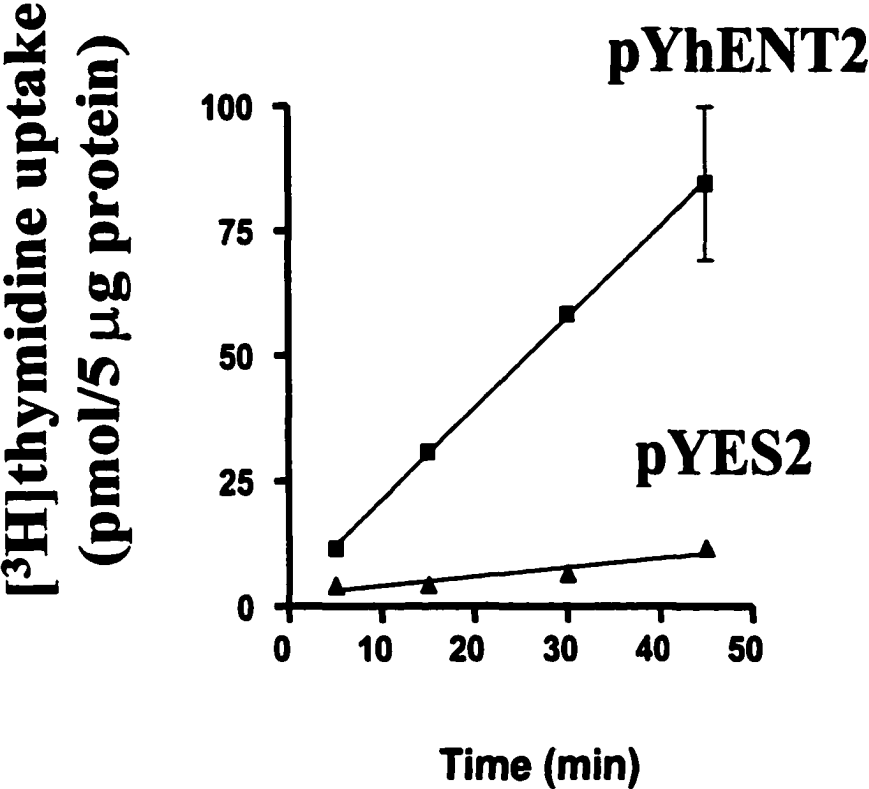


**Figure VI-6      Demonstration of recombinant hENT2 in *S. cerevisiae* membranes by reconstitution of thymidine transport activity**

Crude membranes prepared from yeast with pYhENT2, as described in the legend for Figure VI-4, were solubilized with octylglucoside and reconstituted into liposomes, as described in Chapter II, section II.M. The uptake of 20  $\mu\text{M}$  [ $^3\text{H}$ ]thymidine into proteoliposomes was measured for the indicated timed interval in the absence (-■-, total uptake) or presence (-▲-, non-mediated uptake) of a mixture of transport inhibitors (10 mM adenosine, 10  $\mu\text{M}$  dipyridamole and 10  $\mu\text{M}$  NBTGR). hENT2-mediated uptake of [ $^3\text{H}$ ]thymidine (-▼-) was determined by subtracting the total uptake from the non-mediated uptake. Each point is the average of duplicate determinations (individual values differed from the values shown by  $\leq 7\%$ ). Two experiments gave similar results, yielding an average initial rate of thymidine uptake of 20 pmol/s per mg of protein.

**Figure VI-6**

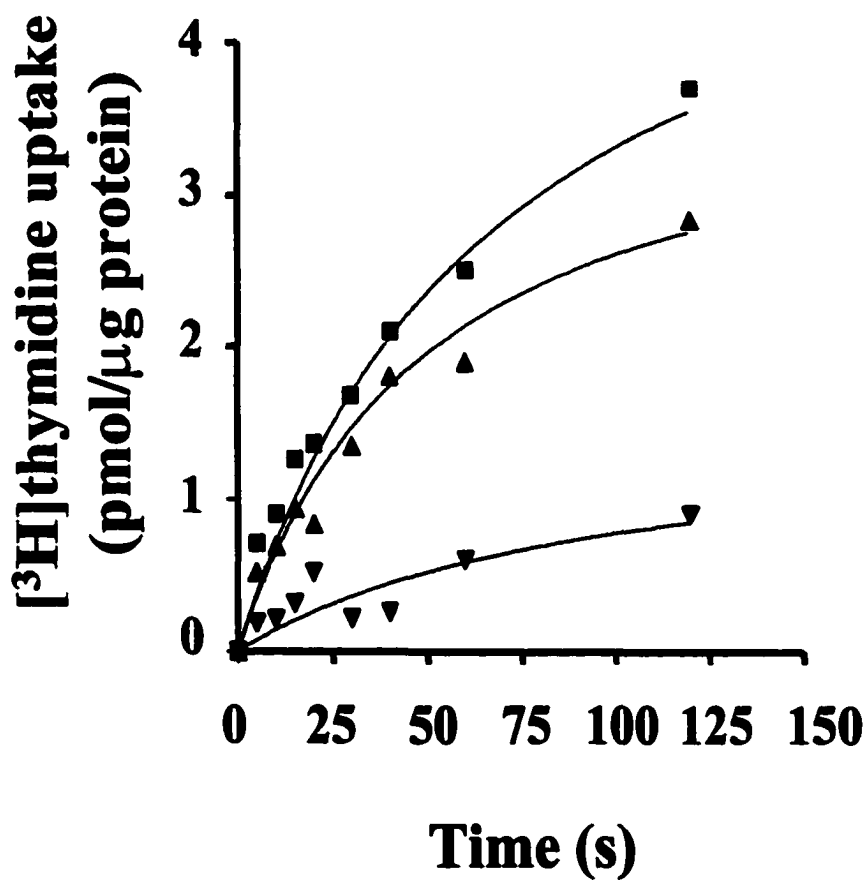




**Figure VI-7      Inhibition of hENT2-mediated complementation of a thymidine transport deficiency in *S. cerevisiae***

Cultures of yeast cells containing either pYES2 or pYhENT2, grown in CMM/GAL medium, were adjusted to an OD<sub>600</sub> of 1.0 and serial dilutions (10<sup>0</sup>-10<sup>-3</sup>) were prepared. Ten-μl portions of the yeast dilutions were spotted onto CMM/GAL/MTX/SAA medium (inducing conditions, thymidylate starvation) that contained 0 μM thymidine, 10 μM thymidine or 1 mM thymidine that also contained a test compound (indicated at left of figure) and the resulting plates were incubated at 30°C as described in Chapter II, section II.B. Growth on plates was assessed after 3.5 days. Two separate experiments, one of which is shown, yielded similar results.

**Figure VI-7**

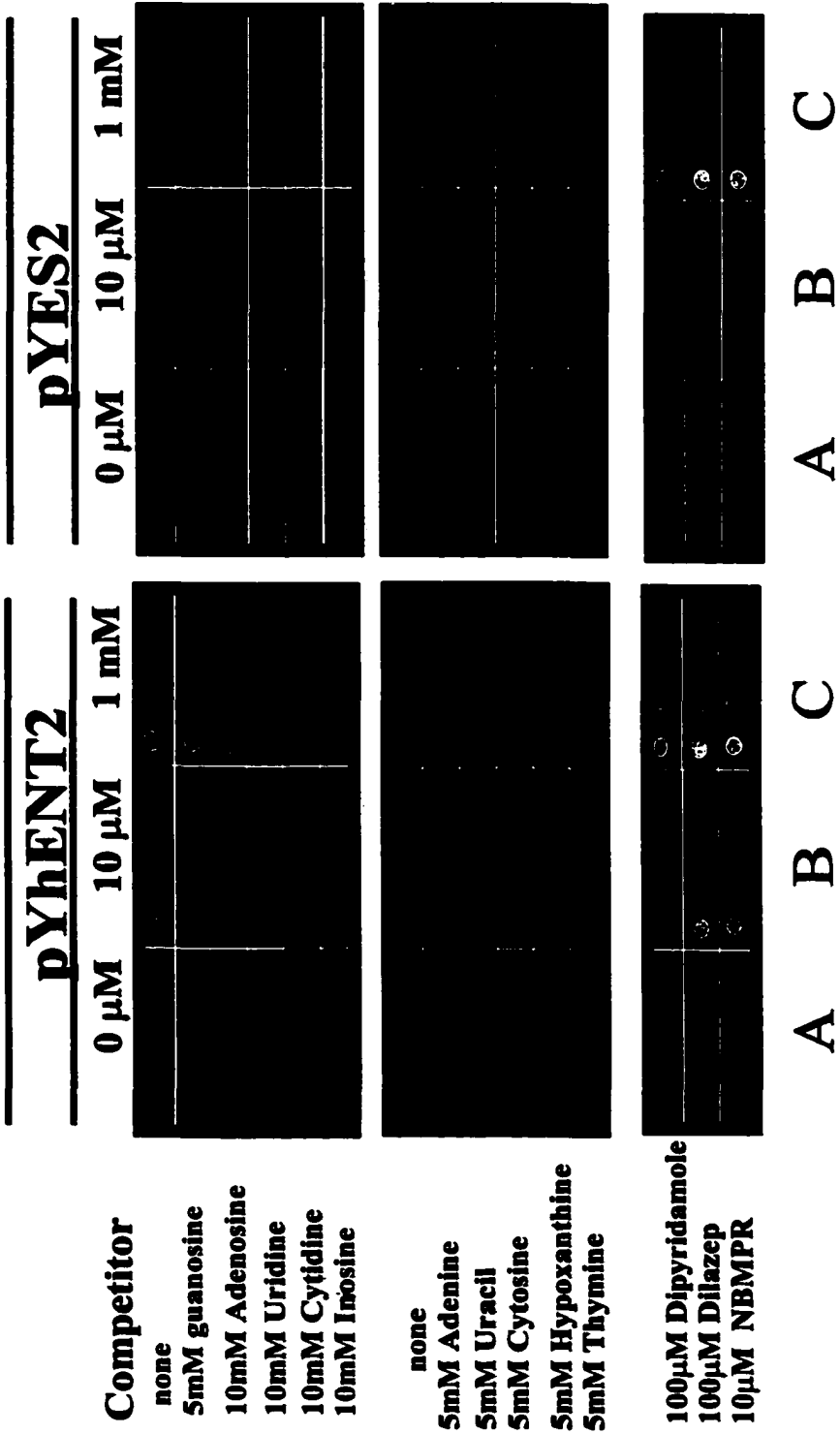


**Figure VI-8      Functional complementation of a thymidine transport deficiency in *S. cerevisiae* by hENT2 glycosylation-defective mutants**

Cultures of yeast containing pYES2, pYhENT2myc, pYN48/57Qmyc, pYN225Qmyc or pYnullmyc, grown in CMM/GAL medium, were adjusted to an OD<sub>600</sub> of 1.0 and serial dilutions (10<sup>0</sup>-10<sup>-3</sup>) were prepared. Ten-μl portions of the yeast dilutions were spotted onto CMM/GAL/MTX/SAA medium (inducing conditions, thymidylate starvation) that contained 0 μM thymidine, 50 μM thymidine, 100 μM thymidine or 1 mM thymidine and the resulting plates were incubated at 30°C as described in Chapter II, section II.B. Growth on plates was assessed after 3.5 days. Two separate experiments, one of which is shown, yielded similar results.

**Figure VI-8**

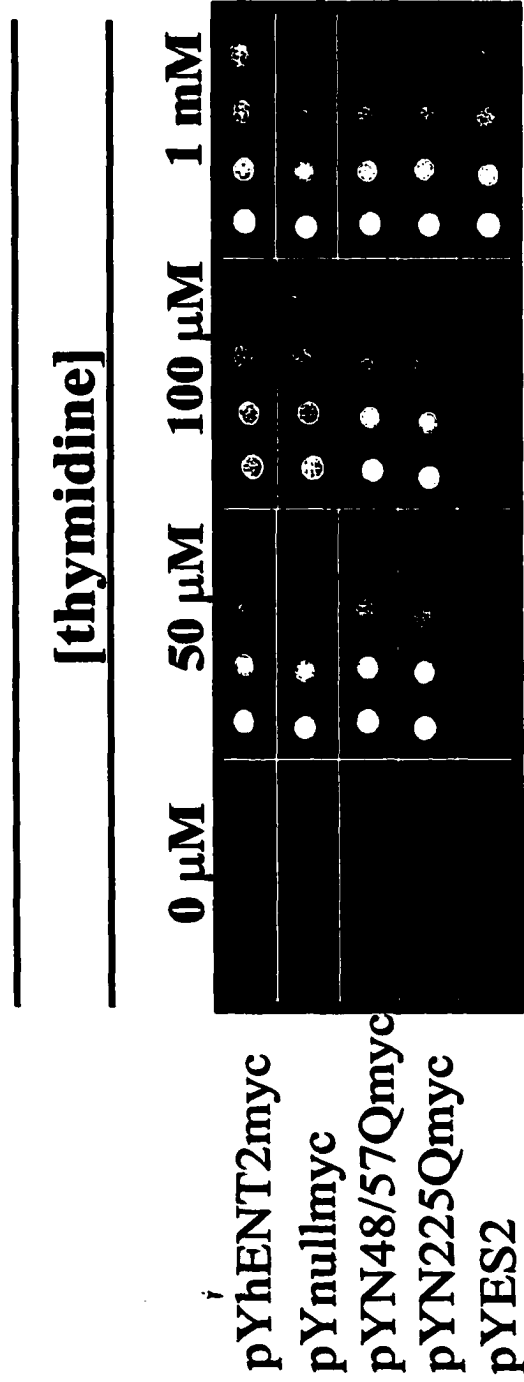
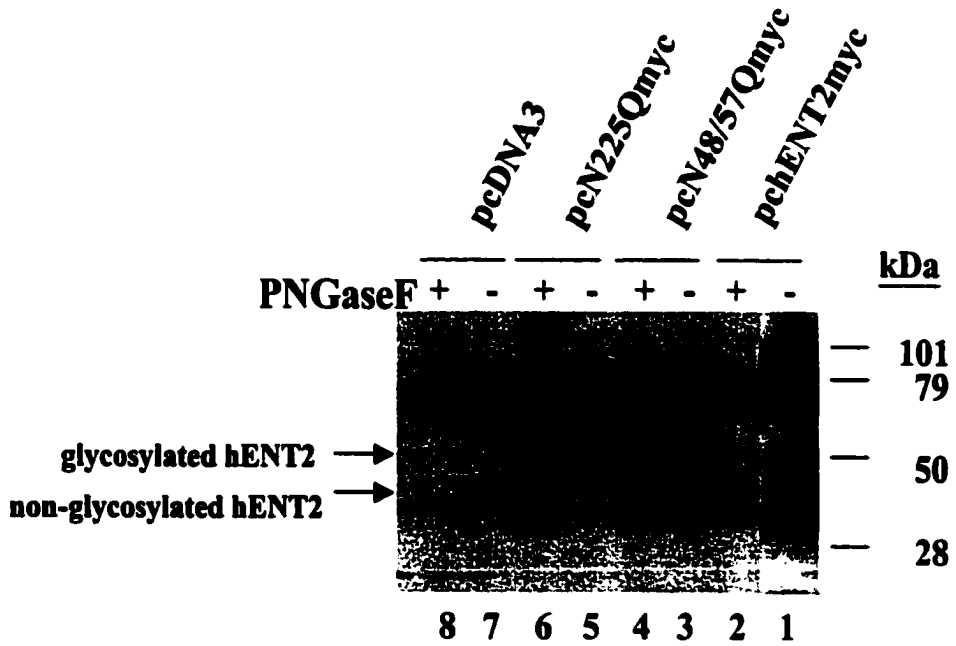


**Figure VI-9            Determination of two topological landmarks in hENT2**

Membranes were prepared, as described in Chapter II, section II.F, from CHO cells transiently transfected with pchENT2myc (lane 1,2), pcN48/57Qmyc (lane pcN225Qmyc 3,4), <sup>-</sup> (lane 4,5) or pcDNA3 (lane 6,7), described in section II.A.v. The resulting membranes were incubated with PNGaseF (+) or buffer alone (-) as described in Chapter II, section II.H, resolved by SDS-PAGE (2 µg protein/lane), transferred to Immobilon-P membrane and subjected to immunoblotting with the anti-hENT2 polyclonal antibodies. The positions of molecular mass markers are indicated in kDa at the left. The position of the glycosylated and non-glycosylated hENT2 immunoreactive species are denoted by arrows. Please note, lane 1 is from the same immunoblot as lanes 2 through 8. Lane 1 represents a longer exposure of the immunoblot to film than for lanes 2 through 8 to permit visualization of the hENT2 immunoreactive species.

-  
.

# Figure VI-9



**VII.**  
**General Discussion**

The initial goal of the work presented in this thesis was to develop procedures for the use of *S. cerevisiae* as an expression system to produce recombinant nucleoside transporter proteins to enable biochemical and molecular studies of relationships between nucleoside transporter structure and function. A substantial effort was devoted to the development and validation of methods to achieve expression of nucleoside transporter cDNAs, focusing initially on members of the CNT protein family and subsequently on members of the ENT family. Nucleoside transporters from bacteria, rat and humans were successfully produced in yeast at levels that were sufficient for a variety of functional studies that addressed questions of current interest in nucleoside transporter biology. The levels of expression achieved were not sufficient to undertake purification of nucleoside transporter proteins.

#### **VII.A The nucleoside transporter proteins of *S.cerevisiae***

A key factor in the development and utilization of a model expression system is knowledge of the host's endogenous nucleoside transport proteins. Therefore, an examination and characterization of the nucleoside transporter proteins of *S. cerevisiae* was undertaken. It was shown that *S. cerevisiae* possess two structurally unrelated nucleoside transporter proteins: (i) FUI1, a uridine-specific transporter protein of the "uracil/allantoin" family of transporters, and (ii) FUN26, a broadly specific, transporter protein of the ENT family. FUI1 was shown to function primarily at the yeast cell surface whereas FUN26 was found in intracellular membranes and thus may function in the translocation of nucleosides between intracellular compartments. These results underscore a feature important not only to the FUI1 and FUN26 transporters of yeast but to nucleoside transporter proteins in general. Nucleoside transporter proteins appear to play a role in the uptake and release of nucleosides also across intracellular membranes. In the case of *S. cerevisiae*, FUN26 may play a role in the salvage of nucleosides released from the degradation of nucleic acids by vacuolar enzymes. In mammalian cells, nucleoside



transporter proteins (or the transport activities) have been shown to be present in both plasma membranes and intracellular membranes (7-9,116).

Future experiments should be aimed at confirming the cellular location and function of native FUN26 to test the hypothesis that FUN26 is a nucleoside transporter protein of vacuolar membranes. Isolation of vacuoles from either wild type yeast or the *fun26*-disruption mutant will allow a direct comparison of nucleoside uptake into the vacuoles to test the hypothesis that FUN26 is a nucleoside transporter of vacuolar membranes. If FUN26 is involved in vacuolar nucleoside transport, uptake of nucleosides into vacuoles isolated from the *fun26*-disruption mutant is expected to be reduced compared to uptake into vacuoles from wild type yeast. A parallel line of investigation using antibodies raised against FUN26 would allow determination of the cellular location of the native protein. Through the use of continuous sucrose gradient fractionation separate organellar membranes, and in conjunction with confocal microscopy, the cellular location of native FUN26 can be determined. Together, these series of experiments will allow us to determine the cellular location of FUN26.

A feature of FUI1 that remains unknown is the identity of the amino acids involved in uridine recognition. Future work with FUI1 should include the identification of the residues involved in uridine recognition. This could be accomplished by taking advantage of the high degree of amino acid identity of FUI1 with FUR4 (50%). Generation of mutant versions of FUR4 with uridine specificity and the reciprocal mutants in which FUI1 is uracil specific would aid in the determination of the domains (and ultimately the amino acid residues) involved in substrate recognition. Uridine appears to be a universal permeant of the mammalian nucleoside transporters (1,2,4), and the identification of the residues of FUI1 that are involved in the interaction of uridine with the transporter will not only provide information about the mechanism of action of FUI1 but may also be informative for mammalian transporters. FUI1 is structurally unrelated to the other nucleoside transport proteins discovered to date. The completed sequencing of the genomes of other

eukaryotic and prokaryotic organisms may reveal additional members of the “uracil/allantoin” family of transporters that have nucleoside transport activity.

#### **V.II.B Development of *S. cerevisiae* as a model expression system**

The validity of the *S. cerevisiae* nucleoside transporter expression system was established using the pyrimidine-nucleoside specific transporters rCNT1, hCNT1 and NUPC. All three CNTs were functionally produced in *S. cerevisiae* and shown experimentally to retain their pyrimidine-specific substrate specificity. The yeast nucleoside transporter expression system was used to demonstrate that open reading frames encoding putative membrane proteins from *H. influenzae* (HI0519) and *H. pylori* (HP1180) encode proteins that are both structural and functional members of the CNT family of proteins. Furthermore, recombinant HI0519 was shown to possess an apparent broadly-specific substrate specificity by assessing the ability of test compounds to block HI0519-dependent phenotypic complementation in yeast subjected to thymidylate starvation. These studies, demonstrated the utility of the yeast nucleoside transporter expression system for identification of novel nucleoside transporters. With the rapid increase in completed genome sequencing projects, a high-capacity screening method such as developed here will aid in the identification and analysis of putative nucleoside transporter cDNAs (e.g., open reading frames from *B. subtilis* and *C. elegans* with sequence similarities to CNT proteins). Future work should be aimed at the continued characterization of the substrate specificity of HI0519 and HP1180.

Additionally, the *S. cerevisiae* expression system could be used as a method for high throughput analysis of inhibitors of nucleoside transporter proteins. This could be accomplished using either the complementation or transport assays to assess the ability of a test compound to block cellular uptake of thymidine or, if the *fuil*-disruption mutant were used as the host strain for production of recombinant transporter protein, uridine (a more robust permeant). Inhibition of colony growth in the thymidine complementation assay or

of uptake of radiolabeled thymidine (or uridine) in the transport assay would be indicative of a substrate or inhibitor of the transporter in question.

In the case of the complementation assay, high throughput could be achieved by plating yeast onto a small surface area in the presence or absence of a test compound. In these experiments yeast could be cultured in 96-well plates on solid media under selective conditions in the presence or absence of test compounds. Growth could readily be assessed visually or under a light microscope. The small size (volume and surface area) of the wells would have the advantage of requiring less test compound to achieve the desired concentration. The use of 96-well plates would minimize the amount of physical space required to screen a large number of test compounds and would facilitate automation of the process in the preparation of plates and the spotting of yeast. This approach to the complementation assay would rapid identification of high-affinity substrates and inhibitors of the nucleoside transporter being tested. This approach would not identify compounds that partially inhibit the transporter as residual activity would likely allow sufficient amounts of exogenously supplied thymidine to enter the cells, thereby permitting cell growth over the course (3.5 d) of the experiments. This approach would also not allow analysis of compounds that are metabolized by the yeast over the course of the experiment.

In the case of direct measure of transport, experiments would be carried out in a fashion similar to that carried out with FU11 in the experiments of Chapter III. In this approach, nucleoside uptake would be measured into yeast in the absence or presence of a single high concentration of a test compound. This approach has an advantage over the plating assay in that low affinity substrates or inhibitors would be identified by the partial inhibition of transport. Once a compound has been identified as inhibiting transport, a more detailed examination of the lead compound could be undertaken in which the apparent affinity of the compound could be determined by carrying out inhibition experiments over a range of concentrations to determine the apparent inhibition constants ( $K_i$ 's).

### **V.II.C Functional expression of hENT1 in *S. cerevisiae***

Studies were undertaken with hENT1, and a glycosylation defective mutant (hENT1/N48Q), to examine the interaction of inhibitors of nucleoside transport with the recombinant proteins produced in the *S. cerevisiae* expression system. Methodologies were developed that permitted the measurement of interaction of the tight-binding inhibitor NBMPR with recombinant hENT1, the first such direct demonstration with recombinant hENT1. Recombinant hENT1 displayed high-affinity NBMPR binding ( $K_d$ , 1.2 nM) similar to that of the native *es* transporter (1,6). The general utility of rapidly assessing the transport capability of mutant versions of hENT1 using the complementation assay, combined with the ability to directly measure binding of radioactive NBMPR to recombinant hENT1, will facilitate future work directed at identifying the amino acid residues involved in the recognition of NBMPR by hENT1. Specifically, hENT1/hENT2 chimeras could be generated which are assess for functionality and NBMPR sensitivity or insensitivity using the phenotypic complementation assay. In these experiments domains of hENT2 could be inserted into the corresponding region of hENT1 with the aim of identifying a mutant version of hENT1 that is functional and insensitive to inhibition by NBMPR. Conversely, domains of hENT1 could be inserted into the corresponding region of hENT2 with the aim of identifying a mutant version of hENT2 that is functional and insensitive to inhibition by NBMPR

### **V.II.D Functional expression of hENT2 in *S. cerevisiae* and CHO cells**

While a great deal is known about the substrate specificity of hENT1, far less is known about the substrate specificity of hENT2 (1,2,4). This is due, primarily, to two factors (i) no cell line has yet been identified that possesses only the hENT2 transport protein, and (ii) hENT2-dependent transport activity constitutes the minority (10% - 13%) of the total transport activity (1,6,148). The yeast nucleoside transporter expression

system was used in this work to undertake indirect studies using the phenotypic complementation assay to assess the substrate specificity of recombinant hENT2. This work, which confirmed the apparent broad specificity of hENT2 for nucleosides, revealed the capacity of hENT2 to interact with the nucleobases, hypoxanthine and thymine. The interaction of hENT2 with nucleobases is in contrast to hENT1, which interacts with nucleosides and not nucleobases (1-3,19). The direct measure of nucleoside and nucleobase uptake will be required to establish which compounds are substrates or inhibitors of hENT2. The high degree of sequence identity (50%) between hENT2 and hENT1 will permit the identification of the region(s) responsible for nucleoside and nucleobase recognition, through the use of chimeric studies.

The topology studies initiated here through the use of scanning N-linked glycosylation mutagenesis has defined the topology of two landmark regions of hENT2. Future work will be necessary to further define the topology of the loop regions (connecting transmembrane domains) of hENT2 through continued use of scanning and insertional N-linked glycosylation mutagenesis. Specifically, tandem N-linked glycosylation consensus sites (NNSS) would be inserted to the predicted loop regions of hENT2. The functionality of these insertion mutants would be confirmed using the phenotypic complementation assay and the glycosylation status would be assessed by expression of the mutants in CHO cells.

#### **V.II.E Nucleoside transporter proteins as therapeutic targets**

Nucleoside analogue drugs are currently used in the treatment of a number of human diseases, including various solid and haematologic cancers, viral diseases and parasitic infections (for recent reviews see (1,2,6,161)). Like physiologic nucleosides, the analogue drugs are generally hydrophilic compounds that require functional transport processes at cell surfaces to enter target cells and exert their therapeutic effects. With the exception of the hENT1-mediated transport processes, the capacity of nucleoside transporters to accept nucleoside analogues as permeants has not been studied in depth

because of the lack of *in vitro* model systems. However, recent advances in the molecular biology of nucleoside transporters has enabled the development of new approaches, based on functional analysis of recombinant transporter proteins.

A number of purine and pyrimidine nucleoside analogues are used in the treatment of haematologic malignancies including cladribine, fludarabine and cytarabine (161). More recently gemcitabine has shown promising results in the treatment of solid tumours including non small-cell lung, breast, bladder, ovarian, and head and neck carcinomas (161). Several of these drugs have been found to be transported with varying affinities by the human nucleoside transporter proteins.

*In vitro* evidence suggests that cellular resistance to anticancer nucleoside analogues is related, in part, to low nucleoside transport capacity (for review, see Mackey *et al.* (161)). A murine T-cell lymphoma (S49) was chemically mutagenized and clones were selected for resistance to toxic concentrations of adenosine (162-164). A resulting adenosine-resistant isolate (AE1) displayed increased resistance to adenosine as well as to several nucleoside analogues (cladribine, gemcitabine, 5-fluorouridine, 5-fluoro-2'-deoxyuridine) that was associated with a decreased capacity for nucleoside uptake(5,164). Similarly, a human T-lymphoblast (CCRF-CEM) cell line was chemically mutagenized and clones were selected for resistance to toxic concentrations of cytarabine (165,166). A resulting clone (ARAC-8C) displayed increased resistance to cytarabine that appears to be due to loss of the hENT1-mediated *es* transport activity (*e.g.*, reduced NBMPR-sensitivity and a smaller number of NBMPR-binding sites).

The recent advances in the molecular biology of nucleoside transporter proteins are providing new approaches to study the role of nucleoside transporters in therapy of human diseases. Immunologic and molecular probes are rapidly becoming available to determine the number and identity of nucleoside transporter proteins (the "nucleoside transporter profile") within heterogeneous tumour populations. It should eventually be possible to tailor nucleoside chemotherapy such that it matches the nucleoside transporter profile of the

target cells within a tumour. For example, gemcitabine is a permeant for recombinant hCNT1, hENT1 and hCNT2 with  $K_m$  values, respectively, of 24  $\mu\text{M}$ , 160  $\mu\text{M}$  and 740  $\mu\text{M}$  (167). The greater abundance of one or more these transporters in malignant cells, compared to the dose-limiting normal tissues, would strengthen the rationale for gemcitabine therapy over non-nucleoside therapies. The schedule of drug administration might also be guided by the target nucleoside transporter profile. For example, a tumour cell population possessing predominantly hCNT1 (high gemcitabine affinity,  $K_m = 24 \mu\text{M}$ ) would be expected to respond to prolonged low-dose gemcitabine administration (168) whereas a tumour cell population possessing predominantly hENT1 and/or hENT2 (moderate to low gemcitabine affinities,  $K_m = 160 \mu\text{M}$  and 740  $\mu\text{M}$ , respectively) would warrant bolus high-dose therapy. Finally, by monitoring the nucleoside transporter profile of target malignant cells throughout the course of treatment, acquired changes in the expression of nucleoside transporter proteins might mandate changes in nucleoside drug dosing and or scheduling, or switching to non-nucleoside chemotherapy.

Nucleoside analogues are currently used extensively in anti-viral therapies. Zidovudine and 2',2'-dideoxycytidine are two components of the triple combination chemotherapy used in the treatment of human immunodeficiency virus (HIV) infection. Treatment of virally infected cells using nucleoside analogue chemotherapy faces similar obstacles to that of the treatment of malignant cells. Zidovudine is not transported by the erythrocyte *es* process and has been shown to be a low-affinity permeant of the pyrimidine-nucleoside selective concentrative transporters from human (hCNT1) and rat (rCNT1,  $K_m = 490 \mu\text{M}$ ) (15,27). Understanding of the nucleoside transporter profile of virally infected cells, as compared to surrounding normal tissues, should allow the preferential targeting of nucleoside chemotherapy to the infected cell population.

Parasitic protozoa, which are unable to synthesize purines *de novo*, salvage purine nucleosides and nucleobases from host tissue fluids through the action of unique parasitic transporters that are inserted in the plasma membranes of host cells as well as in plasma

membranes of parasitic cells (38). A number of parasitic transporter cDNAs have been isolated and the cognate recombinant proteins display transport characteristics that are distinct from those of their mammalian hosts. These differences in transportability, which effectively alter the nucleoside transporter profile of infected cells compared to uninfected cells, should allow the development of nucleoside analogues that are transported by parasitic nucleoside transporter proteins but not mammalian nucleoside transporter proteins.



## VIII.

### Bibliography

1. Cass, C. E., Young, J. D., Baldwin, S. A., Cabrita, M. A., Graham, K. A., Griffiths, M., Jennings, L. L., Mackey, J. R., Ng, A. M. L., Ritzel, M. W. L., Vickers, M. F., and Yao, S. Y. M. (1999) in *Membrane Transporters as Drug Targets* (Amidon, G. L., and Sadee, W., eds) Vol. 12, 1 Ed., 12 vols., Kluwer Academic/Plenum Publishers
2. Cass, C. E., Young, J. D., and Baldwin, S. A. (1998) *Biochem Cell Biol* 76(5), 761-70
3. Griffith, D. A., and Jarvis, S. M. (1996) *Biochim Biophys Acta* 1286(3), 153-81
4. Cass, C. E. (1995) in *Drug Transport in Antimicrobial and Anticancer Chemotherapy* (Georgopapadakou, N. H., ed), pp. 403-451, Marcel Dekker, New York, NY
5. Mackey, J. R., Mani, R. S., Selner, M., Mowles, D., Young, J. D., Belt, J. A., Crawford, C. R., and Cass, C. E. (1998) *Cancer Res* 58(19), 4349-57
6. Baldwin, S. A., Mackey, J. R., Cass, C. E., and Young, J. D. (1999) *Mol Med Today* 5(5), 216-224
7. Mani, R. S., Hammond, J. R., Marjan, J. M., Graham, K. A., Young, J. D., Baldwin, S. A., and Cass, C. E. (1998) *J Biol Chem* 273(46), 30818-25
8. Pisoni, R. L., and Thoene, J. G. (1989) *J-Biol-Chem* 264(9), 4850-6
9. Camins, A., Jimenez, A., Sureda, F. X., Pallas, M., Escubedo, E., and Camarasa, J. (1996) *Life Sci* 58(9), 753-9
10. Flanagan, S. A., and Meckling-Gill, K. A. (1997) *J Biol Chem* 272(29), 18026-32
11. Wang, J., Schaner, M. E., Thomassen, S., Su, S. F., Piquette-Miller, M., and Giacomini, K. M. (1997) *Pharm Res* 14(11), 1524-32

12. Huang, Q. Q., Yao, S. Y., Ritzel, M. W., Paterson, A. R., Cass, C. E., and Young, J. D. (1994) *J Biol Chem* **269**(27), 17757-60
13. Yao, S. Y., Ng, A. M., Ritzel, M. W., Gati, W. P., Cass, C. E., and Young, J. D. (1996) *Mol Pharmacol* **50**(6), 1529-35
14. Che, M., Ortiz, D. F., and Arias, I. M. (1995) *J Biol Chem* **270**(23), 13596-9
15. Ritzel, M. W., Yao, S. Y., Huang, M. Y., Elliott, J. F., Cass, C. E., and Young, J. D. (1997) *Am J Physiol* **272**(2 Pt 1), C707-14
16. Yao, S. Y., Ng, A. M., Muzyka, W. R., Griffiths, M., Cass, C. E., Baldwin, S. A., and Young, J. D. (1997) *J Biol Chem* **272**(45), 28423-30
17. Ritzel, M. W., Yao, S. Y., Ng, A. M., Mackey, J. R., Cass, C. E., and Young, J. D. (1998) *Mol Membr Biol* **15**(4), 203-11
18. Griffiths, M., Beaumont, N., Yao, S. Y., Sundaram, M., Boumah, C. E., Davies, A., Kwong, F. Y., Coe, I., Cass, C. E., Young, J. D., and Baldwin, S. A. (1997) *Nat Med* **3**(1), 89-93
19. Griffiths, M., Yao, S. Y., Abidi, F., Phillips, S. E., Cass, C. E., Young, J. D., and Baldwin, S. A. (1997) *Biochem J* **328**(Pt 3), 739-43
20. Wang, J., Su, S. F., Dresser, M. J., Schaner, M. E., Washington, C. B., and Giacomini, K. M. (1997) *Am J Physiol* **273**(6 Pt 2), F1058-65
21. Crawford, C. R., Patel, D. H., Naeve, C., and Belt, J. A. (1998) *J Biol Chem* **273**(9), 5288-93
22. Pajor, A. M. (1998) *Biochim Biophys Acta* **1415**(1), 266-9
23. Patel, D. H., Crawford, C. R., Naeve, C. W., and Belt, J. A. (2000) *Gene* **242**(1-2), 51-8
24. Huang, Q. Q., Harvey, C. M., Paterson, A. R., Cass, C. E., and Young, J. D. (1993) *J Biol Chem* **268**(27), 20613-9
25. Felipe, A., Valdes, R., Santo, B., Lloberas, J., Casado, J., and Pastor-Anglada, M. (1998) *Biochem J* **330**(Pt 2), 997-1001

26. Anderson, C. M., Xiong, W., Young, J. D., Cass, C. E., and Parkinson, F. E. (1996) *Brain Res Mol Brain Res* 42(2), 358-61
27. Yao, S. Y., Cass, C. E., and Young, J. D. (1996) *Mol Pharmacol* 50(2), 388-93
28. Wang, J., and Giacomini, K. M. (1997) *J Biol Chem* 272(46), 28845-8
29. Fang, X., Parkinson, F. E., Mowles, D. A., Young, J. D., and Cass, C. E. (1996) *Biochem J* 317(Pt 2), 457-65
30. Loewen, S. K., Ng, A. M., Yao, S. Y., Cass, C. E., Baldwin, S. A., and Young, J. D. (1999) *J Biol Chem* 274(35), 24475-84
31. Wang, J., and Giacomini, K. M. (1999) *J Biol Chem* 274(4), 2298-302
32. Kwong, F. Y., Davies, A., Tse, C. M., Young, J. D., Henderson, P. J., and Baldwin, S. A. (1988) *Biochem J* 255(1), 243-9
33. Boleti, H., Coe, I. R., Baldwin, S. A., Young, J. D., and Cass, C. E. (1997) *Neuropharmacology* 36(9), 1167-79
34. Coe, I. R., Griffiths, M., Young, J. D., Baldwin, S. A., and Cass, C. E. (1997) *Genomics* 45(2), 459-60
35. Sundaram, M., Yao, S. Y. M., Ng, A. M. L., Griffiths, M., Cass, C. E., Baldwin, S. A., and Young, J. D. (1998) *J Biol Chem* 273(34), 21519-25
36. Paterson, A. R., Gati, W. P., Vijayalakshmi, D., Cass, C. E., Mant, M. J., Young, J. D., and Belch, A. R. (1993) *Proc Annu Meet Am Assoc Cancer Res* 34, A84
37. Belt, J. A., Marina, N. M., Phelps, D. A., and Crawford, C. R. (1993) *Adv Enzyme Regul* 33, 235-52
38. Berens, R. L., Krug, E. C., Marr, J. J. (1995) in *Biochemistry and Molecular Biology of Parasites* (Marr, J. J., Muller, M., ed), pp. 89-117, Academic Press, Inc., New York

39. Vasudevan, G., Carter, N. S., Drew, M. E., Beverley, S. M., Sanchez, M. A., Seyfang, A., Ullman, B., and Landfear, S. M. (1998) *Proc Natl Acad Sci U S A* **95**(17), 9873-8
40. Carter, N. S., Drew, M. E., Sanchez, M., Vasudevan, G., Landfear, S. M., and Ullman, B. (2000) *J Biol Chem*
41. Maser, P., Sutterlin, C., Kralli, A., and Kaminsky, R. (1999) *Science* **285**(5425), 242-4
42. Sanchez, M. A., Ullman, B., Landfear, S. M., and Carter, N. S. (1999) *J Biol Chem* **274**(42), 30244-9
43. Schwab, J. C., Afifi Afifi, M., Pizzorno, G., Handschumacher, R. E., and Joiner, K. A. (1995) *Mol Biochem Parasitol* **70**(1-2), 59-69
44. Chiang, C. W., Carter, N., Sullivan, W. J., Jr., Donald, R. G., Roos, D. S., Naguib, F. N., el Kouni, M. H., Ullman, B., and Wilson, C. M. (1999) *J Biol Chem* **274**(49), 35255-61
45. Carter, N. S., Ben Mamoun, C., Liu, W., Silva, E. O., Landfear, S. M., Goldberg, D. E., and Ullman, B. (2000) *J Biol Chem* **275**(14), 10683-91
46. Parker, M. D., Hyde, R. J., Yao, S. Y., McRobert, L., Cass, C. E., Young, J. D., McConkey, G. A., and Baldwin, S. A. (2000) *Biochem J* **349**(Pt 1), 67-75
47. Rao, T. V., Verma, R. S., and Prasad, R. (1983) *Biochem Int* **6**(3), 409-17
48. Fasoli, M. O., and Kerridge, D. (1990) *J Gen Microbiol* **136**(Pt 8), 1475-81
49. Fasoli, M. O., Kerridge, D., Morris, P. G., and Torosantucci, A. (1990) *Antimicrob Agents Chemother* **34**(10), 1996-2006
50. Detke, S. (1998) *Yeast* **14**(14), 1257-65
51. Horak, J. (1997) *Biochim Biophys Acta* **1331**(1), 41-79
52. Grenson, M. (1969) *Eur J Biochem* **11**(2), 249-60
53. Jund, R., and Lacroute, F. (1970) *J Bacteriol* **102**(3), 607-15

54. Nelissen, B., Mordant, P., Jonniaux, J. L., De Wachter, R., and Goffeau, A. (1995) *FEBS Lett* **377**(2), 232-6
55. Nelissen, B., De Wachter, R., and Goffeau, A. (1997) *FEMS Microbiol Rev* **21**(2), 113-34
56. Wagner, R., de Montigny, J., de Wergifosse, P., Souciet, J. L., and Potier, S. (1998) *FEMS Microbiol Lett* **159**(1), 69-75
57. Jund, R., Weber, E., and Chevallier, M. R. (1988) *Eur J Biochem* **171**(1-2), 417-24
58. Jund, R., Chevallier, M. R., and Lacroute, F. (1977) *J Membr Biol* **36**(2-3), 233-51
59. Silve, S., Volland, C., Garnier, C., Jund, R., Chevallier, M. R., and Haguenaer-Tsapis, R. (1991) *Mol Cell Biol* **11**(2), 1114-24
60. Volland, C., Garnier, C., and Haguenaer-Tsapis, R. (1992) *J Biol Chem* **267**(33), 23767-71
61. Volland, C., Urban-Grimal, D., Geraud, G., and Haguenaer-Tsapis, R. (1994) *J Biol Chem* **269**(13), 9833-41
62. Galan, J. M., Moreau, V., Andre, B., Volland, C., and Haguenaer-Tsapis, R. (1996) *J Biol Chem* **271**(18), 10946-52
63. Urban-Grimal, D., Pinson, B., Chevallier, J., and Haguenaer-Tsapis, R. (1995) *Biochem J* **308**(Pt 3), 847-51
64. Pinson, B., Chevallier, J., and Urban-Grimal, D. (1999) *Biochem J* **339**(Pt 1), 37-42
65. Seron, K., Blondel, M. O., Haguenaer-Tsapis, R., and Volland, C. (1999) *J Bacteriol* **181**(6), 1793-800
66. Chevallier, M. R., Jund, R., and Lacroute, F. (1975) *J Bacteriol* **122**(2), 629-41
67. Losson, R., Jund, R., and Chevallier, M. R. (1978) *Biochim Biophys Acta* **513**(2), 296-300

68. Brethes, D., Chirio, M. C., Napias, C., Chevallier, M. R., Lavie, J. L., and Chevallier, J. (1992) *Eur J Biochem* **204**(2), 699-704
69. Rodriguez, C., Bloch, J. C., and Chevallier, M. R. (1995) *Yeast* **11**(1), 15-23
70. Pinson, B., Pillois, X., Brethes, D., Chevallier, J., and Napias, C. (1996) *Eur J Biochem* **239**(2), 439-44
71. Reichert, U., Schmidt, R., and Foret, M. (1975) *FEBS Lett* **52**(1), 100-2
72. Brethes, D., Napias, C., Torchut, E., and Chevallier, J. (1992) *Eur J Biochem* **210**(3), 785-91
73. Kern, L. (1990) *Nucleic Acids Res* **18**(17), 5279
74. Barton, A. B., and Kaback, D. B. (1994) *J Bacteriol* **176**(7), 1872-80
75. Craig, J. E., Zhang, Y., and Gallagher, M. P. (1994) *Mol Microbiol* **11**(6), 1159-68
76. Westh Hansen, S. E., Jensen, N., and Munch-Petersen, A. (1987) *Eur J Biochem* **168**(2), 385-91
77. Yao, S. Y. M. (1995) in *Physiology*, pp. 236, University of Alberta, Edmonton
78. Munch-Petersen, A., and Jensen, N. (1990) *Eur J Biochem* **190**(3), 547-51
79. Loike, J. D., Hickman, S., Kuang, K., Xu, M., Cao, L., Vera, J. C., Silverstein, S. C., and Fischbarg, J. (1996) *Am J Physiol* **271**(5 Pt 1), C1774-9
80. Meinild, A., Klaerke, D. A., Loo, D. D., Wright, E. M., and Zeuthen, T. (1998) *J Physiol (Lond)* **508**(Pt 1), 15-21
81. Alper, S. L., Chernova, M. N., Williams, J., Zasloff, M., Law, F. Y., and Knauf, P. A. (1998) *Biochem Cell Biol* **76**(5), 799-806
82. Okuda, M., Urakami, Y., Saito, H., and Inui, K. (1999) *Biochim Biophys Acta* **1417**(2), 224-31
83. Detaille, D., Wiernsperger, N., and Devos, P. (1999) *Eur J Pharmacol* **377**(1), 127-36

84. Rumsey, S. C., Kwon, O., Xu, G. W., Burant, C. F., Simpson, I., and Levine, M. (1997) *J Biol Chem* 272(30), 18982-9
85. Pasyk, E. A., Morin, X. K., Zeman, P., Garami, E., Galley, K., Huan, L. J., Wang, Y., and Bear, C. E. (1998) *J Biol Chem* 273(48), 31759-64
86. Heyer, M., Muller-Berger, S., Romero, M. F., Boron, W. F., and Fromter, E. (1999) *Pflugers Arch* 438(3), 322-9
87. Wang, J., and Giacomini, K. M. (1999) *Mol Pharmacol* 55(2), 234-40
88. Cooper, C. B., Winkfein, R. J., Szerencsei, R. T., and Schnetkamp, P. P. (1999) *Biochemistry* 38(19), 6276-83
89. Bruss, M., Porzgen, P., Bryan-Lluka, L. J., and Bonisch, H. (1997) *Brain Res Mol Brain Res* 52(2), 257-62
90. Suzuki, T., Iwazaki, A., Katagiri, H., Oka, Y., Redpath, J. L., Stanbridge, E. J., and Kitagawa, T. (1999) *Eur J Biochem* 262(2), 534-40
91. Tang, X. B., and Casey, J. R. (1999) *Biochemistry* 38(44), 14565-72
92. Tang, X. B., Kovacs, M., Sterling, D., and Casey, J. R. (1999) *J Biol Chem* 274(6), 3557-64
93. Fujinaga, J., Tang, X. B., and Casey, J. R. (1999) *J Biol Chem* 274(10), 6626-33
94. Schaner, M. E., Wang, J., Zevin, S., Gerstin, K. M., and Giacomini, K. M. (1997) *Pharm Res* 14(10), 1316-21
95. Crawford, C. R., Cass, C. E., Young, J. D., and Belt, J. A. (1998) *Biochem Cell Biol* 76(5), 843-51
96. Schaner, M. E., Wang, J., Zhang, L., Su, S. F., Gerstin, K. M., and Giacomini, K. M. (1999) *J Pharmacol Exp Ther* 289(3), 1487-91
97. Ward, J. L., Sherali, A., Mo, Z. P., and Tse, C. M. (2000) *J Biol Chem* 275(12), 8375-81
98. Sekler, I., Kopito, R., and Casey, J. R. (1995) *J Biol Chem* 270(36), 21028-34

99. Ruetz, S., and Gros, P. (1994) *J Biol Chem* 269(16), 12277-84
100. Huang, P., Stroffekova, K., Cuppoletti, J., Mahanty, S. K., and Scarborough, G. A. (1996) *Biochim Biophys Acta* 1281(1), 80-90
101. Ausubel, F. M., Brent, R., Kingston, R. E., Moore, D. D., Seidman, J. G., Smith, J. A., and Struhl, K. (eds) (1997) *Current Protocols in Molecular Biology*. Current Protocols. Edited by Chanda, V. B. 3 vols., John Wiley & Sons, Inc., New York, N.Y.
102. Winzeler, E. A., Shoemaker, D. D., Astromoff, A., Liang, H., Anderson, K., Andre, B., Bangham, R., Benito, R., Boeke, J. D., Bussey, H., Chu, A. M., Connelly, C., Davis, K., Dietrich, F., Dow, S. W., El Bakkoury, M., Foury, F., Friend, S. H., Gentalen, E., Giaever, G., Hegemann, J. H., Jones, T., Laub, M., Liao, H., Davis, R. W., and et al. (1999) *Science* 285(5429), 901-6
103. Spellman, P. T., Sherlock, G., Zhang, M. Q., Iyer, V. R., Anders, K., Eisen, M. B., Brown, P. O., Botstein, D., and Futcher, B. (1998) *Mol Biol Cell* 9(12), 3273-97
104. DeRisi, J. L., Iyer, V. R., and Brown, P. O. (1997) *Science* 278(5338), 680-6
105. Hogue, D. L., Ellison, M. J., Young, J. D., and Cass, C. E. (1996) *J Biol Chem* 271(16), 9801-8
106. Hogue, D. L., Ellison, M. J., Vickers, M., and Cass, C. E. (1997) *Biochem Biophys Res Commun* 238(3), 811-6
107. Baudin, A., Ozier-Kalogeropoulos, O., Denouel, A., Lacroute, F., and Cullin, C. (1993) *Nucleic Acids Res* 21(14), 3329-30
108. Ito, H., Fukuda, Y., Murata, K., and Kimura, A. (1983) *J Bacteriol* 153(1), 163-8
109. Sambrook, J., Fritsch, E. F., Maniatis, T. (1989) *Molecular Cloning: A Laboratory Manual*. Cold Spring Harbor Laboratory, Cold Spring Harbor, NY



110. Williams, J. B., and Lanahan, A. A. (1995) *Biochem Biophys Res Commun* **213**(1), 325-33
111. Krieg, P. A., and Melton, D. A. (1984) *Nucleic Acids Res* **12**(18), 7057-70
112. Hogue, D. L., Hodgson, K. C., and Cass, C. E. (1990) *Biochem Cell Biol* **68**(1), 199-209
113. Markwell, M. A., Haas, S. M., Tolbert, N. E., and Bieber, L. L. (1981) *Methods Enzymol* **72**, 296-303
114. Laemmli, U. K. (1970) *Nature* **227**(259), 680-5
115. Harley, E. R., Paterson, A. R., and Cass, C. E. (1982) *Cancer Res* **42**(4), 1289-95
116. Boumah, C. E., Hogue, D. L., and Cass, C. E. (1992) *Biochem J* **288**(Pt 3), 987-96
117. Cheng, Y., and Prusoff, W. H. (1973) *Biochem Pharmacol* **22**(23), 3099-108
118. Hammond, J. R. (1991) *Mol Pharmacol* **39**(6), 771-9
119. Hammond, J. R., and Zarenda, M. (1996) *Arch Biochem Biophys* **332**(2), 313-22
120. Jarvis, S. M. (1986) *Mol Pharmacol* **30**(6), 659-65
121. Koren, R., Cass, C. E., and Paterson, A. R. (1983) *Biochem J* **216**(2), 299-308
122. Hammond, J. R. (1994) *J Pharmacol Exp Ther* **271**(2), 906-17
123. Tse, C. M., Belt, J. A., Jarvis, S. M., Paterson, A. R., Wu, J. S., and Young, J. D. (1985) *J Biol Chem* **260**(6), 3506-11
124. Villalba, J. M., Palmgren, M. G., Berberian, G. E., Ferguson, C., and Serrano, R. (1992) *J Biol Chem* **267**(17), 12341-9
125. Nakamoto, R. K., Rao, R., and Slayman, C. W. (1991) *J Biol Chem* **266**(12), 7940-9
126. Darsow, T., Burd, C. G., and Emr, S. D. (1998) *J Cell Biol* **142**(4), 913-22
127. Vickers, M. F., Yao, S. Y. M., Baldwin, S. A., Young, J. D., Cass, C. E. (2000) *J. Biol. Chem.* in press

128. Nagy, M. (1979) *Biochim Biophys Acta* **558**(2), 221-32
129. Matile, P. (1969) *Biochem J* **111**(5), 26P-27P
130. Sato, T., Ohsumi, Y., and Anraku, Y. (1984) *J Biol Chem* **259**(18), 11509-11
131. Sato, T., Ohsumi, Y., and Anraku, Y. (1984) *J Biol Chem* **259**(18), 11505-8
132. Booth, J. W., and Guidotti, G. (1997) *J Biol Chem* **272**(33), 20408-13
133. Ohsumi, Y., and Anraku, Y. (1983) *J Biol Chem* **258**(9), 5614-7
134. Li, Z. S., Szczypka, M., Lu, Y. P., Thiele, D. J., and Rea, P. A. (1996) *J Biol Chem* **271**(11), 6509-17
135. Hogue, D. L., Kerby, L., and Ling, V. (1999) *J Biol Chem* **274**(18), 12877-82
136. Fajor, A. M., and Wright, E. M. (1992) *J Biol Chem* **267**(6), 3557-60
137. Tomb, J. F., White, O., Kerlavage, A. R., Clayton, R. A., Sutton, G. G., Fleischmann, R. D., Ketchum, K. A., Klenk, H. P., Gill, S., Dougherty, B. A., Nelson, K., Quackenbush, J., Zhou, L., Kirkness, E. F., Peterson, S., Loftus, B., Richardson, D., Dodson, R., Khalak, H. G., Glodek, A., McKenney, K., Fitzgerald, L. M., Lee, N., Adams, M. D., Venter, J. C., and et al. (1997) *Nature* **388**(6642), 539-47
138. Fleischmann, R. D., Adams, M. D., White, O., Clayton, R. A., Kirkness, E. F., Kerlavage, A. R., Bult, C. J., Tomb, J. F., Dougherty, B. A., Merrick, J. M., and et al. (1995) *Science* **269**(5223), 496-512
139. Vickers, M. F., Mani, R. S., Sundaram, M., Hogue, D. L., Young, J. D., Baldwin, S. A., and Cass, C. E. (1999) *Biochem J* **339**(Pt 1), 21-32
140. Kwong, F. Y., Wu, J. S., Shi, M. M., Fincham, H. E., Davies, A., Henderson, P. J., Baldwin, S. A., and Young, J. D. (1993) *J Biol Chem* **268**(29), 22127-34
141. Kwong, F. Y., Baldwin, S. A., Scudder, P. R., Jarvis, S. M., Choy, M. Y., and Young, J. D. (1986) *Biochem J* **240**(2), 349-56
142. Cass, C. E., and Paterson, A. R. (1976) *Biochim Biophys Acta* **419**(2), 285-94

143. Agbanyo, F. R., Cass, C. E., and Paterson, A. R. (1988) *Mol Pharmacol* 33(3), 332-7
144. Jarvis, S. M., McBride, D., and Young, J. D. (1982) *J Physiol (Lond)* 324, 31-46
145. Jarvis, S. M., and Young, J. D. (1980) *Biochem J* 190(2), 377-83
146. Jarvis, S. M., Janmohamed, S. N., and Young, J. D. (1983) *Biochem J* 216(3), 661-7
147. Crawford, C. R., Ng, C. Y., Ullman, B., and Belt, J. A. (1990) *Biochim Biophys Acta* 1024(2), 289-97
148. Boumah, C. E., Harvey, C. M., Paterson, A. R., Baldwin, S. A., Young, J. D., and Cass, C. E. (1994) *Biochem J* 299(Pt 3), 769-73
149. Landolt-Marticorena, C., and Reithmeier, R. A. (1994) *Biochem J* 302(Pt 1), 253-60
150. Ellgaard, L., Molinari, M., and Helenius, A. (1999) *Science* 286(5446), 1882-8
151. Popov, M., Tam, L. Y., Li, J., and Reithmeier, R. A. (1997) *J Biol Chem* 272(29), 18325-32
152. Popov, M., Li, J., and Reithmeier, R. A. (1999) *Biochem J* 339(Pt 2), 269-79
153. Snyder, P. M., McDonald, F. J., Stokes, J. B., and Welsh, M. J. (1994) *J Biol Chem* 269(39), 24379-83
154. Turk, E., Kerner, C. J., Lostao, M. P., and Wright, E. M. (1996) *J Biol Chem* 271(4), 1925-34
155. Hresko, R. C., Kruse, M., Strube, M., and Mueckler, M. (1994) *J Biol Chem* 269(32), 20482-8
156. Pollet, J. F., Van Geffel, J., Van Stevens, E., Van Geffel, R., Beauwens, R., Bollen, A., and Jacobs, P. (2000) *Biochim Biophys Acta* 1500(1), 59-69
157. Warnat, J., Philipp, S., Zimmer, S., Flockerzi, V., and Cavalie, A. (1999) *J Physiol (Lond)* 518(Pt 3), 631-8

158. Buteau, H., Pezet, A., Ferrag, F., Perrot-Appianat, M., Kelly, P. A., and Edery, M. (1998) *Mol Endocrinol* **12**(4), 544-55
159. Mahanty, S. K., Rao, U. S., Nicholas, R. A., and Scarborough, G. A. (1994) *J Biol Chem* **269**(26), 17705-12
160. Kaiser, B. N., Finnegan, P. M., Tyerman, S. D., Whitehead, L. F., Bergersen, F. J., Day, D. A., and Udvardi, M. K. (1998) *Science* **281**(5380), 1202-6
161. Mackey, J. R., Baldwin, S. A., Young, J. D., and Cass, C. E. (1998) *Drug Resistance Updates* **1**, 310-324
162. Aronow, B., and Ullman, B. (1985) *J Biol Chem* **260**(30), 16274-8
163. Cass, C. E., Kolassa, N., Uehara, Y., Dahlig-Harley, E., Harley, E. R., and Paterson, A. R. (1981) *Biochim Biophys Acta* **649**(3), 769-77
164. Cohen, A., Ullman, B., and Martin, D. W., Jr. (1979) *J Biol Chem* **254**(1), 112-6
165. Ullman, B., Coons, T., Rockwell, S., and McCartan, K. (1988) *J Biol Chem* **263**(25), 12391-6
166. Ullman, B. (1989) *Adv Exp Med Biol* , 415-20
167. Mackey, J. R., Yao, S. Y., Smith, K. M., Karpinski, E., Baldwin, S. A., Cass, C. E., and Young, J. D. (1999) *J Natl Cancer Inst* **91**(21), 1876-81
168. Pollera, C. F., Ceribelli, A., Crecco, M., Oliva, C., and Calabresi, F. (1997) *Invest New Drugs* **15**(2), 115-21